MERCURY ADSORPTION BY *ARTHOBACTER GLOBIFORMIS* AND *SPIRULINA PLATENSIS*

T. L. Kalabegishvili[1,2], I. Murusidze[2], D. T. Pataraya[3], E. Ginturi[1], M. V. Frontasyeva[4], E. I. Kirkesali[1], Gh. Duca[5], I. Zinicovscaia[4,5*]

[1]*Andronikashvili Institute of Physics, 6, Tamarashvili Str., Tbilisi, 0177, Georgia*
[2]*Ilia State University, 3/5, K. Cholokashvili Ave., Tbilisi 0162, Georgia*
[3]*Durmishidze Institute of Biochemistry and Biotechnology, D. Agmashenebeli Kheivani, 10 km, 0159, Tbilisi, Georgia*
[4]*Joint Institute for Nuclear Research, Joliot-Curie Str., 6, 1419890 Dubna, Russia*
[5]*The Institute of Chemistry of the Academy of Sciences of Moldova, 3, Academiei Str., 2028 Chisinau, R. Moldova*
E-mail: zinikovskaia@mail.ru

Abstract. The increasing contamination of soil, sediment, and water with heavy metals by natural and industrial processes is a worldwide problem. Many bacteria and microalgae have demonstrated ability to absorb toxic elements. To study mercury biosorption by bacteria *Arthrobacter globiformis* and microalga *Spirulina platensis* neutron activation analysis (NAA) was applied. The process of mercury biosorption by these media was described by Freundlich and Langmuir-Freundlich Model. Both microorganisms showed a great potential to be used as biosorbing agents for mercury removal from the environment.

Keywords: Langmuir-Freundlich model, *Arthrobacter globiformis, Spirulina platensis,* biosorption, mercury, neutron activation analysis.

Introduction

Heavy metals are known as a hazardous group of pollutants. The contamination by heavy metals causes a serious problem because they cannot be naturally degraded like organic pollutants and they are accumulated in different parts of the food chain [1]. Physical and chemical methods have been proposed for the removal of these pollutants. Nevertheless, they have some disadvantages, among them cost-effectiveness limitations, generation of hazardous by-products or inefficiency when concentration of polluted materials is below 100 mg/l [2]. Biological methods help to avoid these drawbacks since they are easy to operate, do not produce secondary pollution and show higher efficiency at low metal concentrations. Microorganisms and plants are usually used for the removal of heavy metals. Mechanisms by which microorganisms act on heavy metals include biosorption, bioleaching, biomineralization, intracellular accumulation and enzyme-catalyzed transformations [3].

Mercury occupies the sixth position in the list of hazardous compounds [4-7]. Even its very small doses cause gonadotoxic, mutagenic, neurotoxic and embryotoxic effects. Accumulating mainly in the kidneys, liver and spleen, mercury blocks the biochemical activity of protein molecules and low-molecular weight compounds.

Mercury is a well-distributed element. Its mean content in the earth's crust constitutes 8×10^{-6}%. The total amount of mercury in the atmosphere is 10^{-9} g/m^3, 1×10^{-6}% in soil, and 25×10^{-6}% in plants (dry mass) [8].

Mercury is widely used in industry, medicine, dentistry, batteries, science, and in military applications. Mercurial compounds are also used in agriculture as insecticides, fungicides, herbicides and bactericides [9]. These various industrial and agricultural applications have led to severe mercury localized pollution in the aquatic systems and in soils [10-11]. To prevent the detrimental effects of mercurial compounds, many bacterial species *Alteromonas tagae* sp. nov.*, Alteromona simiduii* sp. nov [5], *Klebsiella pneumonia, Streptomyces* sp. have evolved a sophisticated detoxification system by which Hg(II) can be reduced to Hg(0) followed by volatilization of the relatively non-toxic Hg (0) from aqueous media [7].

Algae have been successfully used for waste, wastewater and soil treatment. *Chlorella pyrenoidosa*, *Oedogonium foveolatum*, *Hydrodictyon reticulatum, Scenedesmus quadricauda,* S*pirulina platensis*, *Spirulina maxima, Mastigocladus laminosus* efficiently remove aluminum, mercury, cadmium, zinc and chromium from wastes [12]. *S. platensis* can be used as a metal adsorbent to accumulate copper, mercury, lead [13-14], chromium [15], and cadmium [16]. *Scenedesmus acutus* and *Chlorella vulgaris* can be used to accumulate cadmium, zinc and chromium from wastewater [17].

In this work, biosorption of mercury by *Arthrobacter globiformis and Spirulina platensis* using neutron activation analysis was studied.

Material and methods

Sample preparation

Cultivation of Arthrobacter globiformis 151B

Samples of *Arthrobacter globiformis* 151B a Gram-positive, Cr(VI)-reducer, aerobic bacterial strain was isolated from basalt samples collected from the most polluted region in the Republic of Georgia (Kazreti). The bacteria were

grown aerobically in the following nutrient medium: 10 g of glucose, 10 g of peptone, 1 g of yeast extract, 2 g of caseic acid hydrolysate, 5 g of NaCl, and 1 liter of distilled water. All chemicals used in the experiment were ACS-reagent grade, produced by Sigma (St. Louis, MO, USA). Bacterial cells were grown in 250 ml Erlenmayer flasks as a suspension. The medium was inoculated with 0.1 ml of overnight broth and incubated at 21 °C being shaken continuously. Hg(II) as [$Hg(NO_3)_2 \cdot H_2O$] was added to the bacterial cell cultures at an early stationary phase of their growth. The concentration of Hg(II) varied within the range of 50–5000 μg/L. After being cultivated for 5 days the cells were harvested by centrifugation (10,000 rpm, 15 min, 4 °C), rinsed twice in a 20 mM phosphate buffer and subjected to NAA analysis. For NAA measurements this wet biomass was placed in an adsorption-condensation lyophilizer and dried. The dry native biomass was finally pelletized to 5 mm pieces using a special titanium press form [18].

Cultivation of Spirulina platensis

Spirulina platensis IPPAS B-256 strain from Timiriazev Institute for Plant Physiology of the Russian Academy of Sciences was cultivated in a standard Zaroukh alkaline water-salt medium at a temperature of +34ºC, illumination ~ 5000 lux, initial pH 8.7 and at constant mixing. Since the Hg(II) ions in alkaline medium form an insoluble residue (mercury hydroxide), in order to avoid the mercury residue, mercury glycinate was used as a nutrient loading. To study the Hg accumulation by the *S. platensis* cells the concentrations of nutrient medium loading by mercury constituted 100, 50, 5, 1, 0.1 μg Hg/L. Initial concentration of *S. platensis* suspension in all the experiments of the series constituted 260 mg/L. Cultivation of the *S. platensis* cells was conducted for 6 days. Samples in all the series were taken every 24 hours. In the course of all the experiments microscopic control of *S. platensis* living cells was performed daily [8].

Analysis

The *Arthrobacter globiformis* 151B samples were irradiated using the facilities of the 2 MW nuclear research reactor "Hoger Onderwijs Reactor" of the Reactor Institute Delft, Delft University of Technology [18]. More details on the operation and quality assurance in this laboratory can be found elsewhere [19-20]. Mercury content in the *Spirulina platensis* samples was determined by epithermal neutron activation analysis (ENAA) at the pulsed fast reactor IBR-2 (FLNP JINR, Dubna) [8]. The description of irradiation channels and pneumatic transport system of the IBR-2 are given in [21]. The ENAA data processing and determination of Hg concentrations were performed using software developed in FLNP JINR [22].

Results and discussion

Two heterogeneity-based models isotherm: Freundlich and Langmuir-Freundlich isotherm model (LF) were used for the evaluation of the sorption characteristic of mercury on bacteria *Arthrobacter globiformis* and microalga *Spirulina platensis.*

Freundlich isotherm model

NAA results obtained for *Spirulina platensis* were expressed by Freundlich (heterogeneous) isotherm model (Fig. 1). The Freundlich equation is often considered to be purely empirical in nature [23].

The Freundlich Adsorption Isotherm is mathematically expressed as

$$x/m = Kc^{1/n}$$

It is also can be written as

$$\log(x/m) = \log K + (1/n) \log c$$

where: x = mass of adsorbate; m = mass of adsorbent; c = equilibrium concentration of adsorbate in solution;
K and n are constants for a given adsorbate and adsorbent at a particular temperature**.**

In work [8] theoretical calculations of the adsorption isotherm for Hg(II) on the basis of the obtained experimental data were performed taking into account both physical adsorption and chemosorption. For various Hg(II) concentrations at the duration of cultivation for 24 hours in the Freundlich coordinates the dependence was obtained

$$\log R = -6.77 + 0.62 \log C$$

where R –concentration of the adsorbed Hg(II), C – concentration of Hg(II) in nutrient medium.

Linear approximation by method of least squares is shown in (Fig. 1). The straight line is cutting off on the Y-axis a section, equal to *log* K. In the present case *log* K = -6.77 and K = $0.17 \cdot 10^{-6}$. The correlation coefficient is R = 0.97. The obtained result can be regarded as a confirmation of predominance of biosorptive processes at the initial stage of the *S. platensis* cell cultivation.

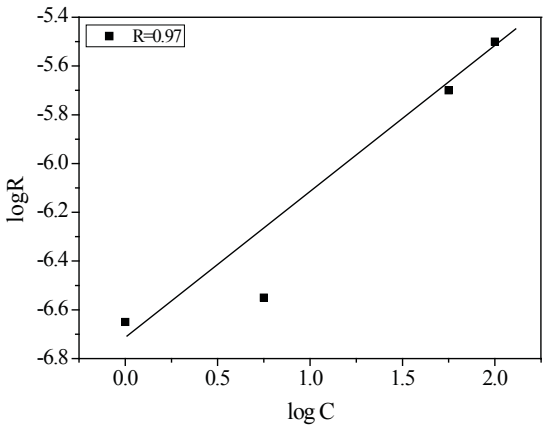

Fig. 1. Freundlich diagram. Linear approximation by method of least squares

The cell surface of many microorganisms, including cyanobacteria, consists of polysaccharides, proteins, and lipids, which act like basic binding sites of heavy metals because they have functional groups, such as amino, carboxylic, sulfhydryl, phosphate, and thiol groups, which can bind metals. The cell wall of *Spirulina platensis* consists of polysaccharides, proteins, and lipids, which have many negative carboxyl and phosphate groups, the dominant binding sites of toxic and heavy-metal cations [24].

It was shown that carboxyl groups of alginate played a major role in the complexation of heavy metals [25].

Langmuir-Freundlich isotherm model

Langmuir isotherm (L) is a useful model to represent the sorption mechanism. This model is based on the assumption that the sorption energy is uniform and homogeneously distributed on the sorbent surfaces.

The Langmuir isotherm model is expressed as:

$$q = q_{max}bc/1+bc$$

Here: c − is the concentration of metal ions; q_{max} − represents the maximum metal accumulation; b − is the affinity parameter of the isotherm reflecting the high affinity of the biosorbent for the sorbate.

The theoretical assumption of the Langmuir model is that the bonding energy on each sorption site is completely equal [22]. The metal uptake (q) was calculated from the initial concentration (C_i) and the analyzed final concentration (C_f) of the metal in solution according to the following formula:

$$q = V(C_i-C_f)/m$$

where V is the liquid sample volume and m is the starting sorbent weight [18].

Some experimental results showed that the theoretical assumption of the Langmuir model failed to explain the sorption of some compounds.

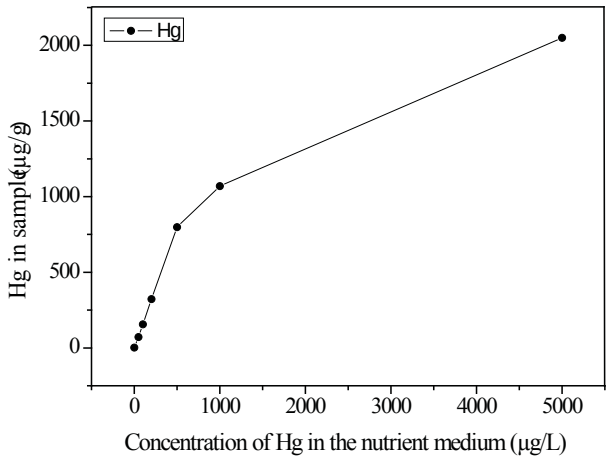

Fig. 2. Accumulation of mercury by *A. globiformis*

Thus, the heterogeneity of sorption energy has been taken into account. The heterogeneity-based isotherm, the Langmuir-Freundlich isotherm model (LF), is then derived as [26].

$$q = q_{max} (bc)^n/1+(bc)^n$$

where n is related to the degree of heterogeneity of a sorbent surface.

Langmuir-Freundlich isotherm was used to describe process of mercury accumulation by bacteria *A. globiformis* (Fig. 2) [18].

Adsorption processes consists of two steps, starting with the rapid one (physical adsorption between the metal ions and the bacterial surface) and continuing with the slow one (chemical adsorption). The rapid process one may last from for several minutes to a few hours, while the slow one lasts from several hours to a few days. The metallic cations form complexes with functional groups (carboxyl, carbonyl, amino, amido, sufonate, phosphate, etc.) present on the surface or inside the porous structure of the biological material [27].

Conclusions

It was shown that the mercury accumulation process fits well the Freundlich and Langmuir-Freundlich models**.** This is obvious evidence that the bacteria *Arthrobacter globiformis* and microalga *Spirulina platensis* can be successfully used as biosorbing agent for mercury removal from the environment.

References

[1]. Jьmejkalová, M.; Mikanová, O.; Borůvka, L. Plant Soil Environ. 49, 2003, 7, 321–326.
[2]. Wang, J.; Chen, C. Biotechnology Advances. 2009, 27, 195- 226.
[3]. Haferburg, G.; Kothe, E. J. Basic Microbiol. 2007, 47, 453-467.
[4]. Oliveira, A.; Pampulha, M. E.; Neto, M. M.; Almeida, A. C. Geoderma. 2010, 154, 359-363.
[5]. Chiu, H.-H.; Shieh, W. Y.; Lin, S. Y.; Tseng, C. M.; Chiang, P.W.; Wagner-Dobler, I. Intern. J. of Syst. and Evol. Microbiol. 2007, 57, 1209–1216.
[6]. Olson, B. H.; Cayless, S. M.; Ford, S.; Lester, J. N. Arch. Environ. Contam. Toxicol. 1991, 20, 226-233.
[7]. Zeroual, Y.; Moutaouakkil, A.; Dzairi, F.Z.; Talbi, M.; Chung, P.U.; Lee, K.; Blaghen, M. Ann. Microbiol. 2003, 53, 149-160.
[8]. Frontasyeva, M. V.; Kirkesali, E. I.; Aksenova, N. G.; Mosulishvili, L. M.; Belokobylsky, A. I.; Khizanishvili, A. I. J. Neutron Res. 2006, 14, 131 – 137.
[9]. Essa, A. M. M.; Macaskie, L. E., Brown, N. L. Biochem. Soc. Trans. 2002, 30(4), 672-674.
[10]. Bargagli, R. Encyclopedia of environmental science. Kluwer Academic Publisher, 1999, pp.402-405.
[11]. Bryan, G.W.; Langston, W. J. Environ. Pollut. 1992, 76, 84-131.
[12]. Radway, J. C.; Wilde, E. W.; Whitaker, M. J.; Weissman, J. C. J. Appl. Phycol. 2001, 13, 451–455.
[13]. Disyawongs, G. J. KMITNB. 2002, 12, 4-8.
[14]. Solisio, C.; Lodi, A.; Torre, P.; Converti, A.; Del Borghi, M. Bioresource Technol. 2006, 97, 1756–1760.
[15]. Mosulishvili, L. M.; Belokobylsky, A. I.; Kirkesali, E. I.; Frontasyeva, M. V.; Pavlov, S. S.; Aksenova, N. G. J. Neutron Res. 2007, 15(1), 49–54.
[16]. Solisio, C.; Lodi, A.; Soletto, D.; Converti, A. Bioresource Technol. 2008, 99, 5933–5937.
[17]. Travieso, L.; Cañizares, R. O.; Borja, R.; Benítez, F.; Domínguez, A. R.; Dupeyrón, R.; Valiente, V. Bull. Environ. Contam. Toxicol. 1999, 62, 144-151.
[18]. Tsibakhashvili, N., Mosulishvili, L., Kirkesali, E.; Murusidze, I.; Frontasyeva, M. V.; Pavlov, S. S.; Zinicovscaia, I. I.; Bode, P.; van Meerten, Th. G. J. Radioanal. Nucl. Chem. 2010, 286, 533–537.
[19]. Bode, P. J. Radioanal. Nucl. Chem. 2000, 245,127-132.
[20]. Koster-Ammerlaan, M.J.J.; Bode, P. J. Radioanal. Nucl. Chem. 2009, 280,445-449.
[21]. Frontasyeva, M.V.; Pavlov, S.S. JINR Preprint E14-2000-177, Dubna, 2000.
[22]. Ostrovnaya, T.M.; Nefedyeva, L.S.; Nazarov, V.M.; Borzakov, S.B.; Strelkova, L.P. Software for INAA on the basis of relative and absolute methods using nuclear database. In «Activation Analysis in Environment Protection». D-14-93-325, 1993, Dubna, 319-326.
[23]. Hussain, A.; Ghafoor, A.; Anwar-ul-Haq, M.; Nawaz, M. Int. J. Agr. Biol. 2003, 5(3), 349-356.
[24]. Dheetcha, A.; Mishra, S. Curr. Microbiol. 2008, 57, 508–514.
[25]. Pan, J.; Lin, R.; Ma, L. Chinese Journal of Oceanology and Linmology. 2000, 18 (3), 260- 264
[26]. Tsai, S. C.; Juang, K. W.; Jan, Y. L. J. Radioanal. Nucl. Chem. 2005, 266 (1), 101-105.
[27]. Fourest, E.; Volesky, B.; 1997. Appl. Biochem. Biotechnol. 1997, 67, 215 – 226.

SYNTHESIS OF NITROGEN-CONTAINING COMPOUNDS FROM HIGHER TERPENOIDS

Aculina Aricu

Institute of Chemistry of the Academy of Sciences of Moldova , Chişinău,
MD-2028, Academiei str. 3, Republic of Moldova
E-mail: aricu_aculina@yahoo.com; Phone: +7 (373 2) 739963; Fax: +7 (373 2) 739775

Dedicated to Academician Pavel Vlad on his 75-th birthday

Abstract: The presence of nitrogen in the molecule is usually accompanied either by the appearance of a new activity or the intensification of original activity characteristic for the native terpenoids. This maintains alive the scientific interest in the synthesis of such compounds. The present communication put into discussion the recently elaborated methods for preparation of the nitrogen-containing terpenic compounds.

Keywords: synthesis, nitrogen-containing compounds, terpenoids, Beckmann rearrangement.

1. Introduction

Many terpenes exhibit various biological activities [1, 2]. In a series of articles it has been reported on the appearance of a new activity or the intensification of the original activity that accompanies the introduction of nitrogen in the molecules of native terpenoids. Therefore the synthesis of the nitrogen-containing terpenic compounds is of great interest for further studies of their biological activity.

2. Synthesis of the nitrogenated derivatives of drimanes and homodrimanes

The nitrogen-containing sesquiterpenic compounds and their biological activity represent a poorly studied area of terpenoid chemistry. The first synthesis of the homodrimanic nitrogen derivatives was reported by Grant P. K. et al. in 1983 [3]. Oxidative degradation of manool (1) [4] gives the intramolecular acetals (2) and (3). The former possesses a powerful ambra-type odour and is being used in the perfumery industry. In this light it was interesting to examine the synthesis of the nitrogen analogues (4) and (5). Reaction of the methylene ketone (6), in turn obtained from the permanganate oxidation of manool (1), with hydroxylamine gave the isomeric oximes (7) and (8) in 5:2 ratio. Their stereochemistry was assigned on the basis of the corresponding amides obtained under Beckmann rearrangement conditions. By direct treating of the oximes with thionyl chloride only low yields of amides were obtained, while by using the base-promoted rearrangement of the tosylate derivatives the yields were greatly increased.

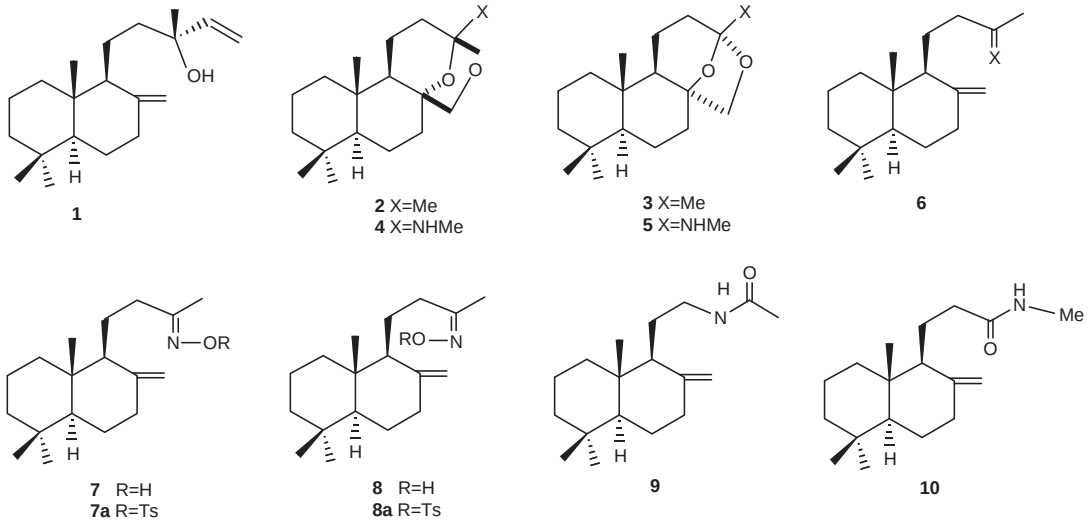

1 **2** X=Me **4** X=NHMe **3** X=Me **5** X=NHMe **6** **7** R=H **7a** R=Ts **8** R=H **8a** R=Ts **9** **10**

Scheme 1

The tosyl derivative (7a) of the less polar oxime (7) furnished the amide (9) in quantitative yield upon treatment with dilute base at room temperature. Since it is known, that Beckmann rearrangement proceeds by a stereospecific *anti*-migration, the *E*-configuration for the oxime (7) has been established. The more polar (O-tosyl) oxime (8a) required

more forcing conditions to effect the rearrangement and gave the amide (10) in 27% yield. Since the amide structure was established to be as depicted in formula (10), this pointed to Z-stereochemistry of the parent oxime (8). The rearrangement of the oxime tosylates under acidic conditions gave the same amide product (9), thus reflecting the facile isomerization of the less stable Z- (O-tosyl)oxime (8a) prior to rearrangement [5].

Later the synthesis was reported by Urones, J.G. et al. [6] describing the use of 12-acetoxy-7,9(11)-drimandien (11), that was in turn prepared from methyl zamoranate (12), as a precursor for C-9 nitrogenated drimanes (Scheme 2). Dien (11) reacts with m-CPBA in a regio- and stereoselective way, affording the epoxide mixture of compounds (13) and (14) [7]. On ulterior derivatisation the α-epoxide afforded carbonates (15) and (17) and carbamates (16) and (18). A1ka1ine hydrolysis of acetate (18) by using a 2N NaOH solution in dioxan (1/1) afforded the corresponding alcohol (19) in 96% yield [8]. Extreme reaction conditions, including saturated solution of KOH and 1,2-ethanediol at 70°C [9] led to the difficultly isolable amino diol (20) in 90% yield. Its treatment with Ac_2O/Py [10] gave the spirodihydrooxazole acetate (21) in 84% yield. In virtue of the amino alcohol high reactivity, the protection of its amino group was required. Hence (21) was treated with $(Boc)_2O$ [11], yielding the N-Boc derivative (22) in 73% yield. Since the latter was resistant to hydrolysis, it could be reduced with DIBAL-H, furnishing diol (23) in good yield (73%).

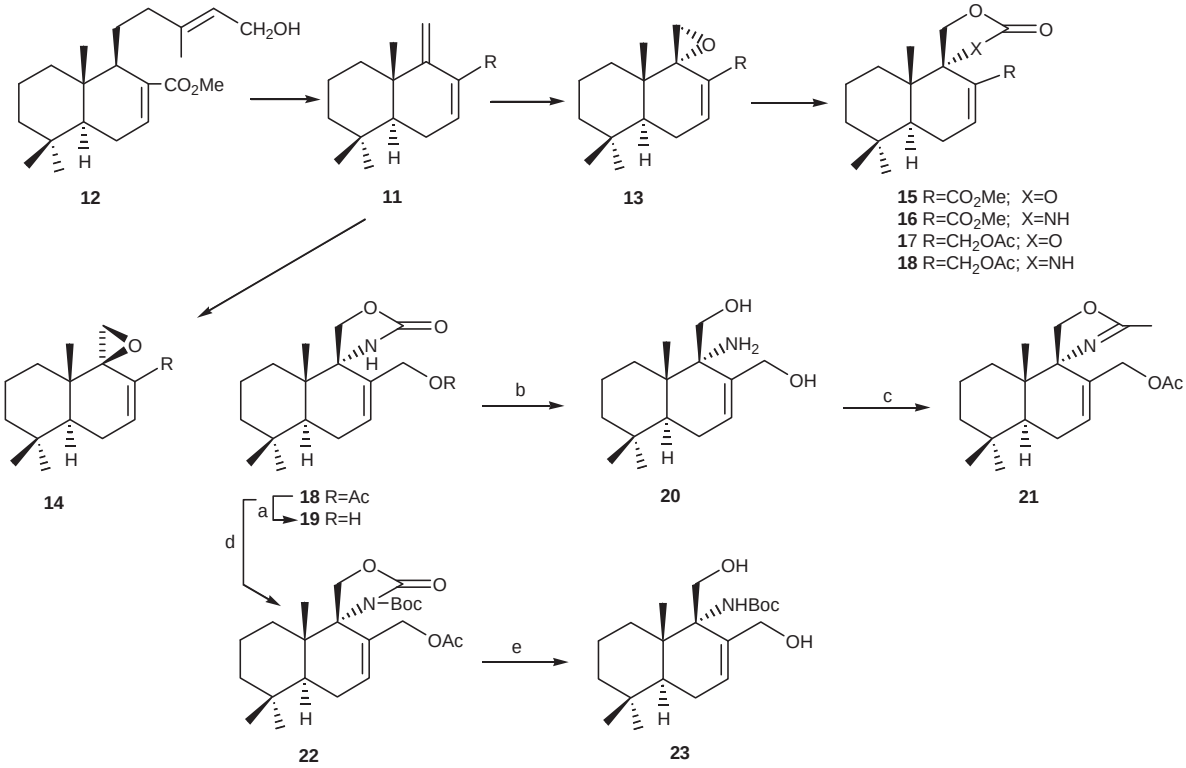

Reagents: a) aqueous 2N NaOH/1,4-dioxane 1/1, 96%; b) saturated KOH in H_2O, 1,2-etanediol, 70°C, 90%; c) Ac_2O, Py, 84%; d) $(Boc)_2O$, Et_3N, DMAP, THF, 73%; e) DIBAL-H, CH_2Cl_2, -78°C, 73%.

Scheme 2

New synthetic strategies to prepare natural drimanes from (-)-sclareol (24) have been reported by Barrero and co-workers [12]. Thus the preparation of natural 9,11-drimen-8α-ol (25) through the nitrogen-containing compounds is described. Synthesis of compound (25) started with the homodrimanic acid (26), in turn obtained from sclareol (24) in 75% overall yield by a two-step sequence [13]. The Curtius rearrangement of the acyl azide derived from (26) represented the key-step in the discussed synthesis. Treatment of (26) with diphenylphosphorylazide (DPPA) in the presence of triethylamine with subsequent reflux in benzene gave the isocyanate (27) [14]. All attempts to transform the latter into the corresponding amine were unsuccessful: hydrolysis of the isocyanate afforded only a very stable cyclic carbamate. Therefore the way was chosen to reduce compound (27) till the formamide (28) that was next treated with potassium hydroxide in methanol to afford the hydroxyacetamide (29) or the aminoalcohol (30), respectively, depending upon the reaction temperature. Then, the transformation of amine (30) into (25) was approached. First of all, diazotization of the amine group was attempted. The main observations were that the amine (30) remained unaltered when it was treated at 0 ºC with sodium nitrite and hydrochloric acid, while at room temperature its decomposition occurred. Hofmann elimination turned out to be also unsuccessful. Treatment of alcohol (30) with potassium *tert*-butoxide in dimethylsulfoxide after exhaustive methylation afforded the methoxyamine (31). In this way the hydroxyl group of compound (28) was protected by treating it with ethyl vinyl ether to give (32). Saponification of the latter

consistently afforded the amine (33), which underwent elimination after exhaustive methylation on treatment under basic conditions yielding (34). The removal of protection subsequently gave (25) (Scheme 3).

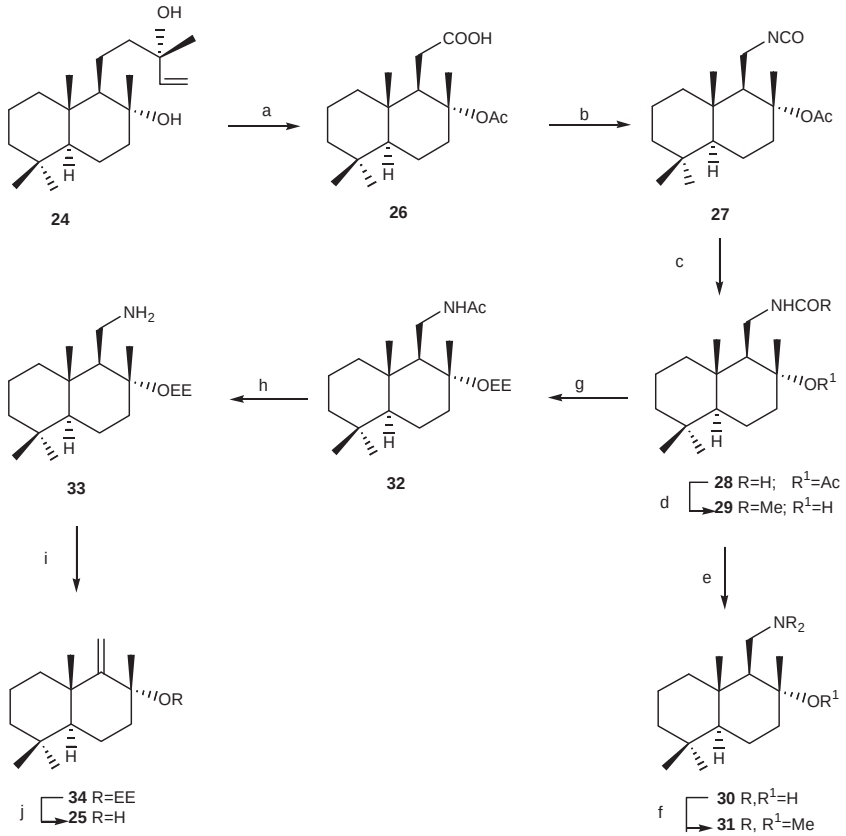

Reagents: a) 1. OsO_4, $NaIO_4$, t-BuOH, 45ºC, 6h.; 2. Jones' oxidation, acetone, 0ºC, 45 min (75% overall yield); b) 1. DPPA (1.1 eq), Et_3N (1.1 eq), Dioxan, 0ºC, 1.5 h; 2. Benzene, reflux; c) $NaBH_4$ (3 eq), EtOH, 0ºC, 30 min. (80%); d) KOH, MeOH, rt, 6 h (96%); e) KOH, MeOH, reflux, 12 h (95%); f) 1. Excess MeI, t-BuOMe; 2. t-BuOK (1.4 eq), DMSO (80%); g) ethyl vinyl ether (8 eq), CSA (0.5 eq), CH_2Cl_2, rt, 25 h (75%); h) KOH, MeOH, reflux, 2 h (91%); i)1. excess MeI, t-BuOMe; 2. t-BuOK (2.7 eq), DMSO (85%); j) AcOH, MeOH, rt, 2 h (95%).

Scheme 3

Many drimane sesquiterpenoids, including their prototype drimenol (35), exibit various biological activities.

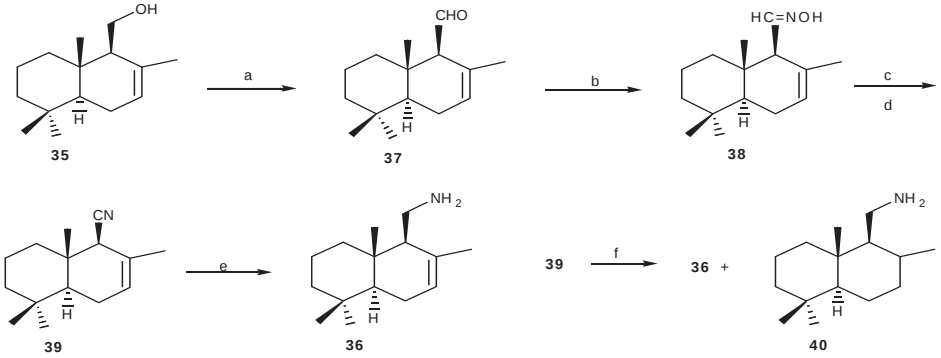

Reagents: a) P_2O_5, DMSO, 20ºC, 95%; b) $NH_2OH{\cdot}HCl$; EtOH, Py, 95%; c) Ac_2O, Py, 64%; d) p-TsCl, Py, 90%; e) $LiAlH_4$, $AlCl_3$, Et_2O, 50%; f) $NaBH_4$, $CoCl_2{\cdot}H_2O$, MeOH, 20ºC, 91%.

Scheme 4

Therefore, it seemed interesting to synthesize the amino- analog of drimenol in order to study its biological properties. We accomplished the synthesis of 11-aminodrim-7-ene (36) from drimenol (35) in four steps [15] (Scheme 4). Drimenol (35) was oxidized into drimenal (37) in 95% yield *via* phosphoric anhydride activated dimethylsulfoxide,

as previously reported [16]. Drimenal oxime (38) was obtained on interaction of drimenal (37) with hydroxylamine hydrochloride in the ethanol-pyridine mixture of solvents. According to TLC, the reaction product consisted of a mixture of *Z*- and *E*-isomers. The oxime of 14,15-bisnorlabd-8-(17)-en-13-one (7) was used as reference to show that the less polar isomer had the *E*-configuration [3]. Since the *E*-configuration of (7) is energetically more favourable, the predominant isomer in the mixture should most probably be the *E*-isomer. In the drimenal oxime (38) obtained by us the above-mentioned less polar isomer predominated. Its content in the mixture after recrystallization from hexane was 80%, the ratio of *Z*- and *E*-isomers being approximately 1:4. Next we investigated the production of drimenylamine (36) *via* the reduction of drimenal oxime (38) by various methods [17-20]. Compound (36) could not be synthesized in satisfactory yield by the reduction of drimenal oxime (38), that is why we decided to convert (38) into the corresponding nitrile (39) and then reduce it to the amine (36). Several methods have been employed by us in order to synthesize (39) [21-27]. As a result, we found as acceptable methods for synthesizing (39) the reactions of (38) with *p*-TsCl or Ac_2O in pyridine. The target- product, 11-aminodrim-7-ene (36), was obtained in 50% yield by refluxing the hydroxylamine (38) with $LiAlH_4$ in Et_2O in the presence of anhydrous $AlCl_3$ [28].

The reduction of nitrile (39) by $NaBH_4$, $CoCl_2 \cdot 6H_2O$ in CH_3OH produced compounds (36) and 7,8-dihydro-11-aminodrimane (40), as a mixture of water-soluble hydrochlorides. The ^1H NMR-spectrum of the mixture indicated on a 2:1 ratio of the hydrochlorides of (36) and (40). The pure compound (36) and its mixture with (40), synthesized by us, are of interest as potentially endowed with biological activity.

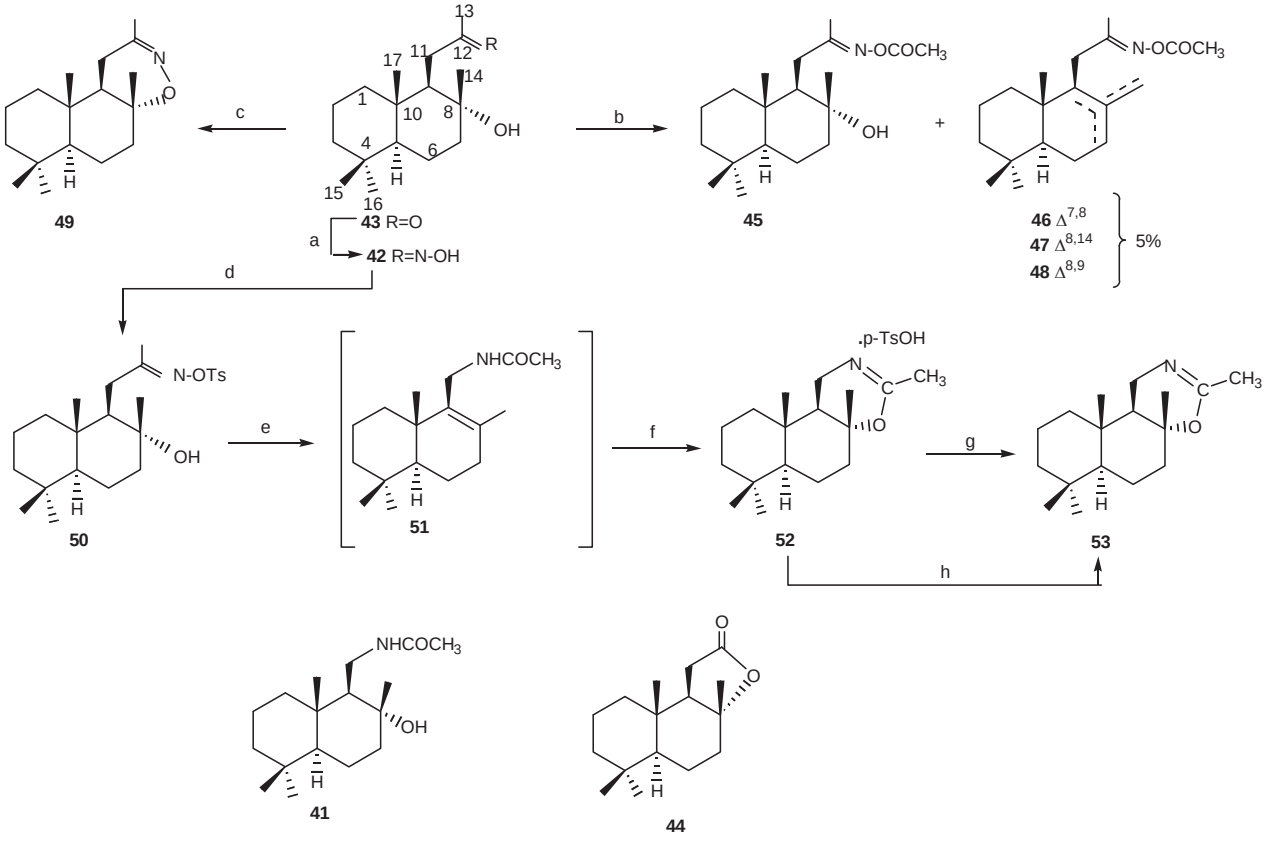

Reagents: a) $NH_2OH \cdot HCl$, EtOH, Py; b) Ac_2O/Py, 105-110°C; c) 86% H_3PO_4, 60-70°C, 82%; d) p-TsCl, Py, 90%; e) CH_3CN, Δ; f) p-TsON, 95%; g) 10% KOH, MeOH, 95%; h) Al_2O_3, 58%.

Scheme 5

The synthesis of amide (41) *via* Beckmann rearrangement of oxime (42) of 11-dihomodriman-8α-ol-12-one (43) was the main our goal we pursued [29]. Hydroxyketone (43) is readily available, being obtained from norambreinolide (44) by the method described by us [30]. Oxime (42) was prepared from compound (43) by its reaction with $NH_2OH \cdot HCl$ in an ethanol-pyridine mixture of solvents. Compound (42) represented a mixture of *Z*- and *E*-isomers, according to its TLC data and ^1H, ^{13}C, and ^{15}N NMR spectra. In virtue of easy conversion of *Z*- into the *E*-isomer as a result of the fact that the latter is energetically more favorable [3], we used (42) for the reactions as a mixture of its *Z*- and *E*-isomers. It was found that on interaction of the oxime (42) with acetic anhydride în pyridine the oxime acetate (45) along with a small amount of the mixture of isomeric dehydrated oxime acetates (46)-(48) were formed. On heating of the solution of the oxime (42) in 86% H_3PO_4 the elimination of water occurred giving 1,2-oxazine (49). Oxime (42) interacts with *p*-tosyl chloride in pyridine affording the oxime tosylate (50). The latter rearranges under reflux in acetonitrile, according to the

Beckmann transpozition, with the elimination of the water and *p*-toluene sulfonic acid, giving the unsaturated amide (51). The reaction of compound (51) with p-TsOH leads to the corresponding salt of cyclic 1,3-oxazine (52) formation, which upon treatment with a metanolic solution of potassium hydroxide furnished compound (53).

The new nitrogen containing drimanic compounds, the 1,2,6-oxazine and N-pyroline oxide derivatives were obtained [31], which are of interest as compounds potentially endowed with interesting biological properties. 11-dihomodriman-8α-ol-12-one (43) was prepared according to the reported protocol [30] and subjected to the dehydration in the presence of the „Amberlist-15" ionite. As result ketone (54) was obtained, which was transformed into oxime (55) by interaction with NH_2OH▪HCl.

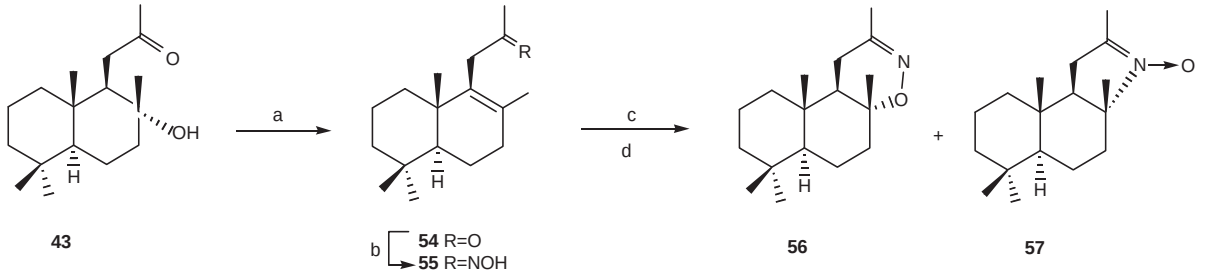

Reagents: a) Amberlist-15, CH_2Cl_2, 20°C, 20 h, 70%; b) NH_2OH·HCl, EtOH, Py, 98%; c) H_3PO_4, (64:65)=36%:56%; CF_3CO_2H, (64:65)=30%:48%.

Scheme 6

By heating at 70-80°C a solution of the oxime (55) in 86% H_3PO_4, the intramolecular cyclization occurred, giving the mixture of (1S,2S,4aS,8aS)-2,5,5,8a-tetrametildecahidro-1H-nafto[1,2][5,6]-3-metil-4,5-dihidro-[1,2,6]-oxazine (56) and (1S,2S,4aS,8aS)-2,5,5,8a-tetrametildecahidro-1H-nafto[1,2-d]-2-metilpirolin-N-oxide (57). The same outcome was reached by heating the oxime (55) in CF_3CO_2H.

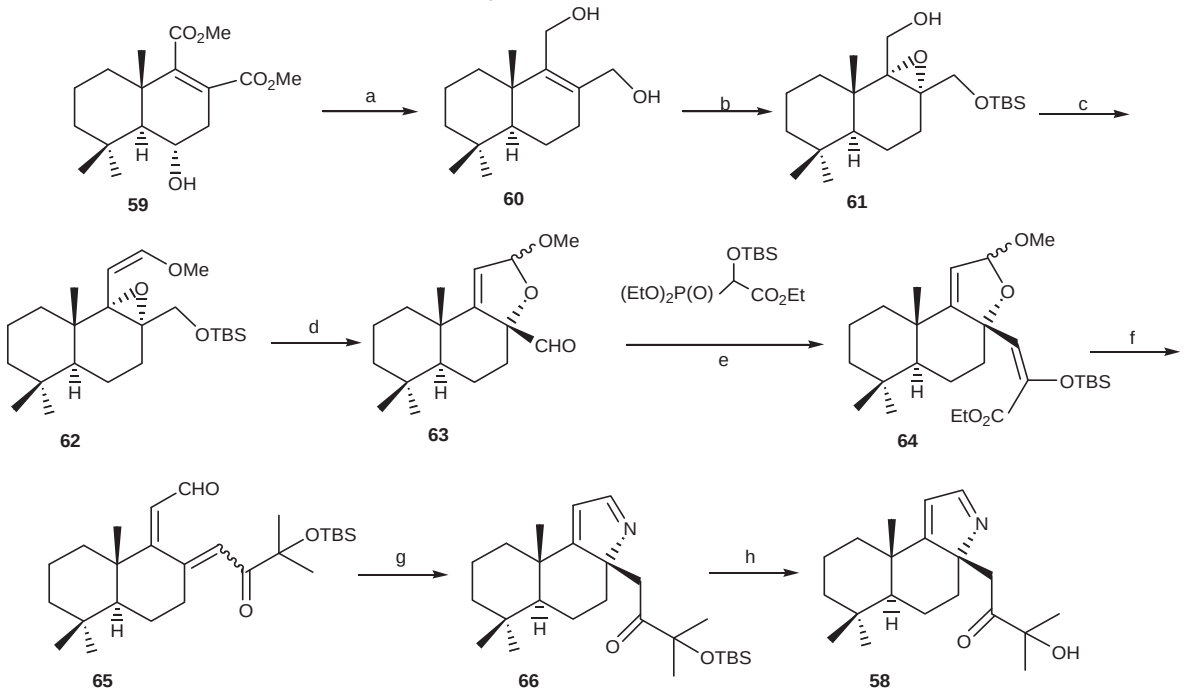

Reagents: a) 1. CTDI, CH_2Cl_2, reflux, 21 h, (94%), 2. n-Bu_3SnH, AIBN, toluene 80°C, 15 min (quant), 3. DIBAL, THF, 0°C, 15 min (98%); b) 1. TBSCl, imidazole, DMF, 0°C to rt, 15 min (97%), 2. MCPBA, CH_2Cl_2, 0°C, 24 h, (α : 62%, β : 30%); c) 1. TPAP, NMO, CH_2Cl_2, rt, 3,5 h, 2. $Ph_3P^+CH_2OMeCl^-$, n-BuLi THF, 0°C, 10 min (60% in two steps); d) 1. TBAF, THF, 0°C to rt, 3 h (86%), 2. Dess-Martin periodinan CH_2Cl_2, rt, 4 h; e) n-BuLi, THF, 0°C to rt, 1 h (48% in two steps α:β=4:1); f) MeLi, THF, 0°C, 10 min (72%, E:Z=4:1); g) NH_3, cat. AcOH, t-BuOH, rt, overnight [65% from (E), 60% from (Z)]; h) TBAF, THF, rt, 1,5 h, (89%).

Scheme 7

A total synthesis of (±) chamobtusin A (58) has been accomplished [32] on the basis of presumed biosynthetic pathway, involving first the imine formation of keto-aldehyde followed then by intramolecular aza-Michael addition. The known alcohol (59) has been selected as a suitable starting material. Its hydroxyl group was converted into thiocarbamate which was then deoxygenated *via* the treatment with *n*-Bu_3SnH and AIBN, and the resulting diester was reduced with DIBAL to give diol (60) in high yield. The less hindered primary alcohol of (60) was selectively protected as the *tert*-butyldimethylsilyl ether. *m*-CPBA oxidation of the double bond gave a mixture of α- and β-epoxides in a ratio of 2:1, and the major R-epoxide (61) was used in the next reaction. After tetra-*n*- propylammonium perruthenate (TPAP) oxidation of the primary hydroxy group of (61), Wittig reaction of the resulting aldehyde under the conditions depicted in scheme 7 afforded enol ether (62) with the only *Z-isomer* of the double bond. The *tert*-butyldimethylsilyl–protection of compound (62) was removed with tetrabutylammonium fluoride (TBAF), and the liberated primary alcohol was oxidized with Dess-Martin periodinane to give the cyclic product (63). Horner-Wadsworth-Emmons reaction of compound (63) with phosphonate gave compound (64) as a mixture of α- and β- isomers in a 4:1 ratio. It was possible to directly convert it into the cyclization precursor (64) by treatment with methyl lithium. Subsequent ring-opening of methyl acetal gave the desired keto-aldehyde (65) as a *E*/*Z* mixture (cca 4:1 ratio) in 72% yield. As expected, the imine formation and subsequent intramolecular aza-Michael addition smoothly proceeded with both geometrical isomers of (66) by treatment with ammonia in the presence of catalytic amounts of acetic acid to afford compound (66) as a single diastereomer in 65% and 60% yield, correspondingly, for *E*- and *Z*-isomer. Finally, the removal of the *tert*-butyldimethylsilyl group gave (±)-chamobtusin A (58). The overall yield of (58) starting from (59) constituted 5.3% in 13 steps.

3. Synthesis of nitrogen-containing compounds from lambertianic acid

During the last decades, the vast series of natural terpenoids has been intensely supplemented by metabolites of plant, microbial and animal origin, whose molecules include various structural fragments attached to the main terpene skeleton through covalent bonds. The unique structure of many so-called mixed metabolites and their important biological activities make them attractive targets of the total synthesis. On the other hand they can serve as plausible models for the design of molecules with useful properties. Among such metabolites, the nitrogen-containing and alkaloid-like compounds continuously attract the scientific interest.

The authors [33] describe a convenient approach to β-carboline diterpenoids as potential models of such metabolites, which is based on the Pictet- Spengler reaction.

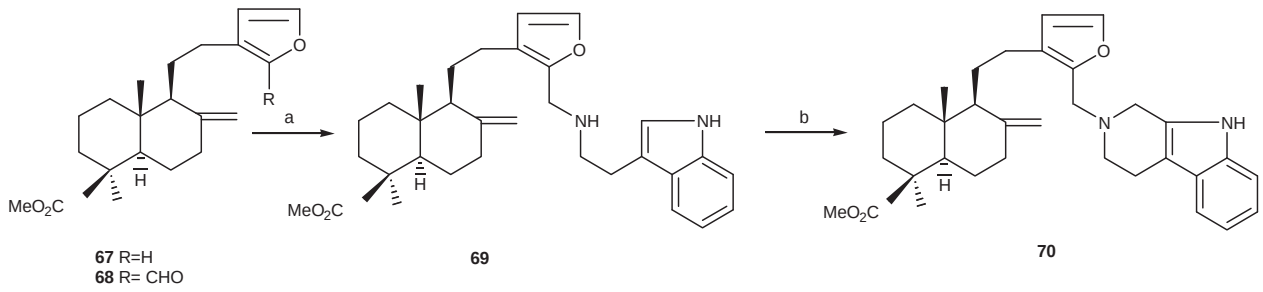

67 R=H
68 R= CHO

69

70

Reagents: a) 1) triptamine, 2) $NaBH_4$; b) CH_2O, TsOH.

Scheme 8

Reductive amination of methyl 16-formyllambertianate (67) or its aldehyde (68) with tryptamine, in the presence of sodium borohydride gives amine (69) in 87% yield. The Pictet-Spengler cyclization of the resulting diterpenoindole amine with formaldehyde furnishes methyl 16-(1,2,3,4-tetrahydro-β-carbolin-2-yl-methyl)lambertianate (70). The reaction of formyl-substituted methyl labdatrienoates and labdadienoates with 2-(3-indolyl)ethylamines provides a convenient approach to 1-diterpeno-β-carbolines.

The Diels-Alder reaction of lambertianic acid (71) with maleic anhydride occurred in a stereoselective fashion and yielded the diastereoisomeric (1*R*,2*S*,6*R*,7*R*)- and (1*S*,2*R*,6*S*,7*S*)-*exo*-adducts (72a) and (72b) [34]. The latter reacted with L-valinol in toluene in the presence of triethylamine to give the corresponding diterpenoid imides, 4-aza-9-oxabicyclo[2.2.1]dec-8-enes (73a) and (73b). The product was a mixture of two diastereoisomers whose ratio (according to the ^1H NMR data of the mixture) was the same as the (1*R*,2*S*,6*R*,7*R*)/(1*S*,2*R*,6*S*,7*S*) ratio in the initial adduct.

Reactions of lambertianic acid (71) with N-substituted maleinimides (74) in the presence of Lewis acids afforded diastereoisomeric adducts having both *exo*- and *endo*- configuration. With the aim of studying the effect of

the N-substituent in the dienophile on the reaction stereoselectivity and biological activity of new nitrogen containing heterocycles of the terpene series, apart from *N*-benzylmaleimide, on synthesized compounds (75-78) with various substituents on the nitrogen. Some transformations of the adducts were examined with a view to obtain cantharidin and dihydroisoindole analogs.

Diels-Alder reaction of lambertianic acid (71) with cyclic dienophiles provides a convenient route to terpenoid cantharidin analogs. The nature of the dienophile is determinant for the stereochemistry of the addition. The reaction of lambertianic acid (71) with maleic anhydride yields exclusively the corresponding *exo* adducts, whereas with N-substituted maleimides both *endo* and *exo* adducts are formed, whose ratio depends on the substituent on the nitrogen. In all the cases, diastereoisomeric pairs were obtained. The obtained products can serve as useful intermediates in the synthesis of diterpenoid analogs of the isoindole and benzophthalimide series.

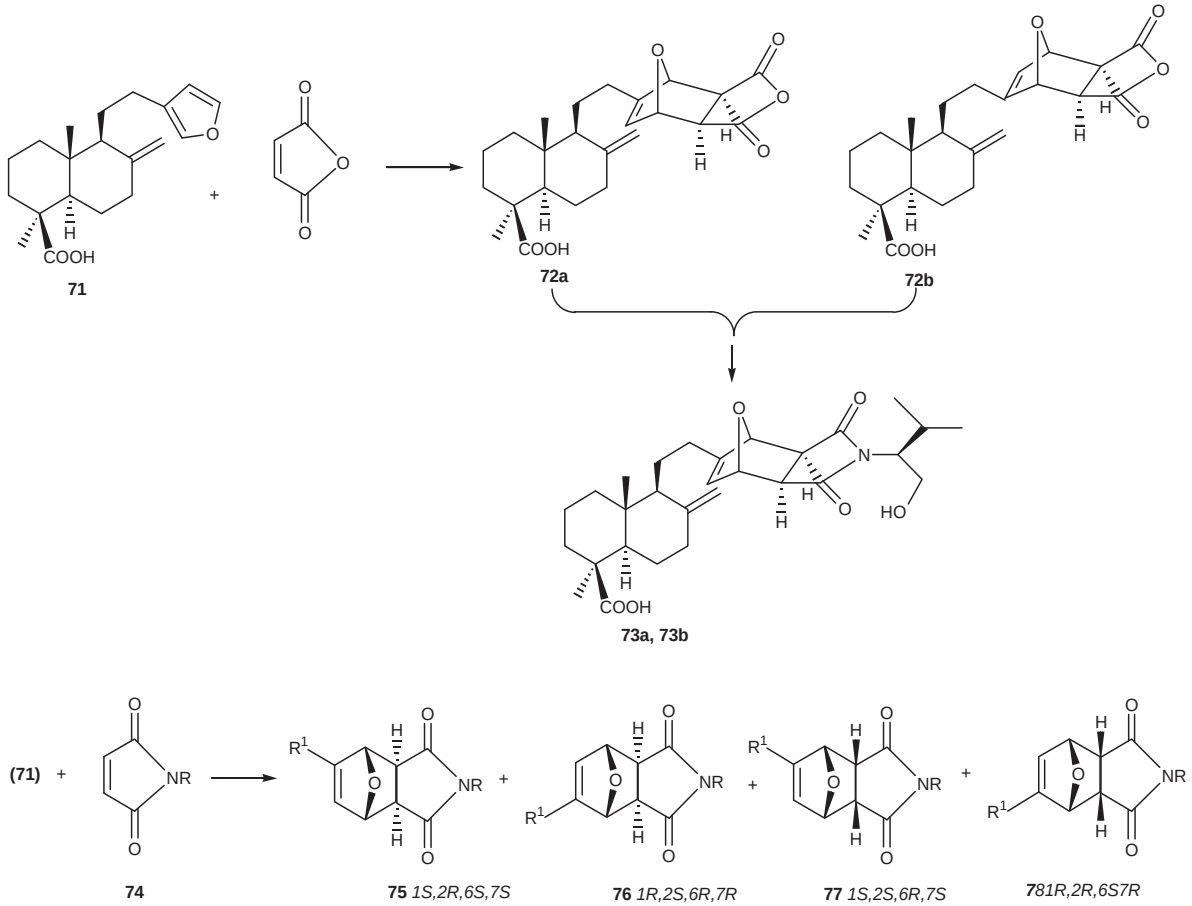

Scheme 9

Heterocyclic derivatives of lambertianic acid were synthesized [35] *via* the reductive amination of carbonyl compounds and subsequent Mannich intramolecular aminomethylation. Treatment of ketone (79) with methylamine-sodum borohydride afforded the mixture of 17-nor-8α-methylamino labdanoid (80) and secondary alcohol (81) in 52% and 33% yield, respectively (Scheme 10). Methylamino derivative (80) reacted with formaldehyde to give hexahydrofuroazocine (82). By the oxidation of 8,12-epoxy-17-hydroxy labdanoid (83) with pyridinium chlorochromate in methylene chloride on obtained the aldehyde (84) that after the reductive amination with methylamine-sodum borohydride gave the amine (85). As aforementioned for (80), the intramolecular aminomethylation of (85) by the action of formaldehyde smoothly led to formation of furoazonine (86). Under analogous conditions, the oxidation of 8-hydroxymethyl labdanoid (87) yielded a mixture of (8*R*)- and (8*S*)- aldehydes (88) at a ratio of 2:1. The subsequent reductive amination of (88) with tryptamine or phenylalanine methyl ester and sodium tetrahydridoborate resulted in the formation of the corresponding amines (89) and (90) as mixtures of stereoisomers. Furoazonine derivatives (91) and (92) have been obtained by cyclization in the presence of formaldehyde. Thus on proposed efficient methods for the synthesis of optically active heteropolycyclic compounds, namely furoazocine and furoazonine derivatives, via transformations of lambertianic acid methyl ester.

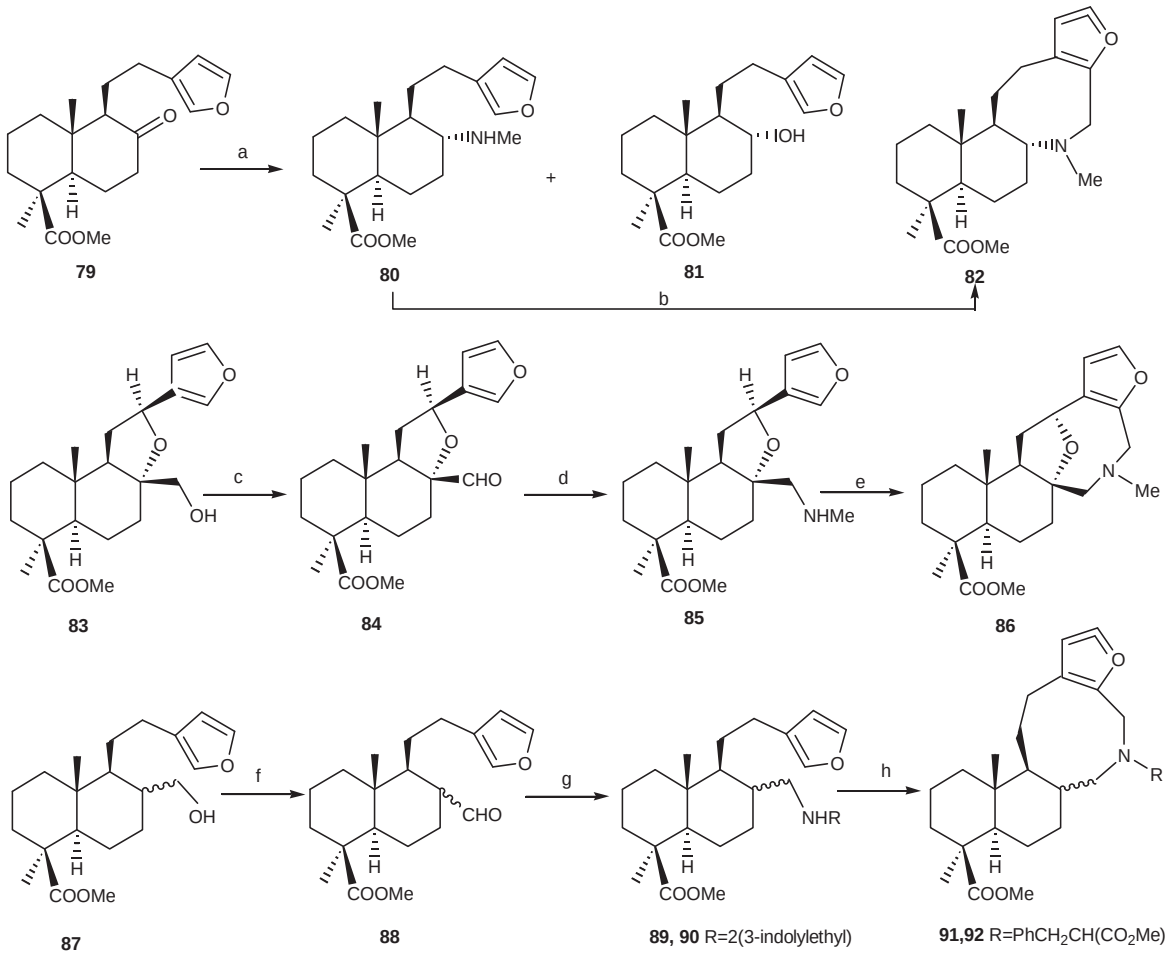

Reagents: a) $MeNH_2/NaBH_4$; b) CH_2O; c) PCC/CH_2Cl_2; d) $MeNH_2/NaBH_4$; e) CH_2O; f) PCC/CH_2Cl_2; g) $MeNH_2/NaBH_4$; h) CH_2O.

Scheme 10

Focusing on the preparation of the new diterpenoids of labdane series that contain a heterocyclic fragment of 10-oxa-3-azatricyclo[5.2.1.01,5]decene (93), the intramolecular [4+2]-cycloaddition reaction of quaternary ammonium salts obtained by quaternization with allyl, methallyl, or propargyl bromides of lambertian acid dialkylaminomethyl derivatives was investigated [36].

Kharitonov Yu.V. et al. [37] report on an interesting approach to the new heterocyclic derivatives of labdanoids that is based on the transformation of 15,16-epoxylabdadiene-15,16-dione (94). The starting compound for this synthesis is readily obtained by oxidative transformations of accessible methyl lambertianate (79).

The oxidation of furan labdanoid (79) with Jones' reagent gave rise to a mixture of the corresponding anhydride (94) and hydroxybutenolides (95) and (96) whose ratio depended on the reaction conditions. By reaction with secondary amines compound (94) gave new terpenyl-containing N-substituted maleimides (97) and (98) (Scheme 11). It is well-known that the reaction of maleic anhydride and its substituted analogs with hydrazines represents an efficient procedure for the preparation of pyridazinediones. The reaction of anhydride (94) with hydrazine hydrate occurred in acetic acid at room temperature and afforded a mixture of 3,6-dioxo-1,2,3,6-tetrahydropyridazine (99) and (N-amino) maleimid (100) (in 47 and 15% yield). The reaction of anhydride (94) with phenylhydrazine required more stringent condition, since 3-hydroxy-l-phenyl-(2H)-pyridazin-6-one (101) and (N-amino)maleimide (102) could be obtained under boiling the reagent mixture in acetic acid in 22 and 38% yield, respectively. Thus diterpenoids of new structural type, labdanopyridazinediones, were prepared for the first time.

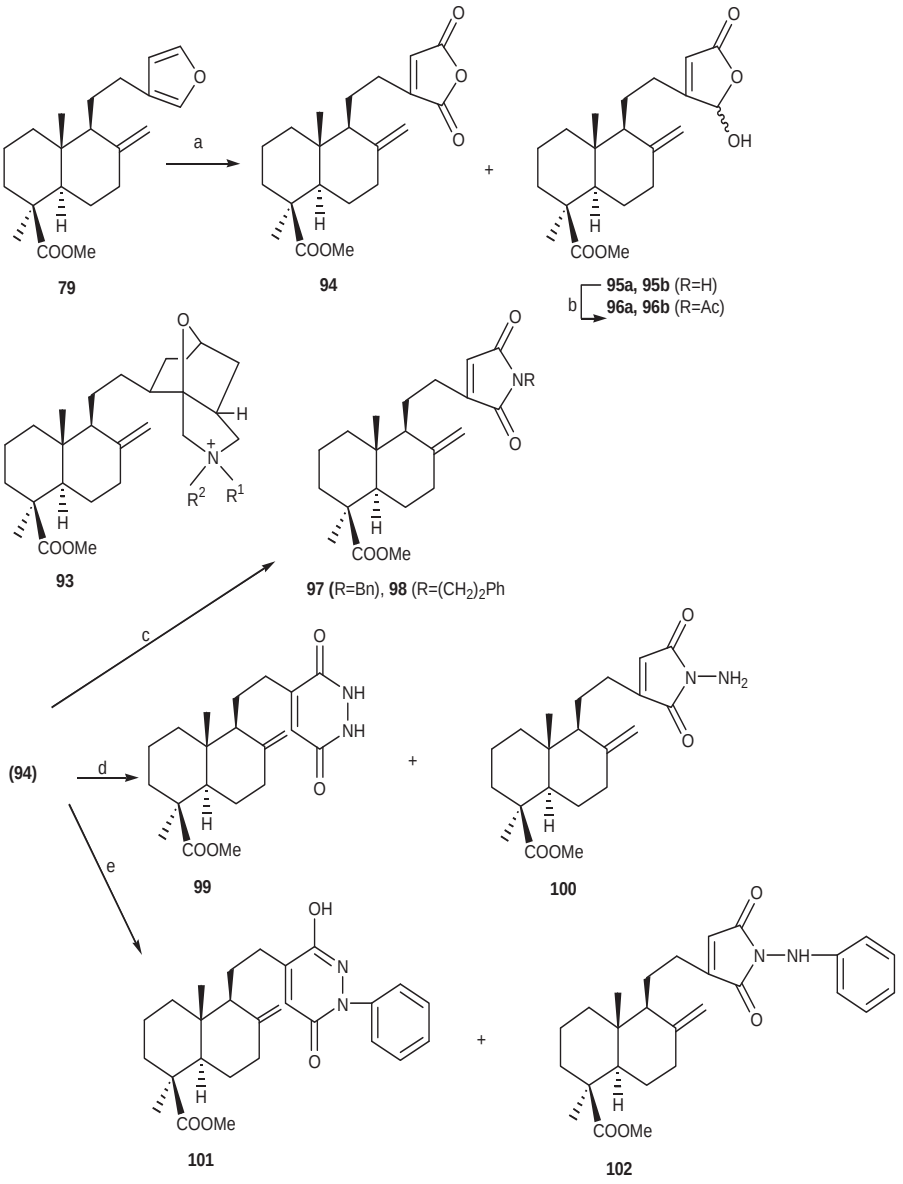

Reagents: a) CrO_3-H_2SO_4; b) Ac_2O-Py; c) RNH_2; d) NH_2NH_2, AcOH, 20°C; e) NH_2NHPh, AcOH, 100°C.

Scheme 11

The goal of the work described by Kharitonov Yu.V. et al. [38] was to synthesize diterpenoid azlactone from 16-formyllambertianic acid methyl ester (103) and study its reactions with nucleophiles. They found that aldehyde (103) reacts with hippuric acid (104) under standard conditions to give labdanoid oxazol-5(4*H*)-one (105) in 44% yield (conversion 56%) (Scheme 12). Azlactone (105) smoothly reacted with primary amines [such as aniline, benzylamines, and phenylethyl (propyl)amines] and 7-aminoheptanoic acid on heating in benzene to give 59–91% conversion into *N*-(1-carbamoylvinyl) benzamides (106)–(115)**.** The lowest yield was observed in the reaction with 3,5,6-trimethoxybenzylamine, while the extension of the alkyl chain between the benzene ring and amino group was noted to increase the product yield. For the interaction of compound (105) with secondary amines (piperidine and *N*-methylphenylmethanamine) the prolonged heating was required and the corresponding terpenoid *N*-(carbamoylvinyl) benzamides (113) and (114) were isolated in 73–80% yield. Treatment of compound (105) with L-proline *tert*-butyl ester smoothly afforded 83% of the pyrrolidine-containing labdanoid (115). Azlactone (105) readily reacted with α-amino acid (leucine and isoleucine) esters, furnishing in 62–78% yield the terpenoid *N*-(2-benzoylaminoacryloyl) amino acid esters (116) and (117). Terpenoid oxazol-5(4*H*)-one (105) undergoes hydrolysis on treatment with a solution of hydrogen chloride in diethyl ether or with 10% alcoholic alkali, the obtained product being identified as individual α-acylamino acid (118) with *Z*- configuration of the double bond.

Thus, the condensation of 16-formyllambertianic acid methyl ester with hippuric acid was investigated that gave the corresponding 4,5-dihydrooxazol-5-one derivatives. Their subsequent transformations open exciting synthetic routes to new nitrogen-containing derivatives of the labdane series.

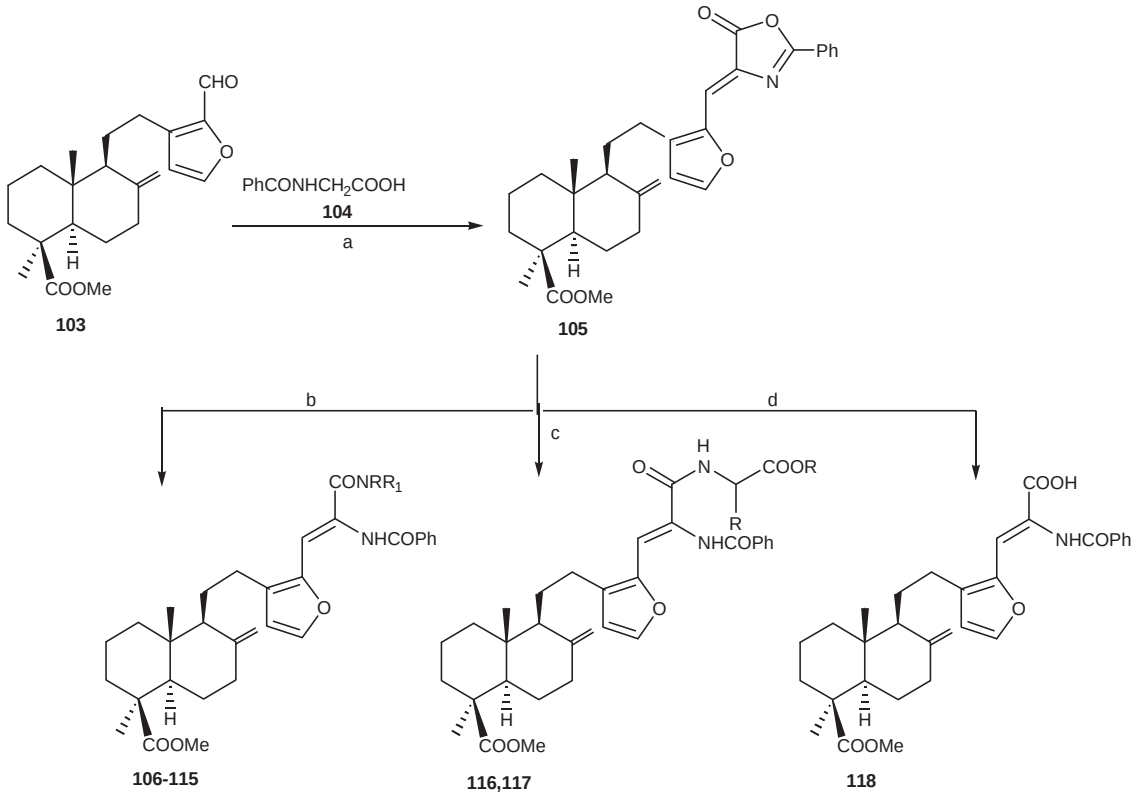

106– 112, R′ = H; 106, R = Ph; 107, R = $PhCH_2$; 108, R = 4-$HOC_6H_4(CH_2)_2$; 109, R = 3,4,5-$(MeO)_3C_6H_2CH_2$; 110, R = 3,5-(*t*-Bu)2-4-$HOC_6H_2(CH_2)_2$; 111, R = 3,5-(*t*-Bu)2-4-$HOC_6H_2(CH_2)_3$; 112, R = $HOCO(CH_2)_6$; 113, R = $PhCH_2$, R′ = Me; 114, RR′ = $(CH_2)_5$; 115, RR′N = 2-(*tert*-butoxycarbonyl)pyrrolidin-1-yl; 116, R = $MeCH_2CH(Me)$, R′ = Me; 117, R = Me_2CHCH_2, R′ = *t*-Bu.

Reagents: a) Ac_2O, K_2CO_3; b) $NHRR^1$, PhH, 75°C; c)$H_2NCHRCOOR^1$, PhH, 75°C; d) H^+.

Scheme 12

Oxidative methoxylation of 8,17-isopropylidenedioxy derivative of lambertianic acid methyl ester (119) with *N*-chlorobenzenesulfonamide in methanol [39] produced almost quantitatively a mixture of stereomeric 2,5-dimethoxydihydrofuran derivatives (120a)–(120d) (Scheme 13). The two *cis* and two *trans* stereoisomers were formed in equal amounts, as concluded from the intensities of signals for methoxy protons and 14-H, 15-H, and 16-H in the ^1H NMR spectra. Hydrogenation of compounds (120a)–(120d) over Raney nickel respectively afforded the 2,5-dimethoxytetrahydrofuran derivatives (121a)–(121d), which were in turn subjected to the reaction with methyl- or ethylamine in acetic acid to give of the corresponding *N*-alkylpyrroles (122) and (123) in 75-84% yield. As it was noted, the extension of the reaction times result in the formation of diols (124) and (125). The glicols (126)-(128) were synthesized in 51–75% yield when the 2,5-dimethoxytetrahydrofurans (121a)–(121d) interacted with allylamine, benzylamine and aniline, respectively, on prolonged heating in acetic acid. By periodate oxidation of diols (124) and (125) that was performed in the presence of acetic acid in methanol, we obtained the decahydronaphtho[1,2-*g*]indoles (129) and (130) in moderate yields (46–51%) as a result of the cyclization of intermediate 8-oxo-17-norlabdanoids. It should be mentioned that the oxidation of compounds (126)–(128) with sodium periodate under neutral conditions gave the 8-oxo-17-nor derivatives (131)–(133) in good yields (76–83%). Ketones (131)–(133) were subjected to the intramolecular ring closure furnishing the N-substituted decahydronaphtho[1,2-*g*]-indoles (134)–(136) in acceptable yields (71–77%).

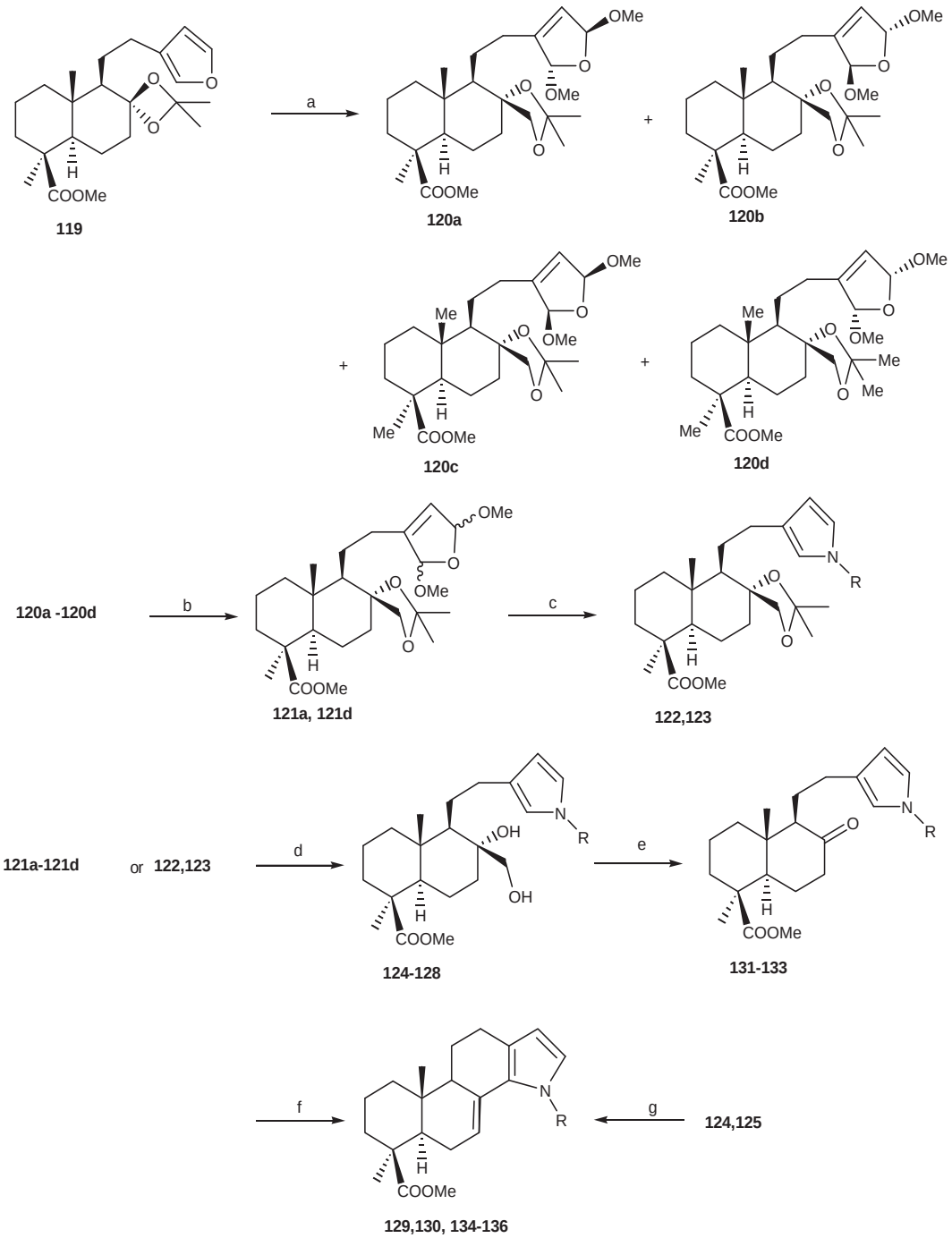

122, 124, 129, R = Me; 123, 125, 130, R = Et; 126, 131, 134, R = $PhCH_2$; 127, 132, 135, R = CH_2=$CHCH_2$; 128, 133, 136, R = Ph.

Reagents: a) $PhSO_2NHCl$, MeOH; b) H_2/Raney Ni, MeOH; c) RNH_2, H_2O, AcOH; d) RNH_2, H_2O, AcOH; e) NaIO4, MeOH; f) MeOH, AcOH; g) $NaIO_4$, H_2O, MeOH, AcOH.

Scheme 13

The work described by Kharitonov Yu.V. et al. [40] was intended to the development of procedures for the synthesis of oxatricyclic γ-lactams with a terpenoid fragment *via* intramolecular [4 + 2]-cycloaddition of *N*-furfuryl amides of accessible labdane diterpenoids. Acylation of methyl 16-(benzylaminomethyl)lambertianic acid methyl ester (137) with 2-methylprop-2-enoyl chloride in chloroform in the presence of triethylamine (1.5 eq.) gave the corresponding methacrylic acid amide (138) in 64% yield. The latter underwent intramolecular cyclization on heating

in boiling benzene (8 h). The only *exo* adducts could be found in the reaction product, as established by analysis of the reaction mixture. The diastereoisomeric methyl (1*R*,5*S*,7*R*)- and (1*S*,5*R*,7*S*)-5-{2-(3-benzyl-5-methyl-4-oxo-10-oxa-3-azatricyclo[5.2.1.01,5]dec-8-en-9-yl)ethyl}-1,4a dimethyl-6-methylidenedecahydronaphthalene-1-carboxylates (139a) and (139b) were obtained in a 1:1 ratio (75% overall yield) (Scheme 14).

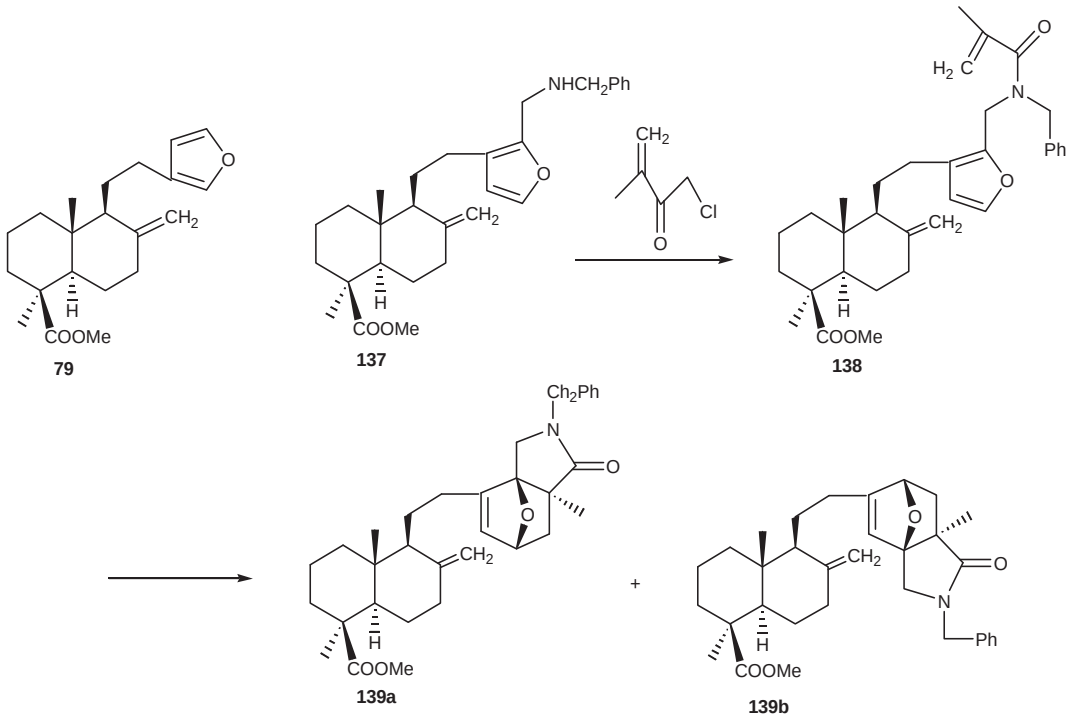

Scheme 14

The smooth isomerisation of lambertianic acid methyl ester (79) into labda-8(9),13(16),14-triene derivative (140) has been achieved by using *p*-toluenesulfonic acid in benzene (89% yield). The magnesium perchlorate assisted acetylation of diterpenoid (140) with acetic anhydride gave a mixture of 16- and 15-acetyl-substituted furanolabdanoids (141) and (142) at a ratio of 1.6:1 in an overall yield of 68%. Acetylfuran (141) easily reacted with benzylamine in the presence of sodium borohydride and titanium isopropoxide to produce 16-[1-(benzylamino)ethyl]-substituted furanolabdanoid (143) in 81% yield as a mixture of (16a*R*)- and (16a*S*)-diastereoisomers. The interaction of furfurylamine (143) with 2-methylprop-2-enoyl chloride in chloroform in the presence of triethylamine at 0–20°C gave the 86% conversion of diastereoisomeric (1*R*,2*S*,5*S*,7*R*)- and (1*R*,2*R*,5*S*,7*R*)-2-methyl-10-oxa-3-azatricyclo-[5.2.1.01,5]decenones (144a) and (144b), differing by their configuration at the C-2 chiral center, at a ratio of 1:1. The intermediate methacrylamide (145) was not isolated, but its formation was detected by ^{1}H NMR spectroscopy after 2 h of mixing the reagents. It has been observed that in the intramolecular cycloaddition the α-methyl-substituted amide (141) is more reactive than its analog (138). Under the acylation of amine (143) with maleic anhydride the mixture of diastereoisomeric (1*R*,2*S*,5*R*,6*R*,7*R*)- and (1*R*,2*R*,5*R*,6*R*,7*R*)-adducts (144a) and (144b) has been obtained in equimolar amounts with an overall yield of 86%.

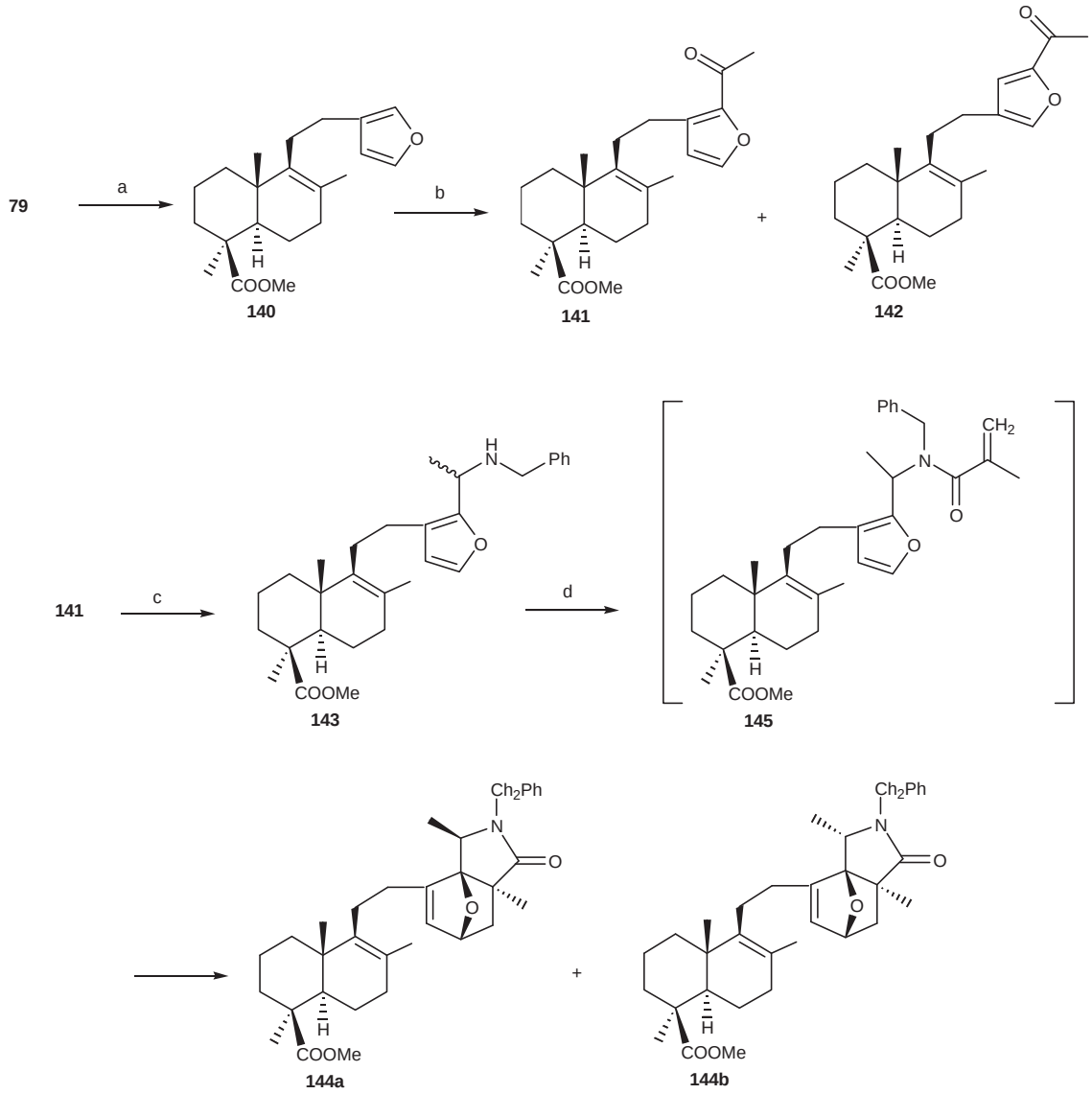

Reagents: a) TsOH, 88%; b) Ac_2O, $Mg(ClO_4)_2$; c) $PhCH_2VH_2$, $NaBH_4$, $(i\text{-}PrO)_4Ti$; d) CH_2=C(Me)COCl

Scheme 15

The aminomethylation of methyl 16-formyllambertianate (103) with L-methionine methyl ester or L-isoleucine *tert*-butyl ester provided the amino acid derivatives of the lambertianic acid (146) and (147) in 63 and 76% yield, respectively (Scheme 16) [41]. The corresponding *N*-furfurylamides (148)–(149) were obtained by the acylation of compounds (146) and (147) with methacryloyl or crotonyl chlorides in chloroform in the presence of triethylamine. Boiling of the amides (148)–(151**)** in benzene solution resulted in their intramolecular cyclization. The analysis of the reaction mixture showed that the reaction afforded exclusively the *exo*-adducts, terpenoid 5-methyl-10-oxa-3-azatricyclo[5.2.1.01,5]dec-8-en-4-ones as a mixture of (1*R*,5*S*,7*R*)- and (1*S*,5*R*,7*S*)-diastereomers (152a), (152b), (154a) and (154b) or 6-methyl-10-oxa-3-azatricyclo-[5.2.1.01,5]dec-8-en-4-ones as a mixture of (1*R*,5*S*,6*R*,7*R*)- and (1*S*,5*R*,6*S*,7*S*)-diastereomers (153a)**,** (153b), (155a) and (155b) (85–89% yields).

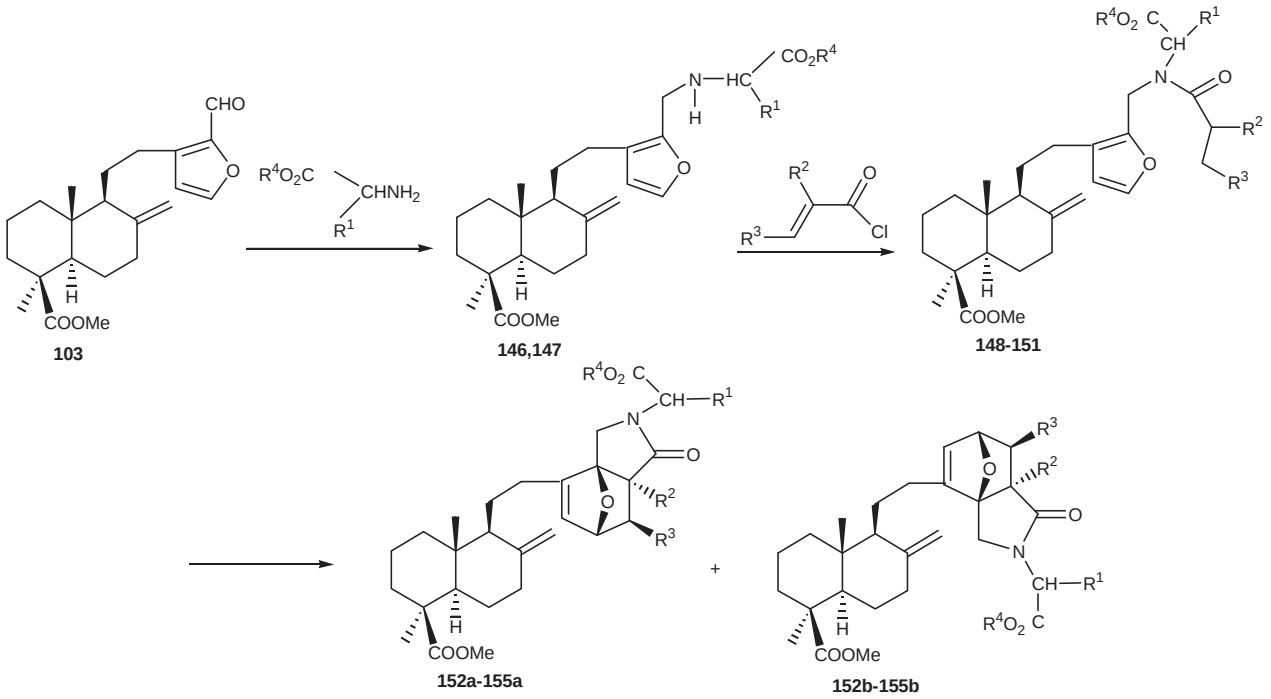

$R^1 = (CH_2)_2SCH_3$, $R^4 = CH_3$ (146); $R^1 = CH(CH_3)CH_2CH_3$, $R^4 = t$-Bu (147); $R^1 = (CH_2)_2SCH_3$, $R^2 = CH_3$, $R^3 = H$, $R^4 = CH_3$ ((148), (152a), (152b)); $R^1 = (CH_2)_2SCH_3$, $R^2 = H$, $R^3 = R^4 = CH_3$ ((149), (153a), (153b));
$R^1 = CH(CH_3)CH_2CH_3$, $R^2 = CH_3$, $R^3 = H$, $R^4 = C(CH_3)_3$ ((150), (154a), (154b)); $R^1 = CH(CH_3)CH_2CH_3$, $R^2 = H$, $R^3 = CH_3$, $R^4 = C(CH_3)_3$ ((151), (154a), (154b)).

Scheme 16

For further studies of the effect of substituents in the dienophilic fragment of terpenoid N-furfurylamides, the synthesis and properties of cyclic N-alkenyl derivatives of labdanoids have been considered. Consequently it was found that methyl 16-formyllambertianate (103) readily reacted with cystamine in benzene at reflux in the presence of triethylamine generating the methyl-16-(thiazolidin-2-yl)lambertianate (156) (Scheme 17).

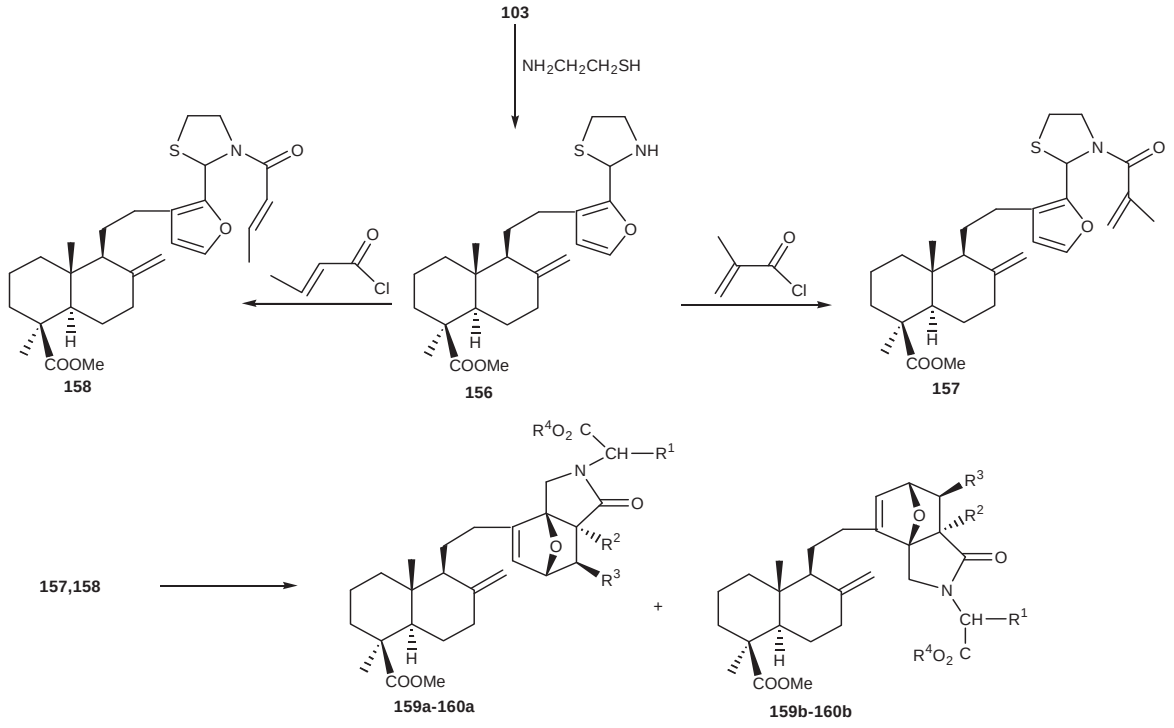

Scheme 17

The acylation of compound (156) with methacryloyl or crotonyl chlorides and assisted by triethylamine in chloroform led to the formation of N-methylacryloyl- (157) or N-crotonyl-2-furylthiazolidines (158) in good yields (75 and 82%, respectively). The intramolecular cyclization of compounds (157) and (158) was achieved by 10 h reflux in benzene and resulted in the corresponding terpenoid derivatives of hexahydrothiazolo[2,3-*a*]isoindolinone (159a)**,** (159b), (160a) and (160b) in 92–96% yields.

The heterocyclic system of dihydroisoindol-1-one constitutes a structural moiety of a number of polycyclic alkaloids, known for the variety of the exhibited biological activities. This motivated the ulterior diggings aimed to the synthesis of functionalized dihydroisoindolones that contain a labdanoid fragment [42]. As starting compound for the synthesis of terpenoid dihydroisoindol-1-ones the accessible furan diterpenoid, phlomisoic acid methyl ester (161) has been selected. Vilsmeier–Haak formylation of phlomisoic acid methyl ester (161) provided a mixture of three compounds, 16-formyllabdatrienoate (162), 15-formyllabdatrienoate (163) and 2-formylmarginatafuran (164) in 79, 8 and 2% yield, respectively (Scheme 18).

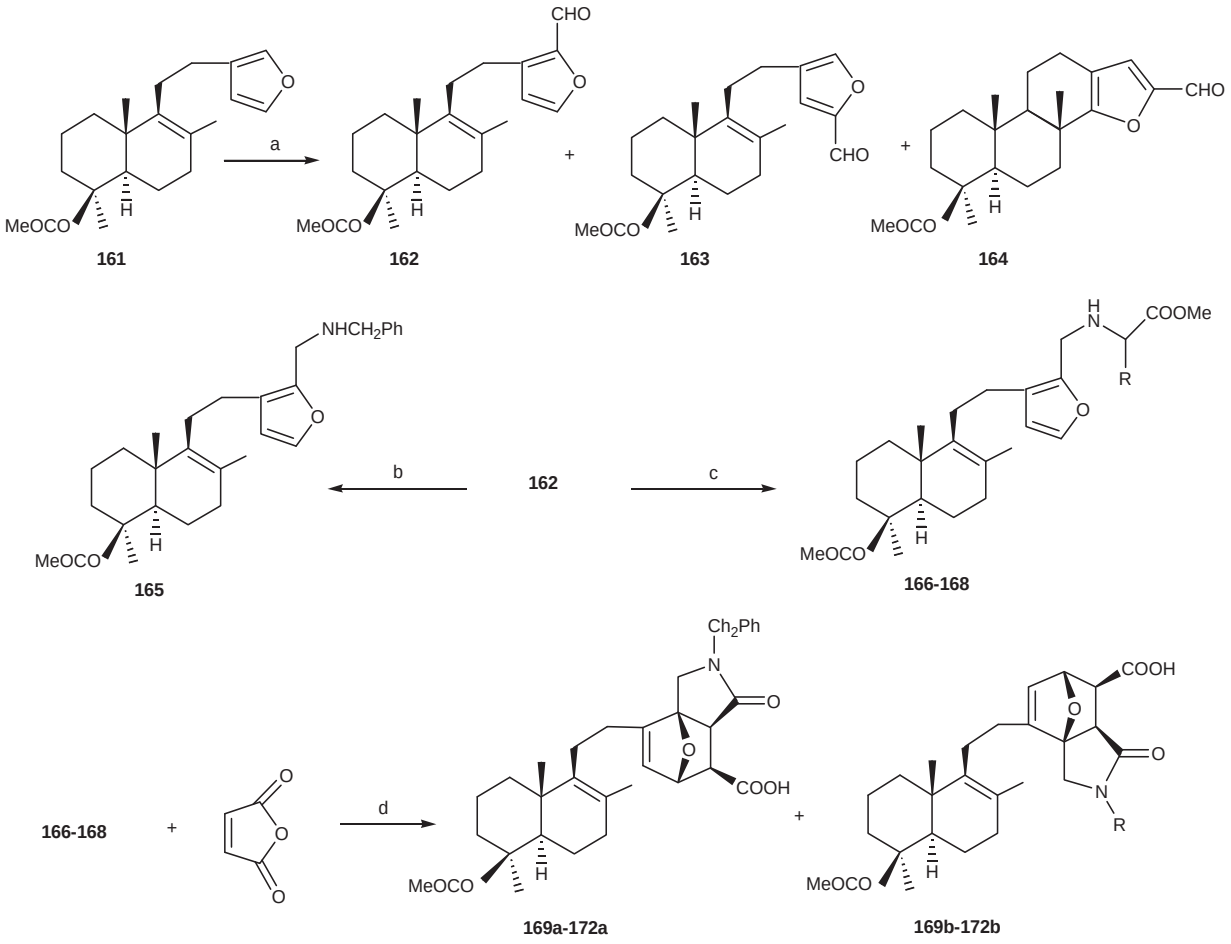

166 R=Me, 167 R=Me_2CH, 168 R=$MeS(CH_2)_2$;169 R=$PhCH_2$; 170 R=$MeCH(CO_2Me)$; 171 R=$Me_2CHCH(CO_2Me)$; 171 R=$MeS(CH_2)_2CH(CO_2Me)$.

Reagents: a) $POCl_3$-DMF, AcONa, H_2O; b) $PhCH_2NH_2$, $NaBH_4$, MeOH; $H_2NCHRCOOMe$, $NaBH_4$, MeOH, c) $H_2NCHRCOOMe$, $NaBH_4$, MeOH; d) PhH, 20°C.

Scheme 18

Reductive amination of methyl 16-formyllabda-8(9),13(16),14-trienoate (162) with benzylamine, or with D,L-α-amino acid methyl esters, in the presence of sodium tetrahydridoborate gave the corresponding labdanoid furfurylamines (165) or furfurylamino acids (164)–(168) in 76–90% yield (Scheme18). In order to obtain the furfurylacrylamides the acylation of compounds (165)–(168) with maleic anhydride and crotonoyl chloride has been examined. The reaction of 16-aminomethyl labdanoids (165)–(168) with maleic anhydride occurred under mild conditions in benzene, at 20°C and

involved the intermediate formation of *N*-furfurylmaleamic acids that were converted into the *N*-substituted 4-oxo-1,7-epoxyhexahydroisoindole-6-carboxylic acids (169)-(172) in 72–96% yield *via* the *exo*-transition state.

4. Synthesis of nitrogen-containing compounds of the enantiomeric series from andrographolide and some of its rearranged derivatives

Andrographolide (173) - the major constituent of the Indian medicinal plant *Andrographis paniculata,* has been lately reported to be conveniently involved in the development of an efficient semi-synthetic procedure for the preparation of structurally diverse labdanes [43]. The proposed method started with the selective oxidative degradation of the C-12(13) olefin bond of the discussed compound (173) into the key-intermediate (174), which served as a precious chiral intermediate (Scheme 19).

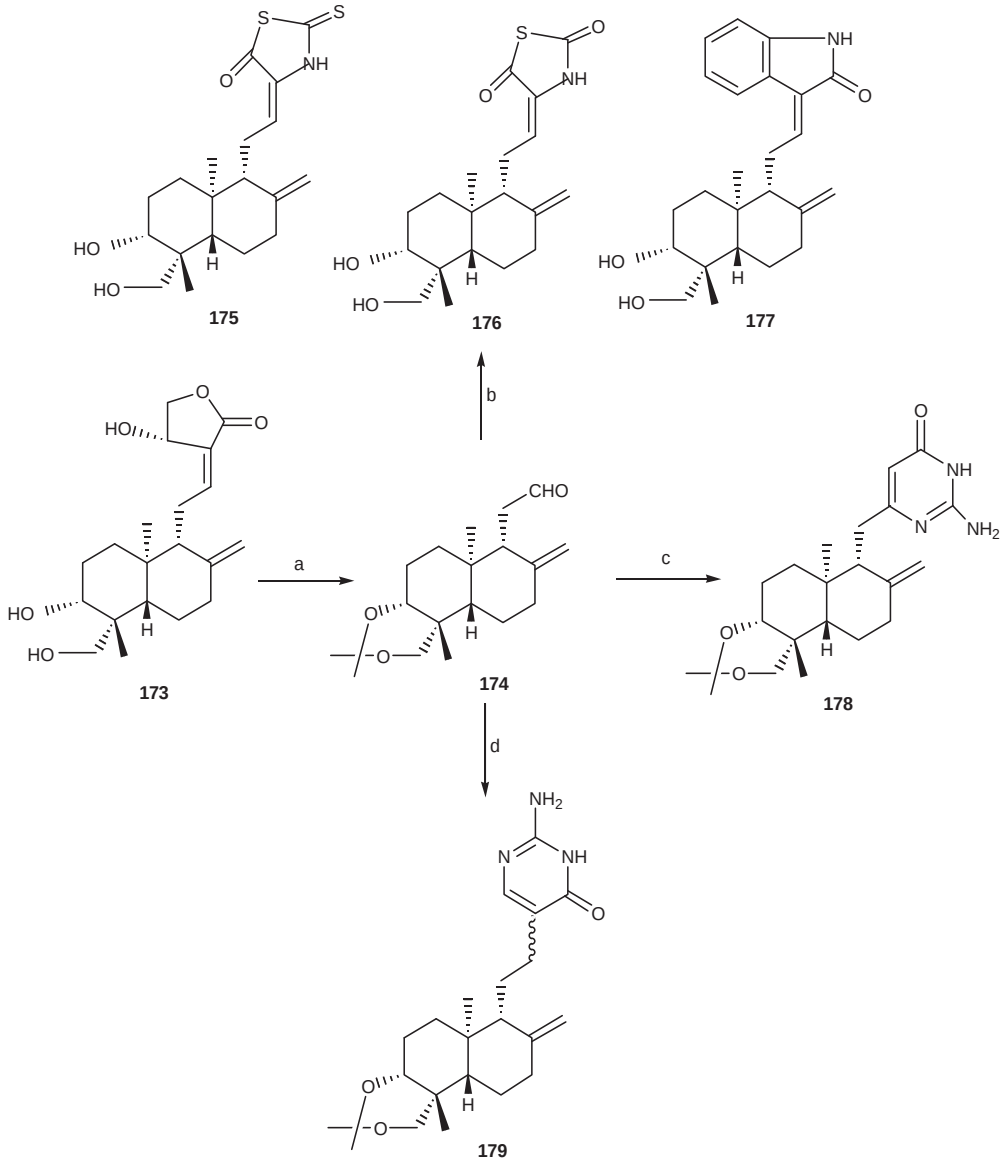

Reagents: a) 1. 2,2-dimethoxypropane/PPTS/benzene/reflux, 95%; 2. Ac_2O/TEA/DCM/rt, 95%; 3. DMAP/DCM/rt, 80%; 4. aq $KMnO_4$/THF, rt, 62%; b) 1. rhodanine/thiazolidinedione/oxindole, b-alanine/benzene/reflux; 2. AcOH/H_2O (7:3), c) 1. $BrCH_2CO_2Et$/Zn/benzene/reflux, (70%); 2. PDC, DCM/rt, (90%); 3. guanidinium chloride/NaOMe/MeOH/reflux, (60%); d) 1. ethyl acetoacetate/$TiCl_4$/py, (70%); 2. $NaBH_4$/MeOH (95%); 3. PDC/DCM, (95%); 4. guanidine hydrochloride/NaOMe/MeOH/reflux (60%).

Scheme 19

The latter was converted into a number of labdane diterpenes by utilizing its aldehyde functionality. Knoevenagel condensation of compound (174) with rhodanine, thiazolidinedione and oxindole, followed by the elimination of the C-3,19-isopropylidene protection, furnished compounds (175), (176) and (177). Compound (178) containing the aminopyrimidone moiety in the side chain was synthesized by Reformatsky reaction of (174) with ethyl bromoacetate, followed by pyridinium dichromate oxidation and condensation with guanidine. The corresponding homologue (179) was prepared as shown in scheme 19 (d).

An effective synthesis of (+)-agelasine C (180) has been achieved from *ent*-halimic acid methyl ester (182) [44]. The structure and absolute configuration of the natural product (-)-agelasine C (180) was established.

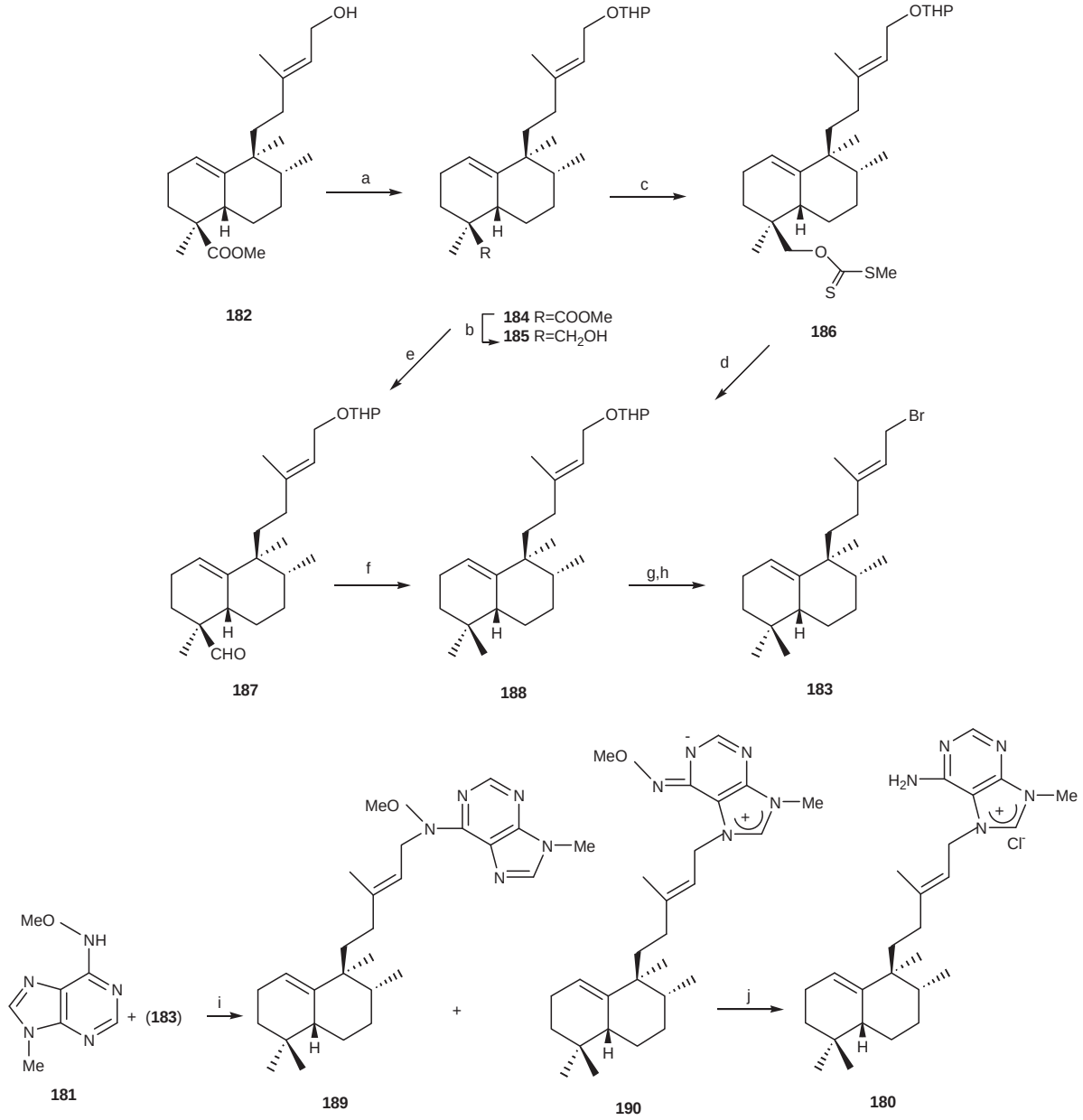

Reagents: a) DHP, p-TsOH, C_6H_6, 15 min, rt, (98%); b) LAH, Et_2O, 8°C and then rt, 4 h, (99%); c) nBuLi, THF, (98%); d) nBu_3SnH, AIBN, toluene, 20 min, (31%); e) TPAP, NMO, DCM, Ar, 45 min, (94%); f) diethylene glycol, $NH_2–NH_2·H_2O$, KOH, (81%); g) p-TsOH, MeOH, 30 min, (81%); h) CBr_4, PPh_3, DCM, 3 h, (76%); i) DMA j) Zn, MeOH, H_2O, AcOH, argon.

Scheme 20

The synthesis of target-compound (180) has been run in a convergent way, considering its purine fragment and the diterpenic part. The purinic fragment (181) was built following the methodology of Fujii [45] from adenine. The

second part of the synthesis comprised the transformation of enthalimic acid methyl ester (182) into the bromoderivative (183). This conversion required the reduction of the methoxycarbonyl group at C-18 to a methyl group, as well as the substitution of the alcohol function in C-15 with bromine. For the aforementioned reduction at C-18 the necessity of suitable protection at C-15 arose and was solved *via* the corresponding tetrahydropyrane derivative (Scheme 20). The reaction of methyl ester (182) with 3,4-dihydro-2H-pyran in *p*-TsOH produced compound (184) that by reduction with lithium aluminium hydride lead to the hydroxyderivative (185). The interaction of the latter with carbon disulphide was followed by the treatment with methyl iodide in alkaline media, which led to the xantogenate (186). It was consequently reducted with tributyltin hydride in the presence of azobisisobutyl nitrile giving the reduction product (188) in a modest yield. The outcome of the reductive conversion could be ameliorated when the Huang–Minlon methodology has been employed upon the aldehyde (187), in turn obtained by oxidation of compound (185) with tetra-*n*-propylammonium perruthenate. Deprotection of the primary hydroxy group, followed by the treatment of the hydroxyderivative with CBr_4 in the presence of thriphenylphosphine afforded the required bromoderivative (183). Once the two basic fragments have been obtained, the synthesis was continued with the alkylation of methoxyadenine (181) by the bromoderivative (183). It gave the mixture of two isomers: compound (199) corresponding to the N in C-6 alkylation and required (190). The latter was finally reduced with Zn in acetic acid giving the target-compound (180).

4. Conclusion

The above-presented data demonstrate that lately the vast series of known natural terpenoids has been intensely supplemented by the nitrogen-containing metabolites of plant, microbial and animal origin. The unique structure of many so-called mixed metabolites, whose molecules include nitrogen, and their important biological properties make them attractive targets of the total synthesis. On the other hand, they can serve as plausible models for designing the molecules with useful functions.

Thus, the scientific interest remains opened to the exploration of new exciting facets of nitrogen-containing terpenoids.

5. References

[1]. Jansen, B. J. M.; de Groot, A. Nat. Prod. Rep., **2004**, 21, (4), 449-477.
[2]. Connolly, I. D.; Hill, R. A. Dictionary of Terpenoids, London: Chapman and Hall, **1991**, vol. 2, pp. 677-809.
[3]. Grant, P. K.; Prasad, J. S.; Rowan, D. D. Aust. J. Chem., **1983**, 36, (6), 1197-1202.
[4]. Schenk, H. L.; Gutmann, H.; Jeger, O.; Ruzicka, L. Helv. Chim. Acta, **1954**, 37, (2), 543-546.
[5]. FIeming, L.; Woodward, R. B. J. Chem. Soc., Perkin Traпs. 1, **1973**, 1653-1657.
[6]. Urones, J. G.; Diez, D.; Gomez, P. M.; Marcos, I. S.; Basabe, P.; Moro, R. F. Nat. Prod. Lett., **1998**, 11, (2), 145-152.
[7]. Urones, J. G.; Marcos, I. S.; Perez, B. O.; Diez, D.; Ligthow, A. M.; Gomez, P. M.; Basabe, P.;. Garrido, N. M. Tetrahredron, **1994**, 50, (37), 10995-11012.
[8]. Cortes, M.; Lopez J.; Diaz, E. Nat. Prod. Lett., **1993**, 2, (1), 37-40.
[9]. Hayashi, T.; Yamamoto, A.; Ito, Y. Tetrahedron Lett., **1988**, 29, (1), 99-102.
[10]. Ardabllchi, N.; Fitton, A. O.; Frost, J. R.; Oppong-Boachie, F. K.; Hadi, A. H.; Sharif, A. M. J. Chem. Soc., Perkin Trans. 1, **1979**, 539-543.
[11]. Kunieda, T.; Ishizuka, T.; Higuchi, T.; Hirobe, M. J. Org. Chem., **1988**, 53, (14), 3381-3383.
[12]. Barrero, A. F.; Alvarez-Manzaneda, E. J.; Chahboun, R.; Gonzalez Diaz, C. Synlett, **2000**, (11), 1561-1564.
[13]. Barrero, A. F.; Alvarez-Manzaneda, E. J.; Altarejos, J.; Salido, S.; Ramos, J. M.; Simmonds, M. S. J.; Blaney, W. M. Tetrahedron, **1995**, 51, (27), 7435-7450.
[14]. Heathcock C. H.; Buse C. T.; Kleschick W. A.; Pirrung M. C.; Sohn J. E.; Lampe J. J. J. Org. Chem., **1980**, 45, (6), 1066-1081.
[15]. Kuchkova, K. I.; Arycu, A. N.;. Vlad, P. F. Chem. Nat. Comp., **2009**, 45, (3), 367-370.
[16]. Kuchkova, K. I.; Arycu, A. N.; Dragalin, I. P.; Vlad, P. F. Khim. Prir. Soedin., **2005**, (2), 152-155 [Chem. Nat. Comp., **2005**, 41, (2), 190-193 (Engl. Transl.)]
[17]. Liu, P. S. J. Org. Chem., **1987**, 52, (21), 4717-4721.
[18]. Nystrom, R. F. J. Am. Chem. Soc., **1955**, 77, (9), 2544-2545.
[19]. Ipaktschi, J. Chem. Ber., **1984,** 117, (2), 856-858.
[20]. Rausser, R.; Weber, L.;. Hershberg, E. B.; Oliveto, E. P. J. Org. Chem., **1966**, 31, (5), 1342-1346.
[21]. Hilgetag, G.; Martin, A., Weygand-Hilgetag Preparative Organic Chemistry, Wiley-Interscience, Chichester, Engl., **1979**, pp. 520.
[22]. Kim, J. N; Chung, K. H.; Ryu, E. K. Synth. Commun., **1990**, 20, (18), 2785-2788.

[23]. Sosnovsky, G.; Krogh, J. K. Synthesis, **1978**, (9), 703-704.
[24]. Boruah, M.; Konwar, D. J. Org. Chem., **2002**, 67, (20), 7138-7139.
[25]. Ganboa, I.; Palomo, C. Synth. Commun., **1983**, 13, (3), 219-224.
[26]. Saednya, A. Synthesis, **1982**, (3), 190-191.
[27]. Capdevielle, P.; Lavingne, A.; Maumy, M. Synthesis, **1989**, (6), 451-452.
[28]. Frejd, T.; Klingstedt, T. Synthesis, **1987**, (1), 40-42.
[29]. Kuchkova, K. I.; Arycu, A. N.; Vlad, P. F.; Deleanu, K.; Nikolescu, A. Chem. Nat. Comp., **2010**, 46, (4), 539-544.
[30]. Kuchkova, K. I.; Chumakov, Yu. M.; Simonov, Yu. A.; Bocelli, G.; Panasenko, A. A., Vlad, P. F. Synthesis, **1997**, (9), 1045-1049.
[31]. Kuchkova, K. I.; Arycu, A. N.; Barba, A.N.; Vlad, P. F. Chem. Nat. Comp., **2011**, 46, (2), 205-210.
[32]. Kuzuya, K.; Mori, N.; Watanabe, H. Org. Lett., **2010**, 12, (21), 4709-4711.
[33]. Chernov, S. V., Shul'ts, E. E., Shakirov, M. M., Tolstikov, G. A. Russ. J. Org. Chem., **2002**, 38, (5), 703-709.
[34]. Kharitonov, Yu. V.; Shul'ts, E. E.; Shakirov, M. M.; Tolstikov, G. A. Russ. J. Org. Chem., **2003**, 39 (1), 57-74.
[35]. Chernov, S. V.; Shul'ts, E. E.; Shakirov, M. M.; Bagryanskaia, I. Yu.;. Gatilov, Yu. V.; Tolstikov, G. A. Russ. J. Org. Chem., **2005**, 41, (4), 547-556.
[36]. Kharitonov, Yu. V.; Shul'ts, E. E.; Shakirov, M. M.; Tolstikov, G. A. Russ. J. Org. Chem., **2005**, 41, (8), 1145-1157.
[37]. Kharitonov, Yu. V.; Shul'ts, E. E.; Shakirov, M. M.; Tolstikov, G. A. Russ. J. Org. Chem., **2006**, 42, (5), 725-735.
[38]. Kharitonov, Yu. V.; Shul'ts, E. E.; Shakirov, M. M.; Tolstikov, G. A. Russ. J. Org. Chem., **2007**, 43, (6), 839–851.
[39]. Chernov, S. V.; Shul'ts, E. E.; Shakirov, M. M.; Tolstikov, G. A. Russ. J. Org. Chem., **2008**, 44, (1), 67–75.
[40]. Kharitonov, Yu. V.; Shul'ts, E. E.; Shakirov, M. M.; Tolstikov, G. A. Russ. J. Org. Chem., **2008**, 44, (4), 521–528.
[41]. Kharitonov, Yu. V.; Shul'ts, E. E.; Shakirov, M. M.; Tolstikov, G. A. Russ. J. Org. Chem., **2009**, 45, (5), 637–649.
[42]. Mironov, M. E.; Kharitonov, Yu. V.; Shul'ts, E. E.; Shakirov, M. M.; Gatilov, Yu. V.; Tolstikov, G. A. Russ. J. Org. Chem., **2010**, 46, (12), 1869–1882.
[43]. Nanduri, S.; Nyavanandi, V. K.; Sanjeeva, S.; Thunuguntla, R.; Velisoju, M.; Kasu, S.; Rajagopal, S.; Kumar, R. A.; Rajagopalan, R.; Iqbal, J. Tetrahedron Lett., **2004**, 45, (25), 4883-4886.
[44]. Marcos, I. S.; Garcia, N.; Sexmero, M. J.; Basabe, P.; Diez, D.; Urones, J. G. Tetrahedron, **2005**, 61, (49), 11672-11676.
[45]. Fujii, T.; Itaya, T. *Tetrahedron*, **1971**, *27*, (2), 351-360.

OCCURRENCE AND CHEMISTRY OF DIHYDROXYFUMARIC ACID

N. Secara, Gh. Duca, L. Vlad, F. Macaev*

Institute of Chemistry of the Academy of Sciences of Moldova,
3 Academy str., MD-2028, Chisinau, Moldova
Tel +373-22-739-754, Fax +373-22-739-954, E-mail: flmacaev@cc.acad.md

Dedicated to academician Pavel F. Vlad on the occasion of his 75th birthday

Abstract: The paper summarizes literature data on occurrence of dihydroxyfumaric acid and its role in biological systems, as well as its chemical properties.

Keywords: dihydroxyfumaric acid, fluorescent sensors, molecular clips, coordination polymers

1. Introduction

The role of many hydroxy acids, such as malic, lactic, glycolic, citric, tartaric, in living organisms and plant metabolism is generally recognized. The interest in plant metabolites as sources of biologically active compounds appeared a long time ago. One of the leaders, due to its potential, in the series of natural sources is the dihydroxyfumaric acid **1**. It is clear that discovery of the relationship between structures and properties can conduct to successful development of new effective antioxidants, drugs etc. In this paper, we tried to systemize literature data based on occurrence of dihydroxyfumaric acid **1** in biological sources and synthetic transformations into target products, which should be convenient (from our point of view) for the chemists. This approach is presented in our review.

2. Structure and occurrence of dihydroxyfumaric acid in biological systems

Dihydroxyfumaric acid is **1** a dicarboxylic hydroxy acid, which is formed from tartaric acid via dehydrogenation or oxidation processes.

For the first time, it was chemically obtained in 1894 by Fenton, as a product of tartaric acid oxidation by hydrogen peroxide, in the presence of Fe(II) [1,2]. Dihydroxyfumaric acid has *trans*- and *cis*- isomers. The *trans*- isomer is called the dihydroxyfumaric acid, and the *cis*- isomer is called the dihydroxymaleic acid. Fenton suggested that the dihydroxyfumaric acid mainly exists in its *cis*- form, therefore in all scientific work before 1950's, the acid is referred to as dihydroxymaleic. At the beginning of the XXth century it was proved [3] that these forms are chemically identical, and in 1953 Hartree [4] showed that in crystalline form, as well as in solution, only the *trans*- isomer exists. Also, it should be mentioned that dihydroxyfumaric acid in solution exists in two tautomeric forms in equilibrium (Scheme 1):

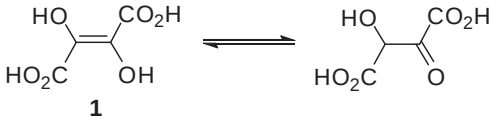

1

Scheme 1

In solution, 80 % of the acid usually corresponds to the enolic group, and the other 20% - to the keto-group [5].

Similarly to tartaric acid, dihydroxyfumaric acid (DHF) plays an important role in nature. The first proofs of its biological significance appeared in 1915 when Neuberg [6] observed that DHF was fermented by yeast. In 1938 Banga and Szent-Gyiirgyi [7] and Banga and Philippot [8] extracted an enzyme, which they called dihydroxyfumaric acid oxidase from plants; the oxidation product was later proved to be diketosuccinic acid. In 1940 Theorell also discovered an enzyme in some plants, which oxidized dihydroxyfumaric acid with oxygen uptake, and he proved that enzyme to be peroxidase.

It was shown that the active centers of dihydroxyfumaric acid oxidase and peroxidase are the coordination compounds of iron ad copper [9]. As it was previously said, these ferments catalyze the transformation of DHF into diketosuccinic acid **2**.

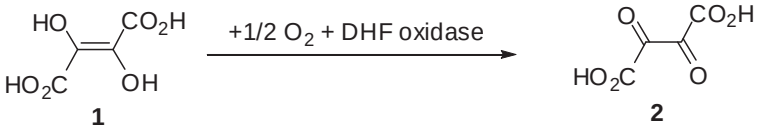

1 **2**

Scheme 2

Therefore, it was suggested [9] that in the system oxygen + DHF-oxidase, the role of DHF is similar to that of ascorbic acid **3** in the ascorbate-oxidase system which afforded α-diketone **4** (see Scheme 3).

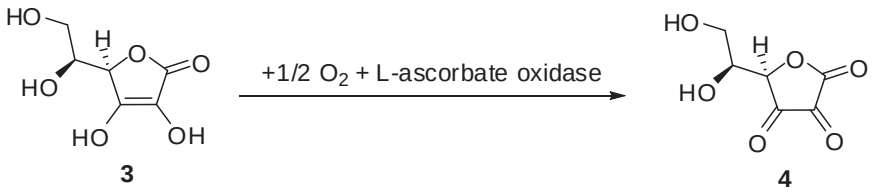

3 **4**

Scheme 3

It may be observed from these schemes that the dihydroxyfumaric acid bears some similarities with the ascorbic acid, and therefore, in biological oxidation, it may play a similar role to that of ascorbate, i.e. intermediate hydrogen carrier from substrates to oxygen.

The oxidase function of peroxidase was later shown towards other compounds, such as: glutathione, hydro- and naphtoquinone, fluoroglycine and others. A necessary condition for the oxydase reaction was proved to be the presence of cofactors – manganese ions and various phenolic compounds. Further information on certain enzymatic reactions of dihydroxyfumaric and diketosuccinic acids in plant tissues was obtained by Stafford, Magaldi, and Vennesland [10] in 1954.

The role of dihydroxyfumaric acid in animal metabolism was evidenced for the first time in 1934 when it was found that the content of glycogen was increased in muscle on incubation with DHF [11]. Latter, was discovered a sequence of enzyme reactions as a pathway for glyconeogenesis, based on the observation suggesting the formation of a pentose (or a pentose phosphate) on addition of DHF and glyceraldehydes (or fructose-l,6-diphosphate and aldolase as a source of glyceraldehyde-3-phosphate) in rabbit muscle extract. The sequence of reactions leading from DHF to 3-ketopentose **5** is given as follows [12].

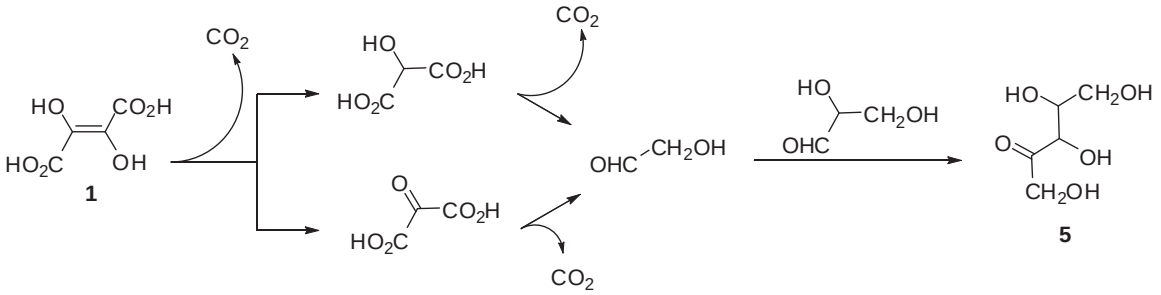

Scheme 4

It is well known that di – and tricarboxylic organic acids play an important role in plant and animal metabolism. Products of carbohydrates transformations, they participate in the biosynthesis of alkaloids, glycosides, amino acids and other biologically active compounds. The dihydroxyfumaric acid is linked to the cycle of di- and tricarboxylic acids, and with the glyoxalic cycle via tartaric acid transformation cycle, as depicted below, in Figure 1.

Without going into details, it should be mentioned that the main function of these cycles consists in that they represent the final collective path of oxidation of carbohydrates, lipids and proteins, as during metabolism processes, glucose, fatty acids and amino acids are transformed either into acetyl-CoA, or in intermediate compounds of cycles mentioned above.

The dihydroxyfumaric acid is formed from tartaric acid by dehydrogenation, in the presence of nicotinamide adenine dinucliotide (NAD) and tartaric acid dehydrogenase, and bivalent iron.

The dihydroxyfumaric acid is involved in metabolism during grapes ripening. Although it is found in small amounts in grapes, it serves as a catalyst for redox reactions. Dihydroxyfumaric acid is easily oxidized by DHF oxidase. Therefore, grapes contain the products of its disintegration: mesoxalic acid, glycolic acid and oxalic acid and glyoxalic acid.

Dihydroxyfumaric acid is of importance in winemaking industry and in food industry. It is well known that organic acids contribute to the formation of acidity of wines – one of the major important wine characteristics. Although its content in wine is small, DHF plays an important role in reduction processes occurring in wine.

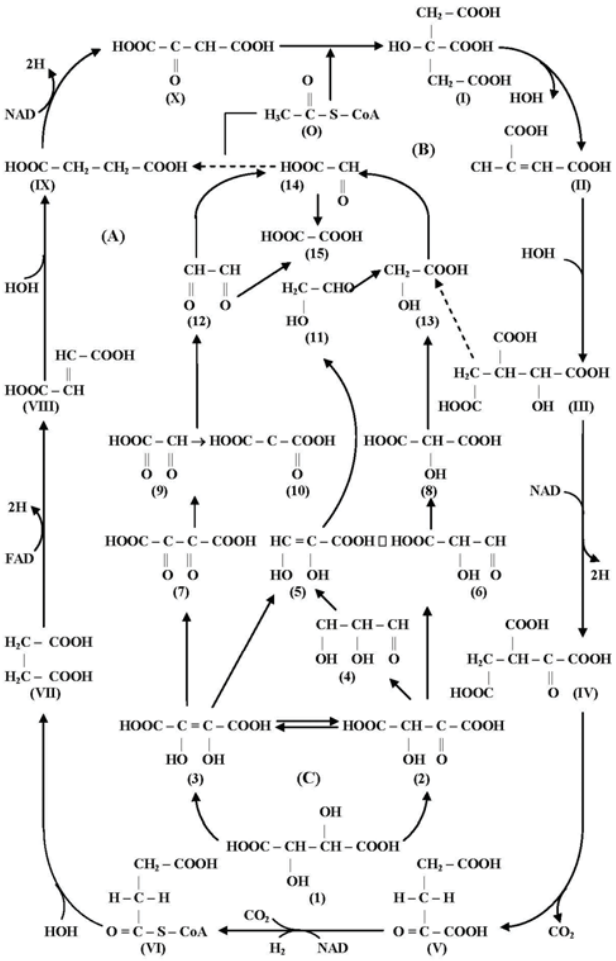

Figure 1 (from [9])**.** Interrelation of metabolic cycles (picture from Duca Gh., PhD thesis, 1979).

(A) – cycle of tricarbonic acids (Krebs cycle), (B) – glyoxalate cycle, (C) – cycle of dicarbonic acids (Baroud cycle). I – citric acid, II – cis-acinitic acid, III – iso-citric acid, IV – oxalo-succinic acid, V – α*-ketoglutalic acid, VI – succinoxo-enzyme A, VII – succinic acid, VIII – fumaric acid, IX – maleic acid, X – oxalo-acetic acid.* 0 – acetyl coenzyme A; 1 – tartaric acid, 2 – oxaloglycolic acid, 3 – dihydroxyfumaric acid; 4 – reductone of triose, 5 – dixydroxyacrilic acid, 6 – semialdehyde of tartronic acid; 7 – diketosuccinic acid, 8 – tartronic, 9 – glyoxylcarbonic, 10 – mezoxalic acids; 11 – glycolic aldehyde, 12 – oxalic aldehyde; 13 – glycolic acid, 14 – glyoxalic acid, 15 – oxalic acid.

If the access of air to wine materials during processing and maturation is limited and within a year the wine absorbs no more than 3-5 mg /L of oxygen, then, according to Rodopulo [13], under these conditions, tartaric acid is oxidized to dihydroxyfumaric acid determining a low redox potential of the wine, and the reductons restore oxidized substances, which contributes to the development of taste and flavor characteristic to table wines. However, DHF decomposes easily in aerobic conditions, and that is the reason for which it is hard to determine it in wines.

To improve the stability of wines in time and to improve their hygienic properties, a series of experiments were performed by Sychev and Duca [14], using dihydroxyfumarate for wine materials preservation. It was shown that due to its pronounced reduction properties DHF transforms oxidized components of grape drinks in their reduced forms. When added to the sample, DHF was consumed by interaction with oxidized polyphenols, while the latter were reduced. That fact reduces the possibility of formation of colloidal haze in wine, and dihydroxyfumarate can be used in certain amounts as a preservative. In this case, oxidation of DHF occurs into diketosuccinic acid, with its further decarboxylation.

It was noticed that compared to the wine obtained according to the conventional technology, the wine made with the addition of dihydroxyfumarate exhibited better taste and a considerably greater stability.

Antioxidant properties of dihydroxyfumaric acid were also appreciated in studies regarding the inhibition of nitrosation of secondary aliphatic amines and amides. It was shown [15] that under the action of DHF, nitrosating agents are inactivated, therefore the formation of harmful nitrosoamines is supressed.

The inhibitory activity of dihydroxyfumaric acid and its sodium salt was investigated in the process of nitrosatoin of metabolites formed in gastric juice. It was found that during albumin and casein proteolysis by proteolytic enzymes, these reagents inhibit the formation of N-nitrozocompounds without having any influence on the content of unhydrolyzed protein substrate or the concentration of formed amino acids [15].

Also, it was found [16] that the sodium salt of DHF decreases the speed of methaemoglobin formation during oxidation of hemoglobin with nitrites, by decreasing the acceleration factor with increasing reducton concentration. Research in the endogenous formation of N'-nitrosonornicotine (one of the most abundant strong carcinogens in unburned tobacco and cigarette smoke) in rats demonstrated efficient inhibition (86%) of this process by dihydroxyfumaric acid [17]. Studies regarding the formation of N'-nitrosoamines in meat products (smoked, fried, dried, salted products) demonstrated that the sodium salt of dihydroxyfumaric acid significantly decreased the concentration of nitrites and nitrates in meat products [15].

3. Chemistry of dihydroxyfumaric acid

It is well known that the spatial structure of a compound significantly affects its properties, including its biological activity. One of the ways used to solve such problems is the implementation of the synthesis of the desired derivative from natural renewable starting materials. In the directed synthesis of substituted 1,2-dihydroxyethylenes a suitable starting compound is dihydroxyfumarate 1 [18-20]. This, along with the peculiar structure makes it an attractive and indispensable source for the implementation of the synthesis of substances with desired properties.

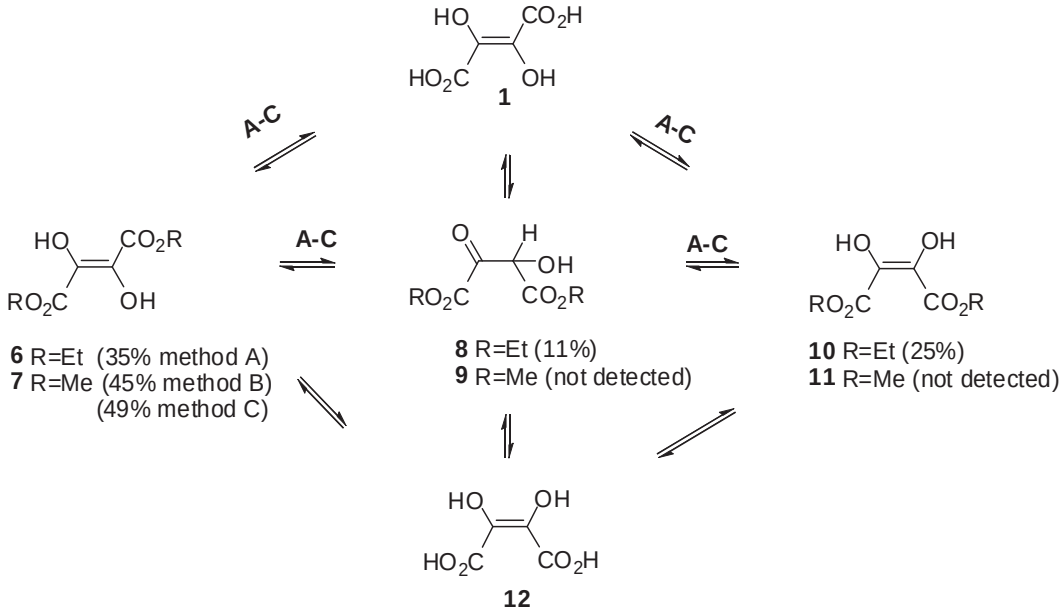

A: EtOH/HCl; **B**: MeOH/HCl; **C**: CH_2N_2/ether

Scheme 5

Given the structure of acid 1, the attack of reagents on its molecule is directed generally to the carboxyl or hydroxyl group. Further transformation of the resulting adducts leads to compounds with greater or smaller number of carbon atoms than the starting material. On the other hand, the tendency to keto-enol tautomerism of substance 1, and as a consequence of the isomerization of *trans*-isomer 1 in the *cis*-isomer 12 made Hartree E. F. explore the configuration of its esters [18].

The mixture of ethylic esters 6,8,10 was synthesized by prolonged maintenance of acid 1 in ethanol/HCl. An analogical approach was used for the homologues 7,9 and 11. However, only the methylic ester 7 was isolated. Alternatively, the substance 7 was synthesized by methylation with diazomethane.

The comparison of acid 1 with compounds of related structure in terms of dissociation constants and chemotactic properties gives evidence for *trans* structure in aqueous solution. The formation of a grey-brown color with $FeCl_3$ (violet on addition of alkali) is in contrast to the customary green color expected with *cis* OH groups. Since both esters retain the ene-diol group they must be considered as *trans* and *cis*, respectively. The fact that ethylation and methylation carried out under very similar conditions with alcohols/HCl yields products of different structures is perhaps due to the different solubility of related ethyl and methyl esters in respective reaction mixtures. Thus after ETOH/HCl treatment, compounds

3 and 5 can be isolated while after MeOH/HCl treatment, only the ester 7 (identical with that prepared with CH_2N_2) can be detected. Since a partial conversion of compound 6 into 10 can be shown to occur under acidic conditions of esterification, and since methyl ester is not accompanied by other isomers after methylation under analogous conditions, it is reasonable to conclude that the *trans* structure is the initial product 1.

Interest in the mechanism of oxidation and isomerization of *cis*- and *trans*-enediols prompted Goodwin *et al* [19] to attempt the preparation of derivatives 13-18 starting from acid 1 (see Scheme 6).

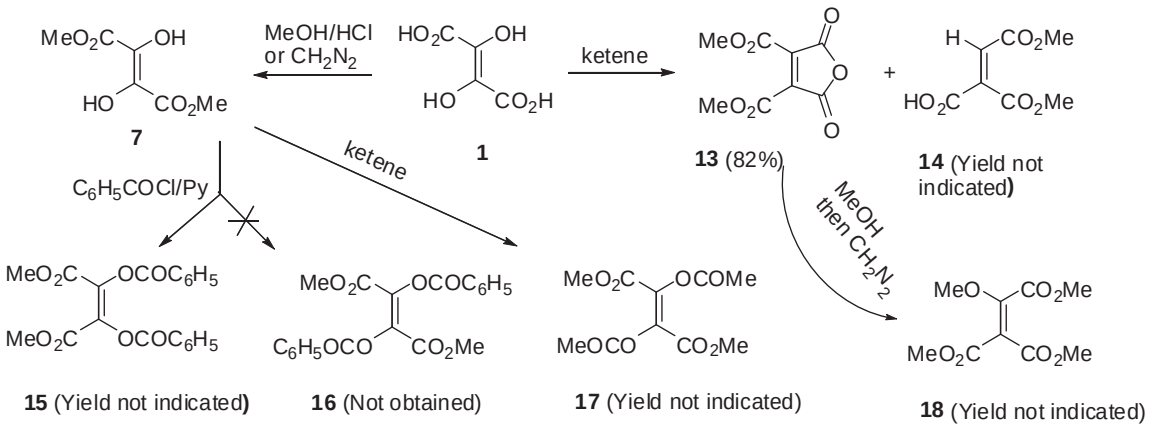

Scheme 6

Benzoylation of *trans*-enediol 7 by action of BzCl/Py leads to centro-symmetrical dimethyl dibenzoylfumarate 15. The formation of *trans*-dimethyl dibenzoylfumarate 16 was not detected. The *trans*- ester 7 with ketene yielded the *trans*-diacetyl ester 17. As a by-product in the preparation of α,β-unsaturated five-membered lactone 13, the compound 14 was isolated. Notable, only if in the acetylation of *trans*-enediol 1, decarboxylation occurred prior to anhydrization the product 14 may have the *trans*-configuration.

The action of various silylating agents on acid 1 has been investigated [20-22].

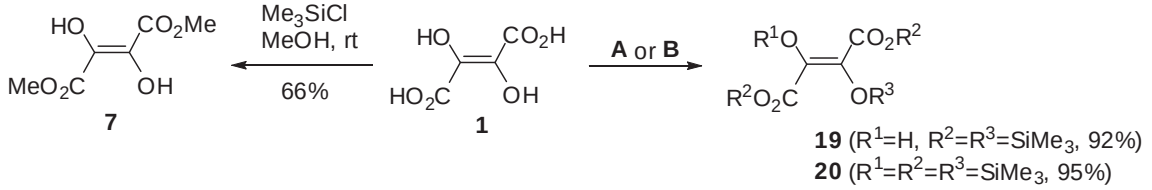

A: Me_3Si-acac, 70^{0}C; **B**: $C_3H_5SiMe_3$, $CF_3SO_3SiMe_3$, MeCN, rt

Scheme 7

2,4-Pentanedione trimethylsilyl enol ethers (Me_3Si-acac) converted enediol 1 into the mono-acid 19.

The product 20 was obtained after the silylation of dihydrofumaric acid 1 with allyltrimethylsilane and trimethylsilyl triflate in acetonitrile at room temperature.

The new esterification of acid 1 with MeOH under the action of trimethylsilyl chloride was performed. An anhydrization with formation of homologue five-membered lactone 13 (see Scheme 7) was not observed in any reactions with participation of silylations agents.

Nitrogen containing derivatives of dihydroxyfumaric acid 1 may open new possibilities in organic synthesis: selecting of appropriate combinations of substituents may allow adjusting the polarity in wide ranges, the solvating ability, catalytic properties and thereby influence the depth and selectivity of the reaction.

The conversion of esters to amides is a useful reaction, and different amides can be prepared this way from appropriate amines. The reaction is particularly useful because the ester is easy to prepare, even in cases where the corresponding acyl halide or anhydride is not. Although more studies have been devoted to the mechanism of acylation of amines with esters than with other reagents, the mechanistic details are not yet entirely clear. Under the normal alkaline conditions, the reaction is base-catalyzed, indicating that a proton is being transferred in the rate-determining step and that two molecules of amine are involved.

In an effort to determine the role of hydrogen bonding in stabilizing secondary structure and to develop means of

predictably enhancing the tendency of functionalized peptides 23 to assume sheet or helical conformations starting from ester 3 has been prepared 2,8-diaminoepindolidione 22 [23].

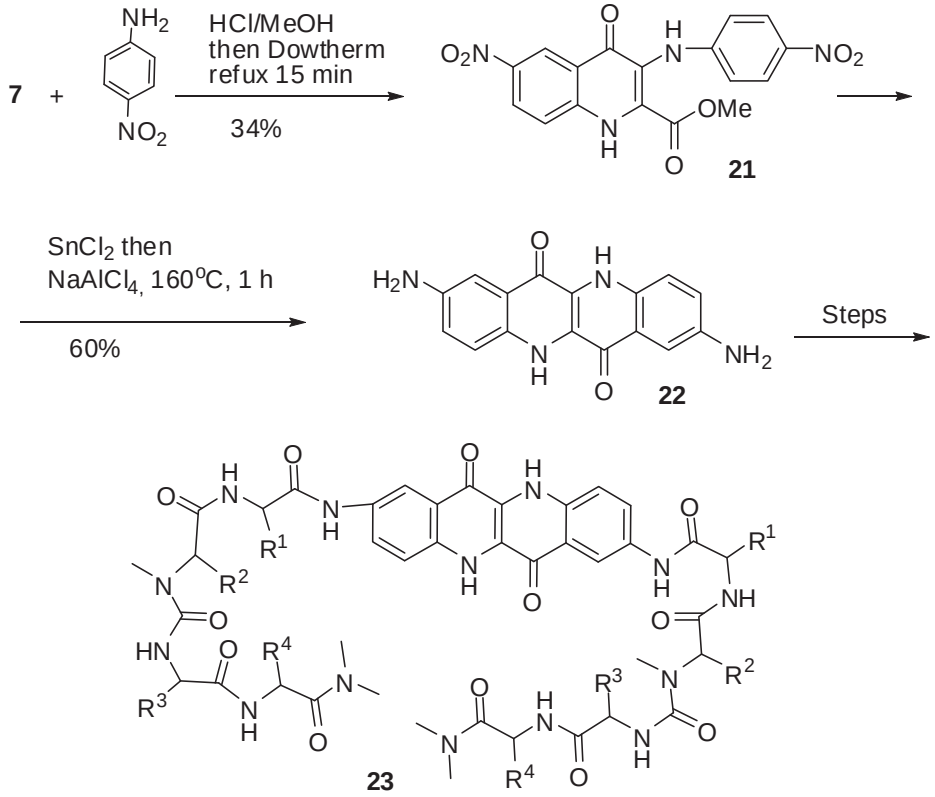

Scheme 8

The amino-de-methylation of the ester 7 by *p*-nitroaniline followed un-catalyzed high-temperature cyclization to form the quinolone 21 in an overall yield of 56%. Diamine 22 derived form carbomethoxyquinolone 21 further was transformed into functionalized peptides 23. The β-turn-forming tendencies of the 2,8-bis-(X-L-Pro-D-Ala) epindolidione, where X=Ac, Boc and COGlyOEt are assigned from ^{1}H NMR evidence.

Our group has been engaged in the synthesis and properties recognition of other amides (Scheme 9) [21].

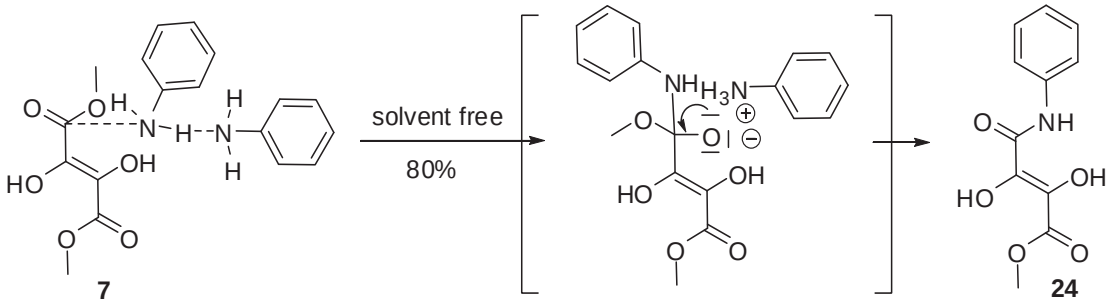

Scheme 9

Heating of the ester **3** in aniline during two hours leads to the formation of monoamide **24**.

Increasing the reaction time and temperature to the boiling point of aniline didn't lead to the formation of bis-anilide. It should be mentioned that the tentative of synthesis of the mixed amide by heating ester **20** with monoethanolamine wasn't successful, either.

An interesting result in the reaction of amidation of ester **7** was obtained when replacing aniline with its nitrogen-containing analogue – 2-aminopyridine (Scheme 10).

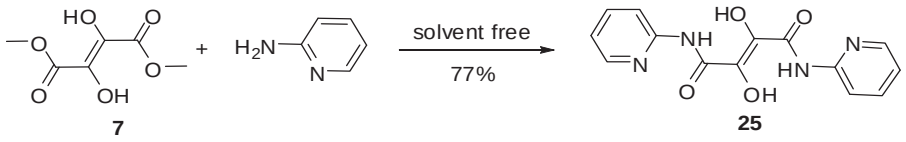

7 25

Scheme 10

Therefore, replacing the carbon atom in the benzene ring with nitrogen in the initial amine, had a significant influence on the character of the formed compound **25**.

The influence of the nature of homologues of monoethanolamine on the reaction rate and physico-chemical properties of dihydroxymaleinic acid amides was investigated.

If the amidation is carried out at room temperature by using ester **7** and monoethanolamine, the reaction product is bis-amidoalcohol **26**.

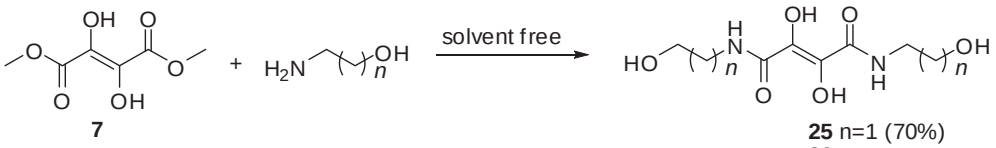

7

25 n=1 (70%)
26 n=2 (60%)

Scheme 11

Increasing the alkyl radical by one methylene fragment in the initial aminoalcohol gave the decrease of the total yield of product **27**.

The presence of two methyl groups in the α-position to the amino group in the initial 2-amino-2-methylpropan-1-ol didn't decrease the yield of the target diamide **27**. Analogically to the previous synthesis, this reaction was performed at room temperature.

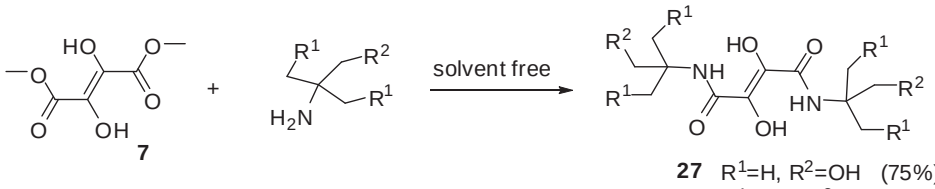

7

27 R^1=H, R^2=OH (75%)
28 R^1=OH, R^2=OH (69%)
29 R^1=R^2=H (70%)

Scheme 12

The transformation into the 2-amino-2-(hydroxymethyl)propane-1,3-diol decreased the reactivity of the amine. According to TLC data, only in the case of heating of initial reagents at 50^{0}C the formation of the product was observed. Following processing of the reaction mass with a yield of 69%, was separated N^1,N^4-bis(1,3-dihydroxy-2-(hydroxymethyl)propan-2-yl)-2,3-dihydroxyfumaramide **28**.

It should be mentioned that the homologue **29** may be synthesized at room temperature by mixing of tert-butyl amine with diether **7**. In this case, the yield of the target product is practically the same with the mentioned above.

The benzimidazole nucleus has been of considerable interest since it was noted that benzimidazole inhibits the growth of certain yeasts and bacteria. Such heterocyclic systems can be modified not only by changing the nature and the number of the connecting atoms but by changing the nature of the substituents in the benzimidazole nuclei as well. Scientific literature revealed the fact that a number of bis-benzimidazoles have been reported but apparently none of them have been synthesized from dihydroxyfumaric acid **1**.

On the other hand the methods were developed to synthesize novel mono and bis-benzimidazoles where the both benzimidazole nuclei are united through their 2-positions either through ethen-1,2-diols (see Scheme 13).

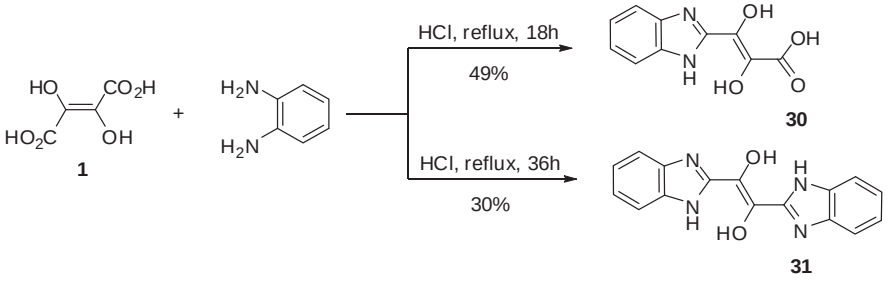

1 30 31

Scheme 13

The benzimidazole **30** was synthesized by hydrochloric acid-catalyzed condensation of the o-phenylenediamine with a dihydroxyfumaric acid **1** an oil bath at 135° under N_2. The same procedure has been used to prepare bis-benzimidazoles **31** by refluxing two moles of diamine with one mole of a dihydroxyfumaric acid **1** in 4 *N* hydrochloric acid.

Cucurbiturils Q[*n*] are substance which composed of 6 glycoluril rings and 12 methylene bridges [24]. It should be noted that cucurbiturils Q[*n*] has been demonstrated different application including the preparation of molecular and ion complexation [25-32], the catalysts [32-34], non-covalent modification of dendrimers [18], molecular necklaces [36,37], molecular switches [38,39], DNA complexes [40] and bowls [41].

Preparation of glycoluril monomers from dihydroxyfumaric acid 1 for expanded cucurbiturils Q[*n*]uril reported in [42]. In the beginning authors investigated the formation of carboxylic acids 30 (Scheme 14).

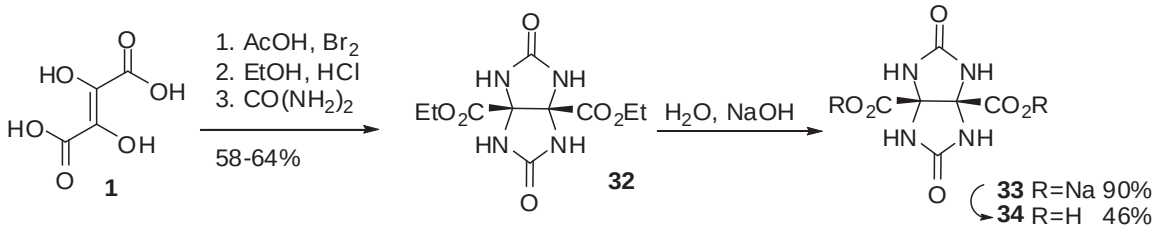

Scheme 14

Conversion of esters 32 into acids 34 was possible by treatment of carboxylic salt 33 with an excess of *p*-toluenesulfonic acid (PTSA). On the other hand, the transformation of esters 32 into cyclic derivatives 36 as well as 37 has been realized according to Scheme 15.

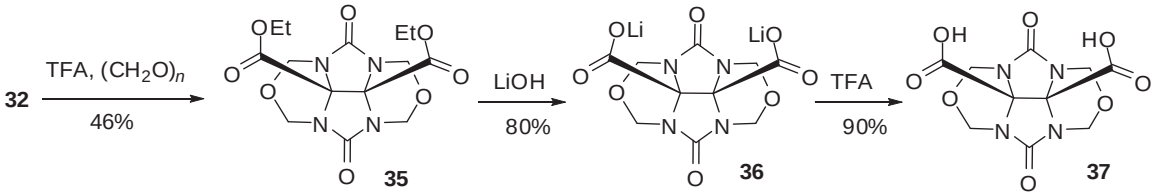

Scheme 15

Direct amidation reactions of esters 32 in neat primary amines at 75-90°C converts the esters into amide functional groups (see Scheme 16).

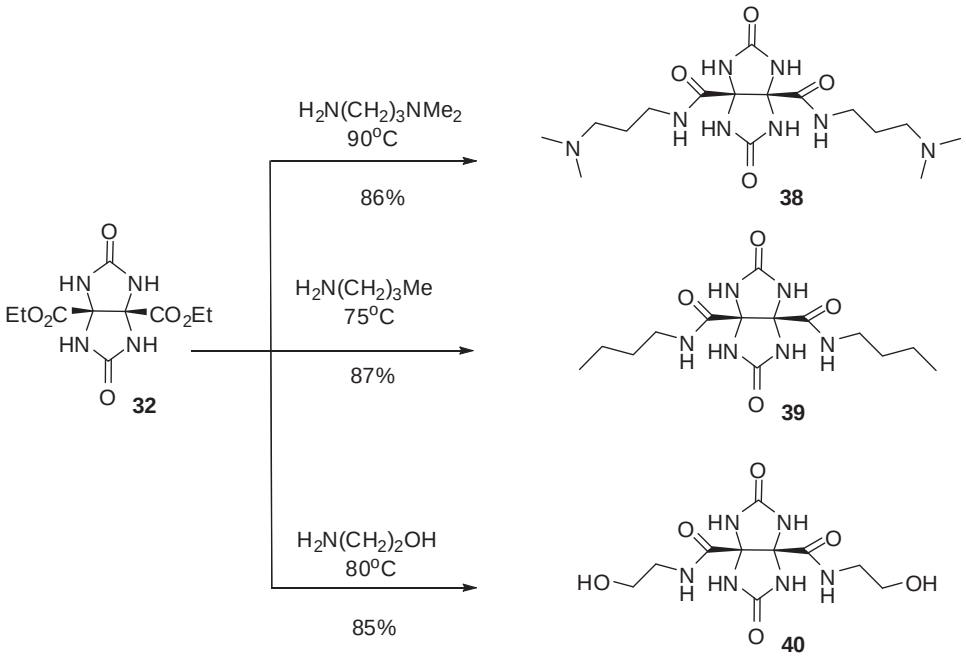

Scheme 16

Discovered that bulky esters 35 was highly reactive in direct amidation reactions with N^1,N^1-dimethylpropane-1,3-diamine, butan-1-amine as well as 2-aminoethanol and provided amides in 88%, 90% and 93% yields, respectively (Scheme 17).

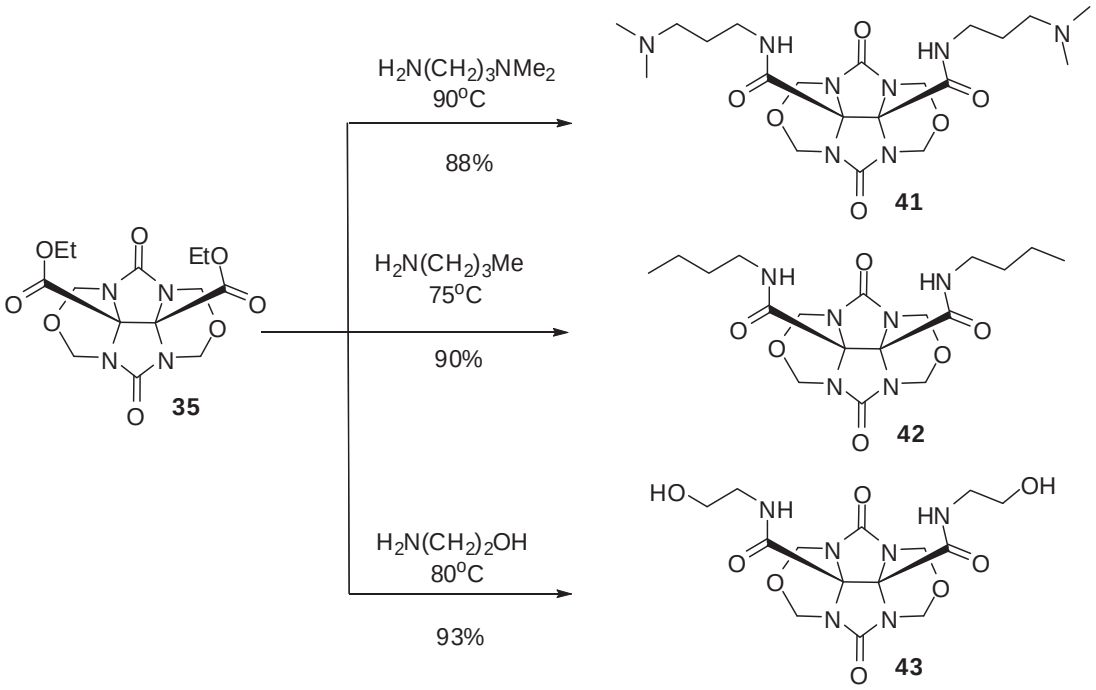

Scheme 17

The amidation of esters 32 and 35 by heating in neat morpholine at temperature up to 128°C afforded ammonium salts 44 and 45 rather than the desired tertiary amides (look Scheme 18).

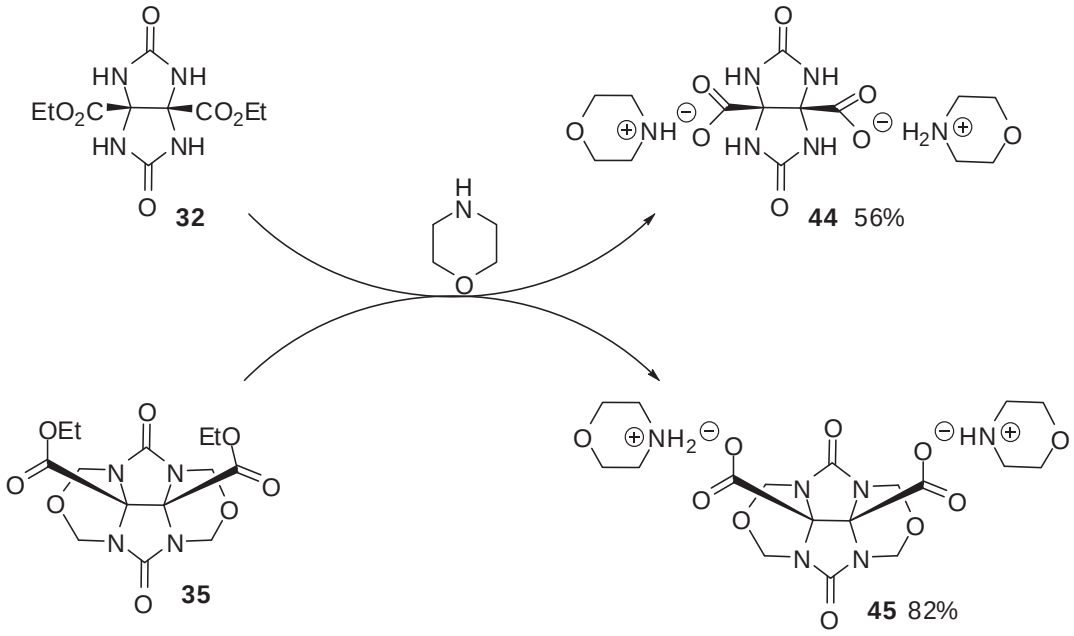

Scheme 18

On the other hand, conversion of diamides 38, 39 into the corresponding imides 46, 47 by treatment with PTSA was realized via Scheme 19.

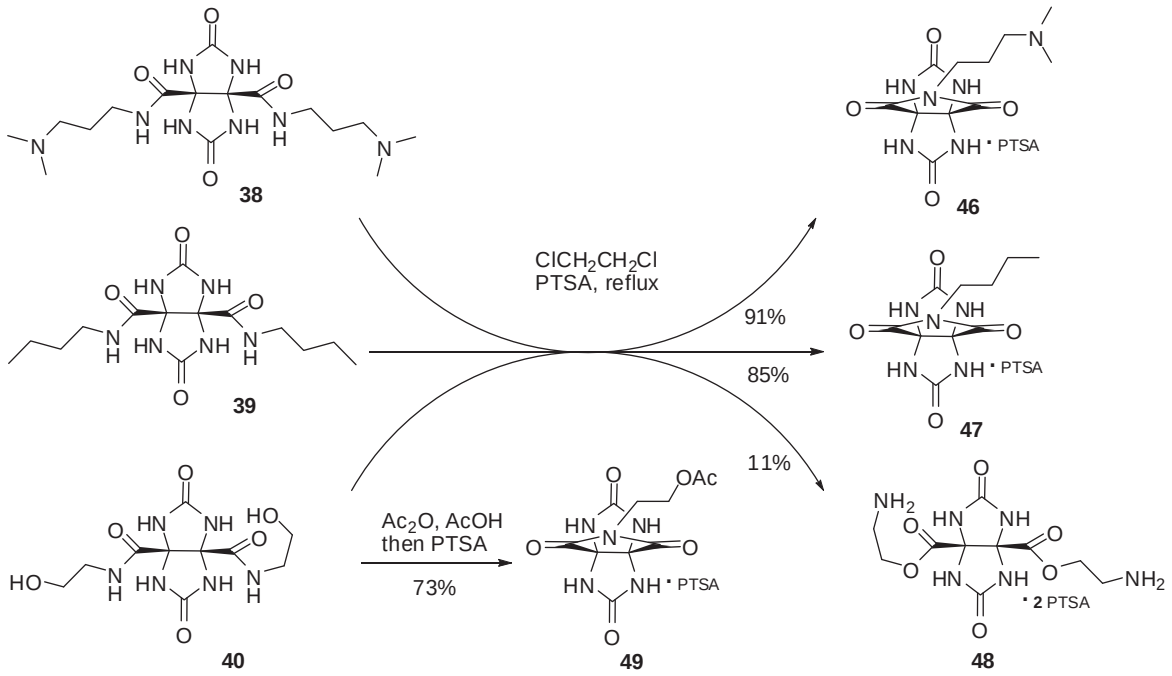

Scheme 19

Heating 40 under similar conditions did not result in the formation of the expected imide. In this case known [43] an N- to O –acyl transfer reaction occurred instead delivering 48 as its PTSA salt. To prevent the N- to O –acyl transfer reaction, acetylation followed ring closure in a single step afforded target compound 49 in 73% yield.

The transformation of compounds 41 and 42 into imides 50 and 51 occurred without incident in comparatively good yields (66% and 82%, respectively) (Scheme 20).

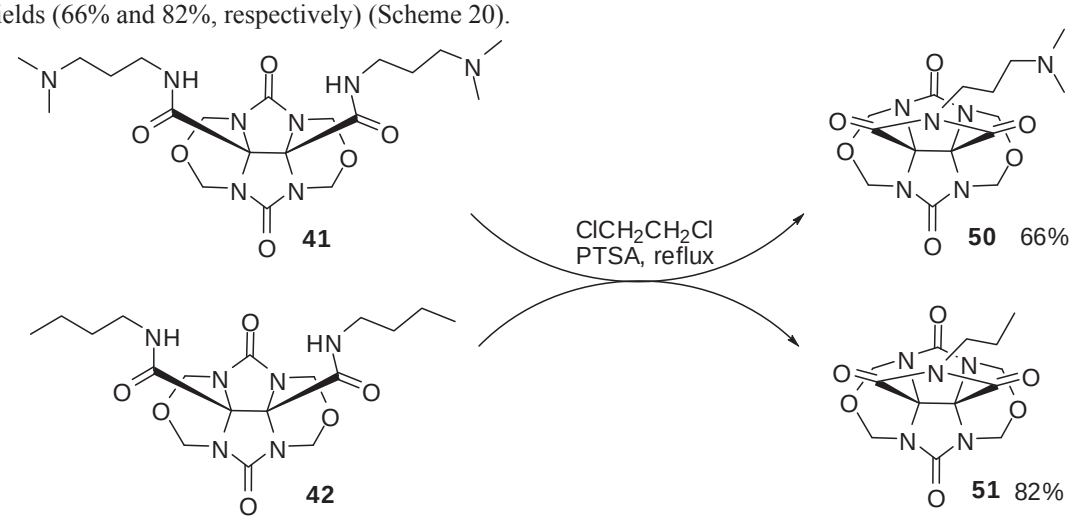

Scheme 20

Similarly with diol **40**, compound **43** was converted into acetate **52** in 73% yields (scheme 21).

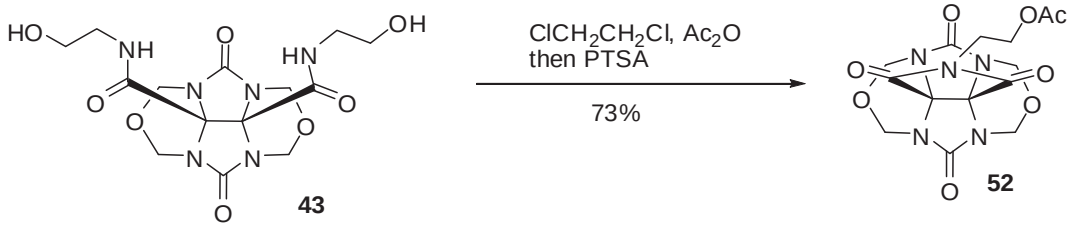

Scheme 21

Synthesized building blocks bearing free ureidyl group and bis-cyclic ethers could be used for construction of cucurbituril, its derivatives, and its congegenes.

The introduction of two aromatic arms would provide π-π-stacking surfaces that encourage strong interactions with substrate. However, aromatic amines have not been reported in such type of Mannich reaction, probably because aromatic amines have lower reactivity compared to aliphatic amines. Other group has developed a new generation of molecular clips from acid 1 with stronger binding capability and rigidity (Scheme 22) [44].

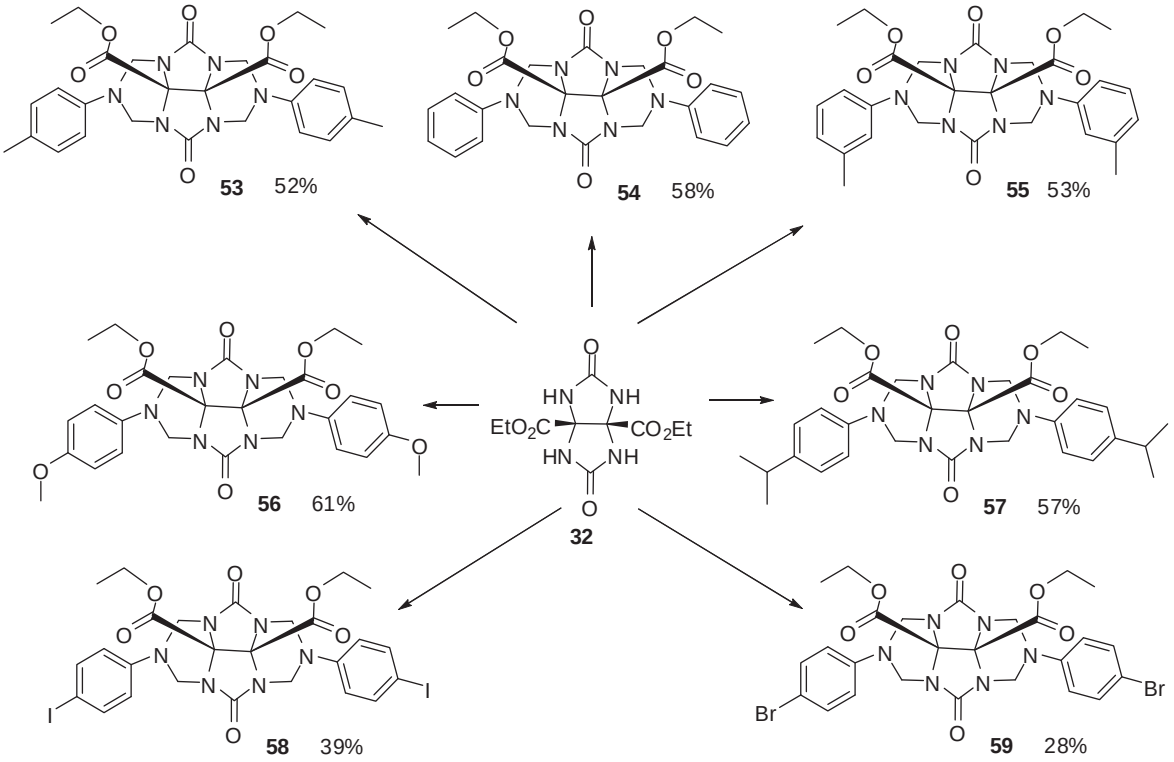

Scheme 22

The esters 32 reacted with aromatic amines in presence of 37% aqueous formaldehyde with formation expected substances 53-59.

Electron-rich amines like para-nitroaniline and para-aminopyridine have not reacted, even when the temperature was elevated and the reaction time was prolonged. DMF was the optimal reaction solvent, because diethoxycarbonyl glycoluril 32 and the products have good solubility characteristics.

Synthesized clips 53-59 can bind 1,3-dihydroxy-substituted aromatic quests by means of hydrogen bonding between the hydroxyl groups of the guest and the urea carbonyl group of the host and by π-π-stacking interactions between the guest and the host sidewall. However such investigation has been realized.

One area of glycoluril derivatives that has been less well explored is their utilization as fluorescent chemosensors for anions [45].

A novel class of fluorescent diethoxycarbobyl glycoluril derivatives with aryl alkyne side chains 61-68 starting from dihydroxyfumaric acid 1 was synthesized via alkylation and subsequent Sonogashira cross-coupling reactions according Scheme 23 [46].

Urea 32 was alkylated with 1,2-bis(bromomethyl)-4,5-dibromobenzene using *t*-BuOK as base in anhydrous DMSO in 59%. The variety of substrates were used in coupling reaction which accomplished using $Pd(PPh_3Cl_2)$/CuI as catalysts in presence of Et_3N in DMF at 100°C. The yields were not affected drastically in the presence of either electron-donating or electron-withdrawing group on arylacetylene. The photophysical properties of synthesized compounds were examined in MeCN. Substances 61, 64 and 65 exhibited a similar λ_{max} of emission (368-370 nm). Fluorescence maximum wavelengths of other derivatives differed from each other. Compared to 61 with an emission maximum at 370 nm, the imission spectrum of 68 exhibited a 32 nm bathochromic shift due to the larger π-conjugation of the naphthyl group as compared to that of the phenyl group of 61. Similarly, red shifts of compounds 62, 63 and 67 with respect to 61 were presumably attributed to more electron-donating nature of the substituent groups.

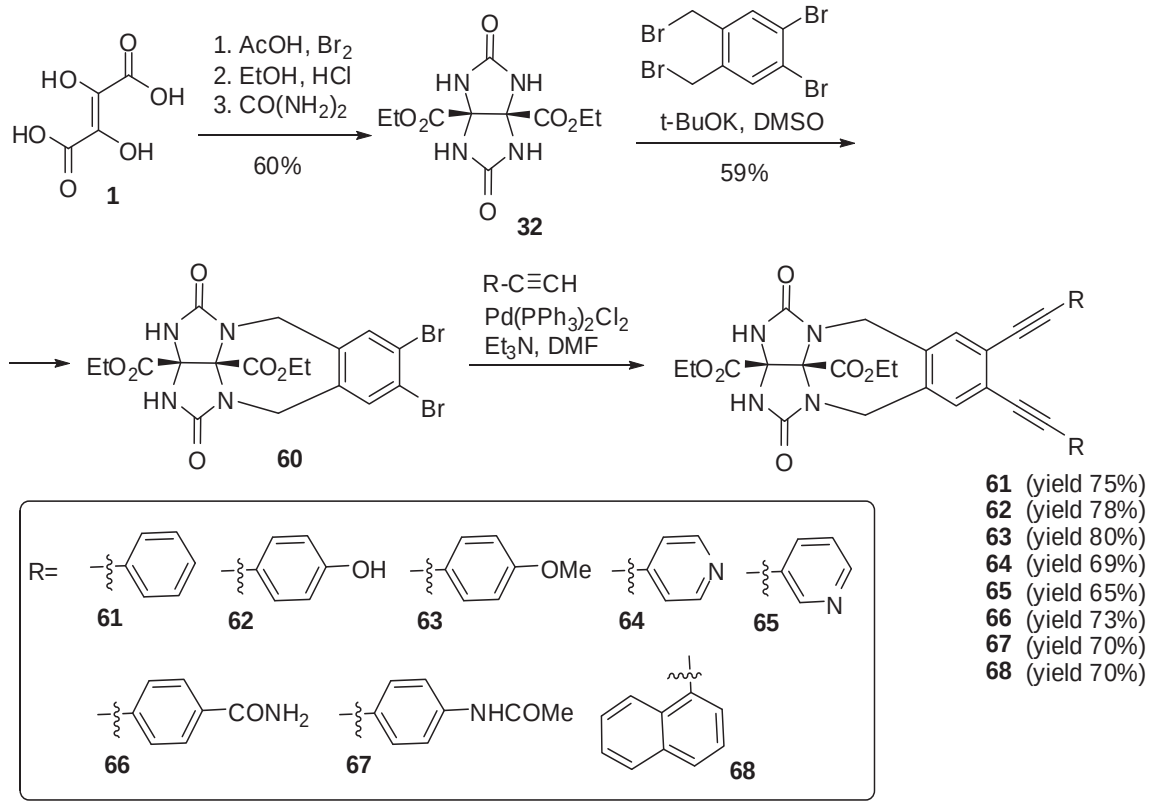

Scheme 23

4-Nitrophenol has mutagenic properties and its use in active ester coupling reactions and previously was complexed by cyclodextrin, calixarene, and cucurbit[*n*]uril molecular containers [47-52]. The synthesis and highly selective recognition properties of fluorescent molecular clip 70 toward 4-nitrophenol reported [53].

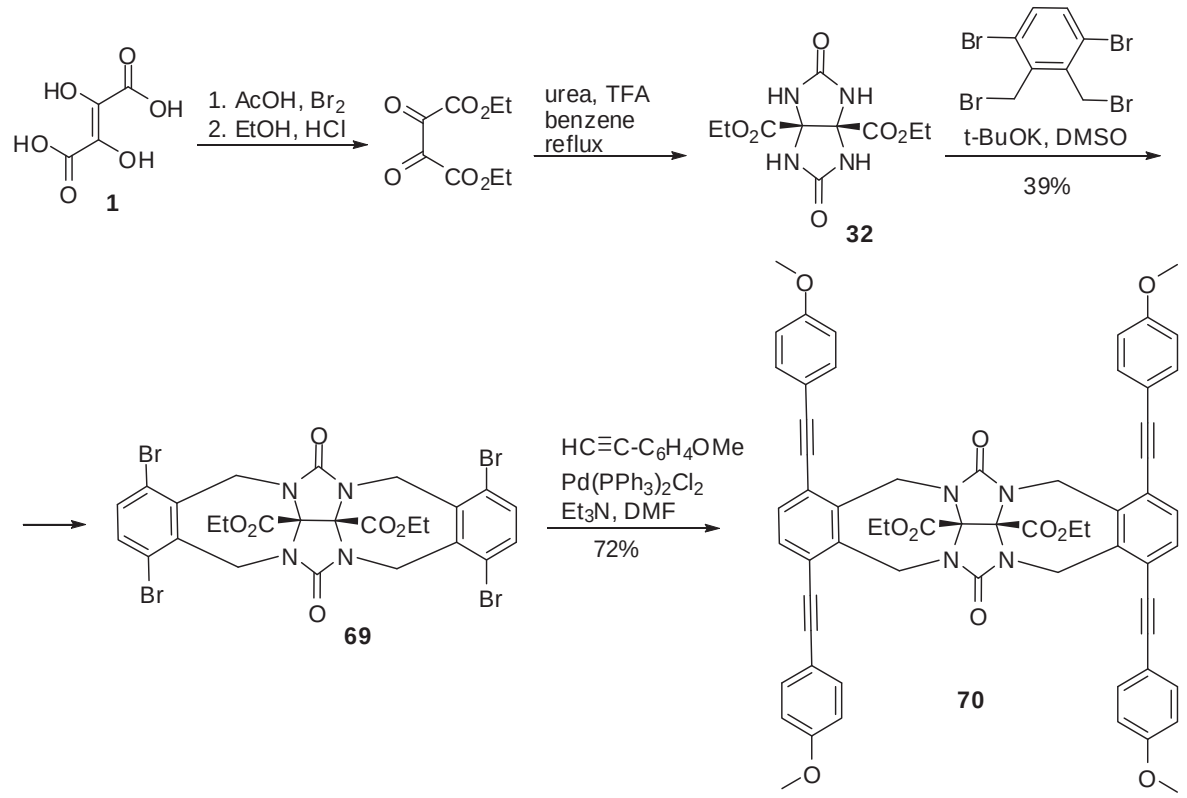

Scheme 24

Alkylation of compound 32 with two equivalent of 2,3-bis(bromomethyl)-1,4-dibromobenzene under basic conditions (see Scheme 19) gave product 69 in 39% yield. Installation of the 4-methoxyphenylethynyl arms by use known method [54] afforded molecular clip 70 in 72 % yield.

It should be noted that significant fluorescence quenching which was observed only for 4-nitrophenol but not for any of other phenols.

Many fluorescent molecular sensors and switches are known for heavy and transition metal ions such as Zn^{2+}, Hg^{2+}, Pb^{2+}, and Cu^{2+} have been developed [55-68]. But, there is examples of specific fluoresensors for Fe^{3+} still scarce [67-72].

Iron is an essential element for humans and plays an important role in biochemical and nutritional processes. Many proteins and enzymes contain ferric ions either for structural purposes or as part of a catalytic site [73].

A pair of novel molecular clips was synthesized from diethoxycarbonyl cyclic urea 35 and 1,2-dihydro-indazol-3-one together with an evaluation of its utility as a new class of as fluorescent Fe^{3+} sensor reported in [74]. Target molecules 71,72 were synthesized as outlined in Scheme 25.

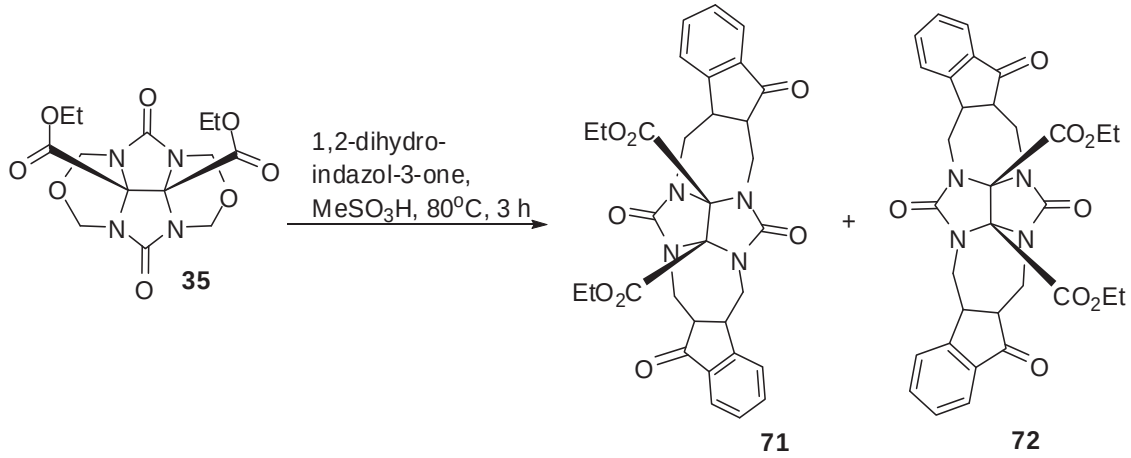

Scheme 25

The condensation of cyclic compound 35 with 2 equivalents of 1,2-dihydro-indazol-3-one in $MeSO_3H$ at 80°C according to the method [75] afforded the pair of diastereomers 71 and 72 in 35% and 26% yields, respectively.

The chemosensory behaviour of isomers 71 and 72 were investigated by fluorescence measurements. It was discovered that sensors 71 and 72 have a higher selectivity for recognition of Fe^{3+} then for K^{+}, Mg^{2+}, Hg^{2+}, Cd^{2+}, Zn^{2+}, Co^{2+}, Ni^{2+}, Cu^{2+}, Pb^{2+}, Ce^{3+} and Cr^{3+}. Moreover, since molecular clips 71 and 72 have the same functional groups but different structures and conformations, in the same conditions, the fluorescence emission response of substance 71 is higher than of isomer 72.

It has been reported that dihydroxyfumaric acid 1, in the presence of certain divalent metal ions, undergoes a sequence of oxidation and benzilic acid rearrangement to produce the trisubstituted methoxide ion $-OC(CO_2-)_3$, a previously undocumented oxidation of carbon, which generates the cubane-like core of a highly symmetrical octa-metallic complex [76]. Figure 2 represents a central molecule acting as a triple H-bond donor to one neighbor and as a triple H-bond acceptor from another neighbor.

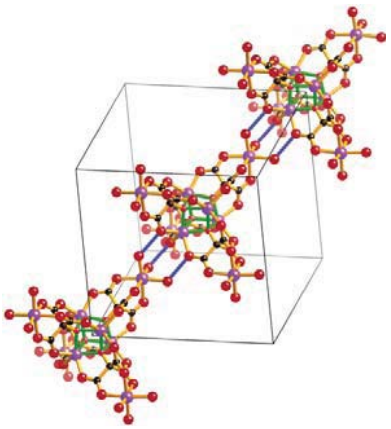

Figure 2. (Picture from [76]).

It was reported that 2,3-dihydroxyfumaric acid in the presence of certain divalent metal ions in basic aqueous solution goes through an aerial oxidation and rearrangement [76,77].

A coordination polymer of composition $[Zn_6(C_4O_7)(C_3HO_5)_3(H_2O)_6](H_3O)\ 8H_2O$ can be obtained in crystalline form (see Figure 3) from basic aqueous reaction mixtures at 40^0C containing Zn(II) together with dihydroxyfumaric acid 1 [78].

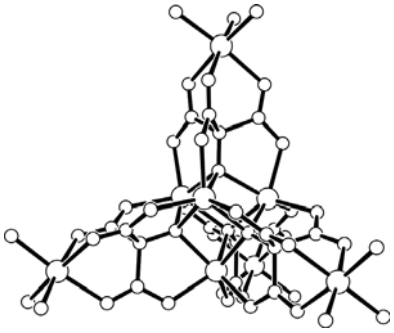

Figure 3 (from [78]).

This redox active compound 1 in basic aqueous solution can play a pivotal role in electron transfer processes, including acting as a reducing agent for a redox couple with high reduction potential and can exhibit rich electrochemistry.

On the other side, the stabilization of CuI complexes at open aerial atmosphere is a great challenge due to its intrinsic instability of the cuprous state and facile oxidation to Cu(II) [79,80].

It was reported the one step facile synthesis of CuI and CuI/CuII mixed-valent coordination frameworks from different CuII-salts in aqueous solution at aerial atmosphere using DHF acid 1 as a reducing agent according Scheme 26 [81].

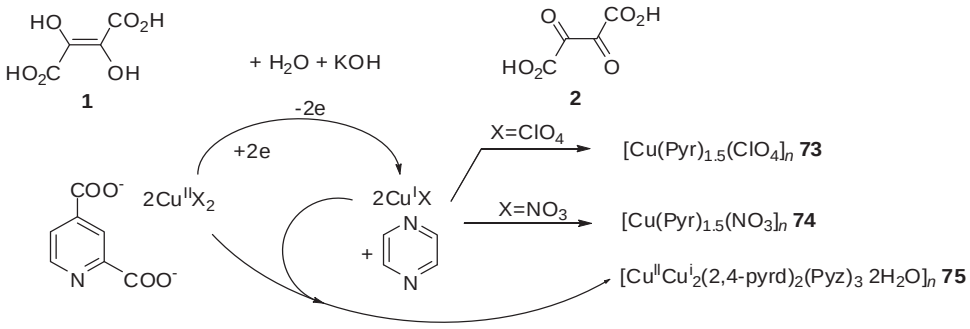

Scheme 26

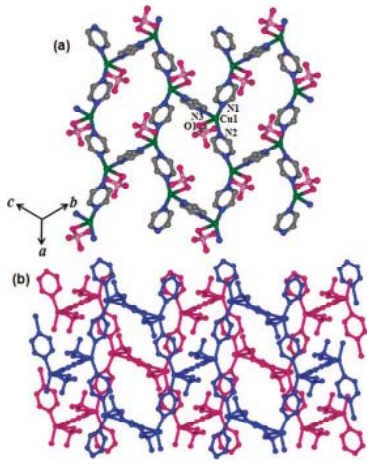

Figure 4

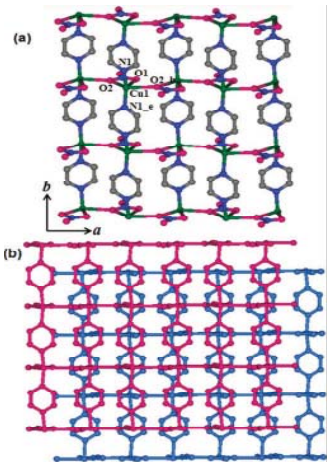

Figure 5

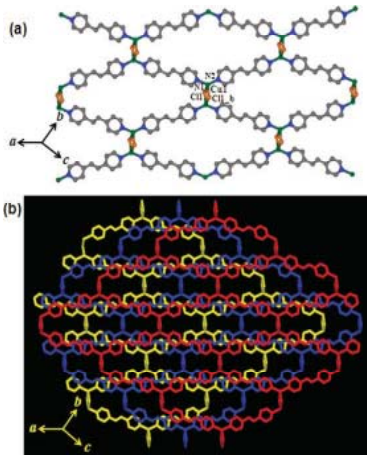

Figure 6

(Pictures from [81]).

By changing the counter-anions, authors were able to produce three different CuI-frameworks with pyrazine and 1,2-bis(4-pyridyl)ethylene linkers {Cu(pyrazine)1.5(ClO_4)}n 73 (Figure 3), {Cu(pyrazine)(NO_3)}n 74(Figure 4), and {[Cu(1,2-bis(4-pyridyl)ethylene)Cl]·2H_2O}n 75 (Figure 5) having different dimensionality and network topology and a mixed-valent porous CuI/CuII framework, [$Cu^{II}Cu^{I}_2$(2,4-pyridinedicarboxylate)3]·2H_2O}n 76 has also been isolated using suitable linkers 2,4-pyridinedicarboxylate and pyrazine by controlling Cu(II) and dihydroxyfumaric acid 1 stoichiometry.

4. Conclusions.

The aim of this review was to give an overview of the data about the occurrence of dihydroxyfumaric acid 1 in biological sources and its synthetic transformations into target products. We concentrated on reactions that relate to a single product. Methods are chosen for their novelty and we only discuss very significant developments and improvements regarding dihydroxyfumaric acid 1. The products derived from dihydroxyfumaric acid 1 can be successfully used to make other materials, but we feel that they will find greater application in the future, hence their position in the review.

5. References

[1]. Fenton, H. J. H., J. Chem. Soc. 1894, 65, 899-911.
[2]. Fenton, H. J. H., Brit. Assoc. Advance Sci. Rep. 1895, 663-671.
[3]. Fenton, H. J. H.; Wilks, W. A., J. Chem. Soc. 1912, 101, 1570-1582.
[4]. Hartree, E. F., J. Am. Chem. Soc. 1953, 75(12), 6244-6249.
[5]. Souchay, P.; Fleury, D.; Fleury, M., C. R. Acad. Sc. Paris 1967, 264, C, 2130-2133.
[6]. Neuberg, C.; Schwenk, E., Biochem. J. 1915, 71, 104-113.
[7]. Banga, I.; Szent-Gyorgyi, A., Z. Physiol. Chem. 1938, 266, 58-63.
[8]. Banga, I.; Philippot, E., Z. Physiol. Chem. 1939, 268,147-152.
[9]. Duca, Gh., PhD Thesis, SUM, Chisinau,1979.
[10]. Stafford, H. A.; Magaldi, A.; Vennesland, B., Science 1954, 120, 265-266.
[11]. Stepanow, A.; Kusin, A., Ber. Dtsch. Chem. Ges. 1934, 67, 723-726.
[12]. Fukunaga, K., J. of Biochem. 1960, 47(6), 741-744.
[13]. Rodopulo, A. K. Bases of winemaking biochemistry (in Russian), Light and food industry Publ., Moscow, 1983.
[14]. Сычев, А. Я., Дука, Г. Г. Виноделие и виноградарство МССР,1985, 12, p. 38.
[15]. Gonta, M., Dr.Sc. Thesis, SUM, Chisinau, 2008.
[16]. Gonta, M., Analele ştiinţifice ale USM, Seria „Ştiinţe chimico-biologice", Chişinău, 2006. p. 71
[17]. Porubin, D.; Hecht, S.; Li, ZZ.; Gonta, M.; Stepanov, I., J. Agric. Food. Chem. 2007, 55 (17), 7199-204.
[18]. Hartree, E. F., J. Am. Chem. Soc. 1953, 75, 6244-6249.
[19]. Goodwin, S.; Witkop, B., J. Am. Chem. Soc. 1954, 76, 5599-5603.
[20]. Secară, N.; Duca, Gh.; Macaev, F., The International Conference dedicated to the 50th anniversary from the foundation of the Institute of Chemistry of the Academy of Science of Moldova". 2009, p. 213.
[21]. Secară, N.; Duca, Gh.; Macaev, F., Chem. J. Moldova 2010, 5 (2), 59-67.
[22]. Yalpani, M.; Wilke, G., Chem. Ber. 1985, 118, 661-669.
[23]. Kemp, D. S.; Bowen, B. R.; Muendel, C. C., J. Org. Chem. 1990, 55, 4650-4657.
[24]. Day, A.; Arnold, P. P.; Blanch, R. J.; Snushall, B. J., Org. Chem. 2001, 66, 8094.
[25]. Buschmann, H. J.; Jansen, K.; Schollmeyer, E., Thermochim. Acta 2000, 346, 33-36.
[26]. El Houaj, M.; Young, H. K.; Luhmer, M.; Kim, K.; Bartik, K., J. Chem. Soc., Perkin Trans. 2. 2001, 2104-2107.
[27]. El Houaj, M.; Luhmer, M.; Ko, Y.; Kim, K.; Bartik, K., J. Chem. Soc., Perkin Trans. 2. 2001, 804-807.
[28]. Marques, C.; Nau, W. M., Angew. Chem. Int. Ed. 2001, 40, 3155-3160.
[29]. Wagner, B. D.; Fitzpatrick, S. J.; Gill, M. A.; MacRae, A. I.; Stojanovic, N., Can. J. Chem. 2001, 79, 1101-1104.
[30]. Mock, W. L.; Shih, N. Y., J. Am. Chem. Soc. 1988, 110, 4706-4710.
[31]. Mock, W. L.; Shih, N. Y., J. Org. Chem. 1986, 51, 4440-4446.
[32]. Mock, W. L.; Shih, N. Y., J. Org. Chem. 1983, 48, 3619-3619.
[33]. Tuncel, D., Steinke, J. H. G., Chem Commun. 2002, 496-497.
[34]. Mock, W. L.; Irra, T. A.; Wepsiec, J. P.; Manimaran, T. L., J. Org. Chem. 1989, 54, 5302-5308.
[35]. Lee, J. W.; Ko, Y. H.; Park, S. H.; Yamaguchi, K.; Kim, K., Angew. Chem. Int. Ed. 2001, 40, 746-749.
[36]. Lee, E.; Kim, J.; Heo, J.; Whang, D.; Kim, K., Angew. Chem. Int. Ed. 2001, 40, 399-402.
[37]. Whang, D.; Park, K. M.; Heo, J.; Ashton, P.; Kim, K.; J. Am. Chem. Soc. 1998, 120, 4899-4900.
[38]. Jun, S. I., Lee; J. W., Sakamoto, S.; Yamagushi, K.; Kim, K., Tetrahedron Lett. 2001, 41, 471-475.
[39]. Mock, W. L.; Pierpont, J., J. Chem. Soc., Chem. Commun. 1990, 1509-1511.

[40]. Isobe, H.; Tomita, N.; Lee, J. W.; Kim, H. J.; Kim, K.; Nakamura, E., Angew. Chem. Int. Ed. 2000, 39, 4257-4260.
[41]. Jeon, Y. M.; Whang D.; Kim K., J. Am. Chem. Soc. 1996, 118, 9790-9791.
[42]. Burnett, C. A.; Lagona, J.; Wu, A.; Shaw, J. A.; Coady, D.; Fettinger, J. C.; Day, A. I.; Isaacs, L., Tetrahedron 2003, 59, 1961-1970.
[43]. Haido, T.; Rudkevich, D. M.; Redek, J. Jr., J. Am. Chem. Soc. 1999, 121, 11253-11254.
[44]. Yin, G.; Wang, Z.; Chen, Y.; Wu, A.; Pan, Y., Synlett. 2006, 1, 49-52.
[45]. Kang, J.; Kim, J., Tetrahedron Lett. 2005, 46, 1759.
[46]. She, N.; Gao, M.; Cao, L.; Yin, G.; Wu, A., Synlett. 2007, 16, 2533-2536.
[47]. Zheng, L. M.; Zhang, Y. Q.; Zeng, J. P.; Qiu, Y.; Yu, D. H.; Xue, S. F.; Zhu, Q. J., Tao Z. Molecules, 2008, 13, 2814-2822.
[48]. Kunsagi-Mate, S.; Szabo, K.; Lemi, B.; Bitter, I.; Nady, G., Kollar. Thermochim. Acta. 2005, 425, 121-126.
[49]. Saki, N.; Akkaya, E. U., J. Inclusion Phenom. Macrocycl. Chem. 2005, 53, 269-273.
[50]. Klaerner, F. G.; Kahlert, B., Acc. Chem. Res. 2003, 36, 919-932.
[51]. Buvari-Bareza, A.; Rak, E.; Meszaros, A.; Barcza, L., J. Inclusion Phenom. Macrocycl. Chem. 1998, 32, 453-459.
[52]. Zimmerman, S. C., Top. Curr. Chem. 1993, 165, 71-102.
[53]. She, N.; Gao, M.; Wu, A.; Isaacs, L., Org. Lett. 2009, 11 (12), 2603-2606.
[54]. Takahashi, S.; Kuroyama, Y.; Sonogashi, Y.; Hagihara, N., Synthesis 1980, 627-630.
[55]. Taki, M.; Wolford, J. L.; O'Halloran, T. V., J. Am. Chem. Soc. 2004, 126, 712-713.
[56]. Maruyama, S.; Kikuchi, K.; Hirano, T.; Urano, Y.; Nagano, T., J. Am. Chem. Soc. 2002, 124, 10650-10651.
[57]. Meng, X. M.; Zhu, M.Z.; Liu, L.; Guo, Q.X., Tetrahedron Lett. 2006, 47, 1559-1562.
[58]. Gong, H. Y.; Zheng, Q. Y.; Zhang, X. H.; Wang, D. X.; Wana, M. X., Org. Lett. 2006, 8, 4895-4898.
[59]. Xiang, Y.; Tong, A. J.; Jin, P. Y.; Ju, Y., Org. Lett. 2006, 8, 2863-2866.
[60]. Martinez, R.; Zapata, F.; Caballero, A.; Espinosa, A.; Tarraga, A.; Molina, P., Org. Lett. 2006, 8, 3235-3238
[61]. Xu, Z. C.; Xiao, Y.; Qian, X. H.; Cui, J. N.; Cui, D. W.; Org. Lett. 2005, 7, 889-892.
[62]. Wang, J. B.; Qian, X. H., Org. Lett. 2006, 8, 3721-3724.
[63]. Guo, X. F.; Jia, L. H., J. Am. Chem. Soc. 2004, 126, 2272-2273.
[64]. Nolan, E. M.; Lippard, S. J., J. Am. Chem. Soc. 2003, 125, 14270-14271.
[65]. Chen, Q. Y.; Chen, C. F., Tetrahedron Lett. 2005, 46, 165-168
[66]. Metiver, R.; Leray, I.; Valeur, B., Chem. Commun. 2003, 996-997.
[67]. Deo, S.; Godwin, H. A., J. Am. Chem. Soc. 2000, 122, 174-175.
[68]. Liu, J. M.; Bu, J. H.; Zheng, Q. Y.; Chen, C. F.; Huang, Z. T., Tetrahedron Lett. 2006, 47, 1905-1908.
[69]. Xiang, Y.; Tong, A., J. Org. Lett. 2006, 8, 1549-1552.
[70]. Tumambac, G. E.; Rosencrance, C. M.; Wolf, C., Tetrahedron 2004, 60, 11293-11297.
[71]. Liu, J. M.; Zheng, Q. Y.; Yang, J. L.; Chen, C. F.; Huang, Z.T., Tetrahedron Lett. 2002, 43, 9209-9212.
[72]. Bricks, J. L.; Kovalchuk, A.; Triefinger, C.; Nofz, M.; Buschel, M.; Tolmachev, A. I.; Daub, J.; Rurack, K., J. Am. Chem. Soc. 2005, 127, 13522-13529.
[73]. Vallee, B. L.; Auld, D. S. In Methods in protein Sequence Analysis. Jornvall H., Hoog J.O., Gustavsson A.M.Eds. Brikhauser, Basel. 1991.
[74]. Hu, S. L.; She, N. F.; Yin, G. D.; Guo, H. Z.; Wu, A. X.; Yang, C. L., Tetrahedron Lett. 2007, 48, 1591-1594.
[75]. Lagona, J.; Fettinger, J. C.; Issaacs, L., Org. Lett. 2003, 5, 3745-3747.
[76]. Abrahams, B. F.; Hudson, T. A.; Robson, R., J. Am. Chem. Soc. 2004, 126, 18624-8625.
[77]. Abrahams, B. F.; Hudson, T. A.; Robson, R., J. Chem. Eur. J. 2006, 12, 7095-7099.
[78]. Abrahams, B. F.; Hudson, T. A.; Robson, R., J. Mol. Struct. 2006, 796, 2-8.
[79]. Gandhi, B.A.; Green, O.; Burstyn, J.N. Inorg. Chem. 2007, 46, 3816-3820.
[80]. Masaoka, S.; Akiyama, G.; Horike, S.; Kitagawa, S.; Ida, T.; Endo, K. J. Am. Chem. Soc. 2003, 125, 1152-1153.
[81]. Mohapatra, S.; Maji T. K., Dalton Trans. 2010, 39, 3412-3419.

VOLTAMMETRIC BEHAVIOR OF SOME STEELS IN AQUEOUS SOLUTIONS OF HNO_3

Gheorghe Nemtoi[1], Liliana Airinei[2], Tudor Lupascu[3] and Alexandru Cecal[1*]

[1]*"Al. I. Cuza" University, Faculty of Chemistry, 11-Carol I Bvd., 700506 – Iasi, Romania*

[2] *Technical College "Gheorghe Cartianu", Traian Bvd., 610143, Piatra-Neamt, Romania*
[3]*Institute of Chemistry, Academy of Sciences of Moldova, Republic of Moldova*
[*]*Email: cecal@uaic.ro*

Abstract: The corrosion process of some steels immersed in HNO_3 solutions of different concentrations by means of voltammetric measurements was investigated. Even if the differences regarding the chemical composition of these steels were relatively low, it was succeeded to establish some electrochemical parameters (R_p, E_{corr}, E_{pc}, I_{pc} ,E_F, I_{pas}, E_{str} and D_{pas}) with different values, in several experimental conditions. For different values of the corrosion potential, or of the contact time solid steel-aggressive medium, were proposed equations of the type: $I = f(E)$,only for linear domains from the given voltammograms.

Keywords: corrosion, electrochemical parameters, nitric acid, steels, voltammograms,

Introduction

Studies on the global process of corrosion were published by several authors both in monographs and in detailed articles [1-7]. There are also scientific papers which deal only with certain aspects of the corrosion process. Thus, Caceres et al. [8] determined the electrochemical parameters and the corrosion rate of carbon steel in NaCl buffered solution, while Sing and Mukherjee [9] dealt with the kinetics of acid dissolution of some mild steels. Nemtoi et al. [10-14] characterized the electrochemical behavior of some steels or non-ferrous alloys in electrolyte medium, under different experimental conditions. Moraru et al. [15] investigated corrosion kinetics of the G105 and P105 steels in 3% NaCl and KCl solutions establishing that the anodic dissolution of iron is described by the exponential equations characteristic to the first order chemical reactions. Moreover there are developed some electrochemical techniques combined with the use of radionuclides, Möessbaer spectroscopy, electronic microscopy, or uv-vis spectrophotometry etc, for the elucidation of the corrosion processes [16-23]

This paper presents an electrochemical study on the corrosion of seven different steels immersed into HNO_3 solutions of different concentrations, pointing out certain parameters that describe the corrosion process in several experimental conditions.

Materials and equipment

The chemical composition of the steels used in the present paper is shown in table 1, the iron content being in the domain 97.772 – 98.782 % g.

Table 1

Chemical composition of the studied steels (% gr)

Steel sample	C	Si	Mn	P	S	Cr	Mo	Ni	Al	Cu	V
2	0.190	0.210	0.610	0.021	0.008	0.050	0.020	0.030	0.036	0.040	0.003
3	0.310	0.220	0.730	0.009	0.006	0.610	0.210	0.030	0.026	0.070	0.007
5	0.140	0.230	0.630	0.010	0.004	0.090	0.020	0.070	0.025	0.170	-
6	0.370	0.260	1.090	0.012	0.019	0.60	0.040	0.120	0.004	0.180	0.005
7	0.320	0.200	0.710	0.010	0.012	0.540	0.190	0.040	0.025	0.140	0.005
11	0.170	0.240	0.810	0.020	0.014	0.040	0.010	0.020	0.035	0.030	0.006
15	0.190	0.230	0.630	0.013	0.009	0.140	0.020	0.050	0.030	0.080	0.003

The experimental data obtained by linear polarization were afterwards processed by the Stern method, [24] using in all the cases the same values of the potential interval (E_{corr} ±15mV) to calculate the polarization resistance R_p.

Supplementary details on the processes that take place in the system may be obtained from analyzing the linear polarization curves on extended potential domains when it **(what is it?)** defines a critical polarization point [25]. This point corresponds to the maximum preceding the passivation process, passivity potential and current, passivation domain and penetration potential E_{str} – corresponding to the end of the passivation domain. These dimensions are pointed out for aqueous solutions of HNO_3, of 0.4 and 4M, while for the 0.04M solutions, over the whole or part of the potential domain, where appears a slight monotonous increase of the current (it is not clear). In order to modify the potential, we started

from a sufficiently high negative potential to reduce all the ionic or molecular species that impurified the alloy surface. The variation rate of the working electrode potential has been relatively high (10 mV/s) to obtain current intensities that be sufficiently to cover the possible accidental system fluctuations, yet sufficiently low to sense all the processes that take place in the solution or on the electrode surface.

For experiments the AutoLab PG STAT 302N Potentiostat (Olanda-Eco Chemie) was used coupled with a GPES software for data processing and interpretation, to determine the open circuit potential (OCP) and for performing the polarization studies. The potentiodynamic anodic polarization tests were performed in nitric acid solutions with 0.04; 0.4 and 4 M concentrations.

All potentiodynamic polarization experiments were performed at room temperature using an electrochemical cell with three electrodes. The reference electrode was the saturated calomel electrode (SCE) and as an auxiliary electrode a platinium wire (Pt) was used. The working electrode, achieved for each steel sample mentioned in table 1, processed in cylindrical form with a diameter of 5 mm embedded into a polymer matrix with 11 mm diameter, so that the part exposed to corrosion was a circular surface, without edges or corners. Before the experimental determinations the working electrodes were mechanically polished with SiC abrasive paper (120 - 2000 gradually) and aluminium paste of 1μm granulation, after which they were washed with water and degreased with ethanol. Before being used in the electrochemical cell, the electrodes were kept in distilled water where a ten minutes nitrogen flow was bubbled to remove oxygen.

Results and discussions

In aqueous solutions of HNO_3 the corrosion potential of metals is attributed to the main "electroactive" species, HNO_2 which is implied in the self-catalytic reactions [26-29].

In the anodic dissolution of iron and its alloys, an important role is played by the water molecules and the anions adsorbed on the metal surface, as a result, Sato [30] proposes the following simplified mechanism:

$$Fe + H_2O \rightarrow Fe(OH)_{ads} + H^+ + e^- \quad (1)$$

$$Fe(OH)_{ads} \rightarrow FeOH^+ + e^- \quad (2)$$

$$FeOH^+ \rightarrow Fe^{2+} + HO^- \quad (3)$$

The corrosion mechanisms of steels in nitric acid should take into account the concentration and the factors that promote trans-passive corrosion by increasing the corrosion potential [31-32]. The appearance of some nitrous acid "electroactive" species by self-catalytic reduction of HNO_3 can be explained due to NO_2 output. Depending on the nitric acid concentration, the temperature and the implied reduction agent, the final corrosion products may be different.

In case of higher concentrations of nitric acid (> 8M HNO_3) or at higher temperatures, the main heterogonous chemical reaction is the self-catalytic reduction of nitric acid to nitrous acid and NO_2 which accumulates in aqueous medium :

$$4HNO_3 \rightarrow 2H_2O + 4NO_2 + O_2 \quad (4)$$

$$NO_2 + e^- \rightarrow NO_2^- \quad (5)$$

$$NO_2^- + H^+ \rightarrow HNO_2 \quad (6)$$

$$HNO_2 + HNO_3 \rightarrow 2NO_2 + H_2O \quad (7)$$

In the case of lower temperatures and concentrations, the reduction of nitrous acid is the main electrochemical reaction and the final product is NO:

$$2HNO_3 \rightarrow HNO_2 + O_2 \quad (8)$$

$$HNO_2 + H^+ \rightarrow NO^+ + H_2O \quad (9)$$

$$NO^+ + e^- \rightarrow NO \quad (10)$$

$$NO + HNO_3 \rightarrow HNO_2 + NO_2 \quad (11)$$

For both the mechanisms, the self-catalytic reduction of nitric acid leads to oxidizers as NO, NO_2 and HNO_2. Similarly, the metal dissolution is self-catalytic in nitric acid because the oxidized cations from solution are available for reduction, as such accelerates the metal dissolution. The electrochemical cathodic reduction has proved to take place at smaller concentrations of HNO_3 (≤ 6M) while the reduction mechanism, followed by the "electroactive" species regeneration that lead to the self-catalytic dissolution of the metal, is real at higher concentrations of HNO_3 (11M), if it is referred to the inoxidable austenitic steels. As it noticed in the present paper, during the corrosion process of steels in the aqueous solutions of HNO_3 there appear brown-red colored precipitations (as rust) around the metallic samples

and may assert that in the respective reactant systems, after a certain contact time: steel-aggressive medium, different transformations may take place, as the following sequences show:

$$Fe + 2HNO_3 \rightarrow Fe^{2+} + 2NO_2 + 2HO^- \quad (12)$$

$$Fe^{2+} + HO^- \rightarrow FeOH^+ \quad (13)$$

$$FeOH^+ + HO^- \rightarrow Fe(OH)_2^+ + e^- \quad (14)$$

$$Fe(OH)_2^+ \rightarrow \gamma FeO(OH) + H^+ \quad (15)$$

$$H^+ + e^- \rightarrow \frac{1}{2}H_2 \quad (16)$$

$$3FeO(OH) + \frac{1}{2}H_2 \rightarrow Fe_3O_4 + 2H_2O \quad (17)$$

$$2FeO(OH) \rightarrow Fe_2O_3 + H_2O \quad (18)$$

The $FeOH^+$ and $Fe(OH)_2^+$ species are intermediaries resulting stable compounds FeO(OH), Fe_3O_4 and Fe_2O_3 fact that will lead to the modification of the respective steel initial structure.

Electrochemical investigations for the study of corrosion

To study the electrochemical corrosion processes, the potentiodynamic method in the variant of line polarization is frequently used [33-37]. The electrochemical polarization technique represents a rapid way to determine the behavior to corrosion of a metal in a given medium and to evaluate the thermodynamic tendency of this process, by immersing the metal or the alloy into an aggressive solution. The corrosion potential, E_{corr}, is a measure of the corrosion tendency of a metal or an alloy immersed into a given electrolytic medium, the modification of which may give indications on the active/passive behavior in metals and alloys. The corrosion potential may be determined by means of linear polarization curves, directly from the voltammogram as being the open circuit potential (OCP) or using the Evans diagrams by representing the logarithms of the current density depending on the potential of the electrode on a overpotential of ±50÷150 mV. In these coordinates, the crossing of the linear parts of the anodic and cathodic branches (as Taffel slopes) of the polarization curve gives, on the potential axis,the values of E_{corr}.

The method of linear polarization resistance serves to determine the corrosion current at the corrosion potential of an alloy by plotting the polarization curve obtained at relatively low overpotentials. The corrosion current determined by this way represents, in fact, the corrosion current that appears at the interface metal/corrosive medium when this solid sample is immersed into solution and cannot be measured directly by means of electrochemical methods. The method is based on the evaluation of the polarization resistance, $R_{p,}$ defined as the tangent slope of the potential curve – the current density [$E = f(j)$] in the poise (E = E_{rev} or overtension η = 0), namely the free corrosion potential:

$$R_p = \left[\frac{\Delta E}{\Delta j}\right]_{E=E_{rev}}, \quad (19)$$

Here, *j* is defined by the relation between measured current intensity (I) at an electrode with a given surface (S).

From potentiometric curves plotted in the coordinates $I = f(E)$, for the domain OPC ± 15mV it was determined the polarization resistance R_p. Such a graphic plot is exemplified below only for sample no.5, yet the values of this parameter are summarized in table 2.

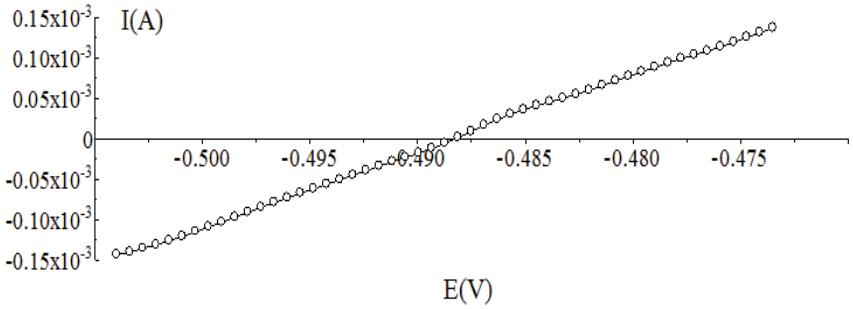

Fig. 1. The voltammogram plotted for sample 5 for determining the polarization resistance in aqueous solution 0.04M HNO_3

Table 2

Voltammetric parameters obtained by the Tafel slopes method

Steel sample	2	3	5	6	7	11	15
0.04 M HNO_3							
-OPC(V)	0.506	0.498	0.461	0.445	0.488	0.543	0.480
R_p (Ω)	111.6	112.4	163.5	64.2	228.5	123.1	112.2
0.4 M HNO_3							
-OPC(V)	0.430	0.344	0.374	0.374	0.357	0.408	0.363
R_p (Ω)	8.34	9.51	10.76	7.63	9.82	10.26	7.917
4.0 M HNO_3							
-OPC(V)	0.309	0.264	0.296	0.257	0.270	0.301	0.288
R_p (Ω)	3.029	2.391	2.177	1.537	1.897	2.343	2.266

The values of potential in the open circuit potential (OCP) were established for all the alloy samples immediately after the immersion of the work electrode into the solution (WE), that indicates the spontaneous formation of passivation film. The open circuit potential is identified with the corrosion potential (E_{corr}) due to the fact that the last is defined as the potential of an electrode measured compared to the control/reference (ER) when the current in the exterior circuit is zero. The transfer of the OCP values to more noble values (reduced) is linked to the more rapid increase of passivation film and this depends on the nature of the formed passive oxide stratum. The R_p values of all the samples are in the concentrated solution (4 M HNO_3), a fact that may be due to the generation of several reduction products of the nitrous "electroactive" species that accumulate during the corrosion process. The dissolution will take place with higher speeds at higher concentration due to the self-catalytic metal dissolution .

By means of the potentiodynamic method we traced the linear voltammograms on extended domain of: -0.6 ÷ 3.0 V out of which it highlighted the critical polarization potential, $E_{pc,}$ with the corresponding value of the I_{pc} current, the passivation potential or the Flade potential, E_F, the passivation current, I_{pas}, the penetrating potential, E_{str}, and the passive domain of each alloy (D_{pas}). These parameters are presented in table 3, characteristics obtained in concentrated solutions of 0.4 and 4 M HNO_3.

Table 3

Corrosion parameters obtained from the potentiodynamic method in solutions of 0.4 and 4 M HNO_3.

Steel sample	E_{corr}(V)	E_{pc}(V)	I_{pc}(mA)	E_F(V)	I_{pas}mA	E_{str}(V)	D_{pas}(V)
4 M HNO_3							
2	-0.309	0.187	63.6	0.342	2.107	1.624	0.34 – 1.62
3	-0.268	0.146	138.7	0.241	2.490	1.646	0.24 – 1.65
5	-0.300	0.413	31.8	0.653	3.723	1.534	0.65 – 1.54
6	-0.260	0.308	73.5	0.343	2.981	1.607	0.45 – 1.59
7	-0.273	0.347	136.6	0.374	2.356	1.683	0.37 – 1.68
11	-0.303	0.305	87.4	0.327	3.105	1.623	0.49 – 1.63
15	-0.292	0.272	78.28	0.355	1.273	1.678	0.35 – 1.68
0.4 M HNO_3							
2	-0.431	0.305	51.3	0.324	2.287	1.497	0.31 – 1.50
3	-0.344	0.290	48.2	0.320	1.656	1498	0.32 – 1.50
5	-0.390	0.336	50.3	0.499	2.309	1.571	0.49 – 1.57
6	-0.375	0.320	52.0	0.541	2.772	1.540	0.54 – 1.54
7	-0.361	0.433	56.5	0.475	3.420	1.558	0.47 – 1.56
11	-0.412	0.408	66.4	0.549	3.864	1.539	0.54 – 1.53
15	-0.368	0.339	49.3	0.476	2.373	1.497	0.47 – 1.50

The voltammograms obtained both in 4 M and 0.4 M HNO_3 solutions are similar for all the alloys studied an active domain being outstanding where the maximum current is I_{pc}, a passive domain, $D_{pas,}$ characterized by a medium current of passivation, I_{pas}, and at high values of the potential of 2.1 V, in the transpassivation domain there appear oscillating currents with amplitudes higher in the more concentrated solution as can be seen in fig. 3. In the solution 0.04 M HNO_3 the alloys behave differently, in the respect that the passive domain is no longer met, there exists a potential

interval in which the current grows lineary. This is also illustrated in fig. 3 where the voltammograms plotted for sample 3 in the three solutions of HNO_3 are shown.

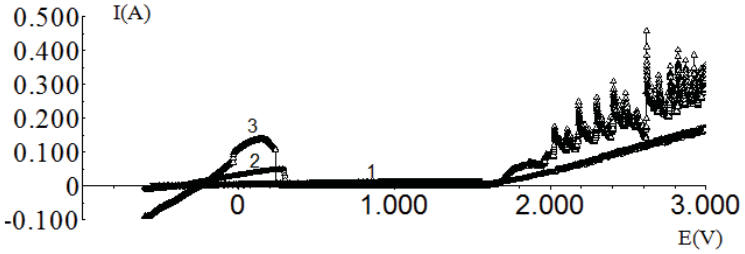

Fig. 3. The linear voltammograms obtained for sample 3 in solutions of different nitric acid concentrations at v=10mV/s; 1) 0.04M; 2) 0.4M; 3) 4M

In table 4, the values of the corrosion potential and the equations of the corrosion current dependency on the potential in its linear part are presented, where the linear correlation coefficient for all the alloy samples is 1.00.

Table 4

Some corrosion parameters obtained from the potentiodynamic method for steels immersed in 0.04 M HNO_3 solution

Steel sample	E_{corr} (V)	The liniar dependency domain (V)	Equation: I(A) = f(E)
2	-0.504	-0.593 – 3.000	$4.758 \cdot 10^{-3} + 9.812 \cdot 10^{-3}$ E(V)
3	-0.495	-0.389 – 0.989	$4.084 \cdot 10^{-3} + 8.114 \cdot 10^{-3}$ E(V)
5	-0.456	-0.564 – 2.122	$4.077 \cdot 10^{-3} + 9.30 \cdot 10^{-3}$ E(V)
6	-0.486	-0.570 – 2.498	$4.88 \cdot 10^{-3} + 10.31 \cdot 10^{-3}$ E(V)
7	-0.479	-0.574 – 3.000	$4.219 \cdot 10^{-3} + 10{,}22 \cdot 10^{-3}$ E(V)
11	-0.538	-0.599 – 3.000	$5.068 \cdot 10^{-3} + 9.396 \cdot 10^{-3}$ E(V)
15	-0.475	-0.596 – 1.729	$5.316 \cdot 10^{-3} + 11.42 \cdot 10^{-3}$ E(V)

In fig. 4 along with the polarization curve obtained with immersing sample 5 in a solution of 0.4 M HNO_3 (a), there is the curve obtained after 4h (b) from the immersion, where one may notice a modification of the critical polarization current (from 50.3 mA decreases to 36.95 mA) and the transfer of corresponding potential (from 0.336V to 0.243V), as well as the current oscillations after 2.1V.

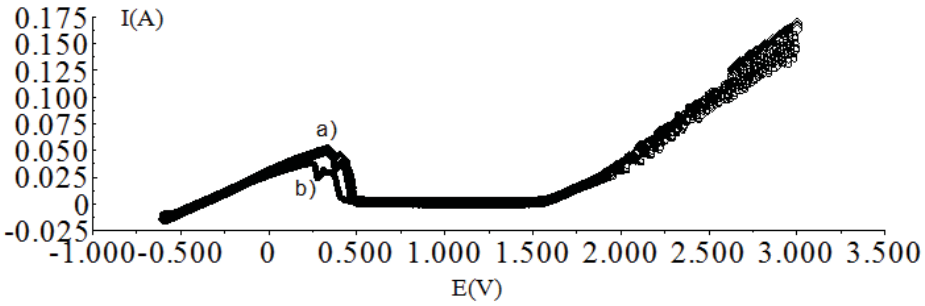

Fig. 4. The linear voltammograms obtained in 0.4M HNO_3 solution for sample 5 at v=10mV/s; a) initially; b) after 4 hours

In fig. 5 the in time modification of the polarization curve for sample 7 after being kept 18 hours in 0.04 M HNO_3, when the corrosion potential transfers to -0.507V (compared to -0.479V) and the corrosion current dependency is given by the equation is shown:

$I(A) = 3.875 \cdot 10^{-3} + 7.79 \cdot 10^{-3}$ E (V) on the whole potential domain (-0.6 – 3.0V).

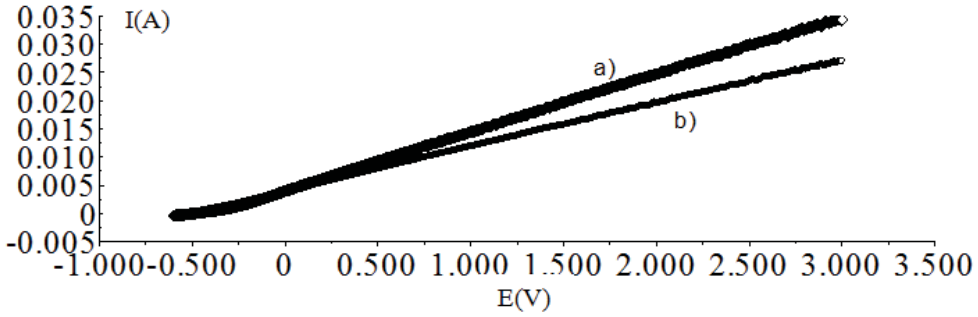

Fig. 5. The linear voltammograms obtained in 0.04M HNO_3 solution for sample 7 at v=10mV/s; a) initially, b) after 18 hours

Fig. 6 presents the linear voltammograms traced for sample 5 in 0.04 M HNO_3 solution at certain immersion moments.

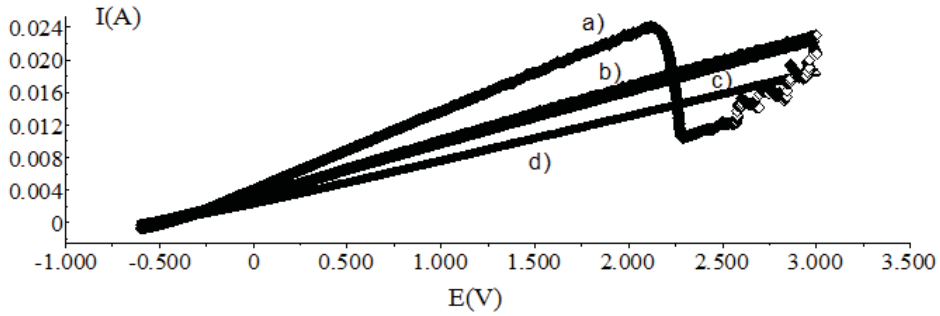

Fig.6. The linear voltammograms obtained in 0.04M HNO_3 solution for sample 5 at v=10mV/s; a) initially, b) after 44 hours, c) after 74 hours, d) after 98 hours

In table 5 the corrosion potential and the dependency of the corrosion current on the potential applied for sample 5 in 0.04 M HNO_3 at different immersion times are presented.

Table 5

Some corrosion parameters of sample 5 in a solution of 0.04 M HNO_3 at different immersion times.

Time from immersion (hours)	E_{corr} (V)	Potential domain (V)	Equation I(A) = f(E)
0	-0.456	-0.564 – 2.122	$4.077 \cdot 10^{-3} + 9.30 \cdot 10^{-3}$ E(V)
44	-0.525	-0.600 – 3.000	$3.226 \cdot 10^{-3} + 6.539 \cdot 10^{-3}$ E(V)
74	-0.547	-0.599 – 3.000	$2.693 \cdot 10^{-3} + 6.24 \cdot 10^{-3}$ E(V)
98	-0.564	-0.600 – 3.000	$2.353 \cdot 10^{-3} + 5.237 \cdot 10^{-3}$ E(V)

If the alloy sample immersion was done into the polarization curve at values higher than 2.10 V there appear current oscillations, which can be observed in table 5 after 44 hours for sample 5, or after 18 hours for sample 7 (fig. 5) .Here did not longer appear current oscillations, its dependency being linear up to 3.00V.

The electrochemical studies pointed out that the seven alloys considered are very close not only from the chemical composition, but also from the structural one, and the different microelements do not significantly change the voltammetric behavior. Yet, for given steels, it was noticed that the corrosion potential (E_{corr}) is higher in the case if the aggressive medium of HNO_3 has a lower concentration. This may be explained by the appearance of some iron oxide protection layers, which reduced the reaction rate on the steel surface undergoing corrosion, a fact that takes place faster when the HNO_3 concentration is higher.

The data obtained in the present paper are added to those published ahead [38-39], referring to the behavior of iron alloys in aqueous solutions of nitric acid having different concentrations.

Conclusions

There are determined experimentally some electrochemical parameters such as; R_p, E_{corr}, E_{pc}, I_{pc}, E_F, I_{pas}, E_{str} and D_{pas} , to characterize the corrosion process of seven steel samples immersed in different HNO_3 solutions. Taking into

account the obtained values from voltammetric studies it can pointed out the different behavior of steels, depending of experimental conditions. For more concentrated HNO_3 solutions the corrosion process develops more slowly due to formation of some protected oxide layers on the steel surface immersed in the aggressive medium. There are presented some mathematical equations having the variables: I=f(E) which described the steels behavior in the corrosion media.

References

[1]. Antropov, L.I., Teoreticescaia Elekrohimija, Visiaia Scolo, Moskva, 1984, p. 109.
[2]. Murgulescu, I.G., Radovici, O.M., Introduction in Physical Chemistry, vol.4, Electrochemistry, Romanian Acad. Ed., Bucharest, 1986, p. 361.
[3]. Oniciu, L., Metal Corrosion , Fundamental Aspects and Anticorrosion protection, Sci. Encicolop. Ed., Bucharest, 1986, p. 68.
[4]. Damaskin, B.B., Prakticum po elekrohimii, Visiaia Scola, Moskva, 1991, p.57.
[5]. Bockris, J.O'M.; Reddy, A.,Gambia-Adelco, M., Electrochemistry in Material Science, in: Modern Electrochemistry 2 B, Kluwer Academic/ Plenum Publ., New York, 1998, p. 1649.
[6]. Nemtoi, Gh., Electrochemistry – Fundamental Aspects , Tehnopress Ed., Iasi, 2011, p. 206.
[7]. Ahmad, Z., Principles of Corrosion Engineering and Control, Elsevier, Amsterdam, 2006, p.72.
[8]. Caceres, L., Vargas, T., Herrera, L., Corros.Sci., **49**, 2007, p. 3168.
[9]. Singh, S.K., Mukherjee, A.K., J. Mater. Sci. Technol., **26**, 2010, p. 268.
[10]. Sutiman, D., Cailean, A., Chiper, C., Nemtoi, Gh., Rev.Chim. (Bucharest), **54**, 2003, p.579.
[11]. Mareci, D., Bocanu, C., Nemtoi, Gh., Aelenei, D., J. Serb. Chem. Soc., **70**, 2005, p.891.
[12]. Gordin, D.M., Goriant, T., Nemtoi, Gh., Mat. Letters, **59**, 2005, p.2959.
[13]. Nemtoi, Gh., Secula, M.S., Cretescu, Ig., Petrescu, S., Rev.Chim., (Bucharest), **57**, 2007, p.952.
[14]. Nemtoi, Gh., Ionica, F., Lupascu, T., Cecal, A., Chem. J. Moldova, **5**, 2010, p.98.
[15]. Moraru, M., Dumitrescu, V., Schiopescu, A., Negoiu, M., Rev. Chim. (Bucharest), **58**, 2007, p.270.
[16]. Vogg, H., Braun, H., Loeffel, R., Lubecki, A., Merz, A., Schmitz, J., Schneider, J., Vehlow, J., J,Radioanal. Chem., **32**, 1976, p.495.
[17]. Cecal, A., Stan, V., Z. Phys. Chem. (Leipzig), **263**,1982, p.117.
[18]. Vehlow, J., KfK-Nachrichten, **15** ,1983, p.31.
[19]. Cecal, A., Electrochim. Acta, **28**, 1983, p.681.
[20]. Cecal, A., Isotopenpraxis, **20**, 1984, p.259.
[21]. Horany, G., Interface Science and Technology, vol.3., Elsevier B.V., Amsterdam, 2004, p.44.
[22]. Homonnay, Z., Szilagyi, P.A., Kuzmann, E., Varga, K., Nemeth, Z., Szabo, A., Rado, K., Schunk, J.; Tilky, P., Patek, G., J. Radioanal. Nucl. Chem., **273**, 2007, p. 85
[23]. Sobkowski, J., INCS-News, **7**, 2010, p.4.
[24]. Stern, M., Geary, A.L., J.Electrochem.Soc., **104**, 1957, p.56.
[25]. Gileadi, E., Electrod Kinetics for Chemists, Verlag Chemie, Weinheim, 1993, p. 73.
[26]. Balbaud, F., Sanchez G., Fauvet, P., Santarini, G., Picard, P., Corros, Sci., **42**, 2000, p.1685.
[27]. Armstrong, R.D., Cleland, G.E., J. Appl, Electrochem., **28**, 1998, p. 1205.
[28]. Balbaud, F., Sanchez, G., Santarini, G., Picard, G., Eur. J. Inorg. Chem., **2**, 1999, p. 277.
[29]. Kolman, D.G., Ford, D.K., Butt, D.P., Nelson, T.O., Corros. Sci., **39**, 1997, p. 2067.
[30]. Sato, N., Corros., **45**, 1989, p. 354.
[31]. Vertes, A.; Czako-Nagy, I. Electrochim. Acta, **34**, 1989, p. 721.
[32]. Jones, D.A., Principles and Prevention of Corrosion, McMillan, New York, 1992, p.115.
[33]. Mansfeld, F., The polarisation resistance techniques for measuring of corrosion current, in Advances in Corrosion Science and Technology, 6, Plenum Press, New York, 1976, p.163.
[34]. Oniciu, L., Constantinescu, E., Electrochemistry and Corrosion, EDP, Bucharest, 1982, p.61.
[35]. Fontana, M.G., Corrosion Engineering, McGraw-Hill, New York, 1987, p.12.
[36]. Kasparova, O.V., Baldokhin, Y.V., Kochetov, G.A., Prot. Metals, **40**, 2004, p. 425.
[37]. Ningshen, S., Kamachi Muladi, U., Amarendra, G., Raj, A., Corros Sci., **51**, 2009, p. 322.
[38]. Cecal, A., Popa, K., Draghici, C., Radiochim.Acta, **93**, 2005, p.115.
[39]. Cecal. A., Ionica, F.,Nemtoi, Gh., Popa, K., Rev.Roumaine Chim., **54**, 2009, p.1127.

THE INFLUENCE OF 2,3-DIHYDROXYBENZALDEHYDE THIOSEMICARBAZONE ON CATALYTIC CURRENTS IN THE SYSTEM MOLYBDENUM(VI) – POTASSIUM CHLORATE IN ACID SULFATE SOLUTIONS

Ludmila Chiriac[a], Tatiana Cazac[a], I. Povar[a]* and M. Revenco[b]

[a] *Institute of Chemistry, Academy of Sciences of Moldova,3 Academiei str., Chisinau MD-2028, Republic of Moldova*
[b] *State University of Moldova, 60 A. Mateevici str., Chisinau MD-2009, Republic of Moldova*
**E-mail: ipovar@yahoo.ca, Phone: +(373) 22 739736*

Abstract: The polarographic catalytic current in acid solutions of Mo(VI), 2,3-dihydroxybenzaldehyde thiosemicarbazone (TSC 2,3-DHBA) and chlorate ions has been investigated. The scheme of reactions, taking place in the solutions and on the electrode, has been proposed. The increase of the catalytic current is explained by the formation of an active intermediate complex [Mo(V)·TSC 2,3-DHBA (ClO^-_3)]. The rate constant of this complex formation $K = 2.56 \cdot 10^6$ $mol^{-1}\cdot dm^3\cdot s^{-1}$, the activation energy $E_a = 15.9$ $kcal\cdot mol^{-1}$ and the reaction activation entropy $\Delta S_a^{\neq} = -23.5$ e.u. have been calculated.

Keywords: voltammetry, catalytic current, molybdenum, thiosemicarbazone 2,3-dihydroxybenzaldehyde, chlorate of potassium.

Introduction

The influence of aromatic hydroxyl-containing compounds on the kinetics and mechanism of reactions in solutions involving molybdenum(VI), chlorate- [1-8] and bromate-ions [9] is rather different. So, in a solution with a small content of phenol and large enough concentrations of Mo(VI) and $KClO_3$ the maximum catalytic wave arises in the area of the potentials matching the second form of Mo(III) on electrode [2].

Catehol [1], 2,3-dihydroxybenzaldehyde (2,3-DHBA) [4] as well as mandelic acid (HMand) [3,5,6] stabilize certain forms of Mo(V) and Mo(III), formed during the polarographic stepwise reduction of Mo(VI) in solutions containing Na_2SO_4 as supporting electrolyte (pH 1 – 2.5). Two reduction waves for Mo(VI) complexes into Mo(V) and Mo(III) complexes were registered on polarograms. The presence of ClO_3^- ions proves a large increase of the catalytic current on the potentials of the first wave of reduction for Mo (VI). This effect allows an increasing of the sensitivity of the Mo(VI) determination.

The catalytic adsorptive voltammetry with accumulation [5-9] allows an additional increasing of the sensitivity for the molybdenum determination.

The present work is dedicated to the investigation of the nature of polarographic current in solutions containing Mo(VI), chlorate-ions and 2,3-dihydroxybenzaldehyde thiosemicarbazone (TSC 2,3-DHBA). The special attention is given to the influence of TSC 2,3-DHBA on the catalytic current in the system Mo (VI) – $KClO_3$, as well as to the comparison of these results with those obtained in the presence of Catehol [1], 2,3-DHBA [4] and HMand [3, 5-9].

Experimental part

The measurements of polarographic catalytic currents were carried out using the polarograph PU-1 (Russia) in the thermostated (25±0.1^{0}C) three-electrode cell containing: the MDE (2.45 $mg^{2/3}\,c\cdot^{-1/2}$) working drop electrode (**a**), the saturated calomel electrode (SCE) as a reference electrode (**b**) and a platinum wire as an auxiliary electrode (**c**).

The pH values were determined with an universal pH-meter with a glass electrode.

The initial molybdenum(VI) solution was prepared from the chemically pure $Na_2MoO_4\cdot 2H_2O$ salt. The purity of other reagents was of the analytical or chemically pure grades. The ligand standard solution (TSC 2,3-DHBA) with the concentration of $5\cdot 10^{-5}$ mol/dm^3 was prepared as follows: an exact weighted amount of the reagent was placed in a 200 cm^3 volumetric flask, then bidistilled water was added, the mixture was carefully mixed until the reagent full dissolution, filled up to the mark and mixed again. The aqueous solution of TSC 2,3-DHBA is unstable to light, thus every two day we prepared fresh solutions of this ligand.

Before the registration of the polarogram, the investigated solutions were deoxygenated by blowing off a current of the electrolytic hydrogen within 20 minutes.

Results and Discussion

In the Mo(VI) acid solutions at pH 1.0 – 2.5 in the presence of chlorate-ions on polarograms there are two catalytic waves. They correspond to the potentials of the first and the second reduction waves of Mo(VI) and testify the catalytic activity for both Mo(V) and Mo(III) species. In the presence of TSC 2,3-DHBA, the catalytic wave in the form of a big maximum, as well as for 2,3-DHBA [4], covers the area of potentials for the first and second waves. However under the conditions of the greatest display of catalytic effects and small concentrations of Mo(VI) (less than $5\cdot10^{-6}$ mol/dm^3), the potential of maximum corresponds to the first catalytic wave in the system Mo(VI) - ClO_3^-, i.e. its occurrence is associated with the formation of an active form of Mo(V).

The occurrence of a maximum and the current falling at potentials more negative than E_{max} are associated with a decreasing of the concentration of Mo(V) active form in the near-electrode layer and transformation of Mo(V) into Mo (III). Moreover, in solutions containing Mo(VI), an oxidant ($KClO_3$) and an organic surface-active ligand (TSC 2,3-DHBA), the occurrence of a wave in the form of a big maximum may be associated with the adsorption of the ligand and /or its complexes with Mo(VI), on the mercury surface. In such a case the concentration in the near-electrode layer is more important, the speed of the chemical reaction is increasing. This processus is determining the speed of the catalytic process entirely. It is necessary to note down that the catalyst complex particles are in the monomeric forme, when the molybdenum (VI) concentration in investigated solutions has been below $1\cdot10^{-4}$ mol/dm^3. In order to explain the nature of the maximum, we have investigated the influence of pH, temperature, height of the mercury column above the capillary as well as the concentrations of TSC 2,3-DHBA, Mo(VI) and ClO_3^- ions on the magnitude of the maximal current I_p.

The catalytic nature of the current in the system Mo(VI) - TSC 2,3-DHBA - ClO_3^- is proved by a high value of the temperature factor equal to 7 % per degree.

The independence of the current magnitude in solutions of Mo(VI) complexes with TSC 2,3-DHBA and ClO_3^- on the height of the mercury column above the capillary confirms the volumetric-kinetic nature of the rate for the rate-determining reaction of the catalytic process.

The dependence of the Ip value from concentration of the oxidant (KClO3), having the form of a curve with an inflection point and a saturation region (Fig. 1, curve 1) testifies about the formation of intermediate active complex (IAC).

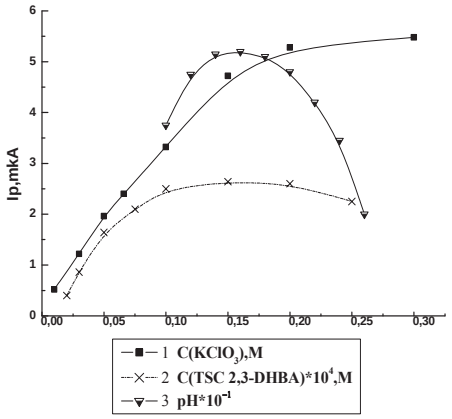

Fig.1. Dependence of I_p on the concentration of $KClO_3$, TSC 2,3-DHBA and pH: 0.2 M Na_2SO_4+ 0.05 M H_2SO_4 (pH 1.4-1.6). The concentrations: $1\cdot10^{-6}$ M Mo(VI) (curves 1, 2 and 3), $1.5\cdot10^{-5}$ M TSC 2,3-DHBA (1,3), 0.1 M $KClO_3$ (2) and 0.2 M $KClO_3$ (3).

The curve of Ip dependence on the ligand concentration (TSC 2,3-DHBA) passes through a maximum (fig. 1, curve 2).

Initially the activating action of the ligand is increasing with the growth of concentration, reaches a peak and then decreases. The presence of the ligand in the coordination area of the catalyst gives rise to acceleration of the IAC formation. When in the coordination sphere of catalyst there are seats accepting the oxidant species $KClO_3$, the catalytic process is in progress. If, under certain conditions the ligand blocks completely the coordination seats around the catalyst, its activity decreases. The maximal value of the current has been observed at the ligand concentration equal to $1.5\cdot10^{-5}$ mol/dm^3.

The optimal pH range is 1.5 – 1.6.The influence of the pH value (fig. 1, curve 3) may be connected with generation of a suitable for coordination form of the molybdenum and/or of the ligand, controlled by photolytic equilibra. Moreover, the ions of hydrogen participate in the redox reaction leading to the regeneration of depolarizer.

The dependence of the catalytic current magnitude on various concentration factors in solutions of Mo(VI) complexes containing 3-DHBA or TSC-2,3-DHBA has the similar character, and is explained by a common mechanism of the catalytic process in these systems. The general scheme of the catalytic process in such systems can be presented by following chemical and electrochemical reactions (for simplicity charges of particles are omitted):

1) Formation in solution of a complex of molybdenum (VI) with the organic ligand L

$$Mo(VI) + L \leftrightarrow [Mo(VI)L] \quad (1)$$

2) Reduction of the formed complex on electrode

$$[Mo(VI)L] + e^- \rightarrow [Mo(V)L] \quad (2)$$

3) Formation of an intermediate active complex with the oxidant species (ClO_3^-) and its adsorption on the electrode surface

$$[Mo(V)L] + ClO_3^- \leftrightarrow [Mo(V)L(ClO_3^-)] \leftrightarrow [Mo(V)L(ClO_3^-)]_{ads.} \quad (3)$$

4) Redox-regeneration of the catalyst.

The IAC, formed according to the reaction (3), undergoes further changes leading to its disintegration in addition to the catalyst regeneration. As it has been shown by the authors [10] by studying the system Mo(VI) – $H_2C_2O_4$ – ClO_3^-, the redox regeneration of the catalyst can occur by two ways:

a) In the polarographically–active complex (PAC) $[Mo(V)L(ClO_3^-)]$ an electronic charge transfer from molybdenum on the oxidant (ClO_3^-) with a subsequent intracomplex oxidation and regeneration of the catalyst in its higher degree of oxidation, takes place

$$[Mo(V)L(ClO_3^-)]+2H^+ \rightarrow [Mo(VI)L]+ClO_2^{\cdot} + H_2O \quad (4)$$

b) An electronic density shift in the PAC from the oxidant to molybdenum occurs and as a result the catalyst is regenerated in the lowest oxidation degree

$$[Mo(V)L(ClO_3^-)]+2H^+ +e^- \rightarrow [Mo(V)L]+ClO_2^{\cdot} + H_2O. \quad (5)$$

The authors of [10] have shown that on the polarograms of molybdenum(VI) and $H_2C_2O_4$ in the presence of ClO_3^- ions , two waves can be observed, second wave being higher the first one. For small Mo(VI) concentrations and $H_2C_2O_4$ concentrations ($\approx 2.5\cdot10^{-3}$ mol/dm^3) only one peak on the polarograms, matching the catalytic current of reduction of complexes Mo (V) in Mo (III) is registered. For this reason authors considered that the catalyst regeneration occurs in its lowest degree of oxidation according equation (5). In our researches we have found, that for small ligand (concentrations (< 3·10- mol/dm^3), one high sharp maximum corresponding to the first wave of reduction of the complex Mo(VI) to Mo(V) has been registered, and therefore it is more probable that the catalyst regeneration proceeds according to the first mechanism, i.e. the catalyst is regenerated in the highest oxidation state.

The investigation of Mo(VI)-Catehol-ClO_3^- [1, 2] and Mo(VI)–2,3-DHBA–ClO_3^- systems [4] show that for small concentrations of ligand ($<5\cdot10^{-5}$ mol/dm^3) one sharp peak is observed on polarograms (see fig. 1, curve 3 [1]). With an increasing of the catehol or 2,3-DHBA concentrations , this peak becomes larger, without a clearly expressed top and the current decreases to more negative potentials. By a further increase of the ligand concentration ($>5\cdot10^{-5}$ mol/dm^3) [4], the peak bifurcates and for concentrations more than $1\cdot10^{-4}$ mol/dm^3 the second maximum becomes slightly higher than the first one. It is quite likely, that this phenomenon is associated not only with an adsorption of complexes on the electrode surface as it was supposed in [6], but also with a regeneration of the catalyst in its lowest degree of oxidation. For TSC 2,3-DHBA the study of influence of higher concentrations on I_p is impossible because of its poor solubility.

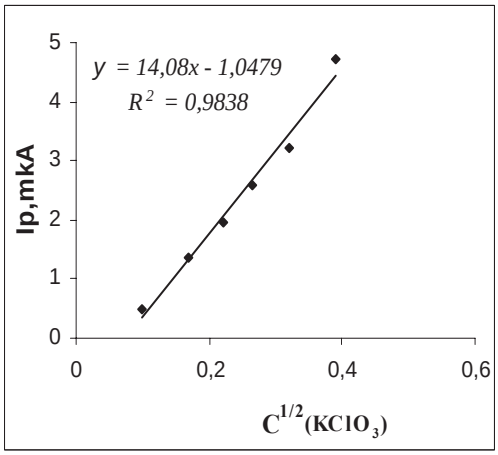

Fig.2. Dependence of I_p on $C^{1/2}(KClO_3)$ with $1\cdot10^{-6}$ M Mo(VI), $1.5\cdot10^{-5}$ M TSC 2,3-DHBA , pH 1.45.

The reaction (3) is the rate limiting and consequently defines the rate of electrode process. The rate constant of PAC formation has been calculated according to Koutetski's equation $i_k/i_d=0{,}81\sqrt{nKC_s t}$ in solutions with the TSC 2,3-DHBA concentration of $1.5\cdot10^{-5}$ mol/dm^3 in the area of I_p linear dependence on $C^{1/2}(KClO_3)$ (fig.2), i.e. in conditions of a pseudo-ion-molecular reaction (where i_k is the catalytic current equal to I_p-I_d; I_d – diffusion current of reduction of the complex Mo (VI) into Mo (V), recalculated for the Mo (VI) concentration of $1\cdot10^{-6}$ mol/dm^3, n – the number of electrons equal to 1; Cs – concentration of oxidant $KClO_3$ and τ is the dropping period of capillary, 3.6 s).

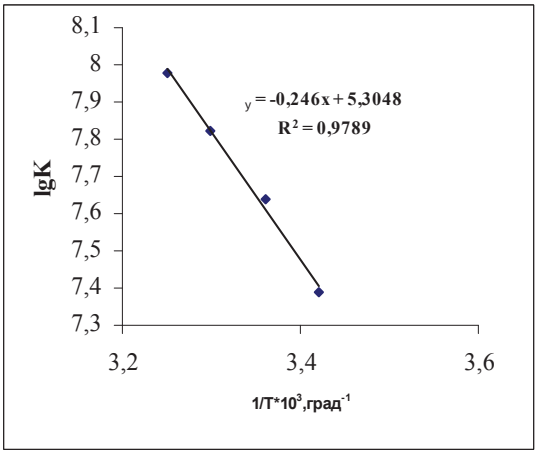

Fig.3. Dependence of log K on 1/T for $1\cdot10^{-6}$ M Mo (VI), $1.5\cdot10^{-5}$ M TSC 2,3-DHBA, pH 1.5.

From the function log K = f(1/T) (fig. 3) within the temperature range of 20 – 35ºC the activation energy and entropy have been calculated according to [11]. The values of the PAC formation rate constant, as well as its activation energy and entropy are presented in Table 1.

Table 1

Kinetic and thermodynamic characteristics of catalytic processes in solutions of Mo (VI) with catehol, 2,3-DHBA, TSC 2,3-DHBA or HMand complexes and chlorate-ions

Ligand - activator	$K\cdot10^6$, $mol^{-1}\cdot dm^3\cdot c^{-1}$	E_a, $kcal\cdot mol^{-1}$	$\Delta S_a^{\pm}$, e. u.	References
Catehol	8.2	16,6	-26,0	1
2,3-DHBA	2.5	14,0	-28,3	4
TSC 2,3-DHBA	2.56	15.9	-23.5	-
HMand	220	14,3	-20,4	3

The found values of the rate constant for PAC formation [Mo(V) TSC 2,3-DHBA (ClO_3^-)], its activation energy and entropy testify about a high catalytic activity of systems. According to the activation influence, TSC 2,3-DHBA is close to catehol and 2,3-DHBA. The large negative values of entropy recognize the spatial difficulties arising at the introduction of ClO_3^- ions in the coordination sphere of Mo(V) complexes. As it can be seen from the values of activation entropy (Table 1), the involvement of ClO_3^- ions in the coordination sphere of Mo(V) complexes with HMand and TSC 2,3-DHBA occurs easier; therefore the activation action of this ligand is higher. On the polarograms of Mo(VI) complexes with TSC 2,3-DHBA and HMand in the presence of $KClO_3$, the peaks have the highest I_p values. The minimum concentration of Mo(VI) ensuring the appearance of the peak on the polarogram is $4\cdot10^{-8}$ mol/dm^3 in the case of HMand while for TSC 2,3-DHBA this value is $2.5\cdot10^{-8}$ mol/dm^3

The catalytic reaction in the system Mo(VI) - TSC 2,3-DHBA - ClO_3^- is very selective and can serve for the metal – catalyst determination of the molybdenum. The optimal conditions for this determination are following: $1.5\cdot10^{-5}$ mol/dm^3 TSC 2,3-DHBA, 0.2 M $KClO_3$, 0.2 M Na_2SO_4, 0.05 M H_2SO_4 (pH 1.4 – 1.6). The linearity of the function $I_p = f(C_{Mo})$ was observed in the concentration range $(0.25 – 10)\cdot10^{-7}$ mol/dm^3. For the Mo(VI) determination the presence of Tl (I), Cu (II), Pb (II), Mn (II), Zn (II), Co (II), Ni (II), Bi (III), Cr (III), Sn (IV), Te (IV), Se (IV) in the ratio 1:10; As (III), Sb (III), Fe (III), W (VI) in the ratio 1:1 do not interfere. The presence of large amounts of As (III), Sb (III), Fe (III)

and any amounts of V (V) and Cr (VI) leads to an increase of the Mo(VI) catalytic wave. The study of this influence is a purpose of our further research. At the ratio Mo(VI) : W(VI) > 1:1, I_p of molybdenum decreases, that is related, possibly, with an involvement of ligand in the complex formation with W(VI) and the formation of catalytic waves of tungsten.

Mandelic acid has been proposed for analytical purposes and is used owing to its good solubility and greater stability. Using the catalytic current of chlorate-ions, Mo (VI) in the presence of HMand has been determined in lizimetric solutions and plants (tobacco leaves, hay beans ashes) [3]. The use of catalytic voltammetry with an adsorptive accumulation has allowed to authors [5-9] developing sensitive methods of the Mo (VI) determination in natural waters [5], while using tairon as a ligand – in river, well and artesian waters, in cucumbers, tomatoes and carrots [8]. The perspective to use the system Mo(VI)) - TSC 2,3-DHBA - ClO_3^- for determination of molybdenum is attractive by its selectivity.

Conclusions

The polarographic catalytic currents in acid solutions, containing Mo(VI), chlorate-ions and 2,3-dihydroxybenzaldehyde thiosemicarbazone (TSC 2,3-DHBA) have been investigated, the schemes of the reactions proceeding in solution and on electrode were proposed. The increase of the catalytic current in the presence of ligand is explained by the formation in solution of an intermediate active complex [Mo(V) TSC 2,3-DHBA (ClO_3^-)]. The rate constant of this complex formation $K = 2.56 \cdot 10^6$ $mol^{-1} \cdot dm^3 \cdot s^{-1}$, the activation energy $E_a = 15.9$ $kcal \cdot mol^{-1}$ and the reaction activation entropy $\Delta S_a^{\neq} = -23.5$ e.u. have been calculated.

These values testify about the high catalytic activity of the studied system. The possibility of the molybdenum determination by means of the catalytic current has been shown.

Acknowledgments

This work was done with the support of the SCOPES 2009-2012 joint research grant

References

[1]. Chikryzova, E.G.; Chiriac, L. The determination of pyrocatechol and oxy-acids using the polarographic catalytic current in solutions of molybdenum (VI) and chlorate-ions / J. Anal. Chem.- 1974 – V. 29, No 12 – p. 2420 – 2426.

[2]. Chiriac, L.; Chikryzova, E.G. The influence of some aromatic hydroxyl-containing compounds on the kinetics and the mechanism of reactions in the solutions of molybdenum (VI) and potassium chlorate. In ” Kinetics and the mechanism of heterogeneous and homogeneous chemical processes ”. Chisinau: Stiinta (Russ.), 1977. – P. 24 – 31.

[3]. Bardin, S.M.; Chikryzova, E.G. Studying of activating influence of mandelic acid and its polarographic determination in acid sulphate solutions of molybdenum and potassium chlorate / J. Anal. Chem.- 1978 – V. 33, No 2 – p. 358 – 363.

[4]. Chiriac, L.; Revenco, M.; Cazac, T.; Cecoi N. The influence of some hydroxyl containing ligands on the polarographic catalytic current in the system Mo(VI) – potassium chlorate / The Int. Conf. dedicated to the 50th Anniversary from the Inst. Chem. Acad. Sci. Moldova. Book of abstracts. Chisinau, 2009 – P.219.

[5]. Kunihiko Yokoil; van den Berg, C.M.G. Simultaneous determination of titanium and molybdenum in natural waters by katodic stripping voltammetry /Anal. Chim. Acta. – 1992 – V.257, No 2. – p. 293 – 299.

[6]. Quentel, F.; Mirceski, V. Catalytic adsorptive stripping voltammetry of molybdenum: redox kinetic measurements / Electroanalysis – 2004 – V.16, No 20. – p.1690 – 1696.

[7]. Safari, A.; Sharns, E. Selective determination of ultra trace concentrations of molybdenum by catalytic adsorptive stripping voltammetry / Anal. Chim. Acta – 1999 – V.396, No. 2-3. – p. 215 – 220.

[8]. Ensafi, Ali A.; Khaloo, Shokooh S. Determination of traces molybdenum by catalytic adsorptive stripping voltammetry / Talanta – 2005. – V. 65 - p. 781-788.

[9]. Li, Hong; Smart, Ronald B. Square wave catalytic stripping voltammetry of molybdenum complexed with dihydroxynaphtalene / J. Electroanal. Chem. – 1997 – V. 429, No 1-2. – p. 169 – 174.

[10]. Bersuker, I.B.; Bardina, S.M. The relation between the electronic structure of molybdenum oxalate complexes and their catalytic activity / Teor. and Experim.. Chem. (Russ.) – 1977 – V. 13, No 14. – p. 455 – 463.

[11]. Koldin, E. Quick reactions in the solutions (Russ.) M.: Mir – 1966- 285 p.

TO THE EQUILIBRIUM MODEL CHOICE IN HETEROGENEOUS AQUEOUS SYSTEMS. 1. THEORETICAL BASIS IN THE CASE OF TWO COEXISTING SOLID PHASES

I. Povar*, Nina Timbaliuc, Tatiana Cazac,
Diana Shepel, Oxana Spinu and Ludmila Chiriac

Institute of Chemistry, Academy of Sciences of Moldova,3 Academiei str., Chisinau MD-2028, Republic of Moldova
**E-mail: ipovar@yahoo.ca, Phone: +(373) 22 739736*

Abstract: An approach has been developed to determine the equilibrium model in heterogeneous aqueous systems containing a mixture of solid phases from the initial composition of the heterogeneous mixture and the equilibrium values of the pH. This approach allows to significantly reduce the quantity of measured data, properly for solubility measurements. By using the new deduced equations it is possible to determine the solubility products of precipitates on the basis of the known composition of initial mixtures and pH values of saturated solutions avoiding some difficult experimental solubility measurements. The derived relations are useful for solving both direct and indirect equilibrium problems.

Keywords: equilibrium model, heterogeneous system, solubility product, pH value, solid phase.

Introduction

The full definition of *equilibrium model* includes the number, nature and stability of chemical species in considered systems [1-4]. Actually, the equilibrium model refers to a set of equilibrium equations and the associated equilibrium constants. The objective of this study is to develop a new method for choice of equilibrium model characteristics that will allow to significantly reducing the number and volume of measured data.

We will analyze the heterogeneous aqueous systems in which, depending on the medium acidity, various individual solid phases may occur. We will be also taking into account the possibility of coexistence of individual precipitates, especially in the cases of closed values for their product solubility values $pK_S = - log K_S$.

There are two main methods to obtain the equilibrium (thermodynamic) constants that characterize the species stability in solid and liquid phases:

a) *Solubility method* or the *method of residual concentrations*. The relation between experimental data obtained by these two methods was revealed in papers [5-7]. Accurate measurement of solubility of sparingly-soluble compounds often requires special experimental consideration and approaches. The traditional saturation shake-flask procedures for measuring the equilibrium solubility are manually intensive, time- and sample-consuming, and may be prone to systematic errors not easily recognized, especially when the pH is not carefully measured, when aggregation or complexation reactions take place (unexpectedly altering spectroscopic properties), or when highly insoluble substances are considered (exceeding the sensitivity of the analytical method) [8].

b) *Potentiometric method* for determination of all the component activities of the precipitate (or precipitates) in saturated solutions [5-7]. This method allows to examine poorly soluble compounds not only in dilute solutions, but in concentrated solutions and in the presence of other electrolytes as well. Recently a new potentiometric method has been proposed which overcomes some of the limitations of standard approaches [9-13]. The new automated potentiometric method [9] was shown to be reliable for determining the solubility-pH profiles of the uncharged substances. Its speed compared to conventional equilibrium measurements (entire solubility-pH profile in 3-10 hr), its sound theoretical basis [9], its ability to generate the full solubility-pH profile from a single titration, and its dynamic range (estimated to be seven orders of magnitude) make the new pH-metric method an attractive addition to traditional approaches.

The first method is associated with complex measurements of the solubility of compounds (or their residual concentrations), while the second one is limited by a narrow assortment of existing stable and reproducible ion-selective electrodes.

Original methods for the determination of solubility products of poorly soluble hydroxides, acids salts and complexonates, based on the potentiometric measurement of only equilibrium pH values of heterogeneous systems as functions of the initial concentrations of the precipitate components, which are known when preparing the mixture were developed in [5-7]. The values for the equilibrium constants as well as the equilibrium and residual concentrations calculated for a series of real systems from known experimental data were in good accordance with those reported in literature under the same conditions.

As it will be shown in this paper, our approach for determining species solubilities and equilibrium constants, based

on new developed equations that require less quantity (and number) of needed experimental data, can be successfully applied as well for the heterogeneous systems containing two coexisting solid phases (precipitates).

Theory, Results and Discussion

The methods of the potentiometric determination of product solubility K_S values for sparingly soluble acids and bases (the systems of type ***a***) as well for sparingly soluble salts of different compositions, in the case of a single solid phase formation (the systems of type b) (avoiding solubility measurements) were developed in [5-7]. For the systems ***a*** and ***b*** the equations for calculating K_S values and the necessary experimental data are summarized in Table 1.

Table 1

Possible composition of individual solid phases and their solubility products

Solid phase composition and medium	Equations for calculation	Needed experimental data
$HA_{(S)}$ *acid solutions*	$K_S = [H]\left(C_A^0 - C_H^0 + [H]\right)$	C_A^0, C_H^0, pH
$MA_{2(S)}$ *acid solutions*	$C_A^0 - C_H^0 - 2C_M^0 + [H] = = \delta - 2\left(K_S'' / \delta^2\right)$, where $\delta = \left(C_H^0 - [H]\right) / K[H]$	C_A^0, C_M^0, C_H^0, pH
$MHA_{(S)}$ *acid solutions*	$C_A^0 - C_H^0 = K_S[M]^{-1}[H]^{-1} - [H]$ $C_M^0 - C_H^0 = [M] - [H] - K_S K[M]^{-1}$	$C_A^0, C_M^0, C_H^0, pH, pM = = -\log[M]$
$M(OH)_{2(S)}$ *alkaline solutions*	$C_{OH}^0 - 2C_M^0 = K_S[H]^{-2}\left(\chi - 2\alpha\right) + K_W[H]^{-1}$ $\alpha = \sum_{i=0} K_i[H]^{-i}, \quad \chi = \sum_{i=1} iK[H]^{-i}$	C_M^0, C_{OH}^0, pH

(Here the indices "*a*", "*b*" and "*s*" represent *acid*, *base* and *salt* respectively).

We will consider comprehensively one of possible cases of coexistence of two precipitates (denoted by the index "s") with a common ion A^-:

$$HA_{(S)} \Leftrightarrow H + A, \quad K_S' = [H][A] \tag{1}$$

$$MA_{2(S)} \Leftrightarrow M + 2A, \quad K_S'' = [M][A]^2 \tag{2}$$

Here and underneath the charges of species are omitted for simplicity.

Using well-known methods of accounting for the non-ideality of real systems, it is easy to calculate the thermodynamic constants from the concentration ones [5-7]. In liquid stage, we shall consider a series coexistent equilibrium. For acid solutions we will take into consideration the side reactions of anion A^- protonation:

$$HA \Leftrightarrow H + A, \quad K = [H][A] \tag{3}$$

The mass balance conditions in this heterogeneous system are defined as follow [5-7]:

$$C_M^0 = P'' + [M] \tag{4}$$

$$C_A^0 = P' + 2P'' + C_A^r = P' + 2P'' + [A] + [HA] = P' + 2P'' + [A]\left(1 + K[H]\right) \tag{5}$$

$$C_H^0 = P' + C_H^r = P' + [H] - [OH] + [HA] = P' + [H] - K_W[H]^{-1} + K[H][A] \tag{6}$$

where P is the amount of the ith ion in the precipitate per 1 unity of the solution volume (expressed in mol/L), C_i^r is the residual (or analytical) concentration of the component "i" of the precipitate in saturated solutions, i.e. its concentration in the solution after the separation of the solid and liquid phases, mol/L [5,6].

The elimination of P from the set of equations above by the linear combination of the mass balance equations (4)-(6) yields:

$$C_A^0 - C_H^0 - 2C_M^0 = C_A^r - C_H^r - 2[M] = \\ = [HA] + [A] - [H] + [OH] - 2[M] \quad (7)$$

Taking into account the MAL (*mass action law*) equations (1) and (2), the equation (7) may be rewritten as follows:

$$C_A^0 - C_H^0 - 2C_M^0 = K_S'[H]^{-1} - [H] - 2\frac{[H]^2 K_S''}{\left(K_S'\right)^2} \quad (8)$$

If the composition of initial mixture (C_i^0) at the measured equilibrium pH value of saturated solutions is known, the equation (8) contains 2 variables: K_S' and K_S''. Measuring the pH values for two different compositions of the initial mixture, we compose a system of two equations with two unknown values K_S' and K_S'', which is unproblematic to solve. Furthermore, from the equations (1) and (2) it is possible to calculate the equilibrium concentrations [*M*] and [*A*]. If the values K_S are known *apriori*, the satisfactory coincidence between calculated results and tabulated data may serve as a proof of the correctitude of the chosen equilibrium model.

If the calculated equilibrium characteristics for a certain equilibrium model keep the constancy of their values within the studied area of the component concentrations, one may affirm that this model is chosen properly.

The other possible compositions of a mixture of solid phases and the equations for their solubility product calculation are summarized in Table 2.

Table 2

Possible composition of a mixture of solid phases and their solubility products

Solid phase composition and medium	Equations for calculation	Needed experimental data
$HA_{(S)} + MA_{2(S)}$ $\downarrow \quad \downarrow$ $K_S' \quad K_S''$ *acid solutions*	$C_A^0 - C_H^0 - 2C_M^0 =$ $= K_S'[H]^{-1} - [H] - 2\left([H]^2 K_S'' \Big/ \left(K_S'\right)^2 \right)$	C_A^0, C_M^0, C_H^0, pH
$HA_{(S)} + MHA_{(S)}$ $\downarrow \quad \downarrow$ $K_S' \quad K_S''$ *acid solutions*	$K_S' = [H]\left(C_A^0 - C_H^0 + [H]\right)$ $K_S'' = K_S'[M]$	C_A^0, C_H^0, pH, pM
$MA_{2(S)} + MHA_{(S)}$ $\downarrow \quad \downarrow$ $K_S' \quad K_S''$ *acid solutions*	$C_H^0 - C_M^0 = [H] + \frac{K_S' K [H]^2}{K_S''} - \frac{\left(K_S''\right)^2}{K_S'[H]^2}$	C_M^0, C_H^0, pH
$MA_{2(S)} + M(OH)_{2(S)}$ $\downarrow \quad \downarrow$ $K_S' \quad K_S''$ *alkaline solutions*	$C_M^0 = \frac{1}{2}\left[C_A^0 - \left(\frac{K_S'[H]^2}{K_S''} \right)^{1/2} \right] + K_S''[H]^2 \alpha +$ $+ \frac{1}{2}\left(C_{OH}^0 - K_W[H]^{-1} + [H] - K_S''[H]^2 \chi \right);$ $\alpha = \sum_{i=0} K_i [H]^{-i}, \quad \chi = \sum_{i=1} iK[H]^{-i}$	$C_A^0, C_M^0, C_{OH}^0 = -C_H^0, pH$

For better understanding the quintessence of the developed approach a real heterogeneous system, that can contain jointly two solid phases, will be examined. The heterogeneous system cadmium caprate-saturated solution can

serve as an example of such system because of the practical significance of polyvalent metal ions in the form of low-soluble soaps with potassium salts of saturated fatty acids [14]. For this system the following constants of equilibrium are known: $\log K' = -10.12$ and $\log K'' = -8.74$ [15]. By means of experimental measurements the authors [14] proved that the simultaneous coo-precipitation of the cadmium caprate $CdA_{2(S)}$ and caprinic (or n-capric) acid $HA_{(S)}$ takes place in acidic solutions, the hydrolysis of cadmium ion can be neglected. The equilibrium pH values in the case of coexistence of two solid phases are calculated by the equation (8). After that, using the above combined equations of the mass action law and the mass balance, we can easily calculate the distribution diagrams of the metal ion and anion in the solid and complex species in aqueous solution, i.e., the heterogeneous equilibrium diagrams (depending on the problem to be solved, one can calculate the distribution of species containing one or other component of solid phases) [16].

Initially, we will introduce the following equations for calculating the partial molar fractions γ_i of species containing the anion A^- in the heterogeneous system, in which reactions (1)-(3) simultaneously occur:

$$\gamma_{HA(S)} = \frac{P'}{C_A^0}, \quad \gamma_{MA2(S)} = \frac{2P''}{C_A^0}, \quad \gamma_{A^-} = \frac{[A]}{C_A^0}, \quad \gamma_{HA} = \frac{[HA]}{C_A^0}, \quad \gamma_{SUM} = \frac{C_A^r}{C_A^0} = \frac{[A]+[HA]}{C_A^0} \qquad (9)$$

The subscript "sum" denotes the sum of the molar fractions of all soluble species. The comparison of the equations (9) with equation (5) implies that

$$\gamma_{HA(S)} + \gamma_{MA2(S)} + \gamma_{SUM} = \gamma_{HA(S)} + \gamma_{MA2(S)} + \sum_{i=0} \gamma_{H_iA} = 1$$

In their appearance, the heterogeneous chemical equilibrium diagrams (see Fig. 1) resemble the distribution diagrams of complex species in a homogeneous solution, but the molar fractions of species γ_i also depend on the initial composition of the mixture and, hence, for the system (1)-(3) are functions of three variables: $\gamma_i = f\left(C_A^0, C_M^0, pH\right)$. From the calculated diagram $\gamma_i = f\left(pH\right)_{C_i^0}$, i.e. $C_A^0 = const$ and $C_M^0 = const$ (Fig.1) one can deduct that the solid phases $CdA_{2(S)}$ and $HA_{(S)}$ coexist within the pH values 5 to 6. So, the equation (8) is valid only inside this pH range. The nature of the formed precipitates can be checked by the IR examination after their isolation from aqueous solution with different pH values [14].

In consequence, knowing one of the equilibrium constants K_S' or K_S'', we can determine the second one by means of the deduced equation (8). The later equation can also be used in the early stage of developing a equilibrium model for the new compounds.

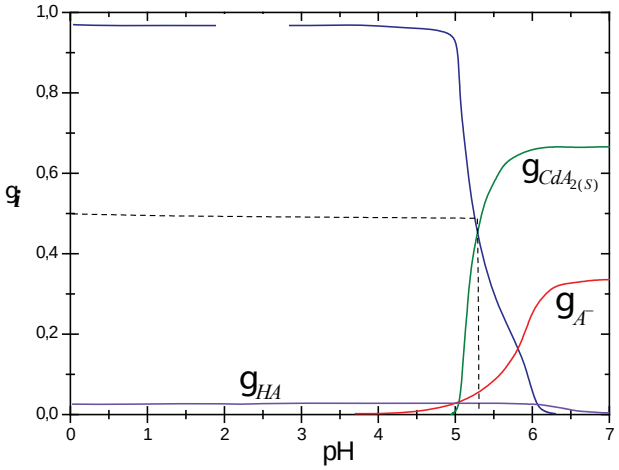

Fig. 1. The distribution of the caprat ion in the heterogeneous system cadmium caprate $CdA_{2(S)}$ – capinic acid $HA_{(S)}$ – aqueous solution as a function of pH at $C_{Cd}^0 = 2.23 \cdot 10^{-3} mol/L$ and $C_A^0 = 6.69 \cdot 10^{-3} mol/L$.

Conclusions

Therefore, the deduced relations are useful for solving both the *direct* (**I**) and *indirect* (**II**) equilibrium problems:

(I) *Direct problem*: calculating the equilibrium composition of heterogeneous mixture using the tabulated constants;

(II) *Indirect problem*: determining the equilibrium constants (the equilibrium model) on the basis of experimental data.

As it can be seen from the data of Table 2, in many cases the obtained equations allow to determine the values of equilibrium constants, mainly K_S, using the pH values of saturated solutions (avoiding this way the traditional, sometimes rather hard, solubility measurements).

The equilibrium constants computed by the developed equations may also produce the "seed" values for the iterative least squares procedure for $logK_S$ refinement, using the existing processing programs.

The developed approach can be applied without difficulty in the case of formation of a mixture of precipitates for arbitrary compositions.

Acknowledgments

This work was done with the support of the SCOPES 2009-2012 joint research grant.

References

[1]. POVAR, I. *Numerical differentiation of the formation function and selection of a chemical equilibrium model.* Russ. J. Inorg. Chem. 1993, **38**, 1787 - 1790.

[2]. POVAR, I. *Derivative of the formation function in respect to equilibrium ligand concentration in the case of polynuclear complex formation in two-component systems*. Russ. J. Inorg. Chem. 1993, **38**, 1782 - 1786.

[3]. POVAR, I. *Functional transformations of experimental data and the chemical model of equilibrium for polynuclear systems - 1. Family of auxiliary concentration functions curves with common cross-over point*. Talanta. 1994, **41**, 1363 - 1368.

[4]. POVAR, I. *Utilization of some partial derivatives of Olerup function for investigating chemical equilibria in polynuclear systems*. Rev. Roum. Chim. 1995, **40**, 319 - 324.

[5]. POVAR, I. *Potentiometric determination of solubility products of poorly soluble hydroxides and acids.* J. Anal. Chem. 1998, **53**, 1113 - 1119.

[6]. POVAR, I. *Potentiometric determination of solubility products and equilibrium ion concentrations for poorly soluble salts*. Russ. J. Gen. Chem. 2000, **70**, 501 - 507.

[7]. POVAR, I. *Determination of the stability of slightly soluble complexonate from pH metric data*. Can. J. Chem. 2001, **79**, 1166-1172.

[8]. AVDEEF, A.; BERGER, C.M.; BROWNELL C. *pH-metric solubility. 2: Correlation between the acid-base titration and the saturation shake-flask solubility – pH methods.* Pharm. Res. 2000, **17**, 85-89.

[9]. AVDEEF, A. *pH-metric solubility. 1. Solubility-pH profiles from Bjerrum plots. Gibbs buffer and pKa in the solid state.* Pharm. Pharmacol. Commun. 1998, **4**, 165-178.

[10]. ROSEMAN, T.J.; YALKOWSKY, S.H. *Physicochemical properties of prostaglandin $F_{2\alpha}$ (tromethamine salt): solubility behavior, surface properties, and ionization constants.* J. Pharm. Sci. 1973, **62**, 1680-1685.

[11]. KAUFMAN, J.J.; SEMO, N.M.; KOSKI, W.S. *Microelectrometric titration measurement of the pK_as and partition and drug distribution coefficients of narcotics and narcotic antagonists and their pH and temperature dependence.* J. Med. Chem. 1975, **18**, 647-655.

[12]. STRENG, W.H.; ZOGLIO, M.A. *Determination of the ionization constants of compounds which precipitate during potentiometric titration using extrapolation techniques.* J. Pharm. Sci. 1973, **73**, 1410-1414.

[13]. TODD, D.; WINNIKE, R.A. *A rapid method for generating pH-solubility profiles for new chemical entities.* Abstr. 9th Ann. Mtng., Amer. Assoc. Pharm. Sci., San Diego, 1994.

[14]. POVAR, I.; SAZONOVA, V.F.; SKRYLEVA, T.L.; SKRYLEV, L.D., *Thermodynamic prediction and experimental substantiation of conditions of phase transformations in the system cadmium caprate - saturated aqueous solution*. Russ. J. Gen. Chem. 1999, **69**, 1698 - 1701.

[15]. KUMOK, V.N.; KULESHOVA O.M.; KARABIN L.A. *Solubility products.* 1983, Novosibirsk: Nauka, 266 p (in Russ).

[16]. POVAR, I. *Method for graphic representation of heterogeneous chemical equilibria in systems sparingly soluble compound - complexing agent - aqueous solution*. Russ. J.Inorg. Chem. 1997, **42**, 607 - 612.

VOLTAMMETRIC CHARACTERIZATION OF THE BEHAVIOR OF BIOLOGICALLY ACTIVE COMPOUND ENOXIL IN VARIOUS MEDIA

Gheorghe Nemțoi[1*], Tudor Lupaşcu[2], Alexandra Ciomaga[1], Alexandru Cecal[1]

[1] *A.I.Cuza University, Faculty of Chemistry, 11-Carol 1 Bvd, 7000506- Iasi, Romania*
[2] *Institute of Chemistry of ASM, 3. Academiei str, Chisinau, 2028 MD, R. Moldova*
E-mail: nemtoi@uaic.ro, tel.+40232201334, fax.+40232201313

Abstract. This paper presents the results of scientific research related to the electrochemical behavior of the complex preparation, Enoxil. It was established that the oxidation-reduction process of Enoxil is quasireversible. The reactivity of Enoxil obtained from alcohol soluble enotannins is more pronounced, compared to that obtained from standard enotannins. The dependence of cathodic current intensity on Enoxil concentration is linear. This can be used to establish Enoxil concentration in solution. Cyclic voltammograms were used to establish reduction and oxidation potential and the formal redox potential on platinum electrode in sodium perchlorate aqueous environment. These features can be used for identification and determination of Enoxil in pharmaceuticals.

Keywords: complex biologically active compound Enoxil, cyclic voltammetry, standard redox potential, dosage of pharmaceuticals.

Introduction

Domestic and imported drugs are subjected to a rigorous control of their correspondence with the quality indices set out in The Analytical and Normative Documentation.

For the identification and determination of pharmaceutical substances in drugs a number of physical, physico-chemical and chemical methods are currently used. The most common physical and physico - chemical methods used for identification and determination of active substance in drugs are IR spectroscopy, UV/Vis, mass spectroscopy, atomic spectroscopy, nuclear magnetic resonance spectroscopy, chromatographic methods, electrochemical methods, etc.

Enoxil is a mixture of substances of natural origin obtained at oxidation of grape seed tannins [1]. As a result of chemical oxidation processes, the breaking of polymer chain takes place in enotannins forming new compounds containing carboxyl, peroxide, alcoholic, aldehyde, ketone, ether, ester, and other functional groups. These new compounds are soluble in water and have an astringent taste. The presence of functional groups listed above has been demonstrated by acid-base titration, and spectral methods [2]. The purpose of the research presented in the current paper is to study the voltammetric behavior of Enoxil.

Electrochemical methods are commonly used in analysis of food tocopherons. Resulted tocopherylquinones give reduction polarographic waves with heights proportional to concentrations, which allows the determination of tocopherol in the initial samples [3]. The synthetic phenolic antioxidants such as Vitamin E and provitamin A can also be detected by electrochemical methods [4-6]. Due to the presence of electroactive groups in natural and synthetic oxidants molecules, the electroanalytical complex evaluation of charge transfer capabilities provides extremely valuable information on the mechanism of reactions involving these compounds in the process of preventing the degradation caused by oxidative stress [7]. Biologically active compound Enoxil exhibits significant antioxidant properties [8].

Experimental

Six types of Enoxil were taken into the study, labeled as follows:

E_1- homogenized Enoxil for Î.M. Farmaco S.A. 2009;
E_2- Enoxil homogenized on 13.XI.2009;
E_3- Enoxil from standard enotannins with μW, 24.03.2010;
E_4- Enoxil from standard enotannins without μW, 25.03.2010;
E_5- Enoxil from enotannins alcohol solution with μW, 24.03.2010;
E_6- Enoxil from enotannins alcohol solution without μW, 25.03.2010.

In 30mL of solution: water (75%vol.) - ethylic alcohol (25%) with electrolytic background 0.1M tetrabutylammonium iodide (ITBA) were added 0.3mL Enoxil (E1) of conc. 5% (5g Enoxil in 100ml aqueous solution), achieving a Enoxil conc. of 4.95×10^{-2}% in the electrochemical cell, the obtained solution being slightly turbid, evidence of precipitate formation tendency.

The cyclic voltamogram (CV) was drawn using the working electrode (WL), platinum disc electrode (EDPt-Φ2mm), reference electrode, SCE (saturated calomel electrode) and the auxiliary electrode (AE), platinum wire electrode, connected to the Electrochemical Combine VoltaLab 32 (Radiometer Copenhagen) and provided with software VoltaMaster2 [9.10], the working temperature being 25 °C. As a result, was obtained a CV characteristic to quasireversible processes, shown in Figure 1. The values of potential are all determined using the SCE used as reference. In order to perform the pH and electroconductivity measurements, the electrochemical multimeter Consort 831 (Belgium) was used.

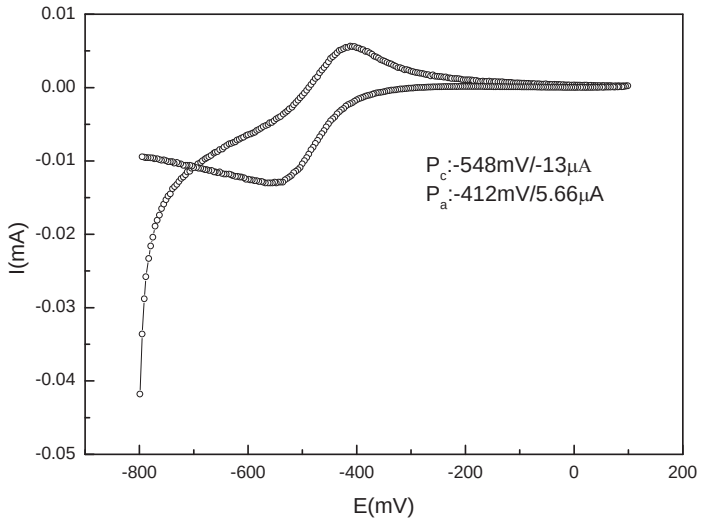

Fig. 1. Cyclic voltamogram of E_1 in ITBA at scan speed of 50mV/s

By further introducing volumes of 0.3mL of E1, the solution becomes more opalescent, thus confirming the tendency of precipitate formation, voltammetric results obtained are presented in Table 1.

Results and discussions

Table 1

Cyclic voltammetry characteristics for E_1 in ITBA at different concentrations and scan speed of 50mV / s

10^2c (g/100mL)	E_{CD} (mV)	E_{PC} (mV)	I_{PC} (μA)	E_{PA} (mV)	I_{PA} (μA)
4.95	127	-548	-13.0	-412	5.66
9.80	125	-648	-20.4	-388	4.71
14.56	123	-676	-28.3	-360	4.74
19.23	120	-723	-34.6	-340	4.19
23.81	122	-735	-42.0	-328	4.24

The following conclusions may be drawn from table 1:

- open-circuit potential values (E_{CD}) change very little with increasing concentration of E_1, proving that no adsorption phenomena take place on the surface of EL;

- shift of the cathodic peak potential (E_{PC}) to more negative values and of the anodic peak potential (E_{PA}) towards more positive values, with increasing Enoxil concentration shows that complexation phenomena occur;

- in dilute E_1 solution ($4.95x10^{-2}$), CV shown in figure 1 highlights a quasireversible process by adding Enoxil, the anode current (I_{PA}) decreases, but it remains practically constant at the following concentrations of E_1, CV highlighting the occurrence of an irreversible process (only the cathodic process takes place) due to precipitation of the formed complex. Figure 2 shows the dependence of the cathodic current intensity on Enoxil concentration, which is linear, and the equation that can serve as standard in the given concentration range.

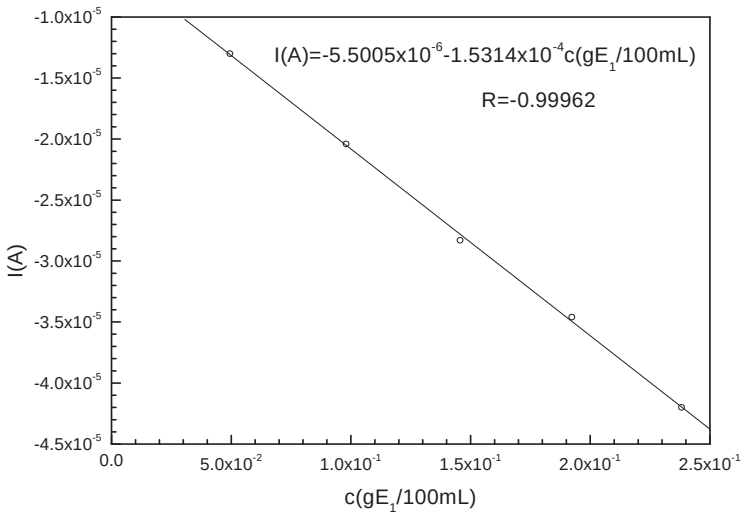

Fig. 2. Dependence of the cathodic current intensity on Enoxil concentration (E_1) in alcohol solution of ITBA

Considering all mentioned above on the voltammetric behavior of Enoxil in alcoholic solution of tetrabutylammonium iodide on platinum electrode, its determination on the basis of the cathodic process can be recommended, using the calibration graph (Fig. 2).

On acidification of solution with $HClO_4$ at a pH below 2.6, no cathodic peak can be revealed (there is a continuous decrease of cathode current), hazing of the solution is more obvious due to the formation of a yellowish precipitate. By alkalinization of the solution with NaOH to pH 8.8 the precipitate darkens, yellow flakes are present, and the CV doesn't present any peaks. The electroreduction process evidenced for the considered above system, may be due to the presence of peroxide group in Enoxil, which is reduced, process facilitated by the presence of iodide ion in the electrolytic background.

In order to avoid the influence of the electrolytic background, we will consider an aqueous solution 0.1M of $NaClO_4$ with pH=5.5 and electronegativity 10.78 mS/cm and using VoltaLab32 we will draw the CV in the range -800÷1200÷-800 with a scan speed of 50 mV/s.

The solutions with 5% (5g Enoxil/100mL solution) were prepared of each type of Enoxil, of which were taken volumes of 0.3mL or 1.0mL (at the end for the last addition) that were added to 30mL 0.1M solution $NaClO_4$ and CV were drawn, at working temperature of 25 °C. Removing oxygen from the solution was achieved by bubbling nitrogen for 5 minutes before plotting the voltamogram. Figure 3 presents the CV obtained for the most diluted solutions of Enoxil ($4.95x10^{-2}$%) and Figure 4 - the 6 types of Enoxil of conc. $19.23x10^{-2}$%.

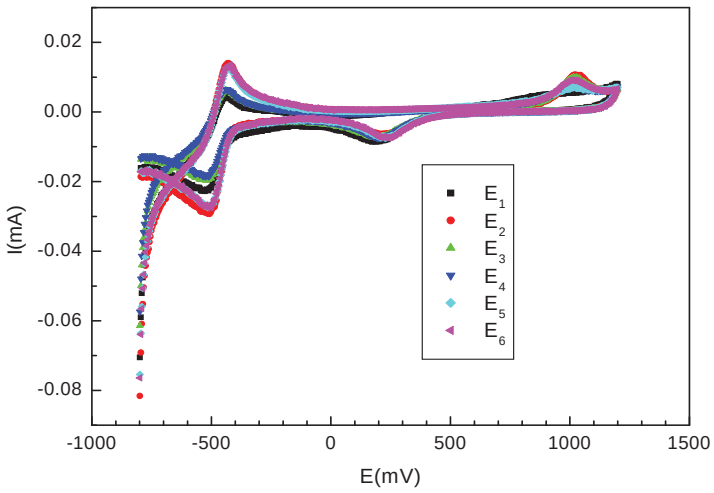

Fig. 3.CV of the 6 types of Enoxil at $4.95x10^{-2}$% in 0.1 M $NaClO_4$ at a scan speed of 50 mV/s

Figure 3 shows that overlapping peaks found in the positive range of potentials can be attributed to electrolytic background, while in the negative range of potentials, the anodic peak coupled with the cathodic one, reveals a quasireversible redox process characteristic to Enoxil. The variation in peak intensities of the anodic processes (I_{PA}) is different from the cathodic ones (I_{PC}) and can be grouped as follows:

$$I_{PA}: E_2,E_5,E_6 > E_3,E_4 > E_1;$$
$$I_{PC}: E_2 > E_5,E_6 > E_1 > E_4,E_3.$$

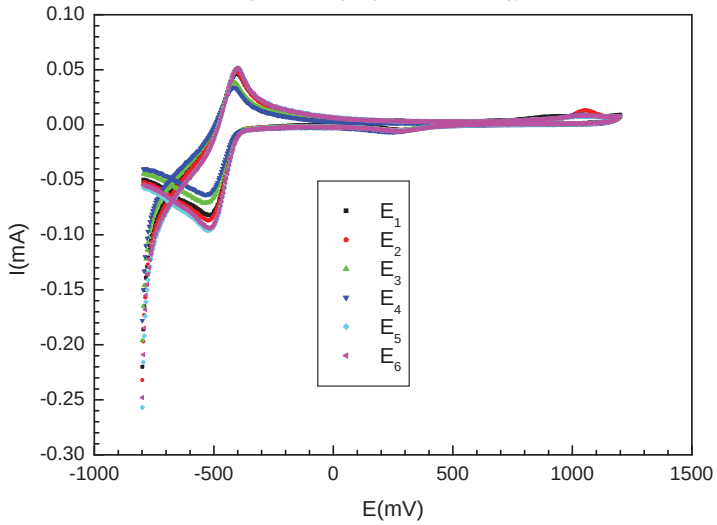

Fig. 4. CV of the 6 types of Enoxil at 19.23x10^{-2}% in 0.1 M $NaClO_4$ at a scan speed of 50 mV/s

CV in figure 4 confirms the existence of peaks in the positive range of potentials due to the medium, and for that reason in figure 5, we will present for E_1, the CVs both for expanded and restricted ranges, where only Enoxil characteristic peaks occur. The reproducibility is very good, given by the overlapping peaks.

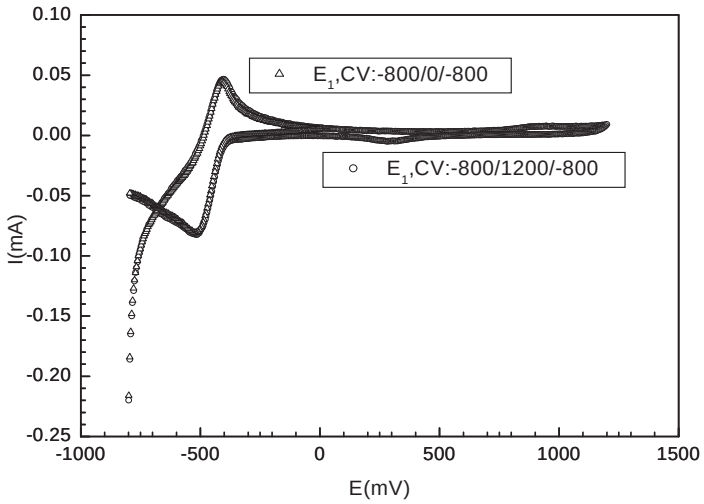

Fig. 5.CV of E_1 at a concentration of 19.23x10^{-2}% in 0.1 M $NaClO_4$ at a scan speed of 50 mV/s for expanded and restricted ranges

Considering the variation of peak current intensity for Enoxil concentration 19.23x10^{-2}%, the 6 types of Enoxil may be grouped as follows:

$$I_{PA}: E_5,E_2,E_6 > E_3,E_4, E_1;$$
$$I_{PC}: E_5,E_6 > E_2 > E_1 > E_3,E_4.$$

There is a slight modification as compared to the Enoxil more diluted solution, but considering that the peak current intensity is directly proportional to the velocity of the redox process, it may be concluded that Enoxil samples E_5 and E_6 are the most reactive, while the E_4 sample is the least reactive. Table 2 presents the collected data obtained by cyclic voltammetry at a scan speed of 50 mV/s for the 6 types of Enoxil on platinum disk electrode in 0.1M $NaClO_4$ solution.

Table 2

Solutions parameters and peak characteristics of CVs
For aqueous solutions of 0.1M $NaClO_4$ of the 6 types of Enoxil

10^2c (g/100mL)	pH	κ mS/cm	$-E_{PC}$ (mV)	$-I_{PC}$ (μA)	$-E_{PA}$ (mV)	I_{PA} (μA)
E_1						
4.95	2.94	11.10	523	22.2	431	6.85
9.80	2.71	11.30	516	45.8	420	25.0
14.56	2.58	11.48	511	65.4	412	37.0
19.23	2.49	11.69	524	88.0	408	45.1
34.16	2.32	12.05	528	132.0	392	62.8
$I_{PC}(\mu A)= 5.3208 – 570.75823c + 492.24991c^2$; R=0.99898 $I_{PA}(\mu A)= -10.91388 + 405.99054c – 558.70508c^2$; R=0.99685						
E_2						
4.95	2.88	11.07	508	29.3	431	14.0
9.80	2.71	11.34	512	48.2	424	28.1
14.56	2.59	11.52	524	68.0	415	38.3
19.23	2.49	11.72	524	87.2	408	48.1
38.46	2.28	12.25	536	155.0	388	82.8
$I_{PC}(\mu A)= -7.36359 – 4.39348c + 0.01437c^2$; R=0.99984 $I_{PA}(\mu A)= 1.09012 + 2.82228c – 0.01819c^2$; R=0.9993						
E_3						
4.95	3.02	11.14	523	19.7	439	6.32
9.80	2.80	11.28	512	40.9	420	22.8
14.56	2.68	11.43	528	57.0	420	31.8
19.23	2.61	11.52	540	71.2	412	38.2
34.16	2.46	11.77	540	112.0	404	60.3
$I_{PC}(\mu A)= 0.54852 – 441.465c + 329.27349c^2$; R=0.99928 $I_{PA}(\mu A)= -6.44928 + 304.78515c – 323.07386c^2$; R=0.99167						
E_4						
4.95	3.04	10.88	511	18.5	432	6.5
9.80	2.84	10.90	516	34.5	428	16.4
14.56	2.72	10.91	519	49.2	420	25.2
19.23	2.64	11.03	536	63.7	416	34.0
34.16	2.48	11.14	559	102	408	55.8
$I_{PC}(\mu A)= -0.97988 – 361.38485c + 191.8709c^2$; R=0.99994 $I_{PA}(\mu A)= -4.44 + 227.15128c – 148.47841c^2$; R=0.9999						
E_5						
4.95	2.86	11.16	516	27.5	428	12.8
9.80	2.63	11.32	512	52.5	416	27.7
14.56	2.51	11.50	508	74.1	408	40.1
19.23	2.41	11.85	528	96.2	404	51.5
34.16	2.24	12.28	527	151	395	61.7
$I_{PC}(\mu A)= -0.3855- 564.72738c + 361.95061c^2$; R=0.99987 $I_{PA}(\mu A)= -7.13662 + 425.25416c – 653.75472c^2$; R=0.99844						
E_6						
4.95	2.85	11.06	516	27.6	424	13.5
9.80	2.63	11.26	516	52.8	412	29.8
14.56	2.50	11.46	516	73.5	412	41.1
19.23	2.41	11.61	524	94.1	400	51.4
34.16	2.25	12.09	532	148.0	388	71.6
$I_{PC}(\mu A)= -1.65877 – 548.01533c + 350.42436c^2$; R=0.99988 $I_{PA}(\mu A)= -3.38475 + 372.85301c – 449.51928c^2$; R=0.99932						

Table 2 shows that increasing concentration of Enoxil in the electrochemical cell where the electrolytic background is sodium perchlorate, leads to a decrease in pH accompanied by a slight increase in electroconductivity (κ), which can be attributed to hydrogen ions generated by Enoxil during dissolution. For every type of Enoxil, the dependency of peak current upon concentration was established, for both the anodic (I_{PA}(μA)) and cathodic (I_{PC}(μA)) processes. Also, the corresponding correlation coefficients (R) are given, with values very close to unity, by 2nd order polynomial fitting of experimental data.

Table 3 presents the mean values of reduction potentials (E_{PC}) and oxidation potentials (E_{PA}) as well as a formal redox potential ($E^{0'}$) calculated according to the formula:

$$E^{0'} = \frac{E_{PC} + E_{PA}}{2}$$

Table 3

The mean values of reduction and oxidation potentials, as well as Enoxil formal redox potential on platinum electrode in aqueous solution of 0.1MNaClO$_4$

Enoxil	$-E_{PC}$ mV	$-E_{PA}$ mV	$-E^{0'}$ mV
E_1	520.4	412.6	466.5
E_2	520.8	413.2	467.0
E_3	528.6	419.0	473.8
E_4	528.2	420.8	474.5
E_5	518.2	410.2	464.2
E_6	520.8	407.2	464.0

The close values of each of the three forms of potential shown in Figure 3, prove that regardless of the type of Enoxil, the electrochemically reactive group of Enoxil is characterized by a reduction potential $\overline{E}_{PC} = -522.8\text{mV}$ and an oxidation potential $\overline{E}_{PA} = -413.8\text{mV}$ and the formal redox potential of this group will be $\overline{E}^{0'} = -468.3\text{mV}$. These values should be qualitative indicators of Enoxil presence and the intensity of the peak current will provide quantitative estimates for a subsequent dosing of Enoxil by voltammetry.

By acidifying the solution with $HClO_4$ gives a marked rise in cathode current (increased speed of the reduction process) and anodic peak flattening, as shown for E_4 in figure 6.

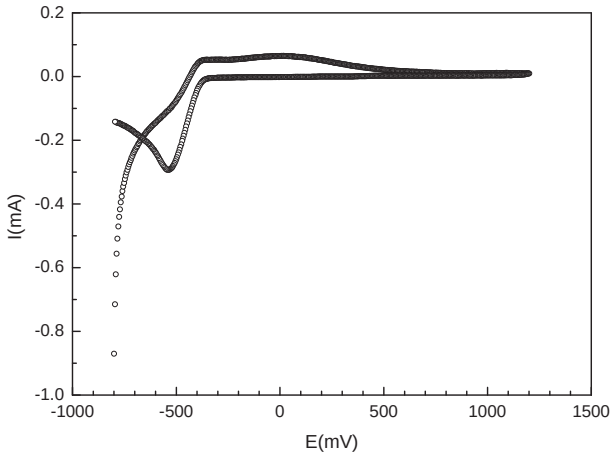

Fig. 6. CV at pH=1.86 for the solution of 34.16x10^{-2}% E_4 in 0.1M NaClO$_4$ at a scan speed of 50 mV/s

By alkalinization of Enoxil solution leads to the decrease of peak intensities and even at a slightly alkaline pH, the peaks characteristic to Enoxil presence practically disappear, as illustrated in Figure 7 for E_4.

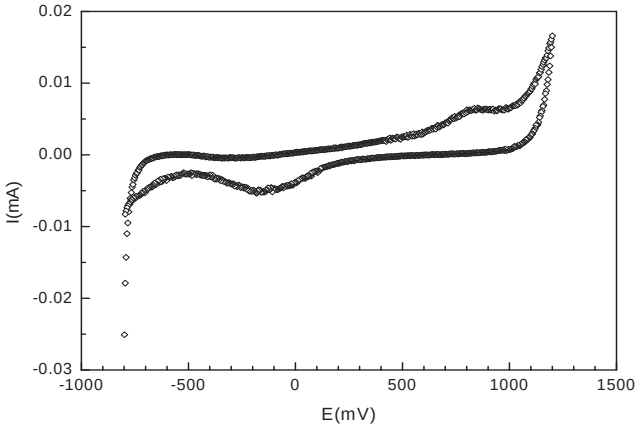

Fig. 7.CV at pH=7.46 for the solution of $34.16x10^{-2}$% E_4 in 0.1M $NaClO_4$ at scan speed of 50 mV/s.

After the voltammetric measurements were performed in 0.1M $NaClO_4$ solution on platinum electrode, as shown in Table 2, pH values are functions of Enoxil concentration, acidification or alkalinization of the solution leading to changes in CV and even annihilation of Enoxil electroreactivity.

This study allows us to conclude that hydrosoluble Enoxil can be studied by voltammetry in aqueous sodium perchlorate medium as electrolytic background on platinum electrode by highlighting a quasireversible redox process.

Conclusions

- The dependence of cathodic current intensity of Enoxil concentration is linear. This can be used to determine the concentration of Enoxil in unknown solutions.
- The analysis of cyclic voltammograms reveals a quasireversible redox process characteristic to Enoxil.
- The Enoxil samples obtained from alcohol soluble enotannins are more reactive over time, compared with enoxil obtained from standard enotannins.
- The analysis of reduction and oxidation potentials and of the formal redox potential of Enoxil samples allows us to estimate these values, which may serve as qualitative indices of Enoxil preparation that can be used for its determination by voltammetry.

References

[1]. Duca Gh., Lupaşcu T., Vlad P., Kulciţki V., Nastas R. Studies on the water solubilization processes of oenotanins and their physico-chemical properties. Chemistry Journal of Moldova. 2006, 1 (1), P. 74-79.
[2]. Lupaşcu T., Duca Gh., Giurgincă M., Vlad P. et. Natural compounds with antioxidant propertes. Key Engeenering Materials, 2009, V. 415, P.P.25-28.
[3]. Wisser K., Heimann W., Fritsche C., Fresenius Z. Anal. Chem., 1967, 230, 189.
[4]. Ruiz M.A., Yanez-Sedeno Poloma, Pingaron J.M., Electroanalysis 1994, 6, 475.
[5]. Ishar M.P.S., Kaur R., Kaur G., Gandhi R.P., Indian J. Chem, 1996, 35B, 641.
[6]. Surez – Fernendaz A.L., Alaines-Varela G, Costa-Garcea A., Electrochimica Acta, 1999, 44, 4489.
[7]. Liteanu S., G.L. Radu. Elemente de bio-electroanaliză a unor principii active antioxidante. Editura Printech, Bucureşti, 2005, 232 p.
[8]. Brevet de Invenție. 3979 MD F 1. Compus cu proprietăți antioxidante. Lupaşcu T., Duca Gh., Lupaşcu L., Giurgincă M., Meghea A. BOPY, nr. 11/2009.
[9]. Nemtoi Gheorghe, Ionica Florica, Lupascu Tudor and Cecal Alexandru,Voltammetric characterirization of the iron behaviour from steels in different electrolytic media, *Chemistry Journal of Moldova. General,Industrial and Ecological Chemistry,* **5,**(1), 2010, 98-105
[10]. Mareci D., Bocanu C., Nemtoi Gh. and Aelenei Delia, Electrochemical behaviour of titanium alloys in artificial saliva, *J.Serb.Chem.Soc.,* 70, 2005, 891-897,

TEMPERATURE INFLUENCE ON PHASE STABILITY OF ETHANOL-GASOLINE MIXTURES

Valerian Cerempei

Institute of Agricultural Technics Mecagro, 7, M. Costin str., MD 2068, Chisinau, R. Moldova
e-mail: icmea_mecagro@yahoo.com

Abstract. The article investigates phase stability of ethanol-gasoline mixtures depending on their composition, water concentration in ethanol and ethanol-gasoline mixture and temperature. There have been determined the perfect functioning conditions of spark ignition engines fueled with ethanol-gasoline mixtures.

Keywords: composition, ethanol, gasoline, mixtures, phase stability, temperature.

Introduction

Researches on phase stability of monoatomic alcohol-gasoline mixtures for different compositions and hydrodynamic conditions were performed previously [1] at constant temperature (18 ... 20° C). In connection with the fact that the smallest capacities of phase stability among studied fuels have been demonstrated by ethanol-gasoline mixtures with ethanol volume fraction up to 50% (E10...E50), the purpose of our research is to study the phase stability of ethanol-gasoline mixtures depending on temperature, water concentration in ethanol and in ethanol-gasoline mixture.

Methodology of experimental researches

For our researches we used ethanol C_2H_5OH (volume fraction of absolute alcohol - 97.0 ... 99.9%) and Regular gasoline-80 with low octane number (LON ≥ 80). In order to research phase stability there were prepared fuel samples, each one having a volume of 100 ml 0.5 ml of water was added to each sample until the appearance of liquid turbidity.

Admissible water concentration for each experiment was determined based on the existing volume of added water and the one existing in ethanol at initial time.

The point of turbidity was assessed according to the existing standard norm GOST5066-91. Based on a bibliographical research [2,3,4,5] it was established that the decrease in temperature increases the danger of phase separation in fuel mixtures. Therefore we studied the range of temperatures below + 18 ºC.

Results and discussions

The obtained results (Fig. 1, 2) confirmed previous results. A drop in temperature from 18 °C to 0 °C reduces the admissible water concentration in ethanol from 6% vol. to 4% vol. in the mixture E10 and from 14.3% vol. to 11.5% vol. in the mixture E70 (Fig. 1). In other mixtures (E20...E50), under mentioned conditions, the reduction of admissible water concentration in ethanol was on average by 2% vol.

It should be mentioned that exceeded admissible water concentration results in liquid turbidity and subsequent separation of phases. The increase of ethanol fraction in the mixture from 10% vol. to 70% vol. enables the dissolution of larger quantities of water. For example, at the temperature 18°C, the admissible water concentration in ethanol is 6% vol. for the mixture E10, and 14.3% vol. for the mixture E70.

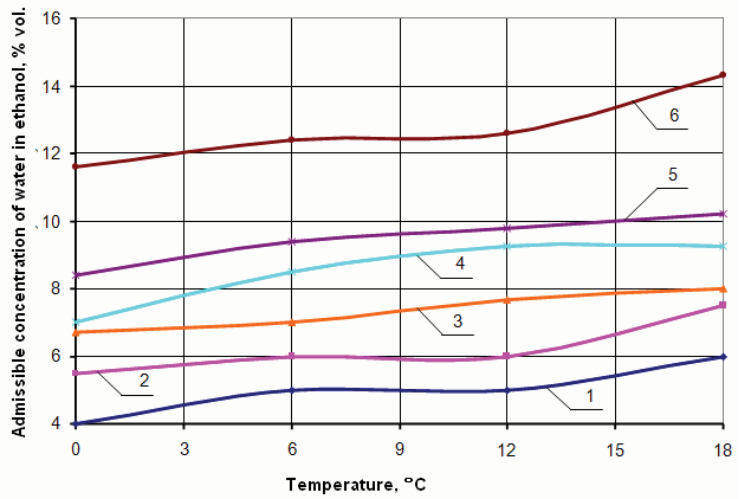

Fig. 1. Dependence of admissible water concentration on the liquide temperature for ethanol – gasoline mixture (1 – 10%; 2 – 20%; 3 – 30%; 4 – 40%; 5 – 50%;6 – 70% vol. ethanol)

After the distillation and rectification, different fractions of ethylic alcohol contain 93 ... 96.6% vol. of absolute alcohol (respectively 7 ... 3.4% vol. of water). Therefore, according to the results of our investigations, the ethanol obtained in these conditions can be used for direct preparation of gasoline mixtures at temperatures above 0° C, if the fraction of ethanol in the mixture exceeds 30% vol. (≥ E 30) (Figure 1.). Otherwise ($C_{ethanol}$ < 30% vol.) it is necessary an additional dehydration of ethanol.

The values of admissible water concentration in ethanol-gasoline mixtures at temperature changements in the range of 0 ... 18 ° C (Fig. 2) vary little: in the mixture E10 - 0.4 ... 0.7% vol. (ΔC = 0.3% vol.), in the mixture E70 - 7.6 ... 9.3% vol. (ΔC = 1.7% vol.). The variation of admissible water concentration in other mixtures (E20...E50) takes intermediate values. It can be noticed the tendency for variation increase of admissible water concentration ΔC along with the increase of ethanol fraction in the mixture from 10% vol. to 70% vol.

Researches results concerning the influence of liquid temperature on the values of admissible water concentration in ethanol and ethanol - gasoline mixtures are necessary in particular for the practical use in preparing and operating these mixtures.

No less important is the dependence of admissible water concentration on the ethanol fraction in the mixture with gasoline. The obtained results demonstrated (Fig. 3) that the increase of ethanol fraction in the mixture from 0 to 90% vol., when changing the values of admissible water concentration, allow to observe four characteristic sectors:

a) Ethanol concentration 0...10% vol.: the gradient of admissible water concentration change is ΔC_{adm}=0,5 % vol./% vol. ethanol;

b) C_{ethan}=10…60 %vol. : ΔC_{adm} =0,11 %vol./% vol. ethanol;

c) C_{ethan}=60…80 %vol. : ΔC_{adm} = 0,3%vol./% vol. ethanol;

d) C_{ethan}=80…90 %vol. : ΔC_{adm} =1,2%vol./%vol. ethanol.

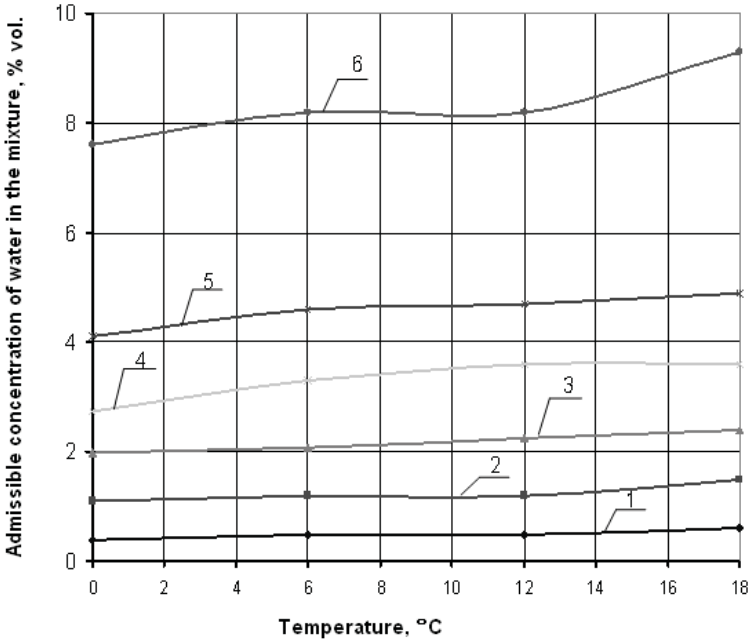

Fig. 2. Dependence of admissible water concentration on the liquide temperature, for ethanol – gasoline mixture (1 – 10%; 2 – 20%; 3 – 30%; 4 – 40%; 5 – 50%; 6 – 70% vol. de etanol)

It is well known that with the increase of ethanol concentration in the mixture with gasoline up to 100%, water solvency in ethanol increases to infinity. Therefore, the domain a) reflects the transition from pure gasoline (C ethanol = 0) to ethanol-gasoline mixture (C ethanol = 10%/vol.), where the influence of ethanol begins absorbing some water (C adm = 5% /vol.) without phases separation. The domain b) shows the influence of ethanol, which increases proportionally and slowly. The domain c) constitutes, as mentioned recently [1], a transition area to the mixtures in which ethanol influence is predominant (sector d).

The use of alimentary alcohol and ether-aldehyde fraction did not essentially change the values of admissible water concentration in ethanol (Fig. 3).

The analysis of research results concerning phase stability in ethanol-gasoline mixtures [1] and admissible water concentration in ethanol (Fig. 3) shows a good concordance.

Taking into account the fact that 5 ml of water were added in the ethanol-gasoline mixture with a volume of 100 ml and the fraction of absolute alcohol in ethanol of 98% vol., we will calculate the real water concentration in ethanol from these mixtures (Table 1). At the same time for the analysis we'll use the values of admissible water concentration in ethanol, determined based on our research (Fig. 3).

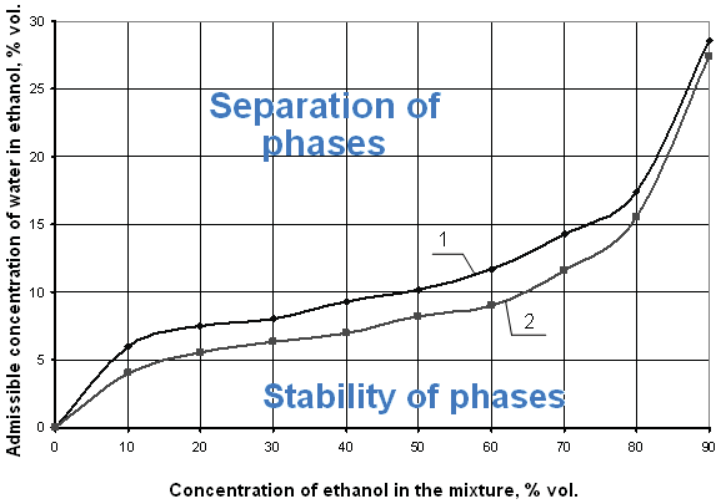

Fig. 3. Dependence of admissible water concentration in the ethanol with gasoline mixture (1 – alimentary; 2 – etero fraction – aldehyde)

When real water concentration in ethanol is higher than the admissible one (mixtures E10 ... E40), is can be clearly observed phases separation with and without agitation. The mixtures E50 and E60, under studied conditions, and as mentioned recently, are in the transition area. Water addition (5ml) in these mixtures without agitation leads to phase separation. Intensive agitation during 20 min stimulates the formation of a transparent and homogeneous liquid in the mixture E60 (Table 1, [1]). Real water concentration in ethanol in the mixture E85 (7.4% vol.) is much smaller than the admissible one (22.5% vol.), and as a result of water addition, the mixture E85 instantly clears for all the studied conditions.

Table 1

Values of real and admissible water concentration in ethanol for different mixtures (t = 18°C)

	Ethanol-gasoline mixtures							
Indicator	E10	E20	E30	E40	E50	E60	E70	E80
1.Real water concentration in ethanol, %vol. [1]	34,7	21,6	16,0	12,9	10,9	9,5	8,5	7,4
2.Admissible water concentration in ethanol, %vol. (fig.3)	5,0	6,5	7,2	8,1	9,2	10,4	13	22,5

Mixtures with high ethanol fraction (E85) are distinguished by increased phase stability, but these mixtures require the change of engine's fuel construction system [2 ... 5]. It was also established [5,6] that the use of ethanol-gasoline mixtures with ethanol fraction up to 30% vol. doesn't require the modification of engine construction, but put stringent requirements concerning admissible water concentration in ethanol. Therefore, for the mixtures E10 and E20, we studied additionally the reaction at low temperatures (down to - 55 ° C).

Although among the results obtained in the two stages mentioned above there are some discrepancies, the study of turbidity temperature dependence of ethanol-gasoline mixtures on the absolute alcohol fraction in ethanol (Fig. 4) demonstrates the same tendencies: at similar temperatures the admissible water concentration is higher in the mixture E20 (compared to E10), and the decrease of turbidity temperature when decreasing water concentration or increasing absolute alcohol concentration in ethanol.

In order to ensure the perfect operation of the engine at temperatures up to -30° C, the mixture E20 should contain water no more than 1.6% vol. (98.4% vol. a.a.) and the mixture E10 - respectively 1.1% vol. of H_2O (98.9% vol. a.a.). For the temperature up to - 20°C, the values of admissible water concentrations increased: in the mixture E20 - up to 2.2% vol., and in the mixture E10 - up to 1.5% vol.

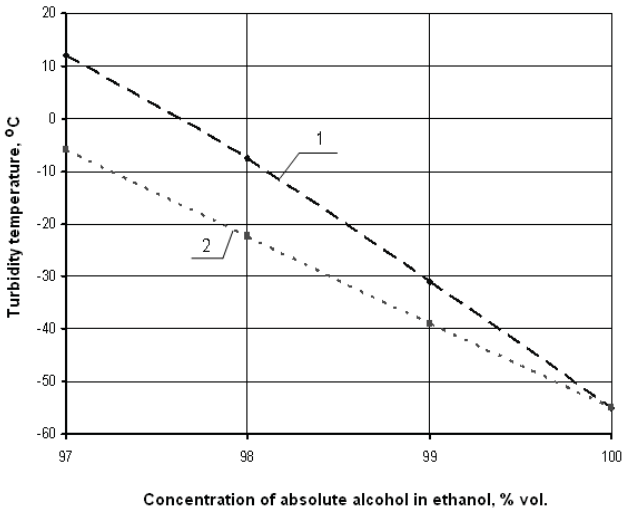

Fig. 4. Dependence of turbidity temperature of ethanol-gasoline mixtures on absolute alcohol concentration in ethanol

Therefore, the obtained results demonstrate that for the existing conditions in the Republic of Moldova, the most efficient solution is to use the mixtures E20 for fuel spark ignition engines. This fact will allow:

- ✓ the use of existing engines without their design modification;
- ✓ perfect operation of the engine having biofuel phase stability at the required level in temperature range up to -20 ...- 30 ° C and water concentration in ethanol less than 2.2...1.6% vol.
- ✓ to reduce the danger of phase separation by shaking the biofuels.

Conclusions

1. The admissible water concentration in ethanol (ethanol-gasoline mixture) depends on biofuel composition and temperature. Temperature increase in the range of 0...+18ºC and ethanol concentration in the mixture allow an increase of admissible water concentration values.

2. The ethanol obtained by distillation and rectification with the help of existing machinery in the Republic of Moldova can be used to prepare directly gasoline mixtures at temperatures above 0°C, if ethanol fraction in the mixture exceeds 30% vol. Otherwise, (at temperatures below 0ºC and C (ethanol) <30% vol.) it is required an additional ethanol dehydration.

3. The change of ethanol fraction in the mixture with gasoline from 0 to 90% vol. allows (t=18°C) to increase admissible water concentration in ethanol from 0 to 28% vol., and to notice four characteristic domains in the gradient of admissible water concentration increase.

4. The use of alimentary alcohol and ether-aldehyde fraction did not essentially change the values of admissible water concentration in ethanol in the mixture with gasoline.

5. In order to ensure the perfect operation of the engine at temperatures up to -30 ° C, the mixture E20 should contain water no more than 1.6% vol. (98.4% vol. a.a.) and the mixture E10 respectively - 1.1% vol. of H_2O (98.9% vol. a.a.). For the temperature up to - 20 ° C, the values of admissible water concentrations increased: in the mixture E20 - up to 2.2% vol. and in the mixture E10 - up to 1.5% vol.

Acknowledgements

The Moldovan Academy correspondent member Dr. I. Habaşescu as well as the scientific researchers D. Ruschih, L. Sîsoev and S. Cojocaru are acknowledged for helpful ideas and discussions.

References

[1]. Cerempei V. Amestecuri combustibile ale alcoolilor monoatomici cu benzină: stabilitatea fazică. Ştiinţa Agricolă, 2010, nr.2, p.70...77

[2]. Смаль Ф. В., Арсенов Е.Е. Перспективные топлива для автомобилей. М.: Транспорт, 1979 – 151 с.

[3]. Manea Gh., Georgescu M. Metanolul – *combustibil neconvenţional*. Bucureşti: Tehnică, 1992 – 84 p.

[4]. Gheorghişor M. *Carburanţi, lubrifianţi şi materiale auto speciale*. Bucureşti: Paralela, 2003 – 324 p.

[5]. Hăbăşescu Ion, Cerempei Valerian, Deleu Vasile et al. Energie din biomasă: tehnologii şi mijloace tehnice/ Chişinău: Bons Offices, 2009 – 368 p.

[6]. Hăbăşescu I., Cerempei V., Esir M., Novorojdin D. Indicii de performanţă a motorului cu aprindere prin scînteie alimentat cu amestec etanol-benzină. Materiale conferinţei internaţionale ”Energetica Moldovei – 2005”, Chişinău: Tipogr. AŞM – p.672-683.

PHASE STABILITY OF MONOATOMIC ALCOHOL-GASOLINE MIXTURES FOR DIFFERENT COMPOSITIONS AND HYDRODYNAMIC CONDITIONS

Valerian Cerempei

Institute of Agricultural Technics Mecagro, 7, M. Costin str., Chisinau, MD 2068 R. Moldova
e-mail: icmea_mecagro@yahoo.com

Abstract: The article investigates phase stability for the mixtures of monoatomic alcohols (ethanol, butanol) with gasoline in the presence of water. There have been determined the optimal storage conditions of mixtures depending on their composition and mixing conditions. The positive influence of butanol on the phase stability of ethanol-gasoline mixtures was detected.

Keywords: butanol, ethanol, gasoline, mixtures, phase stability.

Introduction

In the last 30-40 years, because of a rapid growth in prices for crude oil, the interest for alternative sources of energy including biomass, which the world economy and the Republic of Moldova possess in a sufficient extent, has increased in the world economy [1]. As a result, in order to supply spark ignition engines (SIE), there are increasingly used the mixtures of gasoline with monoatomic alcohols obtained from biomass. During the investigation [2-5] there have been studied physical-chemical and operational properties reflecting the combustion capacity of these mixtures.

Simultaneously, it is well known that monoatomic alcohols, especially methanol and ethanol C_2H_5OH interact with water H_2O thus diminishing phase stability of alcohol-gasoline mixtures. But the existing literature lacks specific information concerning phase stability of the mentioned mixtures.

Therefore, the purpose of our research is to determine the composition of monatomic alcohol - gasoline mixtures and hydrodynamic conditions, which ensure high values of the phase stability.

Methodology of experimental researches

For the researches there have been used: ethanol C_2H_5OH (volume fraction of absolute alcohol - 95.7-98% vol.), butanol C_4H_9OH (absolute alcohol - 99.9% vol.) and regular gasoline – 80 with low octane (RON $\geq$ 80).

There have been studied separately the components forming the mixtures (gasoline 100%, butanol 100%, ethanol 100%) and their mixtures: butanol - gasoline (B10, B20, B30, B50, which contain respectively 10, 20, 30, 50% vol. of butanol), ethanol - gasoline (E10, E20, E30, E40, E50, E60, E85, which contain respectively 10, 20, 30, 40, 50, 60, 85% vol. of ethanol), ethanol - butanol - gasoline (E16 - B16, containing 16% vol. of ethanol, 16% vol. of butanol, 68% vol. of gasoline).

To research the phase stability, there were prepared fuel samples with a volume of 100 ml each one. To these samples there were added 5 ml of water with and without agitation. Shaking was performed by electromagnetic stirring having a constant intensity for all samples and duration of 0.5, 2.0, 5.0, 10.0, and 20.0 minutes. The studied mixtures had an average temperature of +20°C.

Phase stability was assessed visually according to liquid state (cloudy, clear), duration of liquid clearing, the absence or existence of sediment and its volume.

Results and discussions

According to the obtained results (tab. 1, fig. 1), adding water without agitation ($\tau_{agit} = 0$) in any pure fuel has as a consequence practically the instant clearing of these mixtures and the volume fraction of sediments in these fuels is as follows: gasoline – 5 ml, butanol – 4 ml, ethanol – 0 ml.

The agitation of gasoline-water and ethanol-water mixtures does not change the liquid state. After the agitation, the entire quantity of added water (5 ml) settles as sediment in the gasoline, which becomes instantaneously clear. Ethanol also becomes clear in similar conditions, dissolving all the quantity (5ml) of added water.

Butanol, with kinematic viscosity (3.64 mm²/s) 2,4 times higher compared with ethanol and 6.4 times higher compared to gasoline, with the addition of 5 ml of water, dissolves only 1 ml without agitation and the remaining 4 ml deposit as sediment. The agitation stimulates the dispersion of water drops dissolving them in butanol ($\tau_l = 0$ h, $V_s = 0$ ml).

The behavior of gasoline, butanol and ethanol when adding water corresponds to their composition and molecules structure. Because of hydrogen links formation between alcohol and water molecules, the alcohols dissolve well in water. The solubility decrease in water of superior alcohols is a consequence of the increasing influence of

hydrocarbon radical. Gasoline contains C_nH_m hydrocarbons of over 200 types [6], having an average molecular weight within 110-120 kg/kmol and the value of dielectric permeability ε 1,9-2,1 [7]. Ethanol and butanol are monatomic saturated alcohols $C_nH_{2n+1}OH$. Ethanol C_2H_5OH has a molecular weight of 46 kg/kmol and dielectric permeability of 32, and butanol C_4H_9OH -74 kg/kmol and 23 respectively (for comparison, water H_2O molecular weight is 18 kg/kmol, and the dielectric permeability - 81).

Table 1

The influence of mixing conditions of different fuels with water on the duration of liquid clearing τ_l and volume of sediment V_s

Fuel	Duration of agitation, min											
	0		0,5		2		5		10		20	
	τ_l, h	V_s, ml	τ_l,h	V_s, ml	τ_l ,h	V_s, ml	τ_l ,h	V_s, ml	τ_l ,h	V_s, ml	τ_l ,h	V_s, ml
1.Gasoline (100%)	0	5	0	5	0	5	0	5	0	5	0	5
2. Butanol (100%)	0	4	0	0	0	0	0	0	0	0	0	0
3. Ethanol (100%)	0	0	0	0	0	0	0	0	0	0	0	0
4.Mixtures: 4.1. B10	0	5	0,25	5	17,1	5	20,1	5	23,6	5	24,5	5
4.2. B20	0	5	1,2	5	17,4	5	21	4,5	23,7	5	24,8	4,7
4.3. B30	0	5	2,7	5	18,5	5	21,3	4,3	24,1	4,8	25,1	4
4.4. B50	0	5	0,5	2,5	1,5	2	15,8	2	17,5	2	17,8	1
4.5. E10	0	5,5	0,4	13	0,45	12	0,45	13	0,43	13	0,38	12
4.6. E20 (FEA)	0	8	0,37	22	0,42	22	0,38	22	0,32	22	0,33	21
4.7. E20 (alim)	0,8	15	4,55	24	3,43	24	3,2	24	3,02	24	2,45	24
4.8. E30	0	11	0,15	35	0,33	35	0,33	36	0,32	36	0,35	34
4.9. E40	0	12	0,024	50	0,011	44	0,013	50	0,013	50	0,018	50
4.10.E50	0,17	67	0,029	67	0,015	72	0,024	72	0,029	73	0,019	67
4.11. E60	0,033	69	0,015	96	0,13	95	0,17	94	0,17	97	0	0
4.12. E85	0	0	0	0	0	0	0	0	0	0	0	0
4.13. E16 B16 (FEA)	0	5	1,88	4	4,5	5	4,8	5	5	5	5,3	5
4.14. E16B16 (alim)	0	9	1,21	6,5	3,6	7	4,13	7	4,2	7	4,08	7

Dielectric permeability of water and alcohols is influenced by strongly polar group OH^-, which has the greatest influence in water (ε =81), then decreases its influence - in ethanol (ε =32) and butanol (ε =23). The values of listed properties explain practically absolute indissolubility of water H_2O in gasoline, limited water solubility in butanol and unlimited in ethanol.

In most cases, adding water in monoatomic alcohol-gasoline fuel mixtures without agitation has identical consequences - instant clearing (Tab. 1). Only in E50 and E60 mixtures the clearing took 0.17 hours (10 minutes) and 0.03 hours (2 minutes). The volume of sediment in the mixtures butanol-gasoline B10 ... B50, ethanol - butanol - gasoline E16B16 is equal to the volume of added water (5ml). In the mixtures of ethanol-gasoline, sediment volume increased from 5.5 ml (E 10) to 69 ml (E60), decreasing to 0 ml in the mixture E85.

We can assume that in the mixtures E10 ... E40, ethanol increasingly deposits as sediment together with water as its concentration in the mixtures increases. In the mixtures E50 and E60, the sediment includes not only water, ethanol, but also perhaps certain hydrocarbons from gasoline. In the mixture E85 (sediment volume of which is 0 ml), water and gasoline are assimilated (diluted) by ethanol.

The agitation of monoatomic alcohol-gasoline-water mixtures is the cause of water droplets dispersion in monoatomic alcohol-gasoline solutions, thus they becoming cloudy. In all the mixtures with butanol, an increase in the duration of agitation would first of all lead to the increase of the clearing duration τ_l (Fig. 1). Shaking for 0.5 minutes butanol-gasoline-water mixtures B10 ... B50 allows to keep them cloudy, and the clearing duration being for B10 τ_l=0,25 h (sediment volume - 5 ml), B20 – τ_l = 1,2 h (V_s =5ml), B 30 – τ_l =2,7 h (V_s = 5 ml), B50 – τ_l = 0,5 h (V_s=2,5 ml).

When increasing the duration of agitation of butanol mixtures with up to 20 minutes leads to a stabilization of clearing conditions (Fig. 1), maintaining τ_l values at 24.5-25.1 h for B10...B30 and 17.8 h for B50. The volume of sediment in these conditions maintains in the mixture B 10 (5 ml) and decreases in the mixtures B20 ... B50. Its decreasing degree increases while butanol concentration increases: V_s = 4,7 ml in B20, V_s = 4 ml in B30, V_s= 1 ml in B50 (tab 1.). The decrease of sediment volume can be explained by the dissolution of a part of water in butanol.

The agitation of ethanol-gasoline-water mixtures during 0.5 minutes increases the clearing period τ_l compared with stationary conditions up to 0.4 h (E10), the following values being in decrease: τ_l =0,37 h (E20), τ_l = 0,15 h (E30); τ_l =0,024h (E40); τ_l = 0,029 h (E50), τ_l = 0,015h (E60), τ_l = 0 h (E85).

The decrease of clearing period occurs, probably, due to the increase of ethanol fraction and consequently of its influence. All this also explains the increase in sediment volume: V_s = 13 ml (E10), V_s = 22 ml (E20), V_s = 35 ml (E30), V_s = 50 ml (E40), V_s = 67 ml (E50), V_s = 96 ml (E60). In the mixture E85, as already mentioned, the influence of ethanol prevails dissolving
momentaneously the gasoline and water.

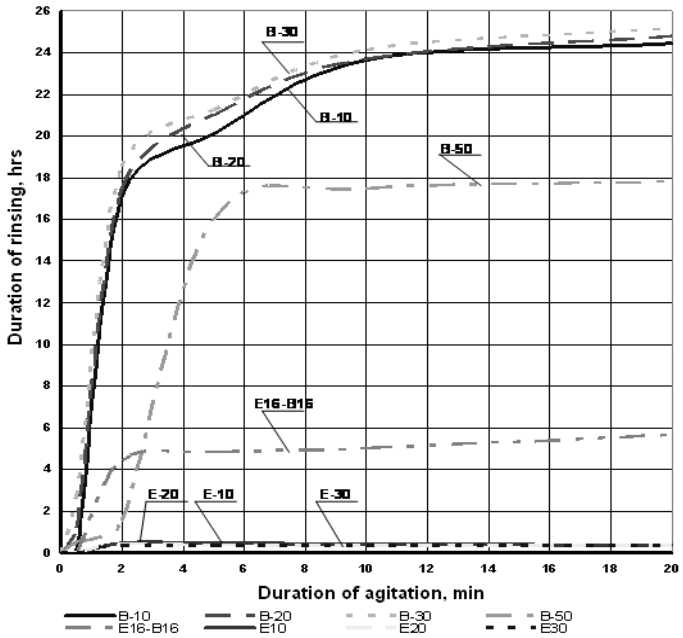

Fig. 1. The influence of the duration of agitation on the duration of clearing of monoatomic alcohol-gasoline-water mixtures

Increasing the duration of agitation up to 20 minutes does not change anything in the behavior of mixtures E10 ... E40, the duration of clearing and volume of sediment varying in narrow limits. The mixtures E50 and E60 present a variant of transition from the mixtures E10...E40 to the mixtures E85...E100. Increasing the duration of agitation up to 20 minutes we reduce sediment volume in the mixture E50 from 73 to 67 ml, and in the mixture E60 - from 97 to 0 ml, the period of clearing decreasing from 0.17 to 0 h.

Our researches proved the dependence of phase stability in mixtures on ethanol composition (Table 1). Using ethero-aldehyde fraction - EAF (98% vol. of absolute alcohol) in the preparation of mixture E20 allows a faster fuel clearing when adding water than in the case when purified alimentary alcohol (95,7 % vol. a.a.) is used.

At the same time when adding water the volume of sediment in the mixtures E20 and E16B16 which are prepared with alimentary alcohol is mostly about 2ml higher than in the mixtures prepared on the basis of ethero-aldehyde fraction. The difference in volumes of sediments is probably linked to differences in the composition of ethylic alcohol, including water fraction.

It should be mentioned that ethero-aldehyde fractions contain relatively large amounts of aldehydes, esters, fusel oil, volatile acids in comparison to alimentary alcohol. This fact influences the properties of alcohol and mentioned mixtures.

Therefore, the accomplished researches prove the dependence of phase stability in biofuels on their composition, agitation regimes, and allow determining the optimal conditions of storage and use of biofuels.

Conclusions

1. Studied pure fuels (gasoline, butanol, ethanol) and their mixtures butanol-gasoline B10 ... B50, ethanol-butanol-gasoline E16B16, have high properties of phase stability. Adding water into gasoline, butanol and their mixtures results in its sedimentation in an equal or less volume than the added volume. The water added in ethanol is completely dissolved.

2. The agitation of butanol-gasoline mixtures increases their clearing period up to 24.5 ... 25.1 hours and reduces the volume of sediment, dissolving a part of the added water in butanol. When increasing butanol fraction in the mixture, water volume increases too, and this is dissolved in butanol.

3. In the triple mixture of ethanol-butanol-gasoline E16B16, water addition has as consequence only its sedimentation, and the remaining ethanol in the fuel mixture obtains high phase stability due to butanol.

4. Butanol, butanol-gasoline mixture B10 ... B30, and ethanol-butanol-gasoline mixture E16B16 require practically identical conditions for the storage process as in the case of gasoline. In this case, the water that gets into fuel (for example, condensed), deposits as sediment for up to 25 hours after which the mixture can be used.

5. Addition of water to ethanol-gasoline mixture E10 ... E30 is the cause of not only water sedimentation but also of ethanol, which can be removed in this way from the fuel mixture. In the mixtures E40 ... E60, together with water and ethanol, certain gasoline fractions decant.

6. Intensive agitation for a relatively long duration (20 minutes) of E60 mixtures allow to obtain a transparent and homogeneous liquid without sediment. The same state can be also achieved in the case of the mixture E85, when adding water with and without agitation due to gasoline and water dissolution in ethanol.

7. Addition of water changes ethanol properties and ethanol-gasoline mixtures while maintaining phase stability in ethanol of the mixtures E60 (with intensive agitation), E85 or excluding it in the mixtures E10 ... E50, E60 (without agitation). Therefore, the mentioned fuels submit more exigent requirements referred to their storage conditions regarding the minimization of water penetration.

8. Faster clearing of ethanol-gasoline mixtures ($\tau_l \leq 0{,}45$ h) compared with butanol-gasoline mixtures ($\tau_l \leq 25$ h) can be explained by ethanol viscosity which is 2.4 times smaller than that of butanol. The obtained results can serve as a basis for establishing the duration of clearing of fuel mixtures in practical conditions.

9. The obtained results allow determining the most efficient agitation regimes of the mixtures ethanol-gasoline and butanol-gasoline with water surplus directly in the composition of supply system of internal combustion engines to achieve optimal composition of combustion air-fuel mixtures.

10. The use of ethylic alcohol of different compositions (purified alimentary alcohol, ethero-aldehyde fraction) changes slightly phase stability, which practically does not affect their conditions of storage and use.

References

[1]. "*World Consumption of Primary Energy Type and Selected Country Groups*, 1980-2004" (XLS). *Energy Information Administration*, U.S. Department of Energy. July 31 2006. http://www.eia.doe.gov/pub/international/iealf/table 18.xls. Retrieved o 2007-01-20.

[2]. Смаль Ф. В., Арсенов Е.Е. *Перспективные топлива для автомобилей*. М.: Транспорт, 1979-151 с.

[3]. Manea Gh., Georgescu M. Metanolul – *combustibil neconvenţional*. Bucureşti: Tehnică, 1992 – 84 p.

[4]. Gheorghişor M. *Carburanţi, lubrifianţi şi materiale auto speciale*. Bucureşti: Paralela, 2003 – 324 p.

[5]. Energie din biomasă: tehnologii şi mijloace tehnice/ Ion Hăbăşescu, Valerian Cerempei, Vasile Deleu şi alţ. Chişinău: Bons Offices, 2009 – 368 p.

[6]. Лышко Г.П. и др. *Топливо, смазочные материалы и технические жидкости.* Кишинев: ГАУМ, 1997 – 486 с.

[7]. Справочник химика, т. 6. Л: Химия, 1967 – 1012 с.

PRODUCTS DERIVED FROM CATALYTIC OXIDATION OF METHYLENE BLUE

T. Lupaşcu*[1], M. Ciobanu[1], O. Bogdevici[2], V. Boţan[1]

[1] *Institute of Chemistry of ASM,* [2]*Institute of Geology and Seismology of ASM*
Email: lupascu@gmail.com

Introduction

A large number of dyes have an important role not only in the textile and dye industries, but also in food, pharmaceuticals, cosmetics, and computers. These new applications bring a series of new problems in the purification of waste water obtained from different technological processes, because colorants are microtoxic, mutagens and carcinogens.

Obtaining of new catalysts, which would oxidize organic pollutants (dyes) in groundwater at relatively low temperatures represents an important goal in developing technologies for purification of wastewater obtained from various processes.

It is known that methylene blue in the presence of various catalysts (in most cases - modified adsorbents) and oxidants, undergoes transformations with the formation of new non-toxic products, whose structure has not yet been established [1-5].

The purpose of this paper is to study the oxidation products of methylene blue, using chromatography and mass spectrometry methods for this purpose.

Results and discussions

The process of oxidation of methylene blue was described in detail in our paper [6]. After 25 cycles of oxidation, the solution was separated from the active carbon CAN-8, subjected to vaporization in vacuum to a ~ 0.5 ml volume. It was subsequently dried in the desiccator with phosphoric anhydride. The obtained content was analyzed using thin-layer chromatography. Two fragments were found in the oxidation products. To determine the structure of these fragments, a fresh aliquot of dye was subjected to oxidation, for 25 cycles, as well. After drying in the desiccator, the content was dissolved in methanol. The solution obtained after rinsing was subjected to liquid-liquid chromatographic and mass spectrometric analyses using Agilent 5973 mass spectrometer.

Figure 1 illustrates the chromatogram of products of catalytic oxidation of methylene blue and the table presents the retention time and their peaks areas.

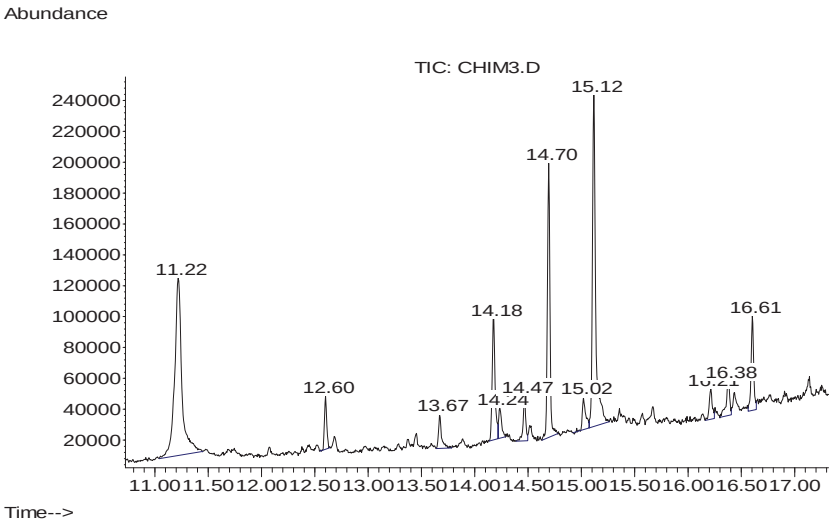

Fig.1. The chromatogram of products of catalytic oxidation of methylene blue

Table 1

Retention time and peaks areas

Compound #	Retention time	Peak Area
1	11.222	5407038
2	12.603	505822
3	13.674	435750
4	14.178	1486617
5	14.237	382915
6	14.469	488206
7	14.696	2875073
8	15.022	443141
9	15.119	4577054
10	16.215	376094
11	16.378	512623
12	16.606	1016222

Figure 2 shows the diethyl phthalate mass spectrum (first peak) from the database.

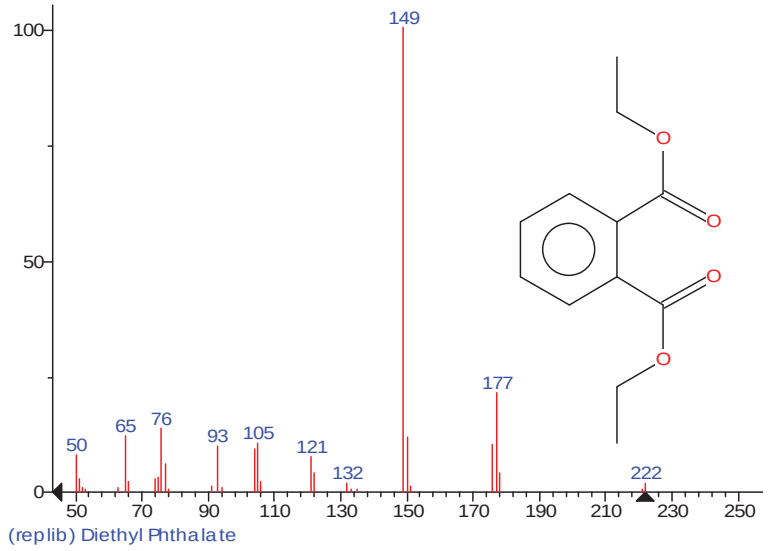

Fig.2. Mass spectrum of diethyl phthalate from the database.

Figure 3 shows diethyl phthalate mass spectrum from the database (a) and the first peak of the oxidation products (b), from figure 1.

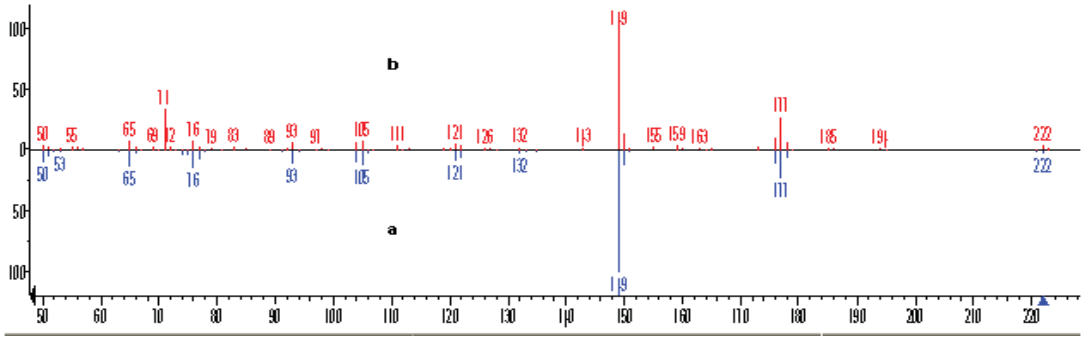

Figure 3. Diethyl phthalate mass spectrum from the database (a) and the first peak of the oxidation products (b).

From the presented data we find a coincidence of more than 90 percent of this substance.

The other peaks in the chromatogram presented in Figure 1 correspond to the retention time 12.6;

14.18;14.47;14.69;15.12;16.61 and, respectively, to the following compounds: methyl tetradecanoate (97%); 1,2-benzenedicarboxylic acid (83%); 9-hexadecenoic acid (91%); hexadecanoic acid (98%); dibutyl phthalate (91%); octadecanoic acid (99%).

Analysis of obtained mass spectra show that the products obtained during the oxidation process, cannot form from the fragmentation of methylene blue, although a catalytic oxidation process of methylene blue is known, giving a series of products, such as butane-2 amine, arridinone, benzylidene, benzacetic acid, benzonitrile [7].

Much of the products obtained by us probably can get into the dry mixture from the vacuum distillation system, or from the methanol used as solvent. It is worth mentioning here that these products make up only 10% of methylene blue used during the 25 cycles. Proceeding from the structural formula of methylene blue (Fig. 4) in the oxidation process, the radical $OH^{\bullet}$, with very high oxidation potential (2.8v) opens the cycle containing nitrogen and sulfur atoms, so that nitrogen can oxidize to nitrates (NO_3^-) or free nitrogen and sulfur may oxidize to sulfates [8].

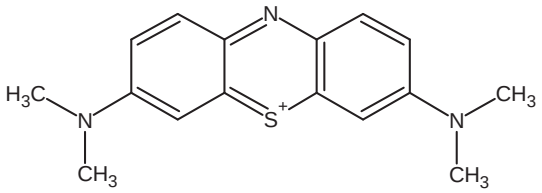

Fig.4. Structure of methylene blue

The attack of $OH^{\bullet}$ radical in the presence of oxygen initiates a complex cascade of oxidation reactions that lead to the mineralization of the resultant product. However, the precise directions of these reactions are not yet well defined. In any case, after the dissolution (after water vaporization) of oxidation products of methylene blue in methanol, an amount remains undissolved, which contains sulfates and nitrates, and which confirms the mineralization of methylene blue in the process of its oxidation.

The study of catalytic oxidation process with a different initial concentration of methylene blue (120 mg/L) produced an unexpected result. As a result there was a complete destruction of methylene blue. In this case the sample with oxidation products was subjected to vaporization in the drying oven at 100 ^{0}C and the dry content dissolved in very pure methanol.

The mechanism of this dye oxidation process is explained by participation of alkaline functional groups and by the fact that during oxygen bubbling through the solution containing methylene blue (C_o = 120 mg/L), on the surface of the activated carbon CAN-8 (at the interface) planar members (hemi-micelles) of dye and oxygen molecules are adsorbed. Thus, there is a potential difference at the interface and the $OH^{\bullet}$ radical is formed, which has a high oxidation potential (2.8V), and which completely catalytically oxidizes methylene blue in the conditions of the experiment. In case of performing the process at a methylene blue concentration of 20 mg/L, the $OH^{\bullet}$ radical acts less effectively at the interface, due to the presence of a smaller number of dye molecules. Methylene blue adsorption occurs, in this case, from the real solutions, and not hemi-micellar ones.

In order to determine if any organic substances are eliminated from the studied active carbon during the oxidation process, we performed blank analysis.

Chromatograms of the zero sample are shown in figure 5 (activated carbon, demineralized water, bubbling with oxygen at 50 ^{0}C) and of oxidation products of methylene blue C_0 – 120 mg/L, activated carbon quantity CAN-8 – 200 mg, Vsol.-100ml, bubbling with oxygen, p-2 atm, T-50 ^{0}C.

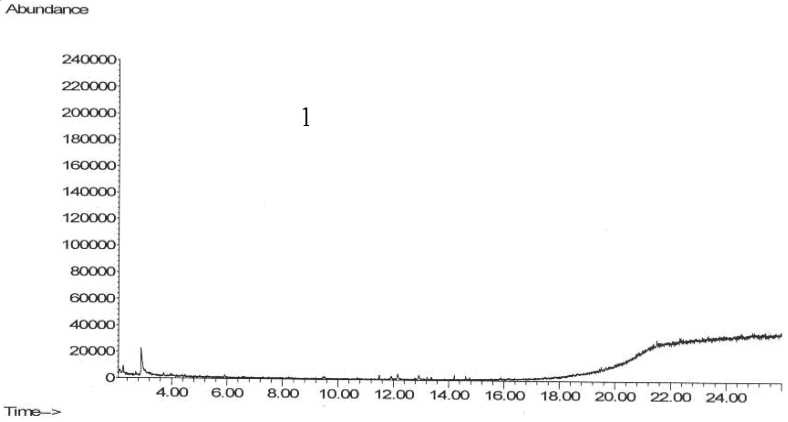

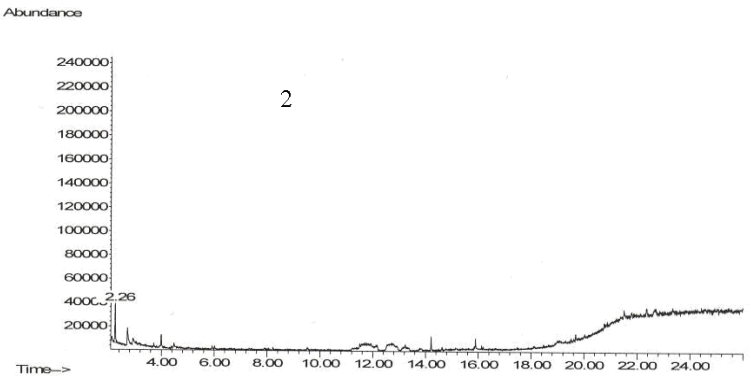

Fig. 5. Chromatogram of the blank sample (activated carbon, demineralized water, bubbling with oxygen at 50 ^{0}C) (1) and chromatogram of oxidation products of methylene blue C_0 – 120 mg/L, activated carbon quantity CAN-8 – 200 mg, Vsol.-100ml, bubbling with oxygen, p-2 atm, T-50 ^{0}C. (2).

It should be noted that in paper [1], where the authors studied the oxidation of methylene blue using as the oxidant - tertiary-butyl hydroperoxide and as a catalyst - manganese oxide with different valences, at room temperature and higher temperatures, the products that are obtained as a result of oxidation are not named, although the mass spectra of obtained products were registered in time (kinetics of the process). Mass spectra for all times were totally different from those we obtained in the present work, which indicates that depending on the catalyst and oxidant studied, and on the concentration of the dye, different intermediate and final products are obtained.

Conclusions

1. It was established that the process of catalytic oxidation of methylene blue, at low concentrations (20 mg/L), i.e. in real solutions, gives sulfates and nitrates and new product, which can be categorized, in their vast majority, as impurities, probably got from the vacuum distillation unit, which make up for only ~ 10 % of methylene blue used in the experiment. Methylene blue adsorption at the interface occurs in real solutions.
2. In case of performing the process at methylene blue concentration of 120 mg/L, hemi-micelles are adsorbed at the interface and the $OH^{\bullet}$ radical acts more effectively due to the presence at the interface of a greater number of dye molecules.

References

[1]. Thamayanthy Sriskandakumar, Naftali Openbe, Chun-Hu Chen, Almec Morey, Cecil King ondu and Steven L. Suib. J.Phys.Chem. A, 2009, 113(8), pp.1523-1530.
[2]. Maximov A.I., Subbotkina I.N., Hliustova A.V. Degradation of organic dyes in a diaphragm discharge in the volume of electrolyte. XXXV International Conference on Plasma Physics and Controlled Fusion, 11-15 February 2008 (in Russian).
[3]. H.S.Silva, N.D.Martinez, A.C.Deiana, J.E.Gonzalez. Catalytic oxidation of methylene blue in aqueous solutions. – 2nd Mercosur Congress on Chemical Engineering. 2005, p.1-8.
[4]. Donaldson J.D.,Grimes S.M., Yasri N.G., Wheals B.: Parrick J; Errington W.E. Anodic oxidation of dye materials methylene blue, acid blue 25, reactive blue 2 and reactive blue 15 and the characterisation of novel intermediate compounds in the anodic oxidation of methylene blue. – J. Chemical Tehnology and Biotechnology, v.77, Number 7, 2002,pp.756-760 (5).
[5]. Li J., Ma W., Huang Y., Cheng M., Zhao J., Yu J.C. A highly selective photooxidation approach using O_2 in water catalyzed by iron (II) bipyridine complex supported on NaY zeolite. – Chem. Commun. 2003. 2214-2215.
[6]. Lupaşcu T., Ciobanu M., Boţan V., Nistor A. Oxidarea catalitică a albastrului de metilen.
[7]. Chemistry Journal of Moldova. 2010. v.5 No.2, p.37-40.
[8]. A. Rodriguez, G. Ovejero, M. Mestanza, V. Callejo, I. Garcia. Degradation of Methylene Blue by catalytic Wer Air Oxidation with Fe and Cu Catalyst Supported on Multiwalled Carbon Nanotubes.- Chemical Engineering Transactions V. 17, 2009, pp. 145-151.
[9]. Rein Munter. Advanced oxidation process – current status and prospects. – Proc. Estonian Acad. Sci. Chem., 2001, 50, 2, 59-80.

HIGH-PERFORMANCE LIQUID CHROMATOGRAPHY FOR DETERMINATION OF AROMATIC ALDEHYDES IN WINE DISTILLATES

Elena Nezalzova

Scientific-Practical Institute of Horticulture and Food Technologies
59, Vierul str., Chisinau, Moldova, e-mail: lena_nezalzova@yahoo.com

Abstract. Quality control of alcoholic beverages, coming into the market, is a defining element in preventing the production and supplying of defective products. One of the main criteria for quality control of wine distillates is to estimate their age, and more precisely the period of maturation as the dominant factor in determining the quality of cognacs and, consequently, their market price. On the opinion of majority scientists, one of the main factors, which determines the age of wine distillates, is the content of aromatic aldehydes, mostly vanillin, and their ratio.

Keywords: wine distillate, age of maturation, aromatic aldehydes, high-performance liquid chromatography.

Introduction

Extraction of natural phenolic compounds from oak wood by wine distillate and their hydrolysis in the process of aging leads to the formation of aromatic alcohols and their subsequent oxidation to aromatic aldehydes. Aromatic aldehydes (vanillin, siringic, sinapic, coniferylic, p-oxybenzoic aldehydes etc.) by their organoleptic properties are involved in formation of cognac's flavor and aroma. In addition, according to many researchers, the concentration of aromatic aldehydes can serve as a marker of duration of the wine distillate's maturation in oak barrels. In this regard, relevant is the correct quantification of aromatic aldehydes in the aged wine distillates, from which subsequently are made cognacs.

From aromatic aldehydes in wine distillates are found mostly compounds of guaiacyl (I) and siringyl (II) series (Table 1) [2, 4].

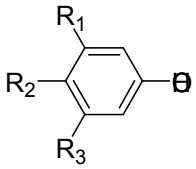

Vanillin: R_1=H; R_2=OH; R_3=OCH_3
Siringic aldehyde: R_1=R_3=OCH_3; R_2=OH
p-oxybenzoic aldehyde: R_1=R_3=H; R_2=OH

I

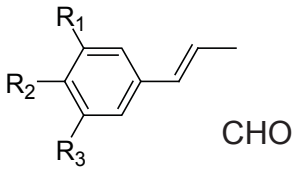

Coniferylic aldehyde: R_1=H; R_2=OH; R_3=OCH_3
Sinapic aldehyde: R_1=R_3=OCH_3; R_2=OH

II

Aromatic aldehydes give characteristic color reactions with various reagents. A number of spectral methods of their quantitative determination is based on this property. However, according to I. Skurikhin, vanillin, siringic and sinapic aldehydes in the ultraviolet absorption spectrum have similar maxima. As a result, the spectrophotometric method can show the total content of these components. Therefore, rather contradictory data on the content of individual aromatic aldehydes in wine distillates and cognacs often appear. It concerns mostly vanillin.

In the present, in the existing regulatory-technical documentation for production of cognacs (SM 145:2003 "Divinuri. Condiții tehnice"), for ageing proof of wine distillates the concentration of an aromatic aldehyde – vanillin is used. But spectrophotometric determination method of analysis is provided for this purpose.

Table 1

Aromatic aldehydes	The content of aromatic aldehydes in wine distillates of 1-15 years old, mg/l	Threshold concentrations, mg/l	
		Aroma	Taste
Vanillin	0,1-1,6	0,01	0,1
Siringic aldehyde	0,2-2,8	50	100
Sinapic aldehyde	0,5-2,4	200	200
Coniferylic aldehyde	0,9-2,6	3	10
Total	1,9-8,7		

I. Skurikhin and others have found that the content of aromatic aldehydes in the process of aging of wine distillates in contact with oak is growing. The relation between simple aromatic aldehydes (vanillin and siringic aldehyde) and aldehydes with the double bond (sinapic and coniferylic aldehydes) is changed ambiguously in the process of aging, so using only vanillin for characterization the degree of wine distillate's maturation without regarding other aromatic aldehydes represents a wrong approach.

The method of high-performance liquid chromatography (HPLC) allows us to identify and quantify the individual aromatic aldehydes from the general group of these compounds, selected by optical methods.

Materials and methods

Spectrophotometric method of SM 145:2003 is based on measuring the optical density of alkaline solution of vanillin in the ultraviolet part of the spectrum at $\lambda = 350$ nm.

The method of high-performance liquid chromatography (HPLC) allows to separate the phenolic compounds and the products of their degradation - aromatic aldehydes and acids extracted by wine distillate from oak wood, on a special chromatographic column, and then to determine them quantitatively. We picked the best mode of separating a mixture of aromatic aldehydes and their predecessors - the aromatic acids and used a method developed for quantitative differential determination of the above mentioned compounds, including vanillin, in wine distillates of different periods of maturation.

For our research we selected about 30 samples of wine distillates of different periods of maturation (young, from 2 to 27 years old), prepared at domestic enterprises and imported into Republic of Moldova.

Determination of aromatic aldehydes and acids by HPLC was performed on the liquid chromatograph LC-20A Prominence, Shimadzu, on the column CC 125/4 Nucleosil 100-5C18 Nautilus. Detector SPD-20AV UV/VIS, by which is equipped this liquid chromatograph, includes deuterium and tungsten halogen lamps, as a result the analytical capabilities are expanded to the visible range. As an eluent we used a mixture of methanol and acetic acid. Separation of standard mixture of aromatic aldehydes was carried out under the following conditions:

The volume of injected sample, µl	100
Wavelength, nm	280
Eluent	Solution A – Methanol. Solution B – 0,5 % Acetic acid
Gradient program:	Start - 5 % solution A, - 95 % solution B
	10 min - 15 % solution A, - 85 % solution B
	45 min - 40 % solution A, - 60 % solution B
	55 min - 92 % solution A, - 2 % solution B
	Stop - 5 % solution A, - 95 % solution B
The rate of the eluent, ml/min	0,8
Duration of analysis, min	60

The content of vanillin was determined on the spectrophotometer СФ-46 by the method indicated in SM 145:2003.

Results and discussion

Figure 1 shows the chromatogram of a standard mixture solution of aromatic aldehydes and acids, on which there is good separation of the peaks and sensitivity.

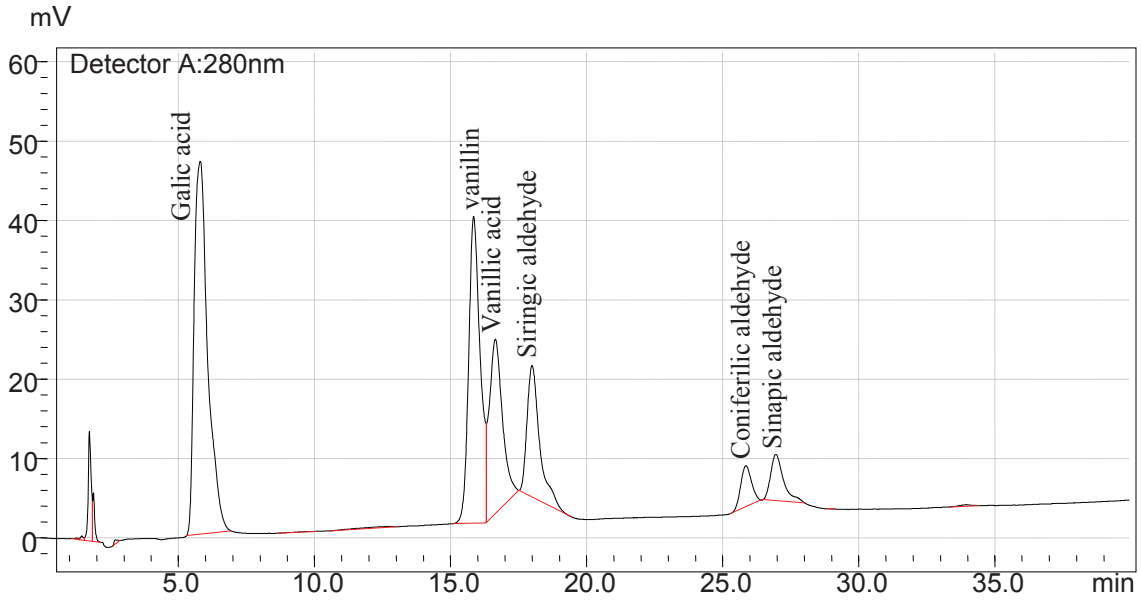

Fig. 1. Chromatogram of standard mixture solution of aromatic aldehydes and acids.

We separated by HPLC method the mixture of aromatic aldehydes and natural sample of the aged wine distillate in the measurement mode of two wavelengths 280 and 254 nm. Figures 2 and 3 show the chromatograms, on which it is seen that the analysis in this mode allows in one step to get a good separation of the peaks of studied substances. Thus, the established modes of analysis by HPLC can differentially determine the concentration of individual aromatic aldehyde and the corresponding aromatic acids in wine distillates.

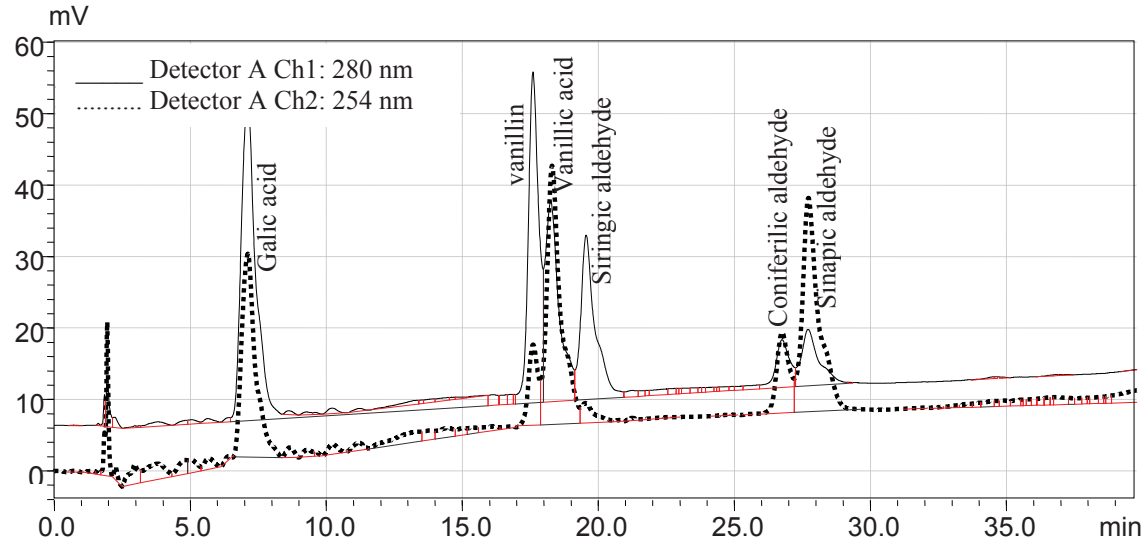

Fig. 2. Chromatogram of standard mixture solution of aromatic aldehydes and acids on two wavelengths: 280 and 254 nm.

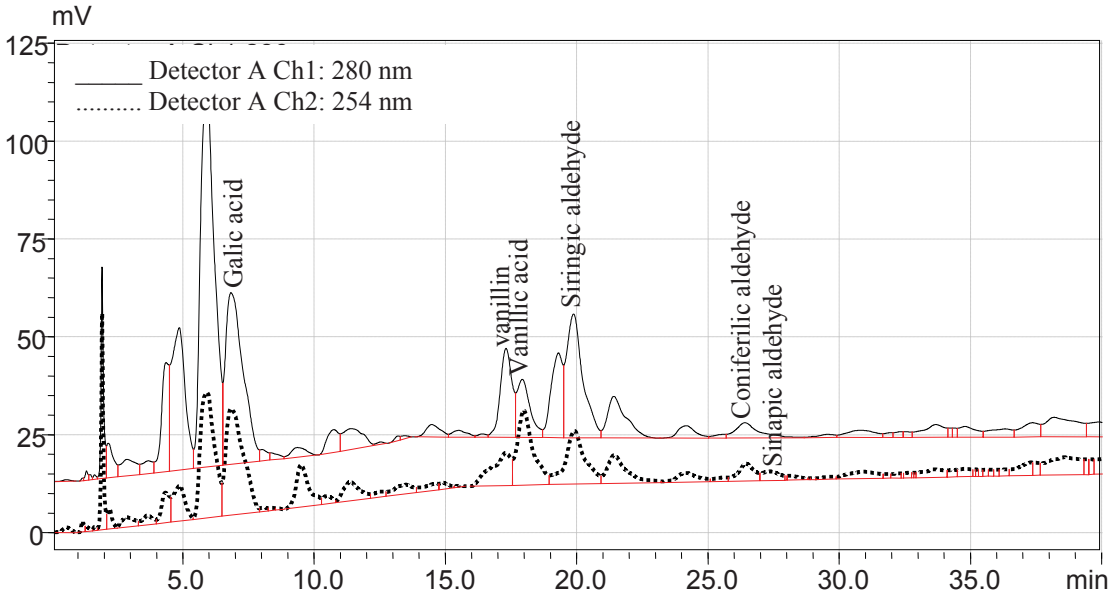

Fig. 3. Chromatogram of composition of aromatic aldehydes and acids of natural sample of the aged wine distillate, year 1980, on two wavelengths: 280 and 254 nm.

We have carried out studies on the comparison of results obtained in determining the content of vanillin in wine distillate of different periods of maturation by the spectrophotometric method in SM 145:2003 "Divinuri. Condiții tehnice" and by high-performance liquid chromatography (HPLC).

We have seen that they differ (Table 2). The content of vanillin, determined by HPLC, was significantly lower than the one, established by spectrophotometric method.

In the current SM 145:2003 "Divinuri. Condiții tehnice" for characterization the physico-chemical composition of aged wine distillates the amount of vanillin is only used, and in wine distillates up to 5 years old this parameter is not normalized, and in the distillate over 6 years old the content of vanillin may not exceed 16 mg/dm^3 /4/. Our studies show that this parameter does not reflect the real picture, the amount of accumulated vanillin is significantly lower than the indicated value.

Table 2

The content of vanillin in aged wine distillates, determined by different methods

The year of laying for maturation	The content of vanillin, mg/dm^3	
	Spectrophotometric method on SM145:2003	High-performance liquid chromatography (HPLC)
1983	13,0	5,6
1985	17,7	6,1
1988	13,5	6,6
1989	14,0	6,6
2003	12,7	7,9
2004	8,5	5,2
2005	6,2	2,7
2005	5,0	3,2
2005	9,5	5,5
2007	2,7	1,2
2007	2,0	0,5
2008	1,2	0,4

Conclusion

The method of determination of aromatic aldehydes in wine distillates by high-performance liquid chromatography has been elaborated. Application of high-performance liquid chromatography (HPLC) allows to eliminate errors at the control of the content of aromatic aldehydes, especially vanillin, in maturated wine distillates.

Acknowledgements

This work was carried out under the direction of Academician Boris Gaina.
Consultant - Elena Scorbanov.

References

[1]. Власов В.Н., Маруженков Д.С. Анализ качества бренди из винограда методом хромато-масспектрометрии, В: Виноград и вино России, 1999, № 1, с.28-31

[2]. Кишковский З.Н., Скурихин И.М. Химия вина. – Москва: Пищевая промышленность, 1976

[3]. Савчук С.А., Колесов Г.М. Хроматографические методы контроля качества коньяков и коньячных спиртов, В: Аналитическая химия, 2005, №8, с.848-868

[4]. Скурихин И.М. Химия коньяка и бренди Москва: Де Ли Принт, 2005.296 с.

[5]. SM 145:2003”Divin.Condiţii tehnice”

[6]. Незальзова Е.Н., Скорбанова Е.А., Гаина Б.С.и др. Выявление объективных показателей возраста коньяков оптическими методами исследования. В: Сборник научных трудов VII международной научной конференции “Лазерная физика и оптические технологии”, Минск, 2008, часть II, с. 215-218.

SYNTHESIS AND IR, NMR CARACTERISATION OF NEW *P*-(N,N-DIPHENYLAMINO) CHALCONES

Sîrbu Dumitru, Marin Ion*

Institute of Chemistry of the ASM, 3 Academiei str., Chisinau, MD-2028, Republic of Moldova
E-mail: marininbox@yahoo.com; tel.: + 373 22 729761.

Abstract: This article reports on the high yield synthesis and novel chalcones with isothiocyanate and imidazol groups. The synthesis was started from N,N-diphenilamine and finished with 4-(N,N-diphenylamino)-4'-(2-thioxo-imidazolidin-4-one)-chalcone, where the cheap and accessible reagents were used.

Keywords : chalcone, isothiocyanat, imidazole, NMR, IR.

Introduction

Since its discovery, chalcones became of interest due to its biological activities such as antibacterial, antifungal, antimalarial and anticancerous properties[1]. The possibility to use chalcones in application domains of luminophore pigments [2], developing of lasers, photographic techniques, photocopying, data storage elements, in dye-sensitized solar cells [3] gave an impulse for the intensification of luminescent chalcones investigation [4].

Results and discussion

In order to obtain 4-(N,N-diphenylamino)benzaldehyde, (4, Scheme 1), two reactions were carried out. Initially, diphenylamine (1) was condensed with iodobenzene (2) to obtain triphenylamine (3). The reaction is catalyzed by activated copper in nitrobenzene [5]. For the introduction of the carbonyl group in the *para* position of the phenyl ring the Vilsmeier reaction was used [6]. The presence of formyl group in the final product (4) was demonstrated by IR spectroscopy (ν (C=O) = 1685 cm^{-1}.

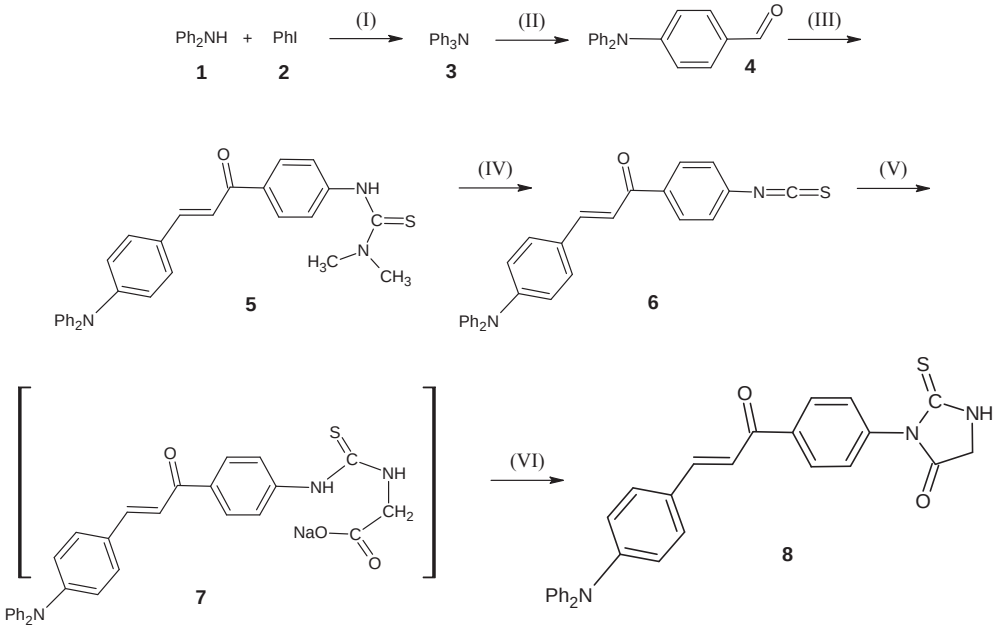

Scheme 1: **Synthetic Route of the 4-(N,N-diphenylamino)-4'-(2-thioxo-imidazolidin-4-one)-chalcone**
(I) Cu/K_2CO_3, $PhNO_2$, reflux (II) $POCl_3$, DMF, 95-100 ºC, 20 h (III) 4-N,N-dimethylthioureidoacetophenone, NaOH, EtOH/DMF, 25 ºC, 5 h (IV) acetic anhydride, dioxane/H_2O, reflux, 2 h (V) glycine, Na_2CO_3, reflux, 2 h (VI) $CHCl_3$, reflux, 1 h.

The synthesis of 4-(N,N-diphenylamino)-4'-(N,N-dimethylthioureido)-chalcone (5) was carried using the alkaline catalysis (Scheme 1). The acetophenone carboanion attack the positively charged carbon of the carbonyl group. As a result, aldol condensation occurs and aldol products are obtained. Thus, by removal of hydroxyl group and formation of the double bond (crotonic condensation), the final compound is obtained (5). To inhibit secondary reactions, alkaline catalysis was carried out at temperatures not more 25 °C.

To confirm the proposed structure of product (5) the 1H-NMR spectrum of this substance was measured. The main information was provided by doublet with chemical shift 7.78 ppm and integral 1 which indicates the presence of the double bond C=C. Also, the peaks for protons of the following groups were found:

- 4'-(N,N-dimethylthioureido) – 3.37 ppm (s, 6H, CH_3) and 9.81 ppm (s, 1H, NH);
- parasubstituted phenyl ring from acetophenone group – 8.01 ppm (d, 2H, 2',6'-C_{ph});
- parasubstituted phenyl ring from 4-(N,N-diphenylamino) group – 7.48 ppm (d, 2H, 2,6-C_{ph});
- Other proton peaks were found as multiplets in the region 7.00 ÷ 7.41 ppm.

Reaction yield is relatively high (70%) compared with those described in the literature for analogue compounds [7].

In order to obtain the isothiocyanato product (6) the elimination of dimethylamine from dimethylthioureidochalconic compound (5) was performed. This was achieved by boiling the latter one in benzene in the presence of acetic anhydride. As a result, the compound (5) was completely consumed and the final product was easily separated.

To confirm the proposed structure of product (6) ^{1}H-NMR, Cosy45–NMR and IR spectroscopy methods were used. The main changing in ^{1}H-NMR spectrum (fig. 1) for compound (6) versus the analog spectrum of the initial compound (5) is the disappearance of the proton peaks for CH_3 and NH groups from 4'-(N,N-dimethylthioureido) fragment. Proton spectrum has provided information about the presence of the following fragments:

- double bond C=C – 7.77 ppm (d, 1H, 2-C);
- parasubstituted phenyl ring from acetophenone group – 8.00 ppm (d, 2H, 2',6'-C_{ph});
- parasubstituted phenyl ring from 4-(N,N-diphenylamino) group – 7.02 ppm (d, 2H, 3,5-C_{ph}), 7.48 ppm (d, 2H, 2,6-C_{ph});
- other proton peaks are overlapped and were assigned to multiplets in the regions – 7.10 ÷ 7.16 ppm (m, 2H, 2*4''-C_{dpha} + 4H, 2*2'',6''-C_{dpha}) and 7.29 ÷ 7.33 (m, 2H, 3',5'-C_{ph} + 4H, 2*3'',5''-C_{dpha} + 1H, 3-C).

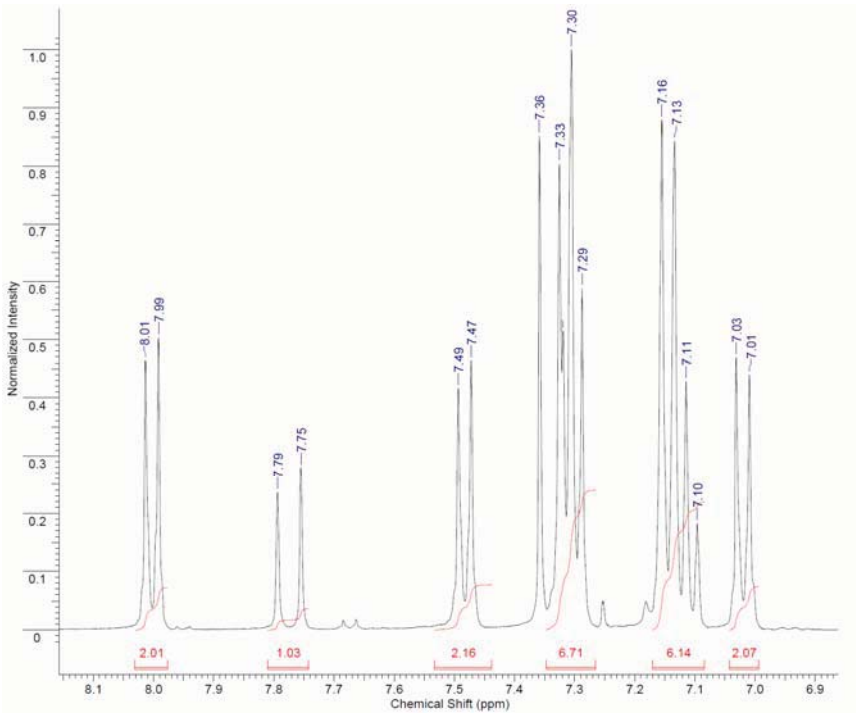

Fig. 1. ^{1}H-NMR spectrum of 4-(N,N-diphenylamino)-4'-isothiocyanato-chalcone

For correct assignment of other proton peaks in the NMR spectrum, Cosy45-NMR spectroscopy was used (fig. 2), that provided information about all protons of compound (6):

- double bond C=C – 7.33 : 7.77 ppm (1H, 3-C : 1H, 2-C);
- parasubstituted phenyl ring from acetophenone group – 7.30 : 8.00 ppm (3',5'-C_{ph} : 2',6'-C_{ph});
- monosubstituted phenyl ring from 4-(N,N-diphenylamino) group – 7.09 : 7.30 ppm (4''-C_{dpha} : 3'',5''-C_{dpha}) and 7.13 : 7.30 ppm (2'',6''-C_{dpha} : 3'',5''-C_{dpha});
- parasubstituted phenyl ring from 4-(N,N-diphenylamino) group – 7.01 : 7.48 (3,5-C_{ph} : 2,6-C_{ph}).

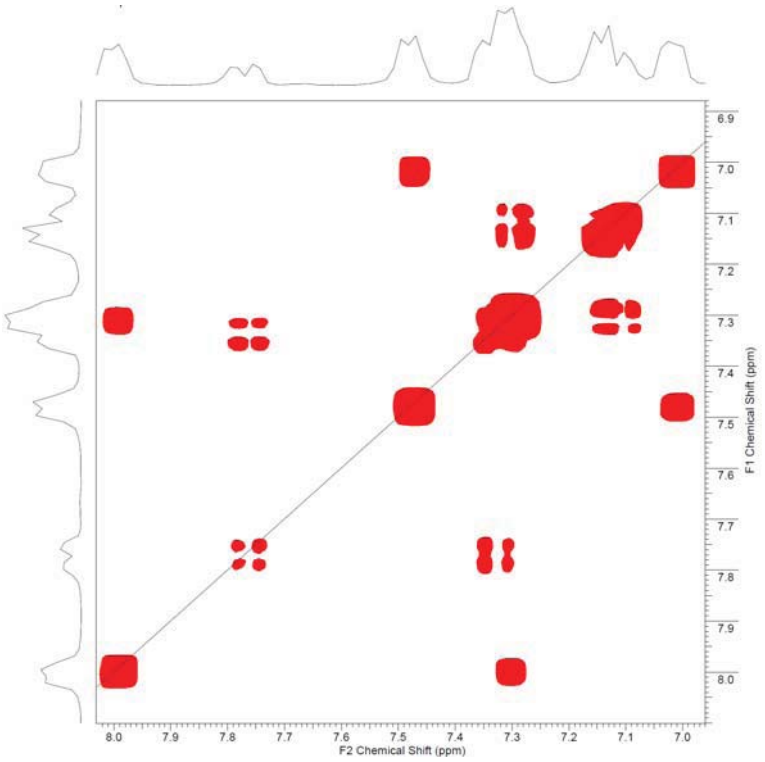

Figure 1: Cosy45-NMR spectra of 4-(N,N-diphenylamino)-4'-isothiocyanato-chalcone

IR spectroscopy was used to demonstrate the presence of functional groups in the studied compound. For product (6) ketone and isothiocyanato groups were studied. Their presence was indicated by intense peaks at following wavelength:

- ν (CO) = 1650 cm^{-1}, medium – ketone group;
- ν (CN) = 2115 cm^{-1}, strong – isothiocyanato group.

^{1}H-NMR, Cosy45-NMR and IR spectroscopic data unequivocally demonstrate the proposed structure of compound (6).

The synthesis of the 4-(N,N-diphenylamino)-4'-(2-thioxo-imidazolidin-4-one)-chalcone (8) was performed by addition of glycine to 4-(N,N-diphenylamino)-4'- isothiocyanato chalcone (6) and subsequent cyclization of the intermediate compound (7). Sodium glycinate is more active in addition reactions as compared to its acid form, therefore glycinic acid was neutralized with sodium carbonate. The addition of sodium glycinate to compound (6) leads to obtaining of sodium chalcone-4-(N,N-diphenylamino)-4'-((carbamothioyl)aminoacetate) (7). The neutralization and subsequent heating in chloroform of the intermediate compound (7) lead to the final product (8).

To confirm the proposed structure of product (8) ^{1}H-NMR and IR spectra were measured. Proton spectrum has provided information about the presence of the following fragments:

- 2-thioxo-imidazolidin-4-one substituted on 3-C – 4.38 (s, 2H, CH_2) and 9.25 (s, 1H, NH);
- parasubstituted phenyl ring from acetophenone group – 8.21 ppm (d, 2H, 2',6'-C_{ph});
- monosubstituted phenyl ring from 4-(N,N-diphenylamino) group – 7.00 ppm (d, 2H, 3,5-C_{ph}) and 7.54 ppm (d, 2H, 2,6-C_{ph});
- parasubstituted phenyl ring from 4-(N,N-diphenylamino) group – 7.75 ppm (m, 4H, 3'',5''-C_{dpha}).
- other protons peaks are overlapped and were assigned to multiplets in the regions – 7.14 – 7.17 ppm (m, 1H, 2-C + 2H, 2*4''-C_{dpha} + 4H, 2*2'',6''-C_{dpha}), 7.36 – 7.40 ppm ((m, 2H, 3',5'-C_{ph} + 1H, 3-C).

Using IR spectroscopy the presence of the following functional groups was demonstrated:

- ν (CO) = 1654 cm^{-1} – ketone group from acetophenone;
- ν (CO) = 1761 cm^{-1} – ketone group from glycine;
- ν (NH) = 3229 cm^{-1} – secondary amine group.

Experimental section

NMR spectra were performed in $CDCl_3$ on BRUKER AVANCE-III 400 MHz spectrometer. NMR methods utilized in this research are: ^{1}H-NMR, ^{13}C-NMR, Cosy45-NMR.

IR spectra were measured at the Spectrum 100 FT-IR Spectrometer Perkin Elmer.

Synthesis of 4-(N,N-diphenylamino)-4'-(N,N-dimethylthioureido)-chalcone (5).

An amount of 5 ml of dried DMF was added to the mixture of 0.40 g (1.45 mmol) 4-((N,N-diphenyl)amino) benzaldehyde and 0.35 g (1.57 mmol) (1:1 equivalent) of 4-N,N-dimethylthioureidoacetophenone. Complete dissolution of initial compounds was observed after addition of solution formed by adding 0.5 g NaOH in 6.5 ml of absolute ethanol. The reaction was performed at 25 ºC under stirring for 5 h. The end of reaction was determined from TLC (Thin Layer Chromatography) analysis by consuming of 4-((N,N-diphenyl)amino)benzaldehyde. The reaction mixture was neutralized with aqueous solution of HCl (4 %) and the precipitate was formed, which was washed with distilled water. The crude product was purified on silica gel column (hexane/benzene, 1/3) to afford the target compound (5) (0.56 g, 70 % yield). ^{1}H-RMN ($CDCl_3$), δ (ppm): 3.37 (s, 6H, CH_3), 7.00 ÷ 7.41 (m, 2H, 3,5-C_{ph} + 2H, 2*4''-C_{dpha} + 4H, 2*2'',5''-C_{dpha}, 2H, 3',5'-C_{ph} + 4H, 2*3'',5''-C_{dpha} + 1H, 3-C), 7.48 (d, 2H, 2,6-C_{ph}), 7.78 (d, 1H, 2-C), 8.01 (d, 2H, 2',6'-C_{ph}) 9.81 (s, 1H, NH).

Synthesis of 4-(N,N-diphenylamino)-4'-isothiocyanato-chalcone (6).

An amount of 0.22 g (2.15 mmol) of acetic anhydride in 4 ml of benzene was added to 1.0 g (2.1 mmol) of 4-diphenylamino-4'-(N,N-dimethylthioureido)-chalcone. The mixture was refluxed for 2 h, the formed precipitate was filtrated, the solvent from filtrate was removed by low pressure distillation. The crude product was purified on silica gel column (hexane/benzene, 1/3) to afford the target compound (6) (0.9 g, 80 % yield). ^{1}H-RMN ($CDCl_3$), δ (ppm): 7.02 (d, 2H, 3,5-C_{ph}), 7.10 ÷ 7.16 (m, 2H, 2*4''-C_{dpha} + 4H, 2*2'',6''-C_{dpha}), 7.29 ÷ 7.33 (m, 2H, 3',5'-C_{ph} + 4H, 2*3'',5''-C_{dpha} + 1H, 3-C), 7.48 (d, 2H, 2,6-C_{ph}), 7.77 (d, 1H, 2-C), 8.00 (d, 2H, 2',6'-C_{ph}). COSY 45 - RMN ($CDCl_3$), δ (ppm): 7.01 : 7.48 (3,5-C_{ph} : 2,6-C_{ph}), 7.09 : 7.30 (4''-C_{dpha} : 3'',5''-C_{dpha}), 7.13 : 7.30 (2'',6''-C_{dpha} : 3'',5''-C_{dpha}), 7.33 : 7.77 (1H, 3C : 1H, 2C), 7.30 : 8.00 (3',5'-C_{ph} : 2',6'-C_{ph}). IR ν (cm^{-1}): 620 w, 643 w, 667 m, 684 m, 694 s, 703 s, 745 m, 756 s, 772 m, 798 m, 810 s, 835 w, 856 vw, 864 vw, 890 w, 929 m, 952 w, 976 m, 1003 m, 1014 m, 1030 s, 1051 w, 1073 m, 1109 w, 1155 m, 1172 s, 1187 s, 1212 s, 1261 m, 1288 m, 1304 s 1314 s, 1337 vs, 1432 m, 1450 m, 1488 vs, 1507 s, 1553 s, 1568 vs, 1576 vs, 1593 s, 1650 m, 1688 w, 1740 vw, 2115 s, 2189 m, 2287 vw, 2510 w, 2600 w, 2743 vw, 2850 w, 2919 w, 3033 w, 3060 w, 3294 vw.

Synthesis of 4-(N,N-diphenylamino)-4'-(2-thioxo-imidazolidin-4-one)-chalcone (8).

The mixture of 0.30 g (0.004 mol) glycine and 0.21 g (0.002 mol) of Na_2CO_3 was dissolved in minimal quantity of water, this solution of sodium glycinate was added drop wise to dioxane solution of 0.86 g (0.002 mol) *4-(N,N-diphenylamino)-4'-isothiocyanato-chalcone*. After refluxing for 2 h, the solution was cooled at room temperature and neutralized with HCl solution ($HCl_{conc.}/H_2O$ = 1/2). The intermediary noncyclic compound was extracted with $CHCl_3$. After refluxing for 1 h, the solvent was removed by low pressure distillation. The crude product was purified on silica gel column (ethyl acetate/benzene, 1/2) to afford the target compound (8) (0.39 g, 40% yield). ^{1}H-RMN ($CDCl_3$), δ (ppm): 4.38 (s, 2H, CH_2), 7.00 (d, 2H, 3,5-C_{ph}), 7.14-7.17 (m, 1H, 2C + 2H, 2*4''-C_{dpha} + 4H, 2*2'',6''-C_{dpha}), 7.36-7.40 (m, 2H, 3',5'-C_{ph} +1H, 3-C), 7.54 (d, 2H, 2,6-C_{ph}), 7.75 (m, 4H, 2*3'',5''-C_{dpha}), 8.21 (d, 2H, 2',6'-C_{ph}), 9.25 (s, 1H, NH). IR, ν (cm^{-1}): 665 w, 696 s, 754 m, 817 m, 897 vw, 959 w, 981 m, 1017 m, 1031 m, 1076 w, 1173 vs, 1187 s, 1215 s, 1269 vs, 1295 s, 1315 s, 1327 s, 1396 m, 1425 m, 1452 m, 1489 vs, 1504 vs, 1580 s, 1603 m, 1654 m, 1761 m, 2599 vw, 2852 w, 2922 w, 3034 w, 3060 w, 3229 w (band).

Acknowledgements: This work was supported by the project 09.832.08.04A.

References

[1]. Ringshi L.; Xiaowu C., Journal of Med. Chem.,1995, Dec. 22, 38(26) : 5031-5037.
[2]. Gorduza V.M.; Tarabasam C.; Atanasiu A.; Pop C.; Coloranți organici. Aplicații neconvenționale. Editura Uni-Press C-68, 2000, 164-190.
[3]. Minigfei Xu; Renzhi Li; Nuttapol Pootrakulchote, J. Phys. Chem. C., 2008, 112, 19770-19776.
[4]. Andries A.; Buzurniuc S.; Verlan V.; Caraman M.; Robu S.; Barbă N., „Fluorescent Nanocomposite Organic Luminophore Compound-Polzmer, The 5th Conference New Research trends in material science" ARM-5, Proceedings vol. III, 2007, 642-644.
[5]. F.D.Hager, Organic Syntheses, Coll. Vol. 1, 1941, 544; Vol.8, 1928, 116.
[6]. G. Lai; X.R.Bu; J. Santos; E.A. Mintz, Synlett 1997, 11, 1275-1276.
[7]. S. Eddarir; N.Cotelle; Y. Bakkour; C. Rolando, Tetrahedron Letters 2003, 44, 5359-5363.

SYNTHESIS AND ANTIVIRAL ACTIVITY OF NEW THIAZOLE, 1,2,4-TRIAZOL AND OXINDOLE DERIVATIVES

[1]Oleg Radul, [1]Natalia Sucman, [1]Serghei Pogrebnoi, [1]Alic Barba,
[2]Athina Geronikaki, [1]Fliur Macaev*

[1]Institute of Chemistry of the Academy of Sciences of Moldova,
Academy str. 3, MD-2028, Chisinau, Moldova
Tel +373-22-739-754, Fax +373-22-739-954, E-mail: flmacaev@cc.acad.md
[2]Aristotelian University of Thessaloniki, Thessaloniki 54124, Greece
Tel.:+302310997616, Fax: +302310997612
E-mail: geronik@pharm.auth.gr

Dedicated to academician Pavel F. Vlad on the occasion of his 75th birthday

Abstract: The synthesis and antiviral activity evaluation of new derivatives of 2-aminothiazole, 1,2,4-triazole, as well as oxindoles has been realized. The synthesized compounds exhibited different cytotoxicity, in particular, oxindols **4** , **5** , **7** , **8** , **9**, **10**, **11**, **12**, **13**, **58** as well as thiazole/triazole **73** and **75** turned out to be the most cytotoxic for MT-4 cell lines. The compounds **11**, **12**, **73**, and **75** are more toxic than reference compound Efavirenz. As far as the antiviral activity is concerned, none of the title compounds turned out active against Reo-1, Sb-1, VSV, RSV, YFV and VV viruses. The results obtained against Bovine Viral Diarrhoea Virus (BVDV) showed that nine compounds (six from oxindol's seria **6**, **12**, **13**, **52**, **56**, **58** and three 73, **75, 77** of triazole homologues) resulted moderate active. Among all of them, the most potent compound was **52**, with EC_{50} of 6.6 μM. Studies of effect of synthesized compounds against Coxsakie Virus (CVB-2) revealed that only two compounds, **13** and **73** exhibit moderate activity (EC_{50} >40 and >18 μM, respectively). It should be noticed that eleven compounds, **4**, **5**, **7**, **8**, **9**, **10**, **11**, **12**, **13**, **58,** and **75** showed moderate activity against HIV-1 (EC_{50} >16 – m >59μM).

Keywords: 2-aminothiazole, 1,2,4-triazol, oxindoles, cytotoxicity, antiviral activity.

1. Introduction

The twentieth century has been characterized both by a drastic reduction in the mortality caused by infectious diseases and by a rise in the control of neoplastic pathologies. The treatment of infectious diseases still remains an important and challenging problem. The therapeutic problem has achieved increasing importance in hospitalised patients, in immuno suppressed patients with AIDS or undergoing anticancer therapy and organ transplants. Oxindoles has posses a different kind of physiological activity [1-21]. 4-Aryl-5-(1*H*-1,2,4-triazol-1-yl)-1,3-thiazol-2-amines are found to be associated with various biological activities such as antifungal, anti-inflammatory, plant-growth regulatory, adenosine receptor antagonists [22-24]. Prompted by these reports and in continuation of search for bioactive substituted thiazole from computer prediction [25] to synthesis and biological evaluation it was contemplated to synthesize 2-aminothiazole containing 1*H*-1,2,4-triazole's moiety starting from 1-benzoylmethyl-1*H*-1,2,4-triazoles.

2. Results and discussion

2.1 Chemistry

Recently, we described the synthesis of substituted oxindoles [11, 26-32]. In the present paper, the synthesis of 3-hydroxyoxindoles **1-18** from easily accessible [32, 33] indol-2,3-diones **25-35** are suggested (Scheme 1).

Our initial studies [27,28] were performed using as catalyst Et_2NH in aq. MeOH, aq. EtOH, aq. *i*-PrOH. The presence of water in reaction media at room temperature showed a positive effect on the reaction of isatine **25** with acetone **19**. However, the use of Et_2NH as a catalyst in 25% aq. ethylene glycol gives the best result (98 %) compared to using of Et_2NH in aq. MeOH (77 %), aq. EtOH (81 %) or aq. *i*-PrOH (88 %). When the temperature was decreased to $5\text{-}10^0$ C, the 3-hydroxyoxindole **1** was obtained only with 60 %. Finally, all the interactions of isatines **26-35** with methylketones **19-24** carried out in 25% aq. ethylene glycol as a solvent using 1 eq. of Et_2NH as catalyst at room temperature gave the novel oxindoles **3-8** and known derivatives **1,2,9-18** with moderate to good yields (see Table 1 and experimental part).

The known transformation [34] of 1-methylindoline-2,3-dione **26** into thiosemicarbazone **44** afforded an antiviral drug that works by inhibiting mRNA and protein synthesis, especially in pox viruses. On the other side, the synthetic approach to Δ^2-1,3,4-thiadiazoline **56** from thiosemicarbazone **46** we published early [35]. This prompted us to find new compounds having a thiadiazoline moiety attached to oxindoles. These compounds can be considered as cyclic thiosemicarbazide derivatives as well.

The synthesis of compounds **43, 45, 47-53** from easily accessible isatines **25, 29, 36-42** was performed according to the method previously reported [35]. Here we report the reaction of 2-oxoindolin-3-ylidene-hydrazinecarbothioamides **43, 45, 47-53** with boiling acetic anhydride (Scheme 1).

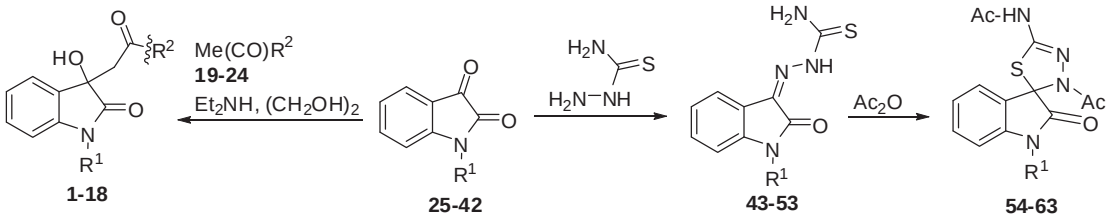

1 R^1= H, R^2=Me
2 R^1= R^2=Me
3 R^1= Et, R^2=Me
4 R^1= Bn, R^2=Me
5 R^1= CH_2CH_2Cl, R^2=Me
6 R^1=$CH_2N(CH_2CH_2)_2O$, R^2=Me
7 R^1=$CH_2N(CH_2CH_2)_2NPh$, R^2=Me
8 R^1= Pr, R^2 = C_6H_5
9 R^1= Me, R^2 = 2,4-Cl_2-C_6H_3
10 R^1= Et, R^2 = 2,4-Cl_2-C_6H_3
11 R^1= Bu, R^2 = 2,4-Cl_2-C_6H_3
12 R^1= hexyl, R^2 = 2,4-Cl_2-C_6H_3
13 R^1= decyl, R^2 = 2,4-Cl_2-C_6H_3
14 R^1= H, R^2= 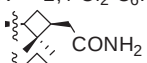
15 R^1= H, R^2= 
16 R^1=H, R^2= 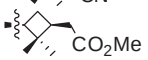
17 R^1= Et, R^2= 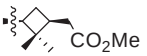
18 R^1= Bn, R^2= 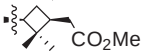

19 R^2 = Me
20 R^2 = Ph
21 R^2 = 2,4-Cl_2-C_6H_3
22 R^2 = 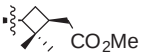
23 R^2 = 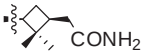
24 R^2 = 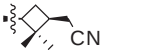

25, **43** R^1= H
26, 44 R^1= Me
27 R^1= Et
28 R^1= Pr
29 45, 55 R^1= Bu
30 R^1= hexyl
31 R^1= decyl
32, 46, 56 R^1= Bn
33 R^1= CH_2CH_2Cl
34 R^1=$CH_2N(CH_2CH_2)_2O$
35 R^1=$CH_2N(CH_2CH_2)_2NPh$
36, 47, 57 R^1= heptyl
37, 48, 58 R^1= nonyl
38, 49, 59 R^1= COMe
39, 50, 60 R^1= $CH_2C(O)CMe_3$
40, 51, 61 R^1= $CH_2CH=C(Me)Cl$
41, 52, 62 R^1= $(CH_2)_2COMe$
42, 53, 63 R^1= $CH_2CH=CH_2$
54 R^1= Ac

Scheme 1

The reaction of thiosemicarbazone **43** with Ac_2O at high temperature afforded isatine-derived Δ^2-1,3,4-thiadiazoline **54** as colorless needles in 71 % yield. Similarly**,** by the reaction of thiosemicarbazone **45, 47-52** and Ac_2O, solid spirooxindoles **54, 55, 57-62** were obtained in good to excellent yields (see Table 1).

Table 1

An analytical data of the synthesized compounds

Compounds	Aggregation M.p. (°C) from EtOH	Yield (%)	Mol. Formula	Elemental analyses (%)		
				C	H	N
				Calcd. / Found	Calcd. /Found	Calcd. / Found
3	155-156	76	$C_{13}H_{15}NO_3$	66.94 / 67.23	6.48 / 6.67	6.00 / 6.32
4	155-157	80	$C_{18}H_{17}NO_3$	73.20 / 73.44	5.80 / 6.21	4.74 / 4.72
5	150-152	78	$C_{13}H_{14}ClN_2O$	58.32 / 58.22	5.27 / 5.68	5.23 / 5.48
6	107-108	76	$C_{18}H_{17}NO_3$	73.20 / 73.44	5.80 / 6.21	4.74 / 4.72
7	165-166	73	$C_{16}H_{20}N_2O_4$	63.14 / 63.22	6.62 / 6.26	9.20 / 9.33
8	149-150	76	$C_{22}H_{25}N_2O_3$	69.64 / 69.77	6.64 / 6.99	11.07 / 10.92
43	252	92	$C_9H_8N_4OS$	49.08/ 49.08	3.66/ 3.49	25.44/ 25.27
45	155	91	$C_{13}H_{16}N_4OS$	56.50/56.34	5.84/6.02	20.27/20.45
46	250	96	$C_{16}H_{14}N_4OS$	61.92/61.77	4.55/4.68	18.05/18.34
47	166-168	90	$C_{15}H_{20}N_4OS$	59.18/59.00	6.62/6.49	18.40/18.11
48	131-132	88	$C_{18}H_{26}N_4OS$	62.39/62.22	7.56/7.33	16.17/16.01
49	251-254	97	$C_{12}H_{12}N_4O_2S$	52.16/51.89	4.38/4.55	20.28/20.11
50	236-237	82	$C_{15}H_{18}N_4O_2S$	56.58/56.38	5.70/5.56	17.60/17.46
51	228	79	$C_{13}H_{13}ClN_4OS$	50.57/50.69	4.24/4.47	18.14/18.11

52	203-205	77	$C_{13}H_{14}N_4OS$	53.78/54.09	4.86/5.02	19.30/19.10
53	176-178	81	$C_{12}H_{12}N_4OS$	55.37/55.21	4.65/4.69	21.52/21.63
54	246-248	71	$C_{13}H_{12}N_4O_3S$	51.31/51.59	3.97/4.25	18.41/18.66
55	211-213	65	$C_{17}H_{20}N_4O_3S$	56.65/56.66	5.59/5.77	15.54/15.34
56	248-249	88	$C_{20}H_{18}N_4O_3S$	60.90/60.88	4.60/4.44	14.20/14.32
57	170-171	71	$C_{19}H_{24}N_4O_3S$	58.74/58.77	6.23/6.50	14.42/14.65
58	202-203	70	$C_{22}H_{30}N_4O_3S$	61.37/61.55	7.02/7.32	13.01/12.96
59	247	59	$C_{16}H_{16}N_4O_4S$	53.32/53.61	4.47/4.35	14.20/14.20
60	250(decom)	82	$C_{19}H_{22}N_4O_4S$	56.70/56.55	5.51/5.69	13.92/14.12
61	176-178	60	$C_{17}H_{17}ClN_4O_3S$	51.97/51.84	4.36/4.54	14.26/14.02
62	189-192	57	$C_{17}H_{18}N_4O_4S$	54.53/54.59	4.85/4.68	14.96/14.89
63	173-175	40	$C_{16}H_{16}N_4O_3S$	55.80/55.98	4.68/4.41	16.27/16.45
70	162-163	75	$C_{11}H_{12}N_6S$	50.75/ 50.97	4.65/ 4.83	32.28/ 32.55
71	194-199	66	$C_{12}H_{14}N_6S$	52.54/52.66	5.14/5.33	30.63/30.76
72	187-190	79	$C_{11}H_{10}Cl_2N_6S$	40.13/40.34	3.06/3.06	25.53/25.67
73	226-236	50	$C_{15}H_{16}N_6O_2S$	52.31/52.33	4.68/4.77	24.40/24.23
74	199	56	$C_{16}H_{18}N_6O_2S$	53.65/53.44	5.07/4.77	24.40/23.37
75	250 (decom)	63	$C_{15}H_{14}Cl_2N_6O_2S$	43.59/43.52	3.41/3.49	20.33/20.31
77	230-232	89	$C_{11}H_8BrN_3S$	C 41.01/40.98	2.50/2.71	21.74/21.72
78	245-246	88	$C_{11}H_8ClN_5S$	47.57/47.83	2.90/2.59	25.22/25.03
79	250(decom)	93	$C_{12}H_{11}ClN_5S$	56.01/56.21	4.31/4.00	27.22/27.47
80	243-244	77	$C_{11}H_7Cl_2N_5S$	42.32/41.98	2.26/2.08	22.43/22.65
81	285-286	77	$C_{13}H_{11}Cl_2N_5S$	45.89/46.32	3.26/3.11	20.58/20.68

N-Allylisatine derivative **53** readily underwent cyclization with Ac_2O to produce the corresponding 1,3,4-thiadiazoline **63**. This compound also appeared to be quite stable in the reaction mixture at this temperature. However, acetamide **63** was obtained in a low yield (only a 40 %). At this condition polymerization to a dark solid material was observed.

The successfull use of thiosemicarbazones in heterocyclization encouraged us to apply available 1-aryl-2-(1*H*-1,2,4-triazol-1-yl)-1-ethanones **66, 68, 69** [36] for the synthesis of compounds **70-72** (schema 2).

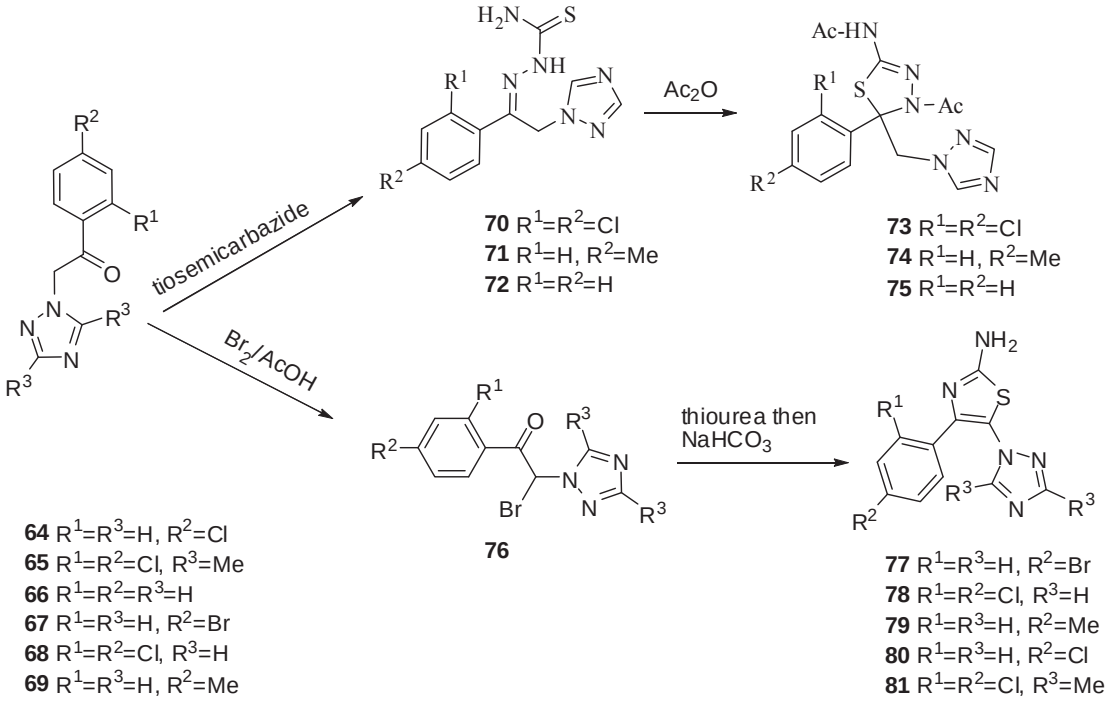

Scheme 2

The thiosemicarbazones **70-72** when reacted with boiling acetic anhydride gave variable yields of 2-acetamido-4-acetyl-5-(aryl)-5-(1*H*-1,2,4-triazol-1-yl-methyl)-Δ^2-1,3,4-thiadiazoline **73-75**.

The second strategy has include transformations of ethanones **64, 65,** and **67-69** into the 1,3-thiazol-2-amines derivative 1,2,4-triazoles **77-81** *via* corresponding α-bromoketones **76**. In the beginning our study the compound **76** (R^1=R^3=H, R^2=Br) was obtained by the halogenation of ketone **67** with Br_2 in mixture HBr/AcOH at 10^0C according to the procedure described in the literature [37]. However, this compound was apparently not very stable. It is worth noting that allylic bromination of ketone **67** using Br_2 followed by condensation of product with thiourea gave the 2-aminothiazole **77** in 89 % yield. The optimized two steps protocol was then expanded to ketones **64, 65, 68,** and **69**. The targets 2-aminothiazole-1*H*-1,2,4-triazoles **78-81** were conveniently isolated as precipitates with good yields (see Table 1). All synthesized compounds were characterized by ellemental analysis (Table 1) as well as spectroscopically (H-NMR, Table 2, MS experimental part).

Table 2

^{1}H NMR spectral data of synthesized compounds

Comp.	δ (ppm)
3	DMSO-d_6: 1.20 (t, 3H, J= 9.17, C$\underline{H}_3$CH$_2$); 2.10 (s, 3H, Me); 2.97 (dd, 2H, CH_2, AB-system, *J*= 11.20 and 14.49), 4.80 (q, 2H, J=6.48 Hz, Me$\underline{CH}_2$); 4.39 (s, 1H, OH), 6.81-7.44 (m, 4H, ArH)
4	DMSO-d_6:2.11 (s, 3H, Me); 2.89, 2.99 (dd, 2H, CH_2, AB-system, *J*=11.55 and 24.32); 4.48 (s, 1H, OH); 4.88 (s, 2H, N-$\underline{CH}_2$-Ph); 6.24-7.41 (м, 9H, arom).
5	$CDCl_3$:2.14 (s, 3H, Me); 3.11-3.66 (m, 3CH_2); 3.97 (s, 1H, OH); 6.91-7.23 (м, 4H, arom).
6	DMSO-d_6:2.09 (s, 3H, Me); 2.50-3.65 (m, 3CH_2); 4.41 (s, 2H, NCH_2), 6.08 (s, 1H, OH); 6.77-7.11 (м, 4H, arom).
7	$CDCl_3$:2.17 (s, 3H, Me); 2.48-3.44 (m, 3CH_2); 4.58 (s, 1H, OH); 4.45 (s, 2H, NCH_2), 6.43-7.27 (м, 9H, arom).
8	$CDCl_3$: 0.90 (t, 3H, J=8.7, C$\underline{H}_3$CH$_2$); 1.62-3.38 (m, 4H, 2CH_2), 2.06 (s, 3H, Me); 2.76 (dd, 2H, CH_2, AB-system, *J* =11.01 and 14.49), 5.99 (s, 1H, OH), 6.83-7.98 (m, 4H, ArH)
43	DMSO-d_6: 7.23-7.89 (m, 6H, NH_2, ArH); 9.10 (s, 1H, NH-CO); 11.13 (s, 1H, NH-CS)
45	DMSO-d_6: 1.00 (t, 3H, J= 8.76, C$\underline{H}_3$CH$_2$); 1.31-3.97 (m, 6H, 3CH_2); 7.21-7.98 (m, 6H, NH_2, ArH), 10.92 (s, 1H, NH-CS)
46	DMSO-d_6: 4.94 (s, 2H, CH_2); 6.93-7.75 (m, 9H, ArH); 8.74-9.10 (m, 2H, NH_2); 12.43 (s, 1H, NH-CS)
47	$CDCl_3$: 0.78 (t, 3H, CH_2-C$\underline{H}_3$, *J*=7.28); 1.02-1.79 (m, 6H, $(CH_2)_3$); 3.64 (q, 2H, CH_2-N, *J*=7.14)
48	$CDCl_3$: 0.78 (t, 3H, CH_2-C$\underline{H}_3$, *J*=5.76); 1.0-1.83 (m, 14H, $(C\underline{H}_2)_7$); 3.64 (t, 2H, CH_2-N, *J*=7.28); 6.65-7.54 (m, 5H, ArH, NH_2); 12.26 (s, 1H, N$\underline{H}$-CS)
49	DMSO-d_6: 2.11 (s, 3H, $COCH_3$); 2.85 (t, 2H, C$\underline{H}_2$-CO-CH_3, *J*=7.28); 3.89 (t, 2H, N-C$\underline{H}_2$-CH_2, *J*=7.2); 7.00-7.70 (m, 4H, ArH); 8.65-9.05 (m, 2H, NH_2); 12.36 (s, 1H, NH-CS)
50	DMSO-d_6:1.20(s,9H,3CH_3); 4.80 (s,2H,CH_2); 6.69-7.76 (m,4H, ArH); 8.71, 8.08(s,s,2H,NH_2);12.29 (s,1H,NH)
51	DMSO-d_6: 2.11 (s, 3H, CH_3); 4.42 (d, 2H, CH_2, *J*=6.06); 5.72 (t, 1H, CH=, , *J*=6.29), 6.93-7.72 (m, 4H, ArH); 8.67, 8.9.06 (s, s , 2H, NH_2); 12.34 (s, 1H, NH)
52	$CDCl_3$:2.13 (s, 3H, Me); 2.70-3.24 (m, 2CH_2); 7.21-7.98 (m, 6H, NH_2, ArH), 10.92 (s, 1H, NH-CS)
53	DMSO-d_6: 4.32 (s, 2H, CH_2); 4.89-5.39 (m, 2H, =CH_2), 5.49-6.2 (m, 1H, CH=), 6.97-7.73 (m, 4H, ArH); 8.59, 8.9.03 (s, s , 2H, NH_2); 12.45 (s, 1H, NH)
54	DMSO-d_6: 2.1, 2.15 (s, s, 6H, 2$COCH_3$); 2.56 (s, 3H, $CONCOCH_3$); 6.65-7.5 (m, 4H, ArH); 12.05 (s, 1H, NH)
55	$CDCl_3$: 0.812 (t, 3H, CH_2-C$\underline{H}_3$, *J*=6.28); 1.13-1.64 (m, 4H, C$\underline{H}_2$-C$\underline{H}_2$-CH_3); 1.91, 2.13 (s, s, 6H, 2$COCH_3$); 3.69 (t, 2H, N- CH_2, *J*=6.51); 6.74-7.39 (m, 4H, ArH); 10.40 (s, 1H, NH)
56	DMSO-d_6: 2.08 (s, s, 6H, 2$COCH_3$); 2.21 (c, 3H, CO-C$\underline{H}_3$), 4.94 (q, 2H, J-16.11, N-C$\underline{H}_2$-C_6H_5); 6.73-7.45 (м, 9H, аром); 12.00 (c, 1H, N$\underline{H}$- CO-CH_3)
57	$CDCl_3$: 0.80 (t, 3H, CH_2-C$\underline{H}_3$, *J*=5.49); 1.15-1.65 (m, 8H, $(\underline{CH}_2)_4$Me); 1.92 (s, 3H, $COCH_3$), 2.12 (s, 3H, $COCH_3$); 3.67 (t, 2H, N- CH_2, *J*=6.91); 6.73-7.38 (m, 4H, ArH); 10.40 (s, 1H, NH)
58	$CDCl_3$: 0.80 (t, 3H, CH_2-C$\underline{H}_3$, *J*=6.64); 1.21-1.84 (m, 14H, $(C\underline{H}_2)_7$Me); 1.93 (s, 3H, $COCH_3$); 2.13 (s, 3H, $COCH_3$); 3.67 (t, 2H, N-CH_2, *J*=6.69); 6.74-7.39 (m, 4H, ArH); 10.35 (s, 1H, NH)
59	$CDCl_3$:2.1, 2.16, 2.22 (s, s, s, 9H, 3$COCH_3$); 4.67 (s, 2H, CH_2); 6.68-7.36 (m, 4H, ArH); 11.72 (s, 1H, NH)
60	DMSO-d_6: 1.19 (s, 9H, CMe_3); 2.08, 2.14 (s, s 6H, 2$COCH_3$); 4.83 (s, 2H, CH_2); 6.79-7.43 (m, 4H, ArH)
61	$CDCl_3$: 1.08 (s, 3H, =C-CH_3); 1.96, 2.12 (s, s, 6H, 2$COCH_3$); 4.45 (d, 2H, CH_2, *J*=7.21); 5.45 (t, 1H, CH=C, *J*=7.07); 6.74-7.38 (m, 4H, ArH); 10.17 (s, 1H, NH)
62	$CDCl_3$: 1.97, 2.02 (s, s, 6H, 2$COCH_3$); 2.05 (s, 3H, $COCH_3$); 2.73 (t, 2H, C$\underline{H}_2$CO, *J*=7.4); 3.82 (t, 2H, N-CH_2, *J*=7.6); 6.69-7.28 (m, 4H, ArH); 11.06 (s, 1H, NH)
63	DMSO-d_6: 2.09, 2.2.16 (s, s, 6H, 2$COCH_3$); 4.20-4.39 (m, 2H, CH_2); 4.89-5.48 (m, 2H, =CH_2), 5.63-5.89 (m, 1H, CH=), 6.88-7.59 (m, 4H, ArH); 12.03 (s, 1H, NH)
70	DMSO-d_6: 5.71 (s, 2H, CH_2); 7.36 (m, 5H, ArH); 7.93 (s, 1H, triazole $C_{(3)}$H); 8.12-8.52 (m, 2H, NH_2); 8.68 (s, 1H, triazole $C_{(5)}$H); 10.97 (s, 1H, NH)

71 DMSO-d_6: 2.26 (s, 3H, CH_3); 5.69 (s, 2H, CH_2); 7.09-7.68 (m, 4H, ArH); 7.94 (s, 1H, triazole $C_{(3)}H$); 8.09-8.44 (m, 2H, NH_2); 8.66 (s, 1H, triazole $C_{(5)}H$); 10.94 (s, 1H, NH)

72 DMSO-d_6: 5.29 (s, 2H, CH_2); 6.98-8.48 (m, 5H, ArH, NH_2); 7.92 (s, 1H, triazole $C_{(3)}H$); 8.48 (s, 1H, triazole $C_{(5)}H$); 10.21 (s, 1H, NH)

73 DMSO-d_6: 1.93, 2.17 (s,s, 6H, $2COCH_3$); 5.30, 5.36 (d,d, 2H, CH_2, AB system, J = 14.43 and 23); 7.41 (m, 5H, ArH); 8.01 (s, 1H, triazole $C_{(3)}H$); 8.55 (s, 1H, triazoile $C_{(5)}H$); 11.55 (s, 1H, NH)

74 DMSO-d_6:1.94, 2.16 (s,s, 6H, $2COCH_3$); 5.24, 5.31 (d,d, 2H, CH_2, AB system, J = 18.67 and 28.92); 7.20, 7.34 (d,d, 4H, ArH, J = 8.65); 8.00 (s, 1H, triazole $C_{(3)}H$); 8.54 (s, 1H, triazole $C_{(5)}H$); 11.50 (s, 1H, NH)

75 DMSO-d_6: 1.97, 2.07 (s,s, 6H, $2COCH_3$); 5.25, 5.32 (d,d, 2H, CH_2, AB system, J = 18.67 and 25.79); 7.54-7,66 (m, 3H, ArH); 8.01 (s, 1H, triazole $C_{(3)}H$); 8.55 (s, 1H, triazole $C_{(5)}H$); 11,55 (s, 1H, NH)

77 DMSO-d_6: 7.31-7.67 m (6H, NH_2, arom), 8.11 s, 8.45 s (2H, 2 Tr-H).

78 DMSO-d_6: 7.18-7.40 m (6H, NH_2, arom), 8.18 s, 8.56 s (2H, 2 Tr-H).

79 DMSO-d_6: 2.26 s (3H, Me), 7.05 broad s (4H, arom), 7.3 s (2H, NH_2), 8.15 s, 8.47 s (2H, 2 Tr-H)

80 DMSO-d_6: 7.23-7.51 m (5H, NH_2, arom), 7.97 s, 8.51 s (2H, 2 Tr-H)

81 DMSO-d_6: 2.00 s, 2.18 s (6H, 2 Me), 7.20-7.50 m (5H, NH_2, arom)

2.2. Antiviral activity

The synthesized thiazole/triazol/oxindols/thiosemicarbazones were evaluated *in vitro* in parallel cell-based assays for cytotoxicity and antiviral activity (Tables **4**) against viruses representative of two of the three genera of the Flaviviridae family, i.e. Flaviviruses (YFV) and Pestiviruses (BVDV), as Hepaciviruses can hardly be used in routine cell-based assays. Title compounds were also tested against representatives of other virus families. Among $ssRNA^+$ were HIV-1 (Retroviridae), CVB-2 and Polio-1 (Picornaviridae); among $ssRNA^-$ were RSV (Paramyxoviridae) and VSV (Rhabdoviridae); among double-stranded RNA (dsRNA) viruses were Reo-1 (Reoviridae). Two representatives of DNA virus families were also included: HSV-1 (Herpesviridae) and VV (Poxviridae).

Compounds exhibited different cytotoxicity, in particular, oxindoles **4** , **5** , **7** , **8** , **9**, **10**, **11**, **12**, **13**, **58** as well as thiazole/triazole **73** and **75** turned out to be the most cytotoxic for MT-4 cell lines (table 3).

Table 3

Bioactivity synthesized compounds against MT-4, MDBK, BHK-21, Vero-76, HIV-1, BVDV, YFV, CVB-2, Sb-1, VSV, VV, HSV-1 (in vitro)

Comps	MT-4	MDBK	BHK-21	Vero-76	HIV-1	BVDV	YFV	CVB-2	Sb-1	VSV	VV	HSV-1
	CC50 [μM]				EC50 [μM]							
1	>100	>100	>100	>100	>100	>100	>100	>100	>100	>100	>100	>100
2	>100	>100	>100	>100	>100	>100	>100	>100	>100	>100	>100	>100
3	>100	>100	>100	>100	>100	>100	>100	>100	>100	>100	>100	>100
4	47	>100	>100	>100	>47	>100	>100	>100	>100	>100	>100	>100
5	55	>100	>100	>100	>55	>100	>100	>100	>100	>100	>100	>100
6	>100	93	>100	>100	>100	>93	>100	>100	>100	>100	>100	>100
7	59	>100	>100	>100	>59	>100	>100	>100	>100	>100	>100	>100
8	49	>100	>100	>100	>49	>100	>100	>100	>100	>100	>100	>100
9	33	>100	>100	>100	>33	>100	>100	>100	>100	>100	>100	>100
10	29	>100	>100	>100	>29	>100	>100	>100	>100	>100	>100	>100
11	17	>100	>100	>100	>17	>100	>100	>100	>100	>100	>100	>100
12	19	>100	>100	>80	>19	85	>100	>80	>80	>80	>80	>100
13	45	>18	>19	>40	>45	>18	>19	>40	>40	>40	>40	>19
14	>100	>100	>100	>100	>100	>100	>100	>100	>100	>100	>100	>100
15	>100	>100	>100	>100	>100	>100	>100	>100	>100	>100	>100	>100
16	>100	>100	>100	>100	>100	>100	>100	>100	>100	>100	>100	>100
17	>100	>100	>100	>100	>100	>100	>100	>100	>100	>100	>100	>100
18	>100	>100	>100	>100	>100	>100	>100	>100	>100	>100	>100	>100
52	>100	>100	>100	>100	>100	6.6	>100	>100	>90	>90	>100	>100
54	>100	>100	>100	>100	>100	>100	>100	>100	>100	>100	>100	>100
56	>100	>100	>100	>100	>100	>94	>100	>100	>100	>100	>100	>100
55	>100	>100	>100	>80	>100	>100	>100	>100	>100	>100	>100	>100
57	>100	>100	>100	>100	>100	>100	>100	>80	>80	>80	>80	>100
58	51	>100	>100	>100	>51	22	>100	>100	>100	>100	>100	>100

59	>100	>100	>100	>100	>100	>100	>100	>100	>100	>100	>100	>100
61	>100	>100	>100	>90	>100	>100	>100	>90	>90	>90	>90	>100
62	>100	>100	>100	>100	>100	>100	>100	>100	>100	>100	>100	>100
63	>100	>100	>100	>100	>100	>100	>100	>100	>100	>100	>100	>100
70	>100	>100	>100	>100	>100	>100	>100	>100	>100	>100	>100	>100
71	>100	>100	>100	>100	>100	>100	>100	>100	>100	>100	>100	>100
72	>100	>100	>100	>100	>100	>100	>100	>100	>100	>100	>100	>100
73	≤3.7	16	>100	18	>100	>16	>100	>18	>18	>18	>18	>100
74	>100	>100	>100	>100	>100	>100	>100	>100	>100	>100	>100	>100
75	16	55	>100	90	>16	>55	>100	>90	>90	>90	>90	>100
77	>100	>100	>100	>100	>100	>87	>100	>100	>100	>100	>100	>100
78	>100	>100	>100	>100	>100	>100	>100	>100	>100	>100	>100	>100
79	>100	>100	>100	>100	>100	>100	>100	>100	>100	>100	>100	>100
80	>100	>100	>100	>100	>100	>100	>100	>100	>100	>100	>100	>100
81	>100	>100	>100	>100	>100	>100	>100	>100	>100	>100	>100	>100

It is worth noting that compounds **11**, **12**, **73**, and **75** are more toxic than reference compound Efavirenz.

As far as the antiviral activity is concerned, none of the title compounds exhibited any activity against Reo-1, Sb-1, VSV, RSV, YFV and VV viruses.

The results obtained against Bovine Viral Diarrhoea Virus (BVDV) showed that nine compounds (six from oxindol's seria **6**, **12**, **13**, **52**, **56**, **58** and three 73, **75, 77** of triazole homologues) resulted moderate active. Among all of them, the most potent compound was **52**, with EC_{50} of 6.6 μM.

Studies of effect of synthesized compounds against Coxsakie Virus (CVB-2) revealed that only two compounds, **13** and **73** exhibit moderate activity (EC_{50} >40 and >18 μM, respectively).

It should be noticed that eleven compounds, **4**, **5**, **7**, **8**, **9**, **10**, **11**, **12**, **13**, **58,** and **75** showed moderate activity against HIV-1 (EC_{50} >16 – m >59μM).

3. Conclusions

In the light of the above-mentioned results, we conclude that synthesized compounds in general not so active as antiviral agent. But some of them showed, good activity against viruses containing a single-stranded positive-sense RNA genome ($ssRNA^+$). In particular, in cell-based assays the compounds **11**, **12**, **52**, **57**, **73**, and **75** results the most potent against MT4 cells, BVDV, and HIV-1, respectively.

4. Acknowledgements

The authors gratefully acknowledge to professor Paola La Colla from University of Cagliari, Italy for providing data an antiviral activity studied compounds.

5. Experimental methods

Solvents and commercially available reagents (1*H*-indole-2,3-dione **25**, 1-methyl-1*H*-indole-2,3-dione **26**, 1-ethyl-1*H*-indole-2,3-dione **27**, 1-benzyl-1*H*-indole-2,3-dione **46**) were purchased from Aldrich and used without additional purification. 1-Alkylindoline-2,3-diones **28-31**, **33-42** were obtained by a known method [32,33]. Melting points were determined on a Boëtius melting point apparatus (PHMK, VEB Wägetechnik Rapido, Radebeul, Germany) and are uncorrected. ^{1}H - NMR spectra were acquired on a Bruker Avance III 400 spectrometer operating at 400.13 MHz for ^{1}H. Chemical shifts δ are given in ppm referring to the signal center using the solvent peaks for reference: DMSO-d_6 2.50 ppm. IR spectra were acquired on apparatus "Perkin-Elmer Spectrum 100 FTIR". Electron ionisation mass-spectra were recorded on a VG-250 spectrometer (VG Labs., Tritech England) with ionisation energy maintained at 70 eV.

General procedure for synthesis of oxindoles 1-18

A mixture of indoline-2,3-dione (10 mmol), ketone (10 mmol), and Et_2NH (0.73 g, 10 mmol) in 25% aq. ethylene glycol (20 ml) was stirred for 6-8 hours at room temperature (TLC control). The precipitate was filtered off, and washed with 25% aq. ethylene glycol (3x10 ml). The crystalline product was used for further synthesis without purification. For analytical purposes, a sample was recrystallized from a suitable solvent.

3-Hydroxy-3-(2-oxopropyl)indolin-2-one 1. M.p. 168-169°C, Ref. [38] 160-165 °C.

3-Hydroxy-1-methyl-3-(2-oxopropyl)indolin-2-one 2. M.p. 147-148°C, Ref. [38] 140-145 °C.

3-(2-(2,4-Dichlorophenyl)-2-oxoethyl)-3-hydroxy-1-methylindolin-2-one 9. Yield 87%, M.p. 162-164°C. Ref. [27] M.p. 161-164 °C.

3-(2-(2,4-Dichlorophenyl)-2-oxoethyl)-1-ethyl-3-hydroxyindolin-2-one 10. Yield 78 %, M.p. 137-138°C. Ref. [27] M.p. 135-138°C.
1-Butyl-3-(2-(2,4-dichlorophenyl)-2-oxoethyl)-3-hydroxyindolin-2-one 11. Yield 95 %, oil. Cal. C 61.24; H 4.88; N, 3.57. $C_{20}H_{19}Cl_2NO_3$. Find. C 61.29; H 4.60; N, 3.58. Ref. [27] Oil.
3-(2-(2,4-Dichlorophenyl)-2-oxoethyl)-1-hexyl-3-hydroxyindolin-2-one 12. Yield 98 %, oil. Cal. C 62.86; H 5.52; N 3.33. $C_{22}H_{23}Cl_2NO_3$. Find. C 62.77; H 5.52; N 3.26. Ref. [27] Oil.
1-Decyl-3-(2-(2,4-dichlorophenyl)-2-oxoethyl)-3-hydroxyindolin-2-one 13. Yield 99 %, oil. Cal. C 65.54; H 6.56; N 2.94. $C_{26}H_{31}Cl_2NO_3$. Find. C 65.39; H 6.56; N 2.88. Ref. [27] Oil.
2-((1S,3S)-3-(2-(3-Hydroxy-2-oxoindolin-3-yl)acetyl)-2,2-dimethylcyclobutyl)-acetamide 14. Yield 68 %, M.p. 206-207°C. Ref. [28] M.p. 205-207°C.
2-((1S,3S)-3-(2-(3-Hydroxy-2-oxoindolin-3-yl)acetyl)-2,2-dimethylcyclobutyl)-acetonitrile 15. Yield 81 %, M.p. 163-164°C. Ref. [28] M.p. 163-164°C.
Methyl 2-((1S,3S)-3-(2-(3-hydroxy-2-oxoindolin-3-yl)acetyl)-2,2-dimethyl-cyclobutyl)acetate 16. Yield 88 %, M.p. 76-77°C. Ref. [28] M.p. 76°C.
Methyl 2-((1S,3S)-3-(2-(1-ethyl-3-hydroxy-2-oxoindolin-3-yl)acetyl)-2,2-dimethylcyclobutyl)acetate 17. Yield 55 %, M.p. 162-163°C. Ref. [28] M.p. 162-164°C.
Methyl 2-((1S,3S)-3-(2-(1-benzyl-3-hydroxy-2-oxoindolin-3-yl)acetyl)-2,2-dimethylcyclobutyl)acetate 18. Yield 79 %, M.p. 152-153°C. Ref. [28] M.p. 152-153°C.

General procedure for synthesis of thiosemicarbazones 43-53, 70-72

The ketones (1 mmol) in EtOH (10 ml) and thiosemicarbazide (1 mmol) in EtOH (10 ml) were mixed at 50°C. Three drops of 30% HCl were added to the mixed solution following by reflux for 1-6 hours (TLC control). The mixture was cooled and precipitate was filtered and recrystallized using an appropriate solvent.

General procedure for heterocyclization of thiosemicarbazones into 1,3,4-thiadiazolines 73-75

After refluxing during 3-6 hours of thiosemicarbazones **70-72** (10 mmol) in Ac_2O (25 ml) the solution was cooled and after addition of H_2O (5 ml) kept overnight at room temperature. The solid was filtered off, washed with cold H_2O, dried over P_2O_5 and recrystallized from appropriate solvent.
N-{5-[(1*H*-1,2,4-Triazol-1-yl)methyl)-4-acetyl-5-(2,4-dichlorophenyl]-4,5-dihydro-1,3,4-thiadiazol-2-yl} acetamide 73. MS, *m*/*z* (relative intensity %): $[M]^+$ 277 (100), 208 (23), 188 (61), 181 (15), 163 (11), 155 (10), 140 (23), 139 916), 138 (56), 137 (38), 132 (8), 123 (7), 114 (8), 113 (9), 111 (17), 102 (12), 90 (8), 86 (10), 81 (8), 76 (8), 75 (13), 70 (10), 60 (89), 32 (25).
N-{5-[(1*H*-1,2,4-Triazol-1-yl)methyl]-4-acetyl-5-p-tolyl-4,5-dihydro-1,3,4-thiadiazol-2-yl}acetamide 74. MS, *m*/*z* (relative intensity %): $[M]^+$ 269 (16), 259(27), 258 (92), 203 (15), 189 (14), 188 (27), 162 (8), 161 (22), 147 (12), 145 (10), 143 (10), 135 (9), 119 (21), 118 (100), 117 (34), 116 (18), 103 (10), 92 (8), 91 (37), 90 (16), 89 (17), 86 (13), 77 (10), 76 (9), 71 (7), 69 (10), 65 (19), 64 (11), 63 (21), 62 (14), 61 (17), 60 (51), 59 (12), 54 (16), 53 (11), 51 (22), 50 (14), 45 (10), 42 (10), 41 (13).
N-{5-[(1*H*-1,2,4-Triazol-1-yl)methyl]-4-acetyl-5-phenyl-4,5-dihydro-1,3,4-thiadiazol-2-yl}acetamide 75. MS, *m*/*z* (relative intensity %): $[M]^+$315 (9), 314 (19), 313 (47), 312 (28), 311 (66), 279 (8), 278 (54), 277 (12), 276 (100), 275 (12), 224 (15), 222(21), 197 (11), 195 (22), 194 (8), 174 (9), 173 (11), 172 (20), 171 (19), 136 (9), 60 (32), 59 (12).

General procedure for the preparation of 4-aryl-5-(1*H*-1,2,4-triazol-1-yl)-1,3-thiazol-2-amines 77-81

The bromination of ketones **64, 65,** and **67-69** were realized with Br_2 in mixture HBr/AcOH at 10°C. The crude product **76** was used without purification in the next step. Mixture of bromide (0.01 mol) **76** and thiourea (0.01 mol) in acetone (20 ml) was stirred at room temperature for 1 hour and after removal of the solvent, the resulting solid was refluxed in ethanol (50 ml) for additional 2 hours. After evaporation of the EtOH, 5% water solution of $NaHCO_3$ (50 ml) was added and mixture was refluxed 8 hours. The solid was collected by filtration, dried and recrystallized from ethanol.

Biological Assays

Compounds were dissolved in DMSO at 100 mM and then diluted in culture medium.

Cells and Viruses.

Cell lines were purchased from American Type Culture Collection (ATCC). The absence of mycoplasma contamination was checked periodically by the Hoechst staining method. Cell lines supporting the multiplication of RNA viruses were the following: $CD4^+$ human T-cells containing an integrated HTLV-1 genome (MT-4); Madin Darby Bovine Kidney (MDBK); Baby Hamster Kidney (BHK-21) and Monkey Kidney (Vero 76) cells.

Cytotoxicity Assays

For cytotoxicity tests, run in parallel with antiviral assays, MDBK and BHK cells were re-suspended in 96 multi-well plates at an initial density of $6x10^5$ and $1x10^6$ cells/mL, respectively, in maintenance medium, without or with serial dilutions of test compounds. Cell viability was determined after 48-96 hrs at 37 °C in a humidified CO_2 (5%) atmosphere by the 3-(4,5-dimethylthiazol-2-yl)-2,5-diphenyl-tetrazolium bromide (MTT) method [39].

Vero 76 cells were re-suspended in 24 multi-well plates at an initial density of $4x10^5$ cells/mL. The cell number of Vero 76 monolayers was determined by staining with the crystal violet dye.

For cytotoxicity evaluations, exponentially growing cells derived from human haematological tumors [$CD4^+$ human T-cells containing an integrated HTLV-1 genome (MT-4)] were seeded at an initial density of $1x10^5$ cells/mL in 96 well plates in RPMI-1640 medium supplemented with 10% fetal calf serum (FCS), 100 units/mL penicillin G and 100 μg/mL streptomycin. Cell cultures were then incubated at 37 °C in a humidified, 5% CO_2 atmosphere in the absence or presence of serial dilutions of test compounds. Cell viability was determined after 96 hrs at 37 °C by the MTT method.

Antiviral assay

Activity of compounds against Human Immunodeficiency Virus type-1 (HIV-1) was based on inhibition of virus-induced cytopathogenicity in MT-4 cells acutely infected with a multiplicity of infection (m.o.i.) of 0.01. Briefly, 50 μL of RPMI containing $1x10^4$ MT-4 were added to each well of flat-bottom microtitre trays containing 50 μL of RPMI, without or with serial dilutions of test compounds. Then, 20 μL of an HIV-1 suspension containing 100 $CCID_{50}$ were added. After a 4-day incubation, cell viability was determined by the MTT method.

Activity of compounds against Yellow Fever Virus (YFV) and Reo Virus type-1 (Reo-1) was based on inhibition of virus-induced cytopathogenicity in acutely infected BHK-21 cells. Activities against Bovine Viral Diarrhoea Virus (BVDV), in infected MDBK cells, were also based on inhibition of virus-induced cytopathogenicity.

BHK and MDBK cells were seeded in 96-well plates at a density of $5x10^4$ and $3x10^4$ cells/well, respectively, and were allowed to form confluent monolayers by incubating overnight in growth medium at 37 °C in a humidified CO_2 (5%) atmosphere. Cell monolayers were then infected with 50 μL of a proper virus dilution (in serum-free medium) to give an m.o.i = 0.01. 1 hr later, 50 μL of MEM Earle's medium, supplemented with inactivated foetal calf serum (FCS), 1% final concentration, without or with serial dilutions of test compounds, were added. After 3-4 days incubation at 37 °C, cell viability was determined by the MTT method.

Activity of compounds against Coxsackie Virus, B-2 strain (CVB-2), Polio Virus type-1 (Polio-1), Sabin strain, and Vesicular Stomatitis Virus (VSV), Vaccinia Virus (VV) and Herpes Virus 1 (HSV-1) and against Respiratory Syncytial Virus (RSV), A-2 strain, in infected Vero 76 cells, was determined by plaque reduction assays in Vero 76 cell monolayers. To this end, Vero 76 cells were seeded in 24-well plates at a density of $2x10^5$ cells/well and were allowed to form confluent monolayers by incubating overnight in growth medium at 37 °C in a humidified CO_2 (5%) atmosphere. Then, monolayers were infected with 250 μL of proper virus dilutions to give 50-100 PFU/well. Following removal of unadsorbed virus, 500 μL of Dulbecco's modified Eagle's medium supplemented with 1% inactivated FCS and 0.75% methyl cellulose, without or with serial dilutions of test compounds, were added. Cultures were incubated at 37 °C for 2 (Sb-1 and VSV), 3 (CVB-2, VV and HSV-1) or 5 days (RSV) and then fixed with PBS containing 50% ethanol and 0.8% crystal violet, washed and air-dried. Plaques were then counted. 50% effective concentrations (EC_{50}) were calculated by linear regression technique.

6. References

[1]. Jiang, X.; Cao, Y.;.Wang, Y; Liu, L.; Shen, F.; Wang, R. J. Am. Chem. Soc., 2010, 132, 15328–15333.
[2]. Satyamaheshwar, P. Current Bioactive Compounds. 2009, 5, 20-38.
[3]. Lawrence, H. R.; Pireddu, R,; Chen, L.; Luo, Y.; Sung, S.-S.; Szymanski, A. M.; Yip, M. L. R.; Guida, W. C.; Sebti, S. M.; Wu, J.; Lawrence, N. J. J. Med. Chem. 2008, 51, 4948-4956.
[4]. Fensome, A.; Adams, W. R.; Adams, A. L.; Berrodin, T. J.; Cohen, J.; Huselton, C.; Illenberger, A.; Kern, J. C.; Hudak, V. A.; Marella, M. A.; Melenski, E. G.; McComas, C. C.; Mugford, C. A.; Slayden, O. D.; Yudt, M.; Zhang, Z.; Zhang, P.; Zhu, Y.; Winneker, R. C.; Wrobel J. E. J. Med. Chem. 2008, 51, 1861–1873.
[5]. Macpherson, L.J.; Dubin, A. E.; Evans, M.J.; Marr, F.; Schultz, P. G.; Cravatt, B. F.; Patapoutian, A. Nature. 2007, 445, 541-545.
[6]. Deiters, A.; Pettersson, M.; Martin, S. F. J. Org. Chem. 2006, 71, 6547–6561.
[7]. Emura, T.; Esaki, T.; Tachibana, K.; Shimizu, M. J. Org. Chem. 2006, 71, 8559–8564.
[8]. Kogure, N.; Ishii, N.; Kitajima, M.; Wongseripipatana, S.; Takayama, H. Org. Lett. 2006, 8, 3085–3088.
[9]. Natarajan, A.; Guo, Y.; Harbinski, F.; Fan, Y.-H.; Chen, H.; Luus, L.; Diercks, J.; Aktas, H.; Chorev, M.; Halperin, J. A. J. Med. Chem. 2004, 47, 4979–4982.
[10]. Macaev, F. Synthesis of spiroindolin-2-ones from 1H-indole-2,3-dione. In INTERBIOSCREEN MONOGRAPH SERIES "Selected methods for synthesis and modification of heterocycles". Vol. 3. The chemistry of synthetic indole systems. IBS press: Moskow, 2004; pp 75-102.

[11]. Geronikaki, A.; Babaev, E.; Dearden, J.; Dehaen, W.; Filimonov, D.; Galaeva, I.; Kraineva, V.; Lagunin, A.; Macaev, F.; Molodavkin, G.; Poroikov, V.; Pogrebnoi, S.; Saloutin, V.; Stepanchikova, A.; Stingaci, E.; Tkach, N.; Vlad, L.; Voronina, T. Bioorganic & Medicinal Chemistry. 2004**,** 12, 6559-6568.
[12]. Takayama, H.; Fujiwara, R.; Kasai, Y.; Kitajima, M.; Aimi, N. Org. Lett. 2003, 5, 2967–2970.
[13]. Woodard, C. L.; Li, Z.; Kathcart, A. K.; Terrell, J.; Gerena, L.; Lopez-Sanchez, M.; Kyle, D. E.; Bhattacharjee, A. K.; Nichols, D. A.; Ellis, W.; Prigge, S. T.; Geyer, J. A.; Waters, N. C. J. Med. Chem. 2003, 46, 3877–3882.
[14]. Bramson, H. N.; Corona, J.; Davis, S. T.; Dickerson, S. H.; Edelstein, M.; Frye, S. V.; Gampe, R. T.; Harris, Jr. P. A.; Hassell, A.; Holmes, W. D.; Hunter, R. N.; Lackey, K. E.; Lovejoy, B.; Luzzio, M. J.; Montana, V.; Rocque, W. J.; Rusnak, D.; Shewchuk, L.; Veal, J. M.; Walker, D. H.; Kuyper, L. F. J. Med. Chem., 2001, 44, 4339–4358.
[15]. Tokunaga, T.; Hume, W. E.; Umezome, T.; Okazaki, K.; Ueki, Y.; Kumagai, K.; Hourai, S.; Nagamine, J.; Seki, H.; Taiji, M.; Noguchi, H.; Nagata, R. J. Med. Chem. 2001, 44, 4641-4649.
[16]. Cravotto, G.; Giovenzana, G. B.; Pilati, T.; Sisti, M.; Palmisano, G. J. Org. Chem. 2001, 66, 8447–8453.
[17]. Carletti, I.; Banaigs, B.; Amade, P. J. Nat. Prod. 2000, 63, 981–983.
[18]. El-Gendy, A. A.; Ahmedy, A. M. Archives of Pharmacia Research. 2000, 23, 310-314.
[19]. Robinson, R. P.; Reiter, L. A.; Barth, W. E.; Campeta, A. M.; Cooper, K.; Cronin, B. J.; Destito, R.; Donahue, K. M.; Falkner, F. C.; Fiese, E. F.; Johnson, D. L.; Kuperman, A. V.; Liston, T. E.; Malloy, D.; Martin, J. J.; Mitchell, D. Y.; Rusek, F. W.; Shamblin, S. L.; Wright, C. F. J. Med. Chem. 1996, 39, 10–18.
[20]. Itakura, K.; Uchida, K.; Kawakishi, S. Chem. Res. Toxicol. 1994, 7, 185–190.
[21]. Takayama, H.; Kitajima, M.; Ogata, K.; Sakai, S. J. Org. Chem. 1992, 57, 4583–4584.
[22]. Ling, S.; Xin, Z.; Qing, Z.; Jian-Bing, L.; Zhong, J.; Jian-Xin, F. Synthetic communications. 2007, 37, 199-207.
[23]. Neil John Press, Roger John Taylor. US Patent, 0053982 A1, 2004.
[24]. Neil John Press, Roger John Taylor. WO Patent, 02/42298 A1, 2002.
[25]. Carosati, E.; Mannhold, R.; Wahl, P.; Hansen, J. B.; Fremming, T.; Zamora, I.; Cianchetta, G.; Baronir, M. J. Med. Chem. 2007, 50, 2117-2126.
[26]. Macaev, F.; Sucman, N.; Shepeli, F.; Zveaghintseva, M.; Pogrebnoi, V. Symmetry. 2011, 3, 165-170.
[27]. Macaev, F.Z.; Radul, O.M.; Sterbet, I.N.; Pogrebnoi, S.I.; Sucman, N.S.; Malinovskii, S.T.; Barba, A.N.; Gdaniec, M. Chem. Heterocyclic Comps. 2007, 3, 374-383.
[28]. Macaev, F.Z.; Radul, O.M.; Gudima, A.P. Russ. Chem. Bull. 2008, 57, 1571-1574.
[29]. Makaev, F. Z.; Radul, O. M.; Gdanets, M.; Malinovskii, S. T.; Gudima, A. P. Russ. J. Struct. Chem. 2006, 47, 796-799. (Engl. Transl.).
[30]. Rekhter, M.A.; Rekhter, B.A.; Yazlovetskii, I.G.; Panasenko, A.A.; Macaev, F.Z. Chem. Heterocyclic Comps. 1998, 34, 275-277.
[31]. Rekhter, M.A.; Macaev, F.Z.; Babilev, F.V.; Grushetskaea, G.N.; Rudakov, S.V. Chem. Heterocyclic Comps. 1996, 32, 418-422.
[32]. Radul, O. M.; Zhungietu, G.I.; Rekhter, M.A.; Bukhanyuk, S.M. Chem. Heterocyclic Comps. 1983, 3, 353.
[33]. Zhungietu, G.I.; Rekhter, M.A. Isatin and its derivatives. Ştiinţa: Chişinău, 1977; pp 36-39.
[34]. Weiss, M.M.; Weiss, P.D.; Mathisen, G.; Guze, P. Clin. Infect. Dis. 2004, 39, 1668-1673.
[35]. Radul, O. M.; Malinovskii, S. T.; Luboradskii, R.; Makaev, F. Z. J. Structural Chem. 2005, 46, 753-758.
[36]. Pogrebnoi, S.I. Ph.D. Thesis, Institute of chemistry of ASM, Chişinău, 2006.
[37]. Fjita, T.; Kitazawa, Y.; Akita, T.; Tani, I. US Patent, 4577032 1989.
[38]. Malkov, A.V.; Kabeshov, M.A.; Bella, M.; Kysika, O.; Malyshev D.A.; Pluhackova, K.; Kocovsky, P. Org. Lett., 2007, 9, 5473-5476.
[39]. Pauwels, R.; Balzarini, J.; Baba, M.; Snoeck, R.; Schols, D.; Herdewijn, P.; Desmyster, J.; De Clercq, E.J. Virol. Methods. 1998, 20, 309.

ON THE PECULIARITIES OF THE RING CONTRACTION REACTIONS OF HOMODRIMANES *VIA* ACID MEDIATED EPOXIDE REARRANGEMENT

Veaceslav Kulcițki*, Tatiana Sîrbu, Nicon Ungur

Institutul de Chimie al AŞ a RM, str. Academiei, 3, MD-2028, Chişinău, Republica Moldova
**Corresponding author: kulcitki@yahoo.com*

Abstract: A selective rearrangement of a epoxi-homodrimanic substrate is described. Using fluorosulfonic acid at low temperature leads by ring contraction to a perhydrindanic structure. On the contrary, using boron trifluoride-diethyl ether at r.t. selectively brings about angular methyl migration.

Keywords: terpenoids, homodrimane, epoxide, rearrangement, hydrindane.

Introduction

Rearrangement reactions of terpenoids leading to ring contraction represent a generally accepted biosynthetic pathway to diverse natural compounds. In general, these reactions are supposed to proceed via an acid-mediated epoxide rearrangement. For a series of important classes of terpenes such biosynthetic schemes have been postulated. We have used a similar bio-mimetic approach [1] for the synthesis of austrodoric acid **1** – a ring contracted nor-drimanic sesquiterpenoid isolated from the Dorid nudibranch *Austrodoris Querguelenensis*. The key step of the synthesis was a bio-mimetic ring contraction of a homodrimanic substrate **2**. This step was performed under the action of a Lewis acid and the yield of target perhydrindane **3** was moderate (cca. 45 %). The structure of the minor reaction products was not reported in our paper and it was the subject of following discussions [2]. We present in the current communication our first results on identification of the minor rearrangement products, which resulted from deeper skeleton transformations of epoxide **2** (Scheme 1).

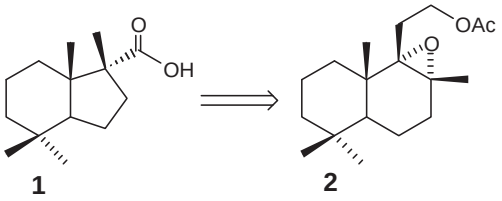

Results and discussion

Rearrangement reaction of epoxides, leading to ring contraction are supposed to proceed via a process, involving acidic attack on the epoxy-group, followed by epoxide opening. A carbonium ion is formed as a result, and its stability assures the following reaction course. Electron-donating groups facilitate carbonium ions formation and in the case of unsymmetrically substituted epoxides, the carbonium ion which is more stabilized by these groups is favoured. In our case, the epoxide group in the substrate **2** is attached to similar substituted carbons, and it is very difficult to estimate the localisation of the positive charge after acidic attack. Consequently, different reaction pathways can lead to different products, diminishing the reaction selectivity.

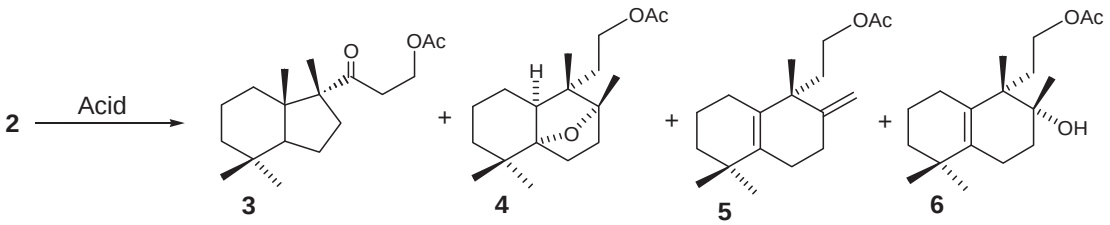

Scheme 1

We have investigated the reaction of epoxide **2** with different acids. All experiments led to similar reaction products, consisting of mixtures of several compounds (Scheme 1). The product composition was also affected by the reaction temperatures and durations. It was established, that the best yield of ring contraction product **3** was highest on treatment of **2** with fluorosulfonic acid at -78°C for 15 min, followed by quenching with triethylamine-hexan mixture.

Using boron trifluoride-diethyl ether complex as initiator turned out to provide selectively the rearranged diene **5** in a similar 66 % yield. Formation of minor amount of **3** was also detected. The results of all isomerisation experiments are presented in the Table 1 below. The relative ratio between reaction products was determined on the basis of ^{1}H NMR data of crude reaction mixtures, by integration of selective proton signals (Figure 1). Separation of individual compounds was performed chromatographically. Structural assignment was performed on the basis of ^{1}H and ^{13}C data of pure compounds, as well as on the basis of IR spectra. Compound **4** was characterized as free alcohol **7**, obtained after hydrolysis (K_2CO_3-MeOH) [3].

Table 1

Exp. No	Solvent	Reaction Temperature, °C	Reaction duration, min	Reaction product distribution, %				Acid
				3	**4**	**5**	**6**	
1	DCM	-20	35	45	14	18	n.d.	$BF_3{\cdot}Et_2O$
2	$MeNO_2$	-25	15	50	17	33	n.d.	$BF_3{\cdot}Et_2O$
3	$MeNO_2$	0	20	47	35	19	n.d.	$BF_3{\cdot}Et_2O$
4	2-NO_2-Pr	22	15	35	n.d.	66	n.d.	$BF_3{\cdot}Et_2O$
5	$MeNO_2$+2-NO_2-Pr (1:1)	-78÷-40	45	54	18	n.d.	27	$BF_3{\cdot}Et_2O$
6	$MeNO_2$+2-NO_2-Pr (1:1)	-50	15	51	28	n.d.	22	$BF_3{\cdot}Et_2O$
7	2-NO_2-Pr	-78	15	65	35	n.d.	n.d.	FSO_3H
8	DCM	22	60	45	20	35	n.d.	*R-$SbCl_6$

*R=tris-(*p*-bromophenyl)-aminium

Explanation of these results can be made on mechanistical grounds. In order for the substrate **2** to form a ring contracted product, the acid attack on the epoxy-group shall lead to formation of C-8 carbonium ion **A** (Scheme 2). It is stabilized by three alkyl groups and by neighbouring acetoxy- group. Following disruption of C9-C10 bond and formation of the new C10-C8 bond occurs through the tri-centered cation and after proton expulsion provide the ring contracted perhydrindane **3**.

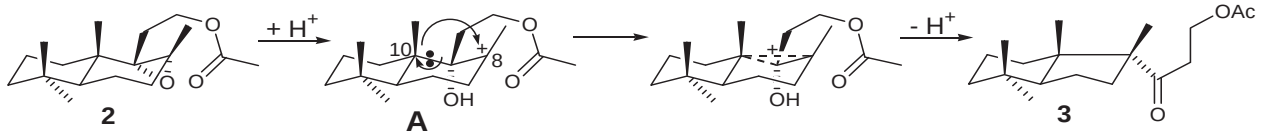

Scheme 2

The other reaction pathway is represented in Scheme 3. Carbonium ion formation occurs at C9, which is also facilitated by three alkyl substituents, but less likely stabilized by acetoxy- group. Instead, it is facilitated by the equatorial disposal of the –OH group and by a facile methyl migration from C10 to C9, to give intermediate carbocation **B**. It can transform either by a following hydride shift and cyclisation through the C8-O- atom into oxide **4**, or by deprotonation to **5** and **6**.

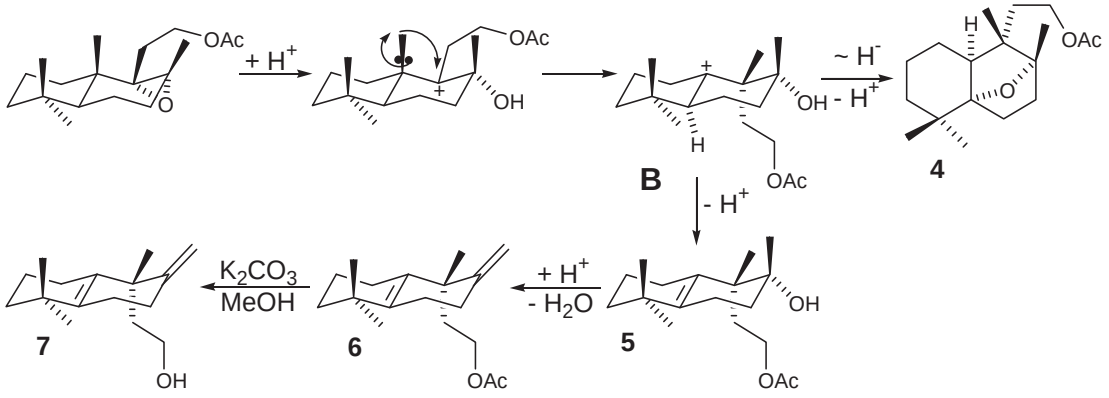

Scheme 3

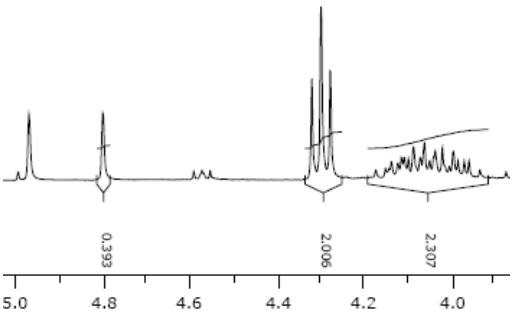

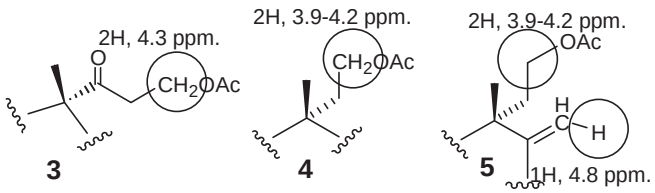

Figure 1. Determination of the isomeric product distribution by integration of selective NMR peaks (experiment No 3). Peak at 4.8 ppm corresponds to one proton of **5**, the triplet at 4.3 ppm – to two protons of **3** and the multiplet 3.9-4.2 represents additive signals from two CH_2-groups of compounds **4** and **5**.

Conclusions

By using different acid inducers and reaction conditions it was possible to finely tune the selectivity of homodrimanic epoxide rearrangements, which besides ring contraction, involve a cascade epoxide opening, followed by methyl and proton shifts. The observed mechanism of epoxide **2** reactivity is confirmed by the similar results in the known transformation of bisnor-labdanic epoxides, reported previously by Halsall and Hadley [4].

Acknowledgements

V.K. acknowledges Alexander von Humboldt foundation for a postdoctoral fellowship.

References

[1]. Kulcitki, V.; Ungur, N.; Gavagnin, M.; Carbone, M.; Cimino, G. *Tetrahedron*: *Asymm*., **2004**, *15* (3), 423-428.

[2]. Alvarez-Manzaneda, E.; Chahboun, R.; Barranco, I.; Cabrera, E.; Alvarez, E.; Lara, A.; Alvarez-Manzaneda, R.; Hmamouchic, M.; Es-Samti, H. *Tetrahedron*, **2007**, *63*, 11943–11951.

[3]. Compound **3**. ^{1}H NMR ($CDCl_3$, 300MHz): 4.31 (t., 2H, J=6Hz), 2.6-2.9 (m., 2H); 2.15-2.25 (m., 1H); 2.00 (s., 3H); 1.17 (s., 3H); 0.87 (s., 3H); 0.86 (s., 3H); 0.84 (s., 3H). IR (liquid film, cm^{-}1): 1734, 1695.
Compound **5**. ^{1}H NMR ($CDCl_3$, 300MHz): 5.00 (s., 1H); 4.83 (s., 1H); 3.96-4.15 (m., 2H); 2.02 (s., 3H); 1.10 (s., 3H); 1.04 (s., 3H); 1.03 (s., 3H). IR (liquid film, cm^{-}1): 2925, 1742, 1460, 1364, 1234, 1034, 880.
Compound **6**. ^{1}H NMR ($CDCl_3$, 300MHz): 4.08-4.27 (m., 2H); 2.03 (s., 3H); 1.14 (s., 3H); 1.00 (s., 3H); 0.99 (s., 3H); 0.97 (s., 3H). IR (liquid film, cm^{-}1): 3460; 2927; 1737; 1461; 1364; 1239; 1142; 1082; 1031.
Compound **7**. ^{1}H NMR ($CDCl_3$, 300MHz): 3.69 (t., 2H, J9Hz); 1.29 (s., 3H); 1.10 (s., 3H); 1.01 (s., 3H); 0.76 (s., 3H). IR (liquid film, cm^{-}1): 3400; 2932; 2870; 1452; 1386; 1073; 1041.

[4]. Hadley, M. S.; Halsall, T. G. *J. Chem. Soc. Perkin Trans. I*, **1974**, 1334-1349.